



Faculteit Farmaceutische, Biomedische en Diergeneeskundige Wetenschappen

Departement Farmaceutische Wetenschappen

Phytochemical, Analytical and Preclinical Investigations on
Plant Extracts as Potential Antitumoural Therapy

Fytochemisch, Analytisch en Preklinisch Onderzoek van
Plantenextracten als Potentieel Antitumorale Therapie

Proefschrift voorgelegd tot het behalen van de graad van Doctor in de Farmaceutische
Wetenschappen aan de Universiteit Antwerpen te verdedigen door

Rica CAPISTRANO I.

Promotoren: Prof. Dr. L. Pieters
Prof. Dr. S. Apers

Antwerpen, 2015

Anyone who has never made a mistake has never tried anything new.

Albert Einstein

TABLE OF CONTENTS

LIST OF ABBREVIATIONS	XI
CHAPTER 1 INTRODUCTION	1
1.1. CANCER	3
1.1.1. What is Cancer?	3
1.1.2. Cancer treatment	6
1.2. MEDICINAL PLANTS AND HERBAL MEDICINES	10
1.3. NATURAL ANTICANCER DRUGS	13
1.4. AIM OF THIS WORK	17
REFERENCES	19
CHAPTER 2 GENERAL EXPERIMENTAL METHODS	25
2.1. CHROMATOGRAPHIC METHODS	27
2.1.1. Solvents and reagents	27
2.1.2. Thin layer chromatography	27
2.1.3. Flash column chromatography	27
2.1.4. High performance liquid chromatography	28
2.1.5. High performance liquid chromatography – Solid phase extraction – Nuclear magnetic resonance spectroscopy	28
2.1.6. Semi-preparative high performance liquid chromatography	29
2.2. SPECTROSCOPIC METHODS	29
2.2.1. Nuclear magnetic resonance spectroscopy	29
2.2.2. Mass spectrometry	30
2.2.3. Optical rotation	30
2.3. BIOLOGICAL METHODS	31
2.3.1. Media and reagents	31
2.3.2. Cell line & culture	31

2.3.3.	Sulforhodamine B assay	33
2.3.4.	Neutral red assay	34
2.3.5.	<i>xCELLigence</i> Real-Time Cell Analysis	34
2.3.6.	Calculation of the IC ₅₀ values	35
REFERENCES		36
CHAPTER 3 <i>STEGANOTAENIA ARALIACEA</i>		37
3.1.	INTRODUCTION	39
3.2.	PHYTOCHEMICAL INVESTIGATION	42
3.2.1.	Plant material	42
3.2.2.	Extraction	42
3.2.3.	Liquid-liquid partition	43
3.2.4.	Thin layer chromatography	43
3.2.5.	Flash column chromatography	44
3.2.6.	Isolation by means of LC-SPE-NMR	45
3.2.7.	Structure elucidation	48
3.2.7.1.	<i>Spiropreussomerin A</i>	48
3.2.7.2.	<i>Conrauiflavonol/afzelin A</i>	56
3.2.7.3.	<i>Protosteganoflavanone</i>	64
3.3.	CYTOTOXICITY STUDY	72
3.4.	DISCUSSION	75
3.5.	SUMMARY AND CONCLUSION	77
REFERENCES		78
CHAPTER 4 <i>GLORIOSA SUPERBA</i>		81
4.1.	INTRODUCTION	82
4.2.	ALKALOIDS	84
4.2.1.	Colchicine	84
4.2.2.	Colchicine derivatives	87

4.3.	PHYTOCHEMICAL CHARACTERISATION	89
4.3.1.	Plant material	89
4.3.2.	Extraction	89
4.3.3.	Isolation of the main constituents	90
4.3.3.1.	<i>Thin layer chromatography of the G. superba crude extract</i>	90
4.3.3.2.	<i>High performance liquid chromatography of the G. superba crude extract</i>	90
4.3.3.3.	<i>LC-SPE-NMR of the G. superba crude extract</i>	91
4.3.4.	Structure elucidation of the main constituents	93
4.3.4.1.	<i>Colchicine</i>	93
4.3.4.2.	<i>3-O-demethylcolchicine</i>	101
4.3.4.3.	<i>Colchicoside</i>	108
4.3.5.	Colchicine-poor extract	115
4.3.5.1.	<i>Liquid-liquid partition</i>	115
4.3.5.2.	<i>Normal phase TLC analysis</i>	116
4.3.5.3.	<i>HPLC analysis of the liquid-liquid partition fractions</i>	117
4.3.5.4.	<i>Isolation of Compound D</i>	119
4.3.5.5.	<i>Identification of colchicosamide</i>	120
4.3.6.	Summary and conclusion	127
4.4.	ANALYTICAL INVESTIGATION	128
4.4.1.	Method development/optimisation	129
4.4.1.1.	<i>Sample preparation</i>	129
4.4.1.2.	<i>Chromatographic conditions</i>	130
4.4.2.	Final analytical method	131
4.4.2.1.	<i>Reference solution</i>	131
4.4.2.2.	<i>Test solution</i>	131
4.4.2.3.	<i>HPLC conditions</i>	132
4.4.3.	Validation of the analytical method	133
4.4.3.1.	<i>Response function – Calibration model</i>	136
4.4.3.2.	<i>Precision</i>	139
4.4.3.3.	<i>Accuracy</i>	144

4.4.3.4.	<i>Specificity</i>	145
4.4.4.	Correction factor	146
4.4.4.1.	<i>Semi-preparative isolation of the two colchicine derivatives</i>	146
4.4.4.2.	<i>Validation</i>	147
4.4.5.	Quantification of the different batches of extract	152
4.4.6.	Summary and conclusion	153
4.5.	PRECLINICAL STUDIES	155
4.5.1.	Introduction	155
4.5.2.	<i>In vitro</i> cytotoxicity	157
4.5.2.1.	<i>Results</i>	157
4.5.2.2.	<i>Discussion</i>	163
4.5.3.	Preliminary <i>in vivo</i> study	165
4.5.3.1.	<i>Materials and methods</i>	165
4.5.3.2.	<i>Results and discussion</i>	166
4.5.4.	<i>In vivo</i> – efficacy study	169
4.5.4.1.	<i>Materials and methods</i>	169
4.5.4.2.	<i>Results</i>	174
4.5.4.3.	<i>Discussion</i>	183
4.5.5.	<i>In vivo</i> – survival study	187
4.5.5.1.	<i>Materials and methods</i>	187
4.5.5.2.	<i>Results</i>	190
4.5.5.3.	<i>Discussion</i>	197
4.5.6.	Conclusion	200
4.6.	SUMMARY AND CONCLUSION	203
	REFERENCES	206

CHAPTER 5 CHELIDONIUM MAJUS **213**

5.1.	INTRODUCTION	215
5.1.1.	Constituents	216
5.1.2.	Biological activities	218

5.1.3.	Ukrain™	220
5.2.	PHYTOCHEMICAL INVESTIGATION	222
5.2.1.	Plant material	222
5.2.2.	Extraction	222
5.2.3.	Defatting	223
5.2.4.	High performance liquid chromatography	223
5.3.	PRECLINICAL STUDIES	225
5.3.1.	<i>In vitro</i> cytotoxicity	225
5.3.1.1.	<i>Results</i>	225
5.3.1.2.	<i>Discussion</i>	230
5.3.2.	<i>In vivo</i> – effect on metastases	232
5.3.2.1.	<i>Materials and methods</i>	232
5.3.2.2.	<i>Results and discussion</i>	235
5.4.	SUMMARY AND CONCLUSION	237
	REFERENCES	238
	CHAPTER 6 GENERAL CONCLUSION & PERSPECTIVES	245
	SUMMARY	251
	SAMENVATTING	257
	ACKNOWLEDGEMENT - DANKWOORD	263
	SCIENTIFIC CURRICULUM VITAE	269

LIST OF ABBREVIATIONS

3T3	mouse fibroblast cells
AIF	apoptosis inducing factor
ANOVA	analysis of variance
ATCC	American type culture collection
BBI	broadband inverse
BEAS-2B	human bronchial epithelial cells
BEGM	bronchial epithelial cell growth medium
BW	body weight
CAM	complementary and alternative medicine
CI	cell index
CD	circular dichroism
CM2	<i>Chelidonium majus</i> crude ethanolic extract
CM2B	<i>Chelidonium majus</i> defatted extract
COL	colchicine
COSY	correlation spectroscopy
CT	computed tomography
DAB	3,3'-diaminobenzidine
DAD	diode array detector
DEPT	distortionless enhancement by polarisation transfer
DMSO	dimethyl sulfoxide
ELSD	evaporating light scattering detector
EtOH	ethanol
ESI	electrospray ionisation
EtOAc	ethyl acetate

FBS	foetal bovine serum
FDG	fluorodeoxyglucose
FMF	Familial Mediterranean Fever
GEM	gemcitabine
GP	general phase
GS	<i>Gloriosa superba</i> crude ethanolic extract
GS2B	Colchicine-poor extract
H&E	haematoxylin & eosin
HMBC	heteronuclear multiple bond correlation
HPLC	high performance liquid chromatography
HPV	human papilloma virus
HRP	horseradish peroxidase
HT-29	human colorectal adenocarcinoma cells
HS	<i>n</i> -heptanesulfonic acid aqueous solution
HSQC	heteronuclear single quantum coherence
IC ₅₀	concentration causing 50% growth inhibition
IHC	immunohistochemical
IM	intramuscular
IP	intraperitoneal
IV	intravenous
LD ₅₀	median lethal dose
MDA-MB-231	human breast adenocarcinoma cells
MeOH	methanol
NCI	National Cancer Institute
NMR	nuclear magnetic resonance
NP	normal phase

NR	neutral red
OD	optical density
PANC-1	human pancreatic epithelioid carcinoma cells
PBS	phosphate-buffered saline
PC-EM002	primary endometrial cancer cell cultures
PC-EM005	primary endometrial cancer cell cultures
PE	petroleum ether
PET	positron emission tomography
Ph. Eur.	European Pharmacopoeia
QTOF-MS	quadrupole-time-of-flight mass spectrometer
RCT	randomised clinical trials
ROI	regions of interest
RP	reverse phase
RSD	relative standard deviation
RTCA	real-time cell analysis (<i>xCELLigence</i>)
RTV	relative tumour volume
SA	<i>Steganotaenia araliacea</i> crude ethanolic extract
SA2A	ethyl acetate fraction of <i>S. araliacea</i>
SD	standard deviation
SE	standard error
SEM	standard error of the mean
SPE	solid phase extraction
SRB	sulforhodamine B
SUV	standard uptake value
T/C	median survival time of the treated animals versus median survival time of the control times

TBST	tris buffered saline with Tween®20
TC	total amount of colchicine and its derivatives expressed as colchicine
TFA	trifluoroacetic acid
TGD	tumour growth delay
TGI	tumour growth inhibition
TLC	thin layer chromatography
TM	traditional medicine
TNF α	tumour necrosis factor α
TQD MS	triple quadrupole mass spectrometer
tris	tris(hydroxymethyl)aminomethane
UPLC	ultra performance liquid chromatography
UV	ultraviolet
VOI	volume of interest
WHO	World Health Organization

CHAPTER 1
INTRODUCTION

1.1. CANCER

Cancer is the leading cause of death worldwide, accounting for 14.1 million new cases and 8.2 million deaths in 2012 and is a major public health burden in both developed and developing countries. Around 57% (8 million) of new cancer cases and 65% (5.3 million) of cancer deaths occurred in the developing countries. Cancer tends to be diagnosed at later stages in many developing countries and this, combined with the limited resources to prevent, diagnose and treat cancer, has an adverse effect on survival. It is estimated that annual cancer cases will rise to 22 million within the next two decades.^[1] On 31st December 2010, it was estimated that 429349 people in Belgium had been diagnosed with at least one type of invasive cancer in the past 20 years. This is approximately 3.9% of the Belgian population or nearly 1 in 25 Belgians.^[2] The global burden of cancer continues to increase largely because of ageing and an increasing adoption of cancer-causing behaviours within economically developing and developed countries.^[2-4]

1.1.1. What is Cancer?

Cancer is a generic term for a large group of diseases that can affect any part of the body, characterised by uncontrolled rapid growth and spread of abnormal cells that grow beyond their usual boundaries. It can invade adjoining parts of the body and spread to other organs. If the spread is not controlled, it can result in death. This process is referred to as metastasis. Metastasis is the major cause of death from cancer.^[5, 6]

Cancer is a disease involving dynamic changes in the genome.^[7] The hallmarks of cancer (Figure 1.1) involve six biological capabilities acquired during the development of tumours. The hallmarks include sustaining proliferative signalling, evading growth suppressors, resisting cell death, enabling replicative immortality, inducing angiogenesis, and activating invasion and metastasis. Sustaining proliferative signalling is the most fundamental trait of cancer cells. Normal tissues control the production and release of growth-promoting signals, thereby ensuring homeostasis of the cell number. Cancer cells show a reduced dependence on exogenous growth stimulation and often generate many of their own growth signals. In addition to the capability of sustaining positively acting growth-stimulatory signals, cancer

cells must also evade growth suppressors. The ability of tumour cell populations to expand in number is determined not only by the rate of cell proliferation but also by the rate of cell attrition. Programmed cell death (apoptosis) represents a major mechanism of cell attrition. Resisting apoptosis is an important acquired capability of cancer cells. The three acquired capabilities so far all lead to the uncoupling of a cell's growth program from signals of its environment. The fourth capability is enabling replicative immortality. Cancer cells require unlimited replicative potential in order to generate macroscopic tumours. This capability stands in contrast to the behaviour of normal cells, which are able to pass through only a limited number of successive cell growth-and-division cycles. The penultimate capability is inducing angiogenesis. Like normal tissues, tumours require sustenance in the form of nutrients and oxygen as well as the evacuation of metabolic waste and carbon dioxide. The tumour-associated neovasculature, generated by the process of angiogenesis, addresses these needs. Sooner or later during the development of most types of human cancer, primary tumour cells invade adjacent tissues and form new colonies. The capability for invasion and metastasis enables cancer cells to escape the primary tumour and colonise new terrain in the body where nutrients and space are not limiting yet.^[7,8]

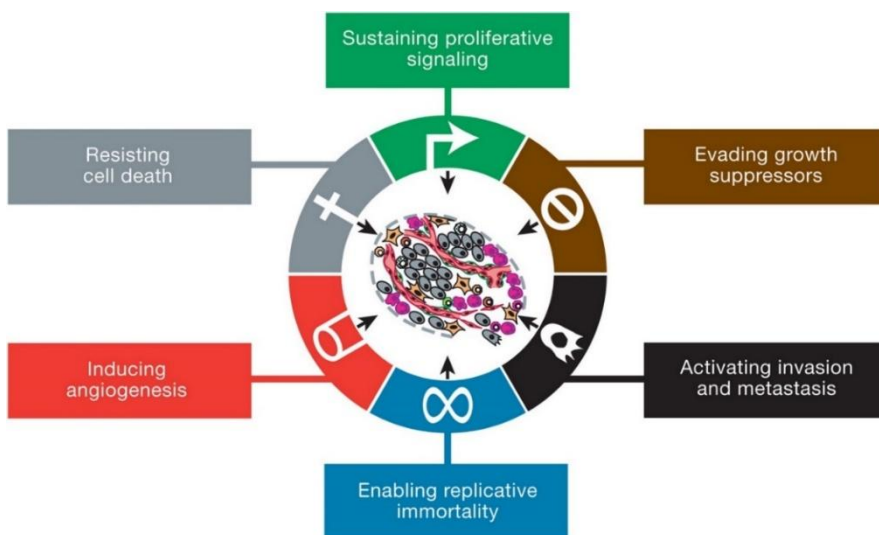


Figure 1.1 The Hallmarks of Cancer (From Hanahan D. and Weinberg R., 2011)

The hallmarks of cancer are defined as acquired functional capabilities that allow cancer cells to survive, proliferate, and disseminate; these functions are acquired in different tumour types via distinct mechanisms and at various times during the course of multistep tumourigenesis. Their acquisition is made possible by two enabling characteristics (Figure 1.2). Most prominent is genome instability, which generates random mutations. A second enabling characteristic involves tumour-promoting inflammation. Conceptual progress in the last decade has added two emerging hallmarks of potential generality to the list of hallmarks, i.e. reprogramming of energy metabolism and evading immune destruction (Figure 1.2). The reprogramming of cellular energy metabolism is needed in order to support continuous cell growth and proliferation. The second emerging hallmark involves active evasion by cancer cells from attack and elimination by immune cells.^[7, 8]

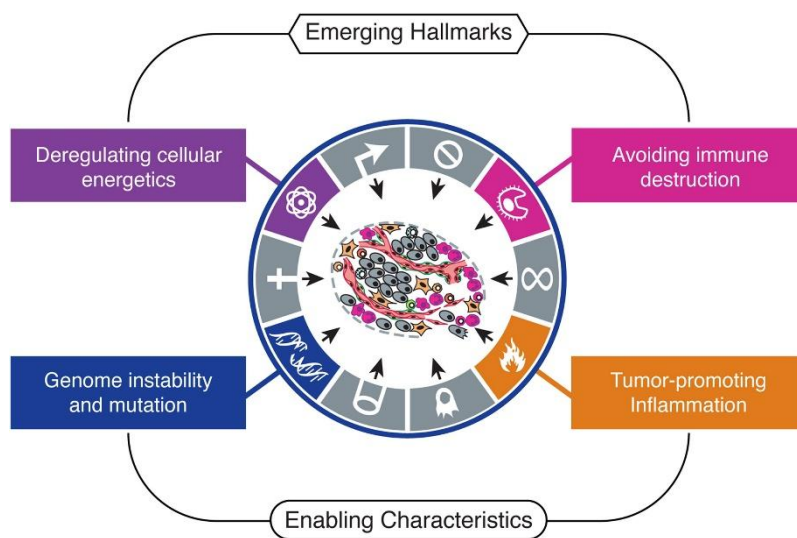


Figure 1.2 Emerging hallmarks and enabling characteristics
 (From Hanahan D. and Weinberg R., 2011)

1.1.2. **Cancer treatment**

Cancer treatment requires a careful selection of one or more interventions, such as surgery, radiotherapy and chemotherapy. The goal is to cure the disease or considerably prolong life while improving the patient's quality of life.^[5] Surgery can be used to diagnose, treat or even help prevent cancer. It offers the greatest chance for cure, especially if the cancer has not spread to other parts of the body. Radiotherapy uses high-energy particles or electromagnetic waves to destroy or damage cancer cells. It is one of the most common treatments for cancer, either by itself or along with other forms of treatment. Usually these two types of therapies are combined with systematic therapy (mainly chemotherapy) to treat metastases or remnant tumours from surgery or radiation therapy. Most classes of chemotherapy have an inhibitory effect on cancer cells or more precisely on rapidly dividing cells by intervening in the proliferation and the normal function of DNA.

Chemotherapeutic drugs can be subdivided into several groups based on their mechanism of action.

Alkylating agents directly damage DNA to prevent the cancer cell from reproducing. As a class of drugs, these agents are not phase-specific; in other words, they act in all phases of the cell cycle (Figure 1.3).^[9] Alkylating agents are used to treat many different cancers, including leukaemia, lymphoma, Hodgkin's disease, multiple myeloma, sarcoma, as well as cancers of the lung, breast, and ovary. There are different classes of alkylating agents, including: nitrogen mustards (e.g. cyclophosphamide) and ethylenimines (e.g. thiotepa). The platinum drugs (cisplatin, carboplatin and oxaloplatin) are sometimes classified as alkylating agents because they kill cells in a similar way.

Antimetabolites are a class of drugs that interferes with DNA and RNA growth by substituting for the normal building blocks of DNA and RNA. These agents damage cells during the S phase. They are commonly used to treat leukaemia, cancers of the breast, ovary, the intestinal tract, as well as other types of cancer. Some examples of antimetabolites are 5-fluorouracil, 6-mercaptopurine, gemcitabine and capecitabine.

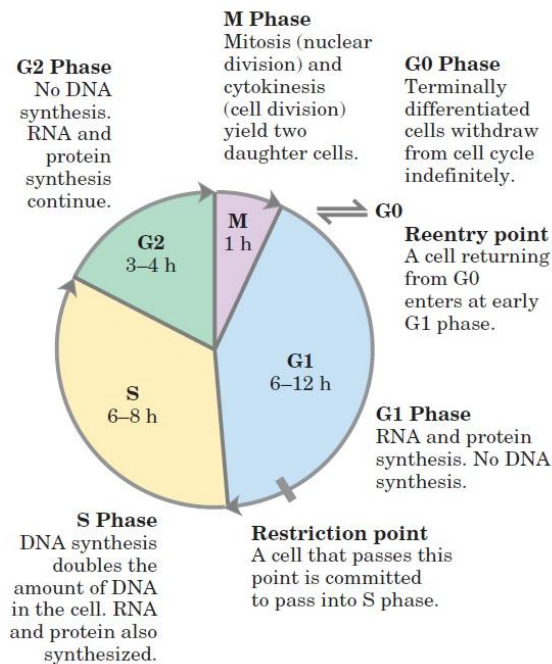


Figure 1.3 Cell cycle (From Nelson D. & Cox M, 2005)

Anthracyclines are antitumour antibiotics that interfere with enzymes involved in DNA replication. These drugs act in all phases of the cell cycle. They are widely used for a variety of cancers. An example of an anthracycline is doxorubicin. Other antitumour antibiotics that are not anthracyclines include bleomycin and mitomycin-C.

Topoisomerase inhibitors are drugs that interfere with enzymes called topoisomerases, which help to separate the two DNA strands so they can be replicated. They are used to treat certain leukaemia, as well as lung, ovarian, gastrointestinal and other cancers. Examples of topoisomerase I inhibitors include topotecan and irinotecan. Examples of topoisomerase II inhibitors include etoposide and teniposide.

Mitotic inhibitors are often plant alkaloids and other compounds derived from natural products. They can stop mitosis or inhibit enzymes from producing proteins needed for cell reproduction. These drugs act during the M phase of the cell cycle but can damage cells in all

phases. They are used to treat many different types of cancer including breast and lung cancer, myelomas, lymphomas, and leukaemia. Examples of mitotic inhibitors include taxanes (e.g. paclitaxel and docetaxel), epothilones (e.g. ixabepilone), vinca alkaloids (e.g. vinblastine, vincristine and vinorelbine) and estramustine.

Other drugs and biological treatments are used to treat cancer, but are not usually considered as chemotherapy. While chemotherapeutic drugs take advantage of the fact that cancer cells divide rapidly, these other drugs have different targets that set cancer cells apart from normal cells. They often have less serious side effects than those commonly caused by chemotherapy because they are targeted to work mainly on cancer cells. Many are used along with chemotherapy. Some of these drugs include differentiating agents, targeted therapies, hormones, and immunotherapy.^[10, 11]

Differentiating agents are based on the concept that cancer cells are normal cells that have been blocked at an early stage of their development and fail to differentiate into functional mature cells. These cells lack the ability to control their own growth and proliferate at an abnormally fast rate. Differentiation therapy aims to force the cancer cell to resume the process of maturation. Although differentiation therapy, e.g. the retinoids (tretinoin and bexarotene), does not destroy the cancer cells, it restrains their growth and allows conventional therapies (such as chemotherapy) to eradicate the malignant cells.^[11, 12]

Targeted cancer therapies are drugs or other substances that disrupt carcinogenesis by targeting certain parts of the cell and the signals that are needed for cancer development and growth. Some targeted therapies inhibit enzymes and are called enzyme inhibitors. These inhibitors slow tumour formation by blocking the signalling cascade for example the tyrosine kinase inhibitor, imatinib. Tyrosine kinase is an enzyme that transfers a phosphate group from ATP to a protein in a cell. Phosphorylation of proteins is an important mechanism in signal transduction and regulating cellular activity, such as cell division. By blocking this enzyme, the cells stop growing. Another way to stop growth of cancer cell is to inhibit growth factor. Gefitinib and erlotinib interrupt signalling through the epidermal growth factor (EGFR) receptor. EGFR is overexpressed in certain types of cancer. This leads to unwanted activation of the anti-apoptotic signalling cascade leading to uncontrolled cell proliferation. Another

example of an enzyme inhibitor is bortezomib, which is a proteasome inhibitor. A proteasome is a complex of enzymes that degrades pro-growth cell cycle proteins and this process is disrupted by proteasome inhibitors.

Hormone therapies use hormone-like drugs that can act on the action or production of female or male hormones. They are used to slow the growth of breast, prostate, and endometrial cancers, which normally grow in response to natural hormones in the body. This treatment prevents the cancer cell from using hormones that is needed to grow, or prevent the body from making these hormones. Drugs such as the anti-oestrogens (tamoxifen), anti-androgens (bicalutamide) and the gonadotropin-releasing hormone (goserelin) are some examples of hormone therapies.

Other cancer drugs are used to stimulate the natural immune system to recognise and attack cancer cells. Immunotherapy works in two ways either by stimulating own immune system or by using antibodies. Immunotherapy includes monoclonal antibodies, cancer vaccines and non-specific immunotherapies. Over the past decades more than a dozen monoclonal antibodies have been approved to treat certain cancers. For example, trastuzumab is an antibody against the HER2 protein, frequently overexpressed in some types of cancers of the breast or prostate. Cancer vaccines work by starting an immune response in the body. The goal is to help treat cancer or to help prevent recurrence. Certain cancers can be prevented by vaccines, for example some strains of the human papilloma virus (HPV) have been linked to cervical, anal, throat and some other cancers. Vaccines against HPV may protect against some of these cancers. In 2010, the first vaccine to treat advanced prostate cancer was approved, but other vaccines for many different types of cancer are being studied at the moment. Non-specific cancer immunotherapies stimulate the immune system in a more general way, some are given as such as cancer treatments, and others are used as adjuvants to boost the immune system. Some examples are the interleukins, interferons or immunomodulating drugs such as thalidomide.^[10, 11]

The natural anticancer drugs or products derived from natural origin will be discussed in detail in section 1.3.

1.2. MEDICINAL PLANTS AND HERBAL MEDICINES

Phytotherapy is the oldest form of therapy worldwide. An estimated two thirds of the world population resorts to medicinal plants derived from folk medicines for their primary health care needs.^[13]

“Traditional medicine” (TM) is a comprehensive term used to refer to systems such as traditional Chinese medicine, Indian Ayurveda and Arabic unani medicine, and to various forms of indigenous medicine. Use of TM remains widespread in developing countries and the broad use is often attributable to its accessibility and affordability.^[14] Sometimes it is the only affordable source of health care for the world’s poorest patients. In Africa up to 80% of the population uses TM to help meet their health care needs. In Asia and Latin America, the populations continue to use TM because of historical reasons and cultural beliefs.^[14] In countries where the primary health care system is based on conventional Western medicine, or where TM has not been incorporated into the national health care system, TM is often termed “complementary”, “alternative” or “non-conventional” medicine. Complementary and alternative medicine (CAM) is often used when referring to traditional medicine in Europe or North America. Use of CAM is increasing rapidly in developed countries, e.g. the percentage of population which has used CAM at least once in Belgium is 38%. TM/CAM therapies include medication therapies and non-medication therapies (e.g. acupuncture). The medication therapies involve mainly the use of herbal medicines.^[14]

Herbal medicines offer several advantages. In many parts of the world, they are easily available and affordable compared to synthetic drugs.^[14] The presence of synergistic and/or side effects neutralising combinations in medicinal plants is a long-established concept.^[15] Usually the plant preparations in their crude form show a more interesting combination of activities than the isolated constituents. So there is a huge potential in the use of medicinal plant extracts.^[16]

However, herbal medicines are not without their own limitations. Clinical data on efficacy and safety are not always available. The concentration of active constituents in a given plant species varies considerably, depending on a number of factors such as the age, the geographical location, the time of harvesting, the harvesting processes, and storing conditions.^[17]

Nevertheless, scientific research can overcome some of these limitations and enable the development of effective medicinal preparations. Therefore its claimed efficacy needs to be established and the toxicity must be assessed. In addition, quality control is essential. Together with the increasing use of TM/CAM, there is a growing demand for evidence on the safety, efficacy and quality of TC/CAM products.^[14]

Because herbal medicines are largely used around the world, the following definitions have been developed in order to meet the need for standard internationally accepted definitions. The World Health Organisation (WHO) has formulated these definitions, which in general are also accepted by the European Pharmacopoeia (Ph. Eur.). According to Ph. Eur. 8.0, herbal drug preparations are homogeneous products obtained by subjecting herbal drugs to treatments such as extraction, distillation, expression, fractionation, purification, concentration or fermentation. Herbal drugs are mainly whole or fragmented, or broken plants, parts of plants, algae, fungi or lichens, in an unprocessed state, usually in dried form but sometimes fresh. Extracts are preparations of liquid (liquid extracts and tinctures), semi-solid (soft extracts and oleoresins) or solid (dry extracts) consistency, obtained from herbal drugs or animal matter, which are usually in dry state. Quantified extracts are adjusted to a defined range of constituents, and adjustments are made by blending batches of extracts, while standardised extracts are adjusted within an acceptable tolerance to a given content of constituents with known therapeutic activity. Standardisation is achieved by adjustment of the extract with inert material or by blending batches of extracts. Other types of extracts are essentially defined by their production process and their specifications e.g. standardised or quantified extracts submitted to purification procedures that increase the typical proportions of characterised constituents with respect to the expected values are referred to as refined extracts.^[18]

Furthermore about three quarters of the plant-derived drugs in clinical use today came to the attention of pharmaceutical companies because of their use in TM.^[13] Most of the plant-derived drugs were originally discovered through the study of herbal cures and traditional medicine and some of these could not be substituted despite enormous advancements in synthetic chemistry.^[16] For example, the precursor of paclitaxel, 10-deacetylbaccatin III, is still extracted from its natural source. The chemical diversity of secondary plant metabolites that resulted from plant evolution may be even superior to that found in synthetic combinatorial chemical libraries.^[19] Natural products represent valuable sources for drug development given the fact that a considerably large amount of drugs is of natural origin.^[20]

There are two basic reasons to work on medicinal plants. The first is to search for new lead compounds to be developed as drugs as such or as synthetic or semi-synthetic analogues. The second reason is the valorisation of traditional medicine and herbal medicinal products and the use of the plant preparations as such.^[21] The use of a plant preparation can be supported if it is safe and if its activity can be scientifically confirmed, if the toxicity and the potential adverse effect have been evaluated and if the quality is controllable and assured.^[22]

1.3. NATURAL ANTICANCER DRUGS

Natural products have been investigated and utilised to alleviate diseases since early human history. In the early 1900s, 80% of all medicines were obtained from plants. In more recent times, natural products have continued to be significant sources of drugs and leads.^[23] The National Cancer Institute (NCI) has shown that more than two thirds of the anticancer drugs approved between the 1940s and 2006 were either natural products or were developed based on the knowledge gained from natural products.^[13] Their dominant role is evident in the approximately 60% of anticancer compounds that are natural products or natural product derivatives.^[23] Natural products belong to the major players in cancer research, since a considerable portion of antitumour agents currently used in the clinic are of natural origin. Drugs of different classes are part of the armatorium to fight the war against cancer, e.g. taxanes (paclitaxel, docetaxel), *Vinca* alkaloids (vincristine, vinblastine, vindesine, vinorelbine), epipodophyllotoxines (etoposide, teniposide), anthracyclines (doxorubicin, daunorubicin, epirubicin, idarubicin), camptothecin and its derivatives (topotecan, irinotecan), and others (Figure 1.4).^[13]

Paclitaxel, also known as Taxol[®], is a good example to illustrate the importance of anticancer drugs of plant origin. It was initially discovered through the NCI program for evaluation of plant preparations for anticancer activity. In 1964, an extract of the *Taxus brevifolia* bark was shown to be highly cytotoxic *in vitro* on cancer cells and the biological activity was confirmed in certain animal models of cancer. In 1971, the structure of paclitaxel was elucidated and it showed a unique mechanism of action in its suppression of the growth of cancer cells. Paclitaxel binds to microtubule polymers and stabilises the microtubules, leading to mitotic arrest. In 1992, paclitaxel was approved for the treatment of refractory ovarian cancer, but because of its complex chemical structure, it was not economically feasible to be synthesised and thus it had to be isolated from a natural source.^[23] Paclitaxel was initially extracted from the bark of *T. brevifolia* but now it is obtained by semi-synthesis from 10-deacetylbaccatin III, which is extracted from the needles of *T. baccata*. Docetaxel, a semi-synthetic taxane also with anticancer activity was directly obtained from 10-deacetylbaccatin III.^[24] The taxanes

paclitaxel and docetaxel show impressive antitumour activity against breast, ovarian and other tumour types in the clinic.^[25, 26]

In the 1970s another breakthrough in the field of anticancer drugs came from the *Catharanthus roseus*, also known as *Vinca rosea*, or the Madagascan periwinkle.^[27] Extracts of *V. rosea* possess many therapeutic effects including antitumour activity. Vincristine and vinblastine were the first alkaloids with antitumour activity to be isolated and identified. The introduction of the vinca alkaloid vincristine resulted in a considerable increase in the cure rates for Hodgkin's disease and some forms of leukaemia. Vinorelbine was the first new second-generation vinca alkaloid to emerge from structural modification studies.^[24, 25] Vinca alkaloids disrupt the mitotic spindle assembly through interaction with tubulin. They bind specifically to β -tubulin and block its ability to polymerise with α -tubulin into microtubules. This leads to destabilisation of microtubules and thus inhibiting mitosis.^[24, 26]

Podophyllum peltatum and *P. emodii* have a long history of medicinal use, including the treatment of skin cancers and warts. The major active constituent, podophyllotoxin was reported in the 1950s. Many closely related podophyllotoxin-like lignans were isolated and several of them were introduced into clinical trials, but were dropped due to lack of efficacy and unacceptable toxicity. Extensive research led to the development of etoposide and teniposide as clinically effective agents. Etoposide and teniposide are semi-synthetic derivatives of an isomer of podophyllotoxin, i.e. epipodophyllotoxin.^[28] Podophyllotoxin binds to tubulin and acts by preventing microtubule formation. Etoposide and teniposide on the other hand inhibit DNA topoisomerase II enzyme thus preventing DNA replication. The different mechanism of action is due to a small change in the configuration of the molecules and the introduction of a bulky substituent.^[24, 27] The microbial-derived anthracyclines (daunorubicin and doxorubicin) also act as inhibitors of topoisomerase II, thus initiating DNA damage. Other mechanisms have also been reported, such as intercalation, i.e. the anthracyclines approach DNA via the major groove of the double helix and intercalate using the planar tricyclic system, thus preventing the replication and transcription. A third mechanism involves the quinone moiety which can chelate iron to form an anthracycline-DNA-iron complex. Reactive oxygen species are then generated, leading to single-strand

breaks in the DNA chain. A fourth mechanism involves interference with DNA unwinding or DNA strand separation and helicase activity.^[29, 30] After daunorubicin and doxorubicin, a series of semi-synthetic compounds, i.e. idarubicin and epirubicin have been approved for use in the clinic. Doxorubicin exhibits a broad spectrum of activity and remains one of the most effective anticancer drugs. It is widely used in the treatment of breast carcinoma, small cell lung cancer, ovarian carcinoma and lymphomas.^[24]

The screening program of NCI also led to the discovery of the extract of *Camptotheca acuminata* characterised by cytotoxic activity against a variety of leukaemia and solid tumours. Camptothecin was identified as the active constituent of the extract. Despite the promising preclinical and clinical antitumour activity the use of camptothecin was hindered by severe and unpredicted toxicity. Years of intense research led to two semi-synthetic analogues, i.e. irinotecan and topotecan. These camptothecin derivatives act as inhibitors of DNA topoisomerase I and cause DNA damage by stabilising the covalent topoisomerase I-DNA complex, thus preventing religation.^[24]

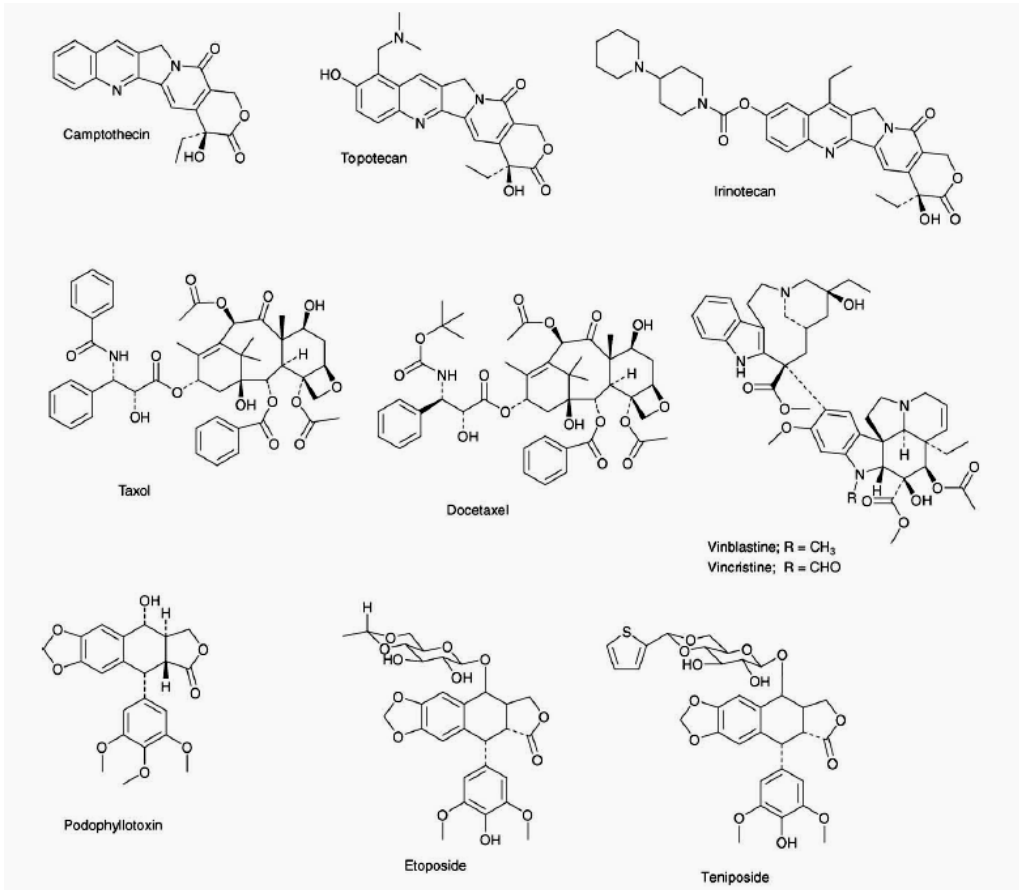


Figure 1.4 Plant-derived anticancer agents (From Cragg, G.M. and D.J. Newman, 2005)

1.4. AIM OF THIS WORK

The aim of this thesis was to perform phytochemical and pharmacological investigations on some promising plant extracts and to evaluate their potential in the treatment of cancer.

Indeed it is frequently observed that herbal medicinal products contain an array of active constituents that may have additive or even synergistic effects. In addition, many plant extracts contain inactive prodrugs, e.g. glycosides that are metabolically activated after oral intake, and result in a gradual release of the active constituents. Both aspects may contribute to reduced toxicity and a better pharmacological profile compared to conventional monotherapy. Since toxic side effects are quite often a limiting factor in chemotherapy, it is hypothesised in this thesis that herbal medicinal products may provide a valuable alternative approach for cancer treatment. Having this in mind, three plants species were selected in this project, i.e. *Steganotaenia araliacea* Hoechst., *Chelidonium majus* L. and *Gloriosa superba* L.

***Steganotaenia araliacea* Hoechst.** (Apiaceae) (**Chapter 3**) is known to contain antitumoural constituents, i.e. cytostatic lignans of which steganacin is the most promising compound. It has thoroughly been studied and compared to podophyllotoxin. Other lignans with similar though less pronounced antitumoural properties present in this plant are steganangin and steganone. Because of its traditional use, previous results on its antitumoural constituents such as the main product steganacin, and the presence of a range of related compounds, *Steganotaenia araliacea* was selected for this study.^[31-34]

***Gloriosa superba* L.** (Liliaceae) (**Chapter 4**) is used in traditional medicine in Asia (Ayurveda) and tropical Africa for several purposes, such as the treatment of gout, rheumatism, snake bites, intestinal worms, etc.^[35-39] The tubers contain colchicine, a well-known medicine against gout. The seeds of this plant even serve as a commercial source of this drug.^[40, 41] Colchicine has antimitotic properties and it has been used in the treatment of cancer. However, because of the low therapeutic index, it is not used as an anticancer drug anymore.^[42, 43] *Gloriosa superba* contains other, very similar alkaloids such as gloriosine, demethylcolchicine and the glycoside colchicoside.^[44-46] Because of the relatively high concentration of colchicoside^[47], a putative prodrug of active colchicine-like molecules, *Gloriosa superba* was selected in this

project, since it nicely fits in with our hypothesis of improving the pharmacological profile by the presence of prodrugs.

***Chelidonium majus* L.** (Papaveraceae) (**Chapter 5**) is a herb that is widely spread in Europe and is used in folk medicine against disorders of liver and bile and for treatment of warts. It contains interesting alkaloids and both the crude extract and its constituents have already shown antitumoural activity, though the pure compounds were often found too toxic for human use. Since 1991 the product Ukrain™ is commercially promoted and has appeared in different clinical trials. It is said to be a semi-synthetic derivative with a trimeric structure containing one thiophosphoric acid and three chelidonine molecules. However, chemical analyses rather concurred with a mixture of *Chelidonium* alkaloids and the trimeric structure has never been retrieved in the Ukrain™ product. Nevertheless, in addition to the many low-quality clinical trials that have been reported, some valid studies have shown promising antitumoural activity in the treatment of pancreatic cancer amongst others. The promising activity of Ukrain™ on the one hand and the ambiguous content of this expensive medicine on the other hand, were the reasons to investigate and evaluate *Chelidonium majus* extract.^[48-50]

The research that was envisaged in this project on the different plant extracts concerned:

- 1) Phytochemical characterisation, i.e. isolation and identification of the active constituents or prodrugs using chromatographic and spectroscopic techniques, focusing on the alkaloids from *Chelidonium majus* and *Gloriosa superba*, and the lignans from *Steganotaenia araliacea*;
- 2) Analytical method development and validation in order to produce standardised plant extracts with constant quality;
- 3) Preclinical *in vitro* and *in vivo* studies to determine the efficacy and toxicity of the plant extracts.

REFERENCES

1. International Agency for Research on Cancer (IARC) and Globocan. *Estimated Cancer Incidence, Mortality and Prevalence Worldwide in 2012*. [cited 17/09/2014]; Available from: http://globocan.iarc.fr/Pages/fact_sheets_cancer.aspx.
2. Stichting Kankerregister. *Cancer Prevalence in Belgium 2010*. [cited 17/09/2014]; Available from: http://www.kankerregister.org/media/docs/publications/PrevalenceinBelgium2010_e-book.pdf.
3. Jemal, A., F. Bray, M.M. Center, J. Ferlay, E. Ward, and D. Forman, *Global cancer statistics*. CA Cancer J Clin, 2011. 61(2): p. 69-90.
4. Ferlay, J., I. Soerjomataram, M. Ervik, R. Dikshit, S. Eser, C. Mathers, M. Rebelo, D. Parkin, D. Forman, and F. Bray. *GLOBOCAN 2012 v1.0, Cancer Incidence and Mortality Worldwide: IARC CancerBase No. 11 2013* [cited 17/09/2014]; Available from: <http://globocan.iarc.fr>.
5. World Health Organization (WHO). *Fact sheet N°297*. February 2014 Available from: <http://www.who.int/mediacentre/factsheets/fs297/en/>.
6. American Cancer Society, *Cancer Facts & Figures 2013*. American Cancer Society, 2013.
7. Hanahan, D. and R.A. Weinberg, *The hallmarks of cancer*. Cell, 2000. 100(1): p. 57-70.
8. Hanahan, D. and R.A. Weinberg, *Hallmarks of cancer: the next generation*. Cell, 2011. 144(5): p. 646-674.
9. Nelson, D. and M. Cox, *Lehninger, Principles of biochemistry*. 2005. p. 466.
10. National Cancer Institute. [cited 17/09/2014]; Available from: <http://www.cancer.gov/>.
11. American Cancer Society. *Chemotherapy principles*. [cited 17/09/2014]; Available from: <http://www.cancer.org/treatment>.

12. Nowak, D., D. Stewart, and H.P. Koeffler, *Differentiation therapy of leukemia: 3 decades of development*. Blood, 2009. 113(16): p. 3655-3665.
13. Efferth, T., *Cancer Therapy with Natural Products and Medicinal Plants*. Planta Medica, 2010. 76(11): p. 1035-1036.
14. World Health Organization, *WHO traditional medicine strategy 2014-2023*. 2014.
15. Gilani, A.H. and Atta-ur-Rahman, *Trends in ethnopharmacology*. Journal of Ethnopharmacology, 2005. 100(1-2): p. 43-49.
16. Ansari, J.A. and N.N. Inamdar, *The Promise of Traditional Medicines*. International Journal of Pharmacology, 2010. 6(6): p. 808-812.
17. Willcox, M.L. and G. Bodeker, *Traditional herbal medicines for malaria*. BMJ, 2004. 329(7475): p. 1156-1159.
18. Ph. Eur., *EUROPEAN PHARMACOPOEIA 8.0*. p. 744-746.
19. Fabricant, D.S. and N.R. Farnsworth, *The value of plants used in traditional medicine for drug discovery*. Environ Health Perspect, 2001. 109 Suppl 1: p. 69-75.
20. Efferth, T., *Personalized Cancer Medicine: From Molecular Diagnostics to Targeted Therapy with Natural Products*. Planta Medica, 2010. 76(11): p. 1143-1154.
21. Xu, Y.J., R. Capistrano, L. Dhooghe, K. Foubert, F. Lemiere, S. Maregesi, A. Balde, S. Apers, and L. Pieters, *Herbal medicines and infectious diseases: characterization by LC-SPE-NMR of some medicinal plant extracts used against malaria*. Planta Med, 2011. 77(11): p. 1139-1148.
22. Vlietinck, A., L. Pieters, and S. Apers, *Legal requirements for the quality of herbal substances and herbal preparations for the manufacturing of herbal medicinal products in the European union*. Planta Med, 2009. 75(7): p. 683-688.
23. McChesney, J.D., S.K. Venkataraman, and J.T. Henri, *Plant natural products: Back to the future or into extinction?* Phytochemistry, 2007. 68(14): p. 2015-2022.

24. Nobili, S., D. Lippi, E. Witort, M. Donnini, L. Bausi, E. Mini, and S. Capaccioli, *Natural compounds for cancer treatment and prevention*. Pharmacol Res, 2009. 59(6): p. 365-378.
25. da Rocha, A.B., R.M. Lopes, and G. Schwartzmann, *Natural products in anticancer therapy*. Curr Opin Pharmacol, 2001. 1(4): p. 364-369.
26. Escuin, D., E.R. Kline, and P. Giannakakou, *Both microtubule-stabilizing and microtubule-destabilizing drugs inhibit hypoxia-inducible factor-1alpha accumulation and activity by disrupting microtubule function*. Cancer Res, 2005. 65(19): p. 9021-9028.
27. Gurib-Fakim, A., *Medicinal plants: traditions of yesterday and drugs of tomorrow*. Mol Aspects Med, 2006. 27(1): p. 1-93.
28. Cragg, G.M. and D.J. Newman, *Plants as a source of anti-cancer agents*. J Ethnopharmacol, 2005. 100(1-2): p. 72-79.
29. Patrick, G., *An introduction to Medicinal Chemistry*. 2005. Third edition: p. 500-502.
30. Gewirtz, D.A., *A critical evaluation of the mechanisms of action proposed for the antitumor effects of the anthracycline antibiotics adriamycin and daunorubicin*. Biochem Pharmacol, 1999. 57(7): p. 727-741.
31. Kupchan, S.M., R.W. Britton, M.F. Ziegler, C.J. Gilmore, R.J. Restivo, and R.F. Bryan, *Tumor Inhibitors .80. Steganacin and Steganangin, Novel Antileukemic Lignan Lactones from Steganotaenia-Araliaceae*. Journal of the American Chemical Society, 1973. 95(4): p. 1335-1336.
32. Wickramaratne, D.B.M., T. Pengsuparp, W. Mar, H.B. Chai, T.E. Chagwedera, C.W.W. Beecher, N.R. Farnsworth, A.D. Kinghorn, J.M. Pezzuto, and G.A. Cordell, *Novel Antimitotic Dibenzocyclo-Octadiene Lignan Constituents of the Stem Bark of Steganotaenia-Araliaceae*. Journal of Natural Products, 1993. 56(12): p. 2083-2090.
33. Meragelman, K.M., T.C. McKee, and M.R. Boyd, *10-demethoxystegane, a new lignan from Steganotaenia araliacea*. Journal of Natural Products, 2001. 64(11): p. 1480-1482.

34. Sackett, D.L., *Podophyllotoxin, Steganacin and Combretastatin - Natural-Products That Bind at the Colchicine Site of Tubulin*. Pharmacology & Therapeutics, 1993. 59(2): p. 163-228.
35. Rajendran, K., P. Balaji, and M.J. Basu, *Medicinal plants and their utilization by villagers in southern districts of Tamil Nadu*. Indian Journal of Traditional Knowledge, 2008. 7(3): p. 417-420.
36. Samy, R.P., M.M. Thwin, P. Gopalakrishnakone, and S. Ignacimuthu, *Ethnobotanical survey of folk plants for the treatment of snakebites in Southern part of Tamilnadu, India*. Journal of Ethnopharmacology, 2008. 115(2): p. 302-312.
37. Kapoor LD, *CRC Handboek of Ayurvedic medicinal plants*. 1990, Florida: CRC press.
38. Nadkarni AK, *Indian Materia Medica*. 2002: Popular Prakashan Ltd.
39. Smith AC, *Flora Vitiensis nova: a new flora of Fiji*. Vol. 1. 1979, Kauai, Hawaii: National Tropical Botanical Garden.
40. Sarin, Y.K., P.S. Jamwal, B.K. Gupta, and C.K. Atal, *Colchicine from Seeds of Gloriosa-Superba*. Current Science, 1974. 43(3): p. 87-87.
41. Kannan, S., S.D. Wesley, A. Ruba, A.R. Rajalakshmi, and K. Kumaragurubaran, *Optimization of solvents for effective isolation of colchicines from Gloriosa superba L. seeds*. Natural Product Research, 2007. 21(5): p. 469-472.
42. Yue, Q.X., X.A. Liu, and D.A. Guo, *Microtubule-Binding Natural Products for Cancer Therapy*. Planta Medica, 2010. 76(11): p. 1037-1043.
43. Hastie, S.B., *Interactions of Colchicine with Tubulin*. Pharmacology & Therapeutics, 1991. 51(3): p. 377-401.
44. Canonica.L, B. Danieli, P. Manitto, G. Russo, and Bombarde.E, *New Alkaloids of Gloriosa Superba L*. Chimica & L Industria, 1967. 49(12): p. 1304.
45. Chaudhuri, P.K. and R.S. Thakur, *1,2-Didemethylcolchicine - a New Alkaloid from Gloriosa-Superba*. Journal of Natural Products, 1993. 56(7): p. 1174-1176.

46. Suri, O.P., B.D. Gupta, K.A. Suri, A.K. Sharma, and N.K. Satti, *A new glycoside, 3-O-demethylcolchicine-3-O-alpha-D-glucopyranoside, from Gloriosa superba seeds*. Natural Product Letters, 2001. 15(4): p. 217-219.
47. Poutaraud, A. and P. Girardin, *Influence of chemical characteristics of soil on mineral and alkaloid seed contents of Colchicum autumnale*. Environmental and Experimental Botany, 2005. 54(2): p. 101-108.
48. Colombo, M.L. and E. Bosisio, *Pharmacological activities of Chelidonium majus L (Papaveraceae)*. Pharmacological Research, 1996. 33(2): p. 127-134.
49. Sokoloff, B., Y. Takeuchi, C.C. Saelhof, and R. Powella, *Antitumor Factors Present in Chelidonium Majus L.I. Chelidonine + Protopine*. Growth, 1964. 28(3): p. 225-231.
50. Kim, H.K., N.R. Farnsworth, R.N. Blomster, and H.H.S. Fong, *Biological and Phytochemical Evaluation of Plants .V. Isolation of 2 Cytotoxic Alkaloids from Chelidonium Majus*. Journal of Pharmaceutical Sciences, 1969. 58(3): p. 372-374.

CHAPTER 2
GENERAL EXPERIMENTAL METHODS

2.1. CHROMATOGRAPHIC METHODS

2.1.1. Solvents and reagents

All solvents, including *n*-hexane, petroleum ether, ethyl acetate, isopropyl alcohol, absolute ethanol (99.99%) (EtOH), diethyl ether and methylene chloride were purchased from Acros Organics (Geel, Belgium) or from Fisher Scientific (Leicestershire, UK) and were at least analytical grade. All reagents, such as trifluoroacetic acid (TFA), glacial acetic acid, phosphoric acid, sulphuric acid ($\geq 95\%$), potassium dihydrogen phosphate, formic acid, dimethyl sulfoxide (DMSO), hydrochloric acid (25%), ammonia (25%), *n*-heptanesulfonic acid and ammonium formate were purchased from Acros Organics or Sigma-Aldrich (St. Louis, MO, USA). Solvents used for HPLC, i.e. methanol (MeOH) and acetonitrile were HPLC grade and purchased from Fisher Scientific. RiOS water was prepared by reverse osmosis and water for HPLC was dispensed by a *Milli-Q* system from Millipore (Bedford, MA, USA) and passed through a 0.22 μm membrane filter. The reference materials, colchicine (97%), chelidone (99.2%), sanguinarine (98%), chelerythrine (97%), protopine (100%) and gemcitabine (100%) were purchased from Sigma-Aldrich. Berberine (97.5%) was purchased from Alfa Aesar, Karlsruhe, Germany.

2.1.2. Thin layer chromatography

Analytical plates for thin layer chromatography (TLC) were purchased from Merck (Darmstadt, Germany). Silica gel 60 F₂₅₄ plates (20 x 20 cm) were used for normal phase (NP) TLC and silica gel 60 RP-18 F₂₅₄ plates (10 x 20 cm) for reverse phase (RP) TLC. The spraying reagent *p*-anisaldehyde was prepared by mixing 0.5 mL *p*-anisaldehyde (Sigma, St. Louis, MO, USA) with 10 mL glacial acetic acid, 85 mL methanol and 5 mL sulphuric acid.

2.1.3. Flash column chromatography

Flash column chromatography was carried out on a Reveleris® iES system from Grace (Columbia, MD, USA) using the Reveleris® *Navigator*TM software. The system consists of a binary pump with four solvent selection, an ultraviolet (UV) and evaporating light scattering

detector (ELSD) and a fraction collector with two trays of 96 tubes. The column used was a pre-packed Flash Grace Reveleris® silica cartridge with a particle size of 40 µm. Detection and collection were based on UV and ELSD. The ELSD carrier solvent was isopropyl alcohol.

2.1.4. **High performance liquid chromatography**

Two high performance liquid chromatography (HPLC) systems were used: an Agilent 1200 series and an Agilent 1260 series both with degasser, quaternary pump, automatic injection sampler, thermostatic column compartment and a diode array detector (DAD) (Agilent Technologies, Eindhoven, The Netherlands). Different silica-based columns were used such as GraceSmart C₁₈ and Apollo C₁₈ (250 x 4.6 mm, 5 µm) (Grace, Columbia, MD, USA), a Phenomenex Luna C₁₈ (2) (250 x 4.6 mm, 5 µm) (Phenomenex, Torrance, CA, USA) and Licrosphere 100 RP-18e (250 x 4.6 mm, 5 µm) (Merck, Darmstadt, Germany). A suitable precolumn was also installed to endure the lifetime of the columns.

2.1.5. **High performance liquid chromatography – Solid phase extraction – Nuclear magnetic resonance spectroscopy**

Liquid Chromatography – Solid Phase Extraction – Nuclear Magnetic Resonance spectroscopy or in short LC-SPE-NMR is an hyphenated technique combining a chromatographic (HPLC) and a spectroscopic NMR system, as well as an SPE system that allows the enrichment of collected compounds. The HPLC compartment consisted of an Agilent 1200 series with degasser, quaternary pump, automatic injection sampler and an UV/VIS detection (variable wavelength) (Agilent Technologies, Eindhoven, the Netherlands). The HPLC is connected to a Bruker/Spark solid phase extraction (SPE) system with HySphere Resin General Phase (GP) cartridges (polydivinyl-benzene material with particle size 5 - 15 µm) to capture and collect the compounds. After the detector, water is added to the eluent stream with a make-up pump (Knauer K 120, Berlin, Germany), to decrease the organic solvent proportion of the elution and to promote better retention of the peaks on the SPE cartridges and this at a flow rate of 3 times higher than the flow rate used during chromatographic analysis. By applying multiple trapping the same compounds were repeatedly captured on the same cartridges. The solvent residues were removed by drying the cartridges with nitrogen gas (N₂). With the Gilson Liquid

Handler 125 the compounds were eluted with deuterated solvents into NMR tubes. Two different silica-based columns were used such as GraceSmart C₁₈ and Apollo C₁₈ (250 x 4.6 mm, 5 μm). A suitable precolumn was also installed to endure the lifetime of the columns.

2.1.6. **Semi-preparative high performance liquid chromatography**

A semi-preparative HPLC (Waters, Milford, MA, USA) with a binary pump, automatic injection sampler, photo diode array detector, triple quadrupole mass spectrometer (TQD-MS) and an automatic fraction collector was used to isolate reference material. A Phenomenex Luna 5 μm C₁₈ (2) 100 Å column with larger internal diameter (250 x 10 mm) was used.

2.2. SPECTROSCOPIC METHODS

2.2.1. **Nuclear magnetic resonance spectroscopy**

Nuclear magnetic resonance (NMR) spectra were recorded on a Bruker DRX-400 instrument (Rheinstetten, Germany), operating at 400 MHz for ¹H and at 100 MHz for ¹³C, employing a 3-mm broadband inverse (BBI) probe or a 5-mm dual ¹H/¹³C probe using standard Bruker pulse sequences. Distortionless enhancement by polarisation transfer spectra (DEPT-135 and DEPT-90) were also recorded. Chemical shifts are given in ppm and coupling constants (*J*) in Hz. The multiplicity is indicated as s for singlet, d for doublet, dd for doublet of doublets, t for triplet and m for multiplet. Not only ¹H and ¹³C spectra were recorded, but sometimes two-dimensional NMR experiments (2D NMR) were necessary in order to elucidate the structure of the compounds. In that case correlation spectroscopy (COSY) experiments for ¹H - ¹H correlations, heteronuclear single quantum coherence (HSQC) for direct ¹H - ¹³C correlations and heteronuclear multiple bond correlation (HMBC) for indirect ¹H - ¹³C correlations were recorded. In order to assist structure elucidation a ¹³C NMR library was used (NMR Predict version 4.8.57 Modgraph). Deuterated solvents including CDCl₃ (99.8% D), DMSO-d₆ (99.9% D), CD₃OD (99.8%D) and CD₃CN (99.8% D) were purchased from Sigma-Aldrich.

2.2.2. Mass spectrometry

An Acquity ultra performance liquid chromatography (UPLC) system, consisting of an autosampler and a binary pump (Waters, Milford, MA, USA) equipped with a 10 μ L loop was used. The UPLC system was coupled to a triple quadrupole mass spectrometer (Waters, Milford, MA, USA) equipped with an electrospray ionisation (ESI) source operated in the positive ion mode to record the mass spectrum of the individual compounds. MS conditions were as follows: capillary voltage 3.4 kV, extractor voltage 2 V, cone voltage 30 V, source temperature 150 $^{\circ}$ C, desolvation temperature 450 $^{\circ}$ C, RF lens 0.1 V, desolvation gas flow 950 L/h, cone gas flow 50 L/h. Compounds were separated on an Acquity HSS C₁₈ column (2.1 x 100 mm, 1.8 μ m) also from Waters. The column was maintained at a temperature of 30 $^{\circ}$ C. The flow rate was set at 0.5 mL and the mobile phases were (A) water and (B) acetonitrile. The used gradient was 0 min, 10% B; 1 min, 10% B; 5 min, 40% B; 7.5 min, 100% B; 10 min, 100% B and 2.5 μ L was injected using partial loop with needle overfill injection. All data were recorded and processed using Masslynx software, version 4.1 (Waters).

High resolution mass spectra were obtained with an Agilent 6530 quadrupole-time-of-flight mass spectrometer (QTOF-MS) equipped with an Agilent Jetstream source that was used with the following parameters: gas temperature 325 $^{\circ}$ C, gas flow 7 L/min, nebuliser pressure 40 psi, sheath gas temperature 325 $^{\circ}$ C, sheath gas flow 11 L/min. Capillary, fragmentor, and skimmer voltages were set to 3500 V, 150 V, and 65 V, respectively and the OCT 1 RF V_{pp} was set at 750 V. The mass spectrometer was operated in the positive and negative ion mode at 20000 resolution. The instrument was calibrated and tuned with a tune mix (G1969-85000) and during acquisition the accuracy was monitored by using an ES-TOF reference mass solution kit (G1969-85001) from Agilent. The Mass Hunter (Agilent Technologies) software was used for data acquisition and processing.

2.2.3. Optical rotation

The specific optical rotation was determined on a Jasco P-2000 Polarimeter. The samples were dissolved in methanol and the optical rotation was recorded at 589 nm with a path length of 50 mm.

2.3. BIOLOGICAL METHODS

2.3.1. Media and reagents

All cell culture reagents and media were purchased from Life Technologies (Ghent, Belgium). All cell lines were maintained at 37 °C and 5% CO₂/95% air in a humidified incubator. All other reagents, including sulforhodamine B, tris(hydroxymethyl)aminomethane (tris) and trichloroacetic acid were purchased from Sigma-Aldrich or Acros Organics.

2.3.2. Cell line & culture

Malignant human cell lines of different origin (breast, pancreas and colon) were used for the *in vitro* cytotoxicity assessments. The breast cancer cell line that was used was the MDA-MB-231 cell line. These are breast adenocarcinoma cells that were isolated from a pleural effusion of a cancer patient in 1973.^[1] These cells form loosely cohesive grape-like or stellate structures consistent with the more invasive phenotype, therefore these cells are regarded as invasive *in vitro*.^[2] The second human cancer cell line that was used was the pancreatic epithelioid carcinoma (PANC-1) cells. They were cultured from a 56-year-old male with an adenocarcinoma in the head of the pancreas which invaded the duodenal wall^[3] and the colorectal adenocarcinoma cells (HT-29) was isolated from a primary tumour in 1964 by J. Fogh using the explant culture method.^[4] MDA-MB-231 cells were cultured in RPMI 1640 medium enriched with 10% foetal bovine serum (FBS), 1% L-glutamine, 1% sodium pyruvate and 1% penicillin/streptomycin. PANC-1 and HT-29 cells were cultured in DMEM also supplemented with 10% FBS, 1% L-glutamine and 1% penicillin/streptomycin. Two normal cell lines were also used to investigate the cytotoxicity of the crude extract. Human bronchial epithelial cells (BEAS-2B) were cultured in bronchial epithelial cell growth medium (BEGM) and the mouse fibroblast (3T3) were cultured in DMEM with all the supplements mentioned above. All previous mentioned cell lines were obtained from the American type culture collection (ATCC).

Primary endometrial cancer cell cultures (PC-EM005 and PC-EM002) were also tested and established from patients undergoing surgery at the Division of Gynaecologic Oncology,

University Hospital Gasthuisberg, Leuven (Belgium). Only after informed consent, patients were included in the study. Tumour samples were placed into sterile RPMI 1640 medium supplemented with penicillin/streptomycin (1000 U/mL) and fungizone (0.5 µg/mL) for transport from the surgery room to the cell culture laboratory. Tumour tissue was subsequently washed with phosphate-buffered saline solution (PBS) supplemented with penicillin/streptomycin and fungizone, and tissue was minced with sterile blades. Tumour tissue was digested with collagenases type IV (1 mg/mL; Roche) in RPMI 1640 medium supplemented with penicillin/streptomycin and fungizone. Also DNase I (0.1 mg/mL; Roche) was added to the digestion medium. Digestion was performed while shaking for 3 h at 37 °C. Thereafter, single cell suspension was prepared by filtration through a 70 µm filter and red blood cells were lysed using ammonium chloride solution (Stem Cell Technologies). Single cells were finally plated into a 25 cm² culture flask and medium was changed the day after. After 1 - 3 weeks, when cells reached 60 - 70% confluency, fibroblasts were removed using mouse anti-human CD90 (Clone AS02; Dianova) and negative selection with Mouse Pan IgG Dynabeads (Life Technologies). Afterwards the cells were cultured in RPMI 1640 medium with all the supplements described above.

The murine pancreatic adenocarcinoma cells (PANC02) were a kind gift from Prof. Dr. C. Gravekamp (Albert Einstein College of Medicine, New York, USA) and were cultured in RPMI 1640 medium supplemented with 10% FBS, 1% L-glutamine, 1% sodium pyruvate and 1% penicillin/streptomycin.

2.3.3. Sulforhodamine B assay

The sulforhodamine B (SRB) assay was performed at the Centre for Oncological Research (CORE) of the University of Antwerp. The SRB assay is a colorimetric assay used for cell density determination, based on the measurements of cellular protein content. It is used to measure drug-induced cytotoxicity. The SRB assay was performed according to the method of Papazisis et al, with minor modification.^[5] Cells were harvested from exponential phase cultures by trypsinisation and counted with the Scepter™ 2.0 (Merck Millipore, Darmstadt, Germany), which is an automated cell counter based on the Coulter principle. Optimal seeding densities were determined to ensure exponential growth and were incubation time and cell line dependant. Table 2.1 shows the used cell density per cell line and incubation time. In each experiment 7 different concentrations of plant extract were tested on the different cell lines and 6 replicate wells per concentration were used. Two different incubation times were evaluated, i.e. 24 h and 72 h. The stock solution was prepared by dissolving the plant extracts in sterile water and by passing the solution through a 0.22 µm filter. After incubation, culture media was removed prior to fixation, which was done by adding 200 µL of 10% cold trichloroacetic acid onto the cells. After one hour at 4 °C, the cells were washed five times with deionised water. The cells were then stained with 200 µL 0.1% SRB in 1% acetic acid for 15 min at room temperature. To remove the unbound stain the cells were washed with 1% acetic acid four times. The plates were left to dry at room temperature. The protein-bound stain was re-dissolved with 200 µL 10 mM unbuffered tris and transferred to 96-well plates for the optical density (OD) reading at 540 nm (Biorad 550 microplate reader and iMark Microplate Absorbance Reader, Nazareth, Belgium).

Table 2.1 Cell density per cell line and incubation time

Cell lines	Cell density (cells/well)	
	24 h	72 h
MDA-MB-231	4000	3200
PANC-1	3000	3000
HT-29	4500	3500
PANC02	500	500

2.3.4. **Neutral red assay**

The neutral red (NR) assay was only used for the cytotoxicity determination on the BEAS-2B cells. This experiment was performed by VITO NV in Mol (Belgium). BEAS-2B cells were seeded in 96-well plates (6400 cells/well suspended in 200 μ L growth medium). After 48 h of incubation, wells were exposed to a concentration range (7 concentrations) of the crude extract for 24 h (6 replicate wells per concentration). After incubation, neutral red staining solution (1% dissolved in growth medium) was added to the cells and incubated for 2 h. Cells were subsequently washed with PBS. Neutral red was extracted from the cells by adding 200 μ L of 10% acetic acid in ethanol to each well. The optical density was measured at 540 nm using a spectrophotometer. Cell viability inhibition was calculated relative to solvent control.

2.3.5. ***xCELLigence* Real-Time Cell Analysis**

Experiments carried out on the endometrial cell lines and the mouse fibroblast cells were performed using the *xCELLigence* Real-Time Cell Analysis (RTCA) DP instrument (Roche Diagnostics GmbH, Mannheim, Germany) at the Division of Gynaecologic Oncology, Department of Oncology at KU Leuven. Cell proliferation and cytotoxicity experiments were performed using modified 16-well plates (E-plate, Roche Diagnostics GmbH, Mannheim, Germany) that were placed in the RTCA DP instrument which was kept in a humidified incubator at 37 °C and 5% CO₂/95% air. Microelectrodes were attached at the bottom of the wells for impedance-based detection of attachment, spreading and proliferation of the cells. Initially, 100 μ L growth medium was added to the wells. After leaving the plates at room temperature for 30 min, the background impedance for each well was measured. Cells were harvested from exponential phase cultures by trypsinisation with 0.05% Trypsin-EDTA and counted by using a Fuchs Rosenthal Counting Chamber. In every well 100 μ L (5000 cells/well for the PC-EM005 and PC-EM002 cell lines, 2000 cells/well for the 3T3 cell line) of the cell suspension was seeded. Water was added to the space surrounding the wells of the E-plate to avoid evaporation from media out of the wells. After leaving the plates at room temperature for 30 min to allow cell attachment, in accordance with the manufacturer's guidelines, they were locked in the RTCA DP device in the incubator. The impedance value of each well was

automatically monitored by the *xCELLigence* system and expressed as a cell index value (CI). For the cytotoxicity experiments, CI was monitored every 5 or 15 min with the *xCELLigence* system. Twenty-four hours after cell seeding, cells were treated during 48 h with the crude extract at five different concentrations in triplicate. PBS was added to control wells also in triplicate.

2.3.6. Calculation of the IC₅₀ values

For the SRB assay, the survival percentages of the cells were calculated from the optical density readings as: (mean OD of treated cells/mean OD of control cells) x 100%. These survival percentages were then fitted in a curve. The concentration of the crude extract causing 50% of growth inhibition (IC₅₀) was then determined by non-linear regression analysis of the data with the WinNonlin® software (Pharsight, St. Louis, MO, USA)

For the RTCA system, the impedance value of each well was automatically monitored by the *xCELLigence* system in real-time and expressed as CI. A real-time plot of the *xCELLigence* experiment is then graphed by the system and after normalisation of the CI, a dose-response curve was plotted and the IC₅₀ value was calculated. The endpoint that was selected to calculate the IC₅₀ value was approximately 48 h after addition of the crude extract.

REFERENCES

1. Brinkley, B.R., P.T. Beall, L.J. Wible, M.L. Mace, D.S. Turner, and R.M. Cailleau, *Variations in cell form and cytoskeleton in human breast carcinoma cells in vitro*. *Cancer Res*, 1980. 40(9): p. 3118-3129.
2. Holliday, D.L. and V. Speirs, *Choosing the right cell line for breast cancer research*. *Breast Cancer Res*, 2011. 13(4): p. 215.
3. Deer, E.L., J. Gonzalez-Hernandez, J.D. Coursen, J.E. Shea, J. Ngatia, C.L. Scaife, M.A. Firpo, and S.J. Mulvihill, *Phenotype and genotype of pancreatic cancer cell lines*. *Pancreas*, 2010. 39(4): p. 425-435.
4. Fogh, J., J.M. Fogh, and T. Orfeo, *127 Cultured Human Tumor-Cell Lines Producing Tumors in Nude Mice*. *Journal of the National Cancer Institute*, 1977. 59(1): p. 221-226.
5. Papazisis, K.T., G.D. Geromichalos, K.A. Dimitriadis, and A.H. Kortsaris, *Optimization of the sulforhodamine B colorimetric assay*. *Journal of Immunological Methods*, 1997. 208(2): p. 151-158.

CHAPTER 3

STEGANOTAENIA ARALIACEA

3.1. INTRODUCTION

Steganotaenia araliacea Hochst., also known as carrot tree or cabbage tree, belongs to the family of the Apiaceae (Figure 3.1). It is a small soft-wooded, sparsely branched, deciduous tree or shrub with thick bark. The leaves are pinnate and crowded towards the branch ends. The leaflets are 2 - 3 pairs on a leaf stalk, ovate and margin toothed. The leaf stalk is about 10 cm long with an expanded base around the stem. The flowers are small, yellowish brown and are in rounded compound clusters at twig ends. The fruits are cream-brown, dehiscent, flat and heart shaped.^[1, 2] The plant occurs over a wide range of altitude, but is abundant in low-altitude woodland or on rocky outcrops.^[2]



Figure 3.1 *Steganotaenia araliacea* Hochst.

S. araliacea is widely spread in tropical Africa (Figure 3.2) and it is often used in Eastern Uganda, Eastern Somalia and Cameroon for the treatment of diarrhoea, oedema, malaria, helminth and wound infections.^[3] The extract of the stem bark also exhibited diuretic and antibacterial properties. In South Africa the root is used for the treatment of headache and snake bites, and the tree trunk has been reported to show snake deterring activity. The scented leaves are used as vermifuge in Sierra Leone, as ophthalmic lotion in Democratic Republic of Congo, and as an anticonvulsant in Gambia.^[1, 4] The leaves are also rubbed on wounds as general disinfectant.^[2] The extract of *S. araliacea* showed intermediate toxicity against the highly pathogenic parasite *Strongyloides papillosus*.^[5]

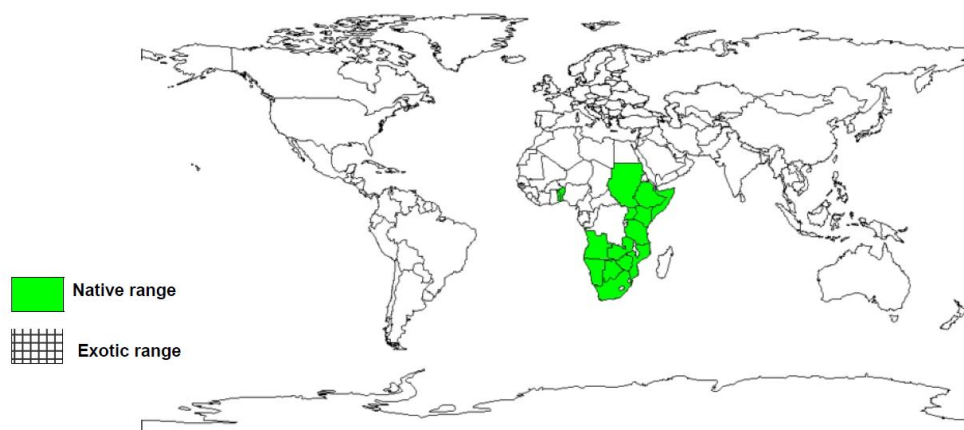


Figure 3.2 Distribution of *S. araliacea* (From Orwa et al., 2009)

S. araliacea has been studied for its biologically active dibenzocyclo-octadiene lactone lignans and their analogues. Steganangin and steganacin were isolated from the stem bark and stem wood and found to exhibit significant antileukaemic activity in the *in vivo* murine P-388 lymphocytic leukaemia test system (Figure 3.3).^[6] *In vitro* it has been shown that steganacin inhibited the assembly of tubulin into microtubules by interacting with the colchicine binding site.^[7, 8] In the study of Wickramaratne et al. six constituents were isolated from the stem bark. Three new compounds, i.e. episteganangine, steganoate A and steganoate B and three known compounds, i.e. steganacin, steganangin and steganolide A were found. All of these lignans

demonstrated cytotoxic activity when tested against a panel of eleven human tumour cell lines, with the exception of steganoate A.^[9]

The organic extract of *S. araliacea* also showed cytotoxic activity in the NCI screening program. This led to the isolation of 10-demethoxystegane by means of bioassay-guided purification together with steganone and prestegane B. These three isolated compounds were tested against ovarian (OVCAR-3) and colon (COLO-205) cancer cells, but only steganone showed activity against OVCAR-3 and COLO-205.^[10]

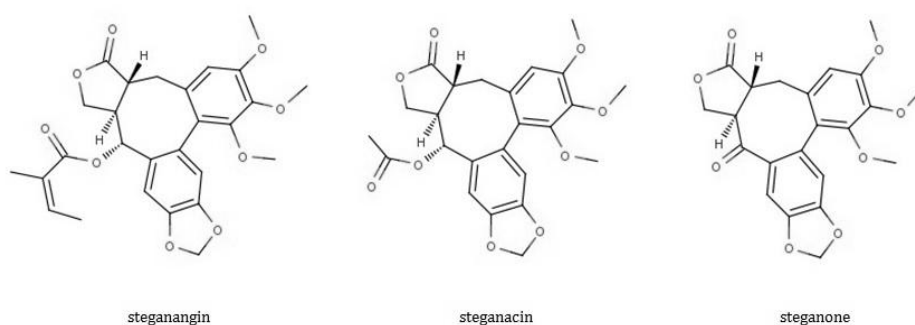


Figure 3.3 Lignans isolated from *S. araliacea* (From Wickramaratne et al., 1993)

Aside from the lignans found in the bark, saponins with steganogenin as aglycon have been isolated and identified from the leaves. Also the composition of the essential oil has been studied.^[11] Moudachirou et al. investigated the leaf oil from plants harvested in different areas of Benin and Togo by means of GC-MS. More than 20 constituents were identified and the main compounds were limonene, β -phellandrene, sabinene, β -caryophyllene and cryptone.^[12] In a study of Noudjou et al. more than 20 major compounds have also been identified by GC-MS analysis in the essential oil of leaflets from Cameroon. This oil was found to contain a high percentage of monoterpene hydrocarbons, mainly represented by limonene, α -pinene and β -pinene. Also sesquiterpene hydrocarbons, such as γ -elemene, ar-curcumene and β -caryophyllene, were identified.^[13]

3.2. PHYTOCHEMICAL INVESTIGATION

3.2.1. Plant material

The stem bark of *Steganotaenia araliacea* Hochst. (Figure 3.4) was collected on 15/7/2010 and 25/11/2010 in Tountouroun (prefecture of Labé, Guinea-Conakry) and identified by Prof. Aliou Baldé from the Department of Pharmacy, University Gamal Abdel Nasser of Conakry, Guinea, and Research and Valorization Center on Medicinal Plants, Dubreka, Guinea, where a voucher specimen (n° 7HK1) was deposited. The material was dried in the shade in open air to reduce deterioration of the plant material.



Figure 3.4 *Steganotaenia araliacea* stem bark

3.2.2. Extraction

The air-dried stem bark was ground and 2.85 kg was exhaustively and consecutively extracted with 20 L of 80% ethanol. The ethanol was removed under reduced pressure at 40 °C and the aqueous extract was lyophilised, yielding 140 g of dried crude extract (SA).

3.2.3. Liquid-liquid partition

A first raw separation of the crude extract was performed by liquid-liquid partition. Approximately 2 g of crude extract (SA) was dissolved in 100 mL MeOH 90%. The partition was performed according to the method used by Wickramaratne et al., with minor modification.^[9] The scheme is shown in Figure 3.5. The dissolved SA was extracted three times with 100 mL petroleum ether (PE). Both fractions were dried under reduced pressure at 40 °C. This first extraction step yielded 0.16 g petroleum ether fraction (SA1A) and 1.28 g methanolic fraction (SA1B). About 1.05 g SA1B was then dissolved in 100 mL water and extracted three times with 100 mL ethyl acetate (EtOAc). The EtOAc fraction (SA2A) was dried under reduce pressure at 40 °C and yielded 0.30 g. The aqueous fraction (SA2B) was lyophilised and yielded 0.61 g.

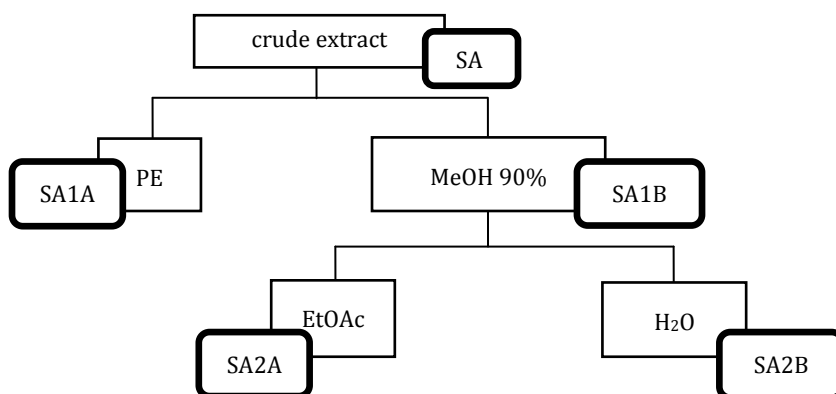


Figure 3.5 Liquid-liquid partition scheme

3.2.4. Thin layer chromatography

The different fractions were subjected to TLC (NP and RP). About 5 mg/mL solutions were prepared of all fractions and 10 µL was applied as a band of 5 mm and developed over a path of 8 cm using a mixture of 75% methylene chloride, 20% *n*-hexane and 5% methanol as mobile phase. The TLC plates were examined at a wavelength of 254 nm and 366 nm. The developed plates were also sprayed with the *p*-anisaldehyde reagent and heated at a temperature of 105 °C until maximal visualisation. The TLC profile (Figure 3.6) of the SA

fractions shows concentrated zones for SA1A, but because the lipids and waxes were expected to be found in this fraction, it was not selected for further purification. The main components of the SA extract were obviously concentrated in fraction SA2A. Therefore fraction SA2A was selected for further phytochemical analysis.

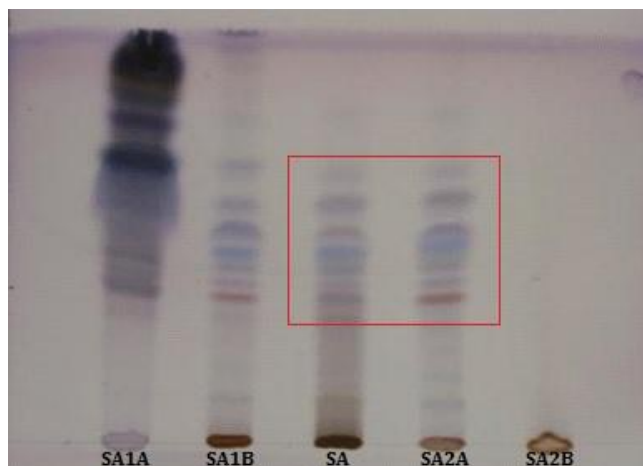


Figure 3.6 NP-TLC profile of SA and fractions, sprayed with *p*-anisaldehyde

3.2.5. Flash column chromatography

The SA2A fraction was then subjected to flash column chromatography for further fractionation. About 0.23 g was dissolved in 2.5 mL methanol and mixed with 0.5 g silica. This silica-sample mixture was dried with N₂ and loaded onto the silica column. The column used was a pre-packed Flash Grace Reveleris® silica cartridge of 12 g and a gradient from methylene chloride to ethyl acetate, followed by methanol was used to elute compounds from the column. The detection and collection were based on UV and ELSD. Two different UV wavelengths were used, i.e. 230 nm and 300 nm and the threshold was set at 0.05 AU. The ELSD carrier solvent was isopropyl alcohol and the threshold was set at 20 mV.

After flash chromatography the obtained subfractions were evaluated with NP-TLC and similar TLC-profiles were pooled resulting in 26 subfractions.

3.2.6. Isolation by means of LC-SPE-NMR

HPLC chromatograms were recorded for all obtained subfractions, as well as the SA2A fraction and the crude extract. The samples were prepared with a concentration ranging from 0.4 – 14.6 mg/mL in methanol. Twenty microliter of each sample was injected into the LC-SPE-NMR and with the use of the Apollo column, the compounds were separated. The mobile phases were (A) water + 0.05% TFA and (B) methanol. The gradient was 0 min, 5% B; 5 min, 5% B; 55 min, 100% B; 60 min, 100% B. The flow rate was 1 mL/min and the chromatograms were recorded at 230 nm. The chromatogram from SA2A (Figure 3.7) showed three major separated peaks with retention time 32.8, 34.0 and 34.6 min. The peak with a retention time of 26.0 min was found to be a mixture of minor compounds that have not been identified. Subfraction SA2A_10 (Figure 3.8) contained two major peaks, **SA2A_10A** and **SA2A_10B** with retention time 32.8 and 34.6 min, respectively. Subfraction SA2A_17 (Figure 3.9) showed one major peak, **SA2A_17A**, with retention time 34.0 min. These three peaks corresponded with the major peaks in fraction SA2A and therefore these compounds were isolated and identified by means of LC-SPE-NMR.

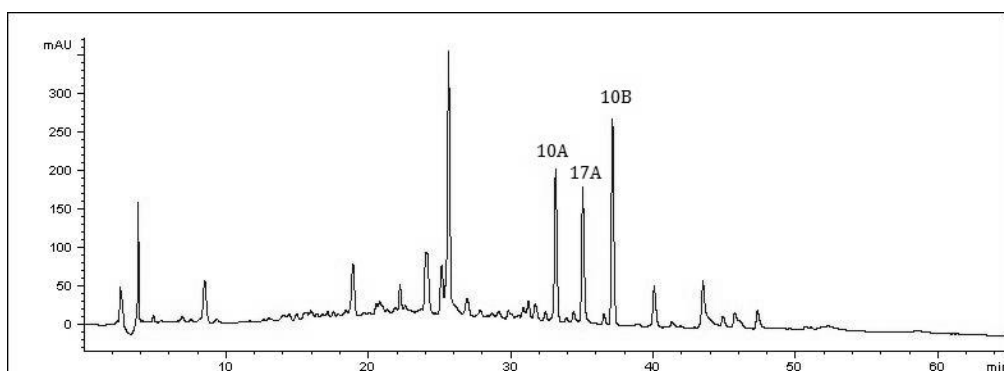


Figure 3.7 Chromatogram of fraction SA2A

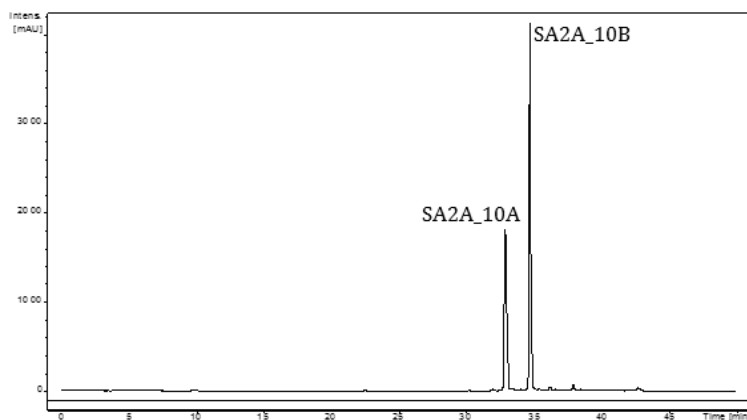


Figure 3.8 Chromatogram of subfraction SA2A_10

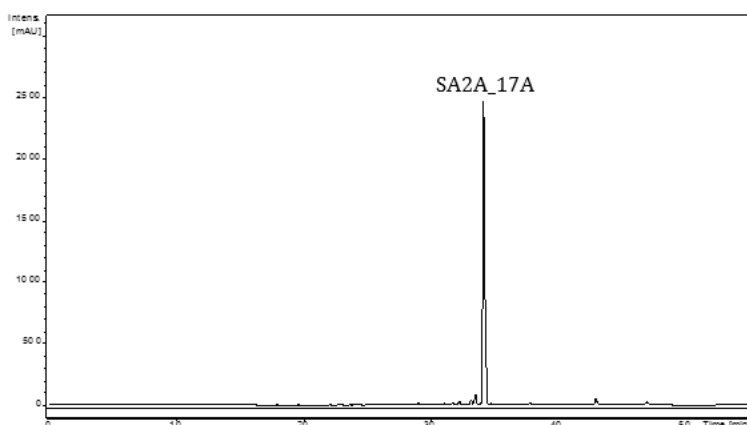


Figure 3.9 Chromatogram of subfraction SA2A_17

For the isolation of **compound SA2A_10A** and **SA2A_10B**, a concentrated solution (5.9 mg/mL) of subfraction SA2A_10 was used and 20 μ L of this solution was injected. The flow rate was set at 1.0 mL/min and the detector at 230 nm. Mobile phase A was water containing TFA (0.05%) and B was acetonitrile. The gradient was adjusted to shorten the run time, thus lowering the solvent consumption. The adjusted gradient was 0 min, 45% B; 5 min, 45% B; 25

min, 68 % B; 27.5 min, 100% B and 32.5 min, 100% B. Nineteen multiple trappings were performed and the two compounds were trapped automatically on the HySphere resin GP cartridges by setting a threshold. The cartridges were then dried with N₂ to remove all residual solvents and the compounds were eluted with deuterated acetonitrile (99.8% atom D) in 3 mm NMR tubes.

For the isolation of **compound SA2A_17A**, a concentrated solution (6.0 mg/mL) of subfraction SA2A_17 was used and 10 µL of this solution was injected. The flow rate and wavelength were the same as above as well as the mobile phases. The gradient was again adjusted to shorten the run time and the used gradient was 0 min, 45% B; 5 min, 45% B; 20 min, 63 % B; 22.5 min, 100% B and 27.5 min, 100% B. Thirty-six multiple trappings were performed and compound SA2A_17A was repeatedly trapped on a cartridge by setting a threshold. The cartridge was then dried with N₂ and the compound was eluted with deuterated acetonitrile in 3 mm NMR tubes.

The ¹H NMR and ¹³C NMR spectra were then recorded for all compounds as well as 2D NMR spectra (COSY, HSQC and HMBC).

3.2.7. Structure elucidation

The structures of the isolated compounds were elucidated mainly by NMR spectroscopy, and confirmed by mass spectrometry.

3.2.7.1. Spiroreussomerin A

The structure of compound SA2A_10A was elucidated by ^1H , ^{13}C (also DEPT-135, DEPT-90) and 2D NMR (COSY, HSQC and HMBC) as **spiroreussomerin A** (Figure 3.10).

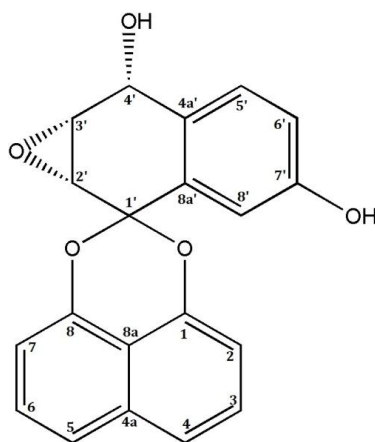


Figure 3.10 Structure of compound SA2A_10A (spiroreussomerin A)

Library search on the ^{13}C NMR data (Table 3.1 and Figure 3.11Figure 3.12) suggested this compound to be a deoxyreussomerin analogue and the data were compared with data found in the literature.^[14] Analysis of the ^1H (Table 3.1 and Figure 3.12) and COSY (Figure 3.13) spectra showed two isolated three proton spin systems 7.07 (H-2), 7.53 (H-3), 7.61 (H-4) ppm and 7.59 (H-5), 7.47 (H-6), 6.94 (H-7) ppm that corresponded to 110.5 (C-2), 129.0 (C-3), 122.0 (C-4), 121.9 (C-5), 128.9 (C-6) and 110.0 (C-6) ppm subunits in the HSQC spectrum (Figure 3.14). HMBC correlations (Figure 3.15) of H-4 and H-5 with two quaternary carbons, C-4a and C-8a, as well as correlations of H-2 and H-3 with C-1, and H-6 and H-7 with C-8, indicated that the subunits C-1 to C-4 and C-5 to C-8 were attached at C-4a and C-8a, leading to the identification of a naphthalene moiety. The chemical shifts of C-1 and C-8 (148.6 ppm)

suggested a 1,8-dioxynaphthalene. The signal at 98.9 ppm suggested an acetal carbon (C-1'). In addition, a three proton spin system with signals at 3.65 (d, $J = 4.0$ Hz, H-2'), 3.53 (dd, $J = 4.0$ and 2.4 Hz, H-3'), and 5.49 ppm (d, $J = 5.4$ Hz, H-4') was observed in the ^1H NMR spectrum and confirmed by the COSY. The chemical shifts in the ^1H and ^{13}C NMR spectra, 51.4 (C-2'), 54.3 (C-3'), and 61.5 (C-4') ppm indicated epoxidation between C-2' and C-3' and an hydroxyl group (3.74 ppm) at C-4'. The HMBC correlations of H-5' (7.29, d, $J = 2.7$ Hz) to C-6' (117.8 ppm) and C-7' (156.3 ppm), H-6' (6.99, dd, $J = 5.8$ and 2.7 Hz) to C-7' and C-8' (119.0 ppm), and H-8' (7.27, s) to C-8a' (133.6 ppm), and C-1', as well as H-2' to C-1' and C-8a' (133.6 ppm), H-3' to C-4a' (135.4 ppm), and H-4' to C-8a', revealed that C-1' to C-4' and C-5' to C-8' subunits were attached at C-4a' and C-8a', forming a decalin fragment, with C-1' as a spiro center between the decalin and 1,8-dioxynaphthalene moieties. The chemical shift of C-7' and the proton signal at 8.02 ppm suggested an hydroxyl group at position 7'. The relative configuration of compound SA2A_10A was proposed by analogy with data found in the literature for spiropreussomerin A. ^1H and ^{13}C NMR assignments were in agreement with those reported in CDCl_3 by Chen et al.^[14] Spiropreussomerin A was first obtained from a liquid culture of *Preussia* sp., an endophytic fungus isolated from a mature stem of *Aquilaria sinensis* (Lour.) Gilg (Thymelaeaceae). It belongs to the spirobisanaphthalenes, a series of fungal secondary metabolites consisting of a 1,8-dihydroxynaphthalene-derived spiroketal unit linked to a second, oxidised naphthalene moiety. The possibility that spiropreussomerin A isolated in this work originates from an endophytic fungus in *Steganotaenia araliacea* can therefore not be excluded.^[14]

The UV spectrum showed UV absorption maxima at 226 and 288 nm and the high resolution mass spectrum was recorded showing a pseudo molecular ion $[\text{M} - \text{H}]^-$ with m/z 333.0779 (calculated m/z 333.0763) consistent with a molecular formula of $\text{C}_{20}\text{H}_{14}\text{O}_5$.

Table 3.1 ¹H and ¹³C NMR assignments for compound SA2A_10A (spiropreussomerin A) recorded in CD₃CN

Position	δ_H (ppm); multiplicity; J (Hz)	δ_C (ppm)
1	-	148.6
2	7.07; d; 7.7	110.5
3	7.53; t; 7.7, 8.3	129.0
4	7.61; d; 8.3	122.0
4a	-	135.4
5	7.59; d; 8.3	121.9
6	7.47; t; 7.7, 8.3	128.9
7	6.94; d; 7.7	110.0
8	-	148.6
8a	-	113.8
1'	-	98.9
2'	3.65; d; 4.0	51.4
3'	3.52; dd; 4.0, 2.4	54.3
4'	5.41; d; 5.4	61.5
4a'	-	123.2
5'	7.29; d; 2.7	130.5
6'	6.99; dd; 5.9, 2.7	117.8
7'	-	156.3
8'	7.27; s	119.0
8a'	-	133.6
OH (4)	3.74; d; 6.1	-
OH (7')	8.02; s	-

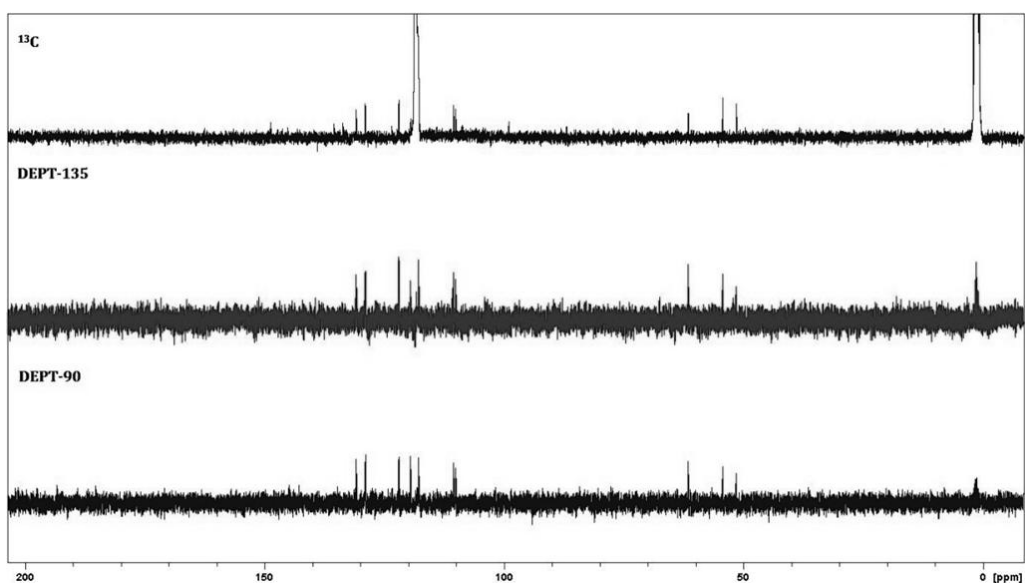
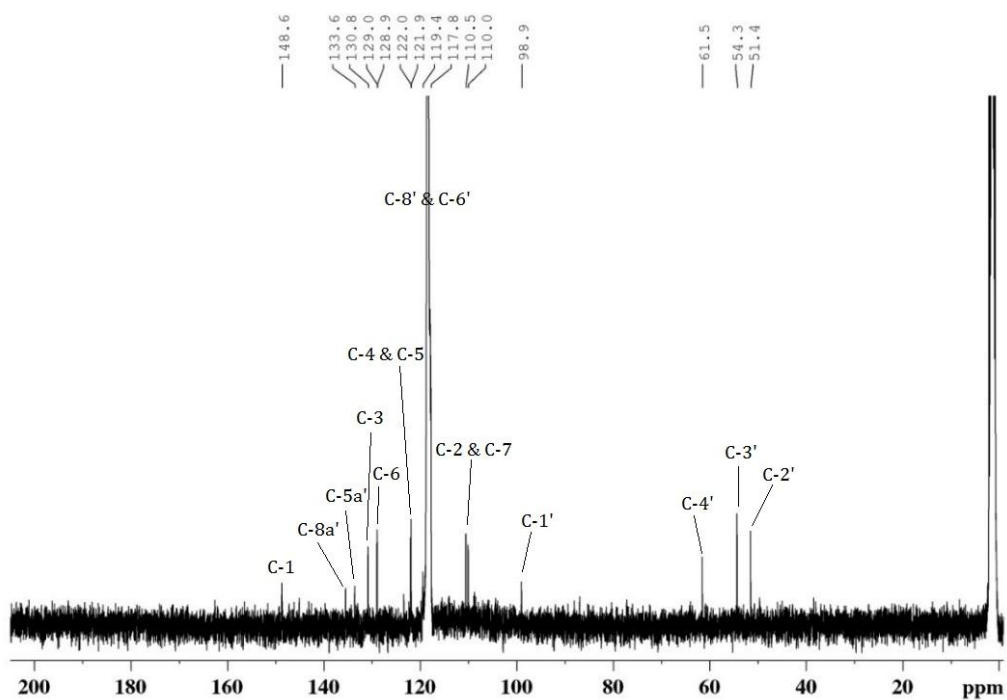


Figure 3.11 ^{13}C spectra, including DEPT-135 and DEPT-90 of compound SA2A_{10A} (spiropreussomerin A)

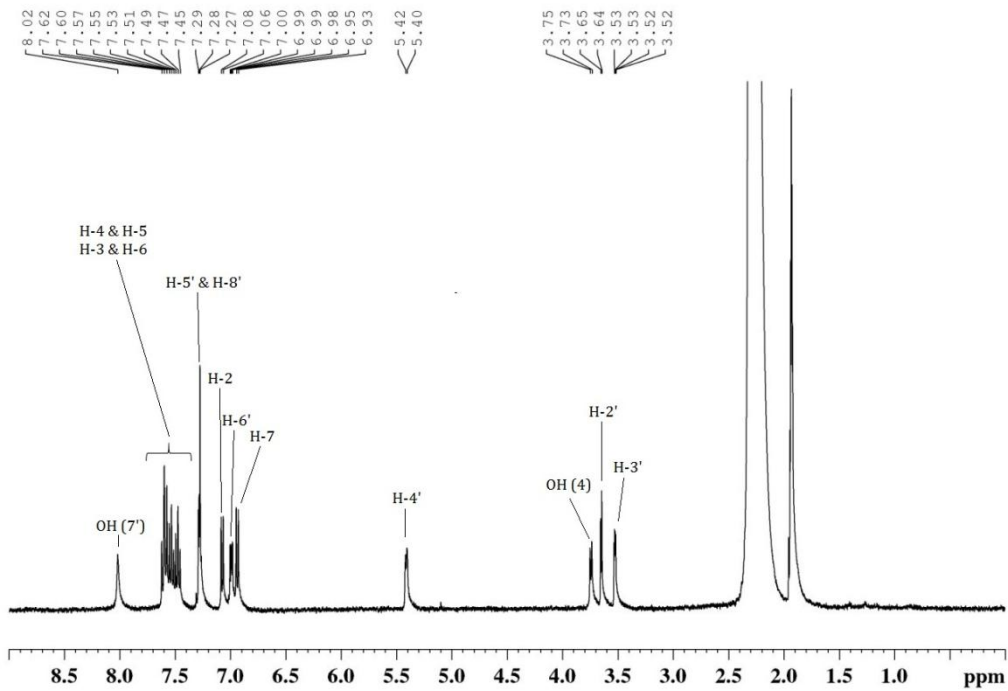


Figure 3.12 ^1H spectrum of SA2A_10A (spiropreussomerin A)

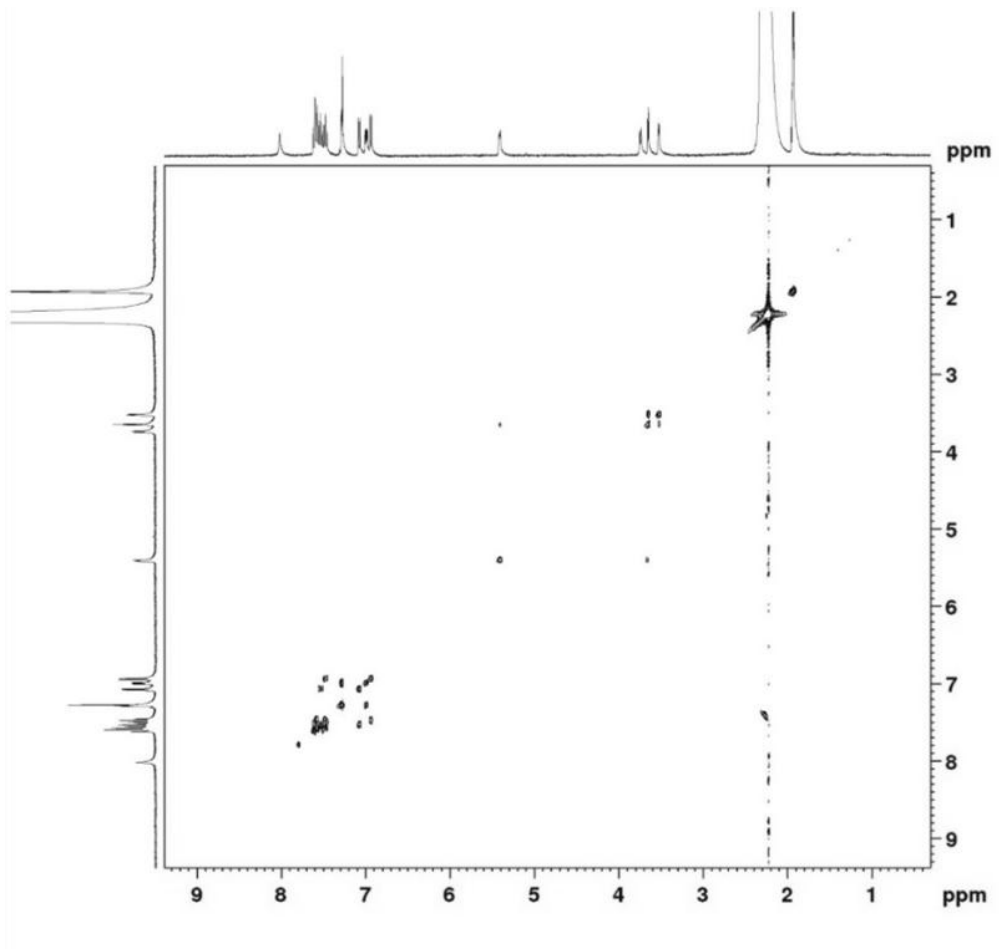


Figure 3.13 COSY spectrum of SA2A_10A (spiropreussomerin A)

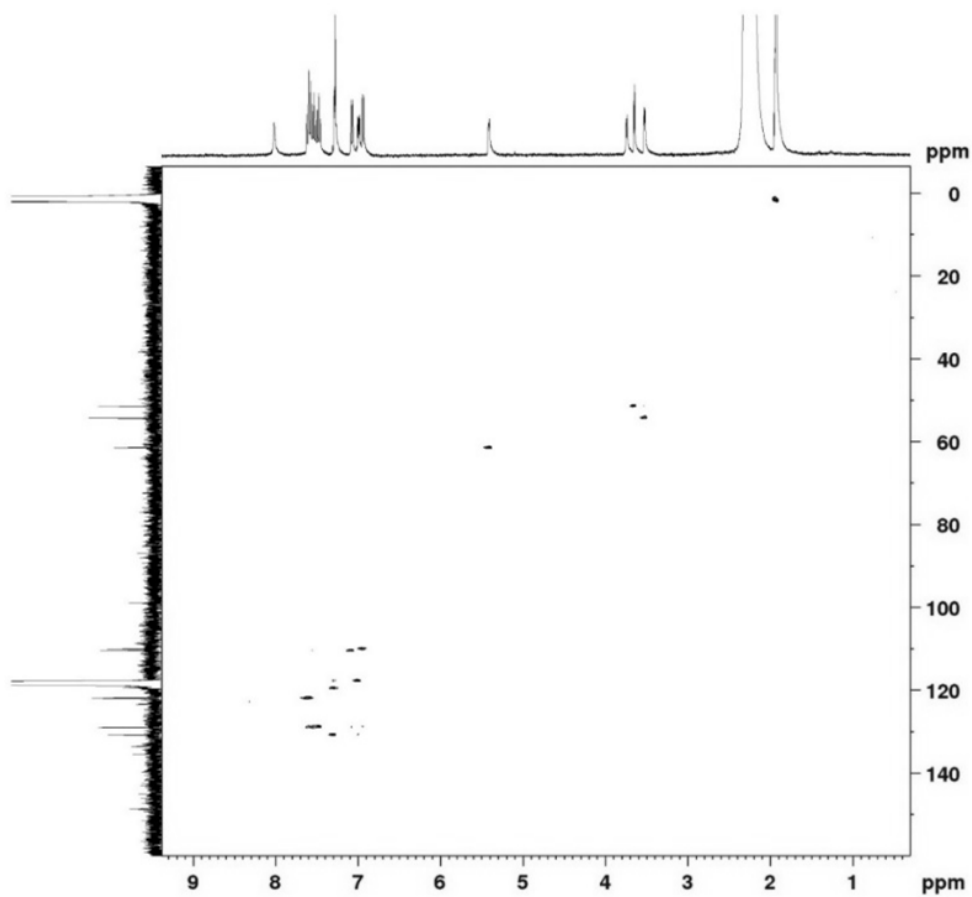


Figure 3.14 HSQC spectrum of SA2A_10A (spiropreussomerin A)

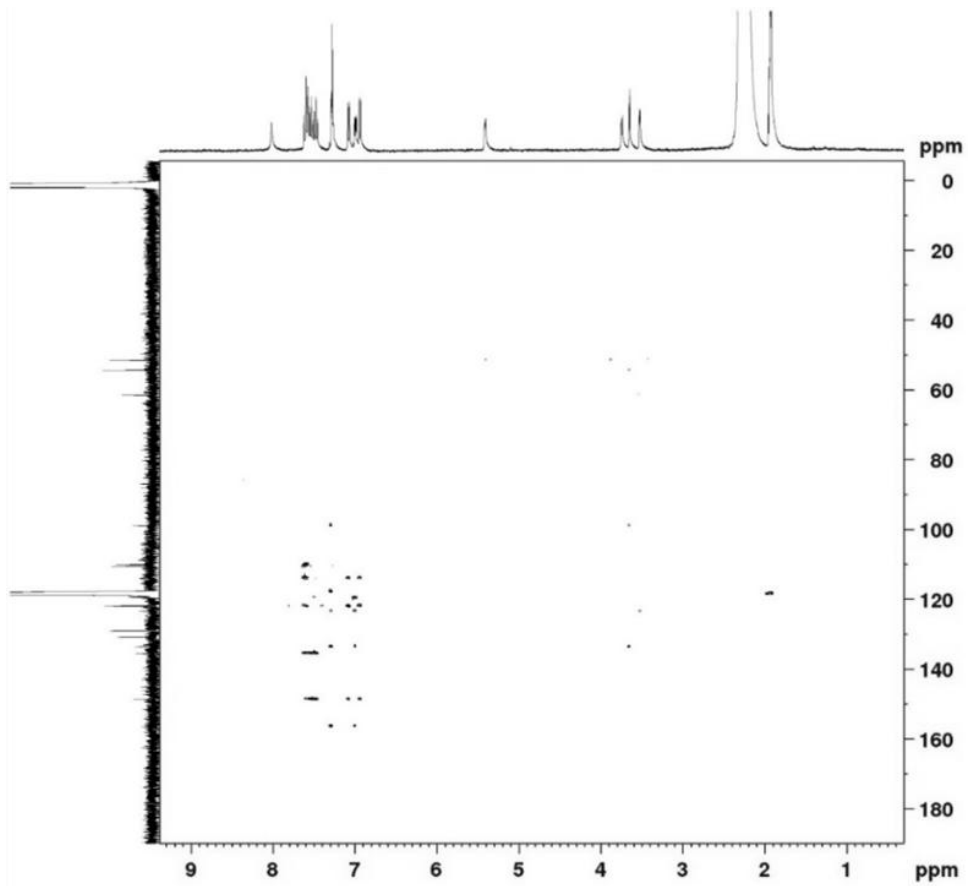


Figure 3.15 HMBC spectrum of SA2A_10A (spiropreussomerin A)

3.2.7.2. Conrauiflavonol/afzelin A

The structure of compound SA2A_10B was elucidated by ^1H , ^{13}C (also DEPT-135, DEPT-90) and 2D NMR (COSY, HSQC and HMBC) as 6,7-(2'',2''-dimethylpyrano)-5,4'-dihydroxyflavanonol, or **conrauiflavonol**^[15], or **afzelin A**^[16] (Figure 3.16). They were first isolated from *Ficus conraui* (Moraceae) and *Hymenostegia afzelii* (Caesalpinaceae), respectively.

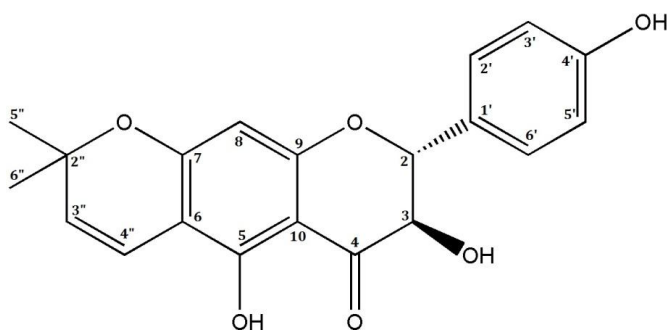


Figure 3.16 Structure of compound SA2A_10B (conrauiflavonol/afzelin A)

Library search on the ^{13}C NMR data (Table 3.2 and Figure 3.17) using the NMR Predict database and the ^1H NMR data (Table 3.2 and Figure 3.18) suggested that this compound had a flavanone skeleton with a 2'',2''-dimethyl pyran ring. By analysis of the COSY (Figure 3.19), HSQC (Figure 3.20) and HMBC (Figure 3.21) correlations the structure was elucidated, and the spectral data corresponded with those reported in the literature.^[15, 16] The carbons C-2 and C-3 of the flavanone skeleton showed signals at 84.4 and 73.2 ppm, respectively. The quaternary carbons C-5, C-7 and C-9 were assigned to the signals at 158.9, 163.2 and 163.6 ppm, respectively. The quaternary carbons in position 6 and 10 showed signals at 104.0 and 102.2 ppm. The signal at 97.0 ppm was assigned to C-8 and the carbonyl group of the flavanone moiety at 198.7 ppm. The aromatic carbons C-2'/6' and C-3'/5' were assigned to the signals at 130.6 and 116.3 ppm, respectively. On the same aromatic ring C-1' was assigned to the signal at 129.1 ppm and C-4' to the signal at 158.9 ppm. The presence of the dimethyl pyran ring was supported by the carbon signals observed at 115.6 ppm (C-4''), 128.2 ppm (C-3''), 79.6 ppm (C-2'') and the two methyl groups at 28.7 and 28.6 ppm. The HMBC correlations

from H-3'' to carbons C-2'' and C-6, and from H-4'' to carbons C-2'', C-6, C-7 and C-5, indicated that the pyran ring was attached to C-7 and C-6 of the flavanonol skeleton.

The ¹H NMR spectrum displayed the typical flavanonol signals at 5.04 ppm (H-2) and 4.60 ppm (H-3) with a coupling constant of 11.8 Hz. This value suggested a *trans* configuration between H-2 and H-3.^[17] The singlet observed at 5.88 ppm was assigned to H-8. The two aromatic protons H-2' and H-6' were assigned to the signal at 7.34 ppm and the two other aromatic protons (H-3' and H-5') were assigned to the signal at 6.86 ppm. H-4'' and H-3'' corresponded with the two coupled doublets (*J* = 10.1 Hz) at 6.57 and 5.62 ppm, respectively. The protons (H-5'' and H-6'') from the methyl groups at position 2'' were assigned to the singlet at 1.40 ppm. The protons of the hydroxyl group gave signals at 4.01 ppm (3-OH), 11.86 ppm (5-OH) and 7.68 ppm (4'-OH).

Conrauiflavonol was isolated from *Ficus conraui* (Moraceae) by Kengap et al. (2011)^[15] and afzelin A from *Hymenostegia afzelii* (Caesalpiniaceae) by Awantu et al. (2011)^[16]. It can be noted that the name conrauiflavonol is somewhat misleading since it is not a flavonol but a flavanonol (or a dihydroflavonol). The difference between conrauiflavonol and afzelin A is not completely clear. The absolute configuration of conrauiflavonol was established as 2*R*, 3*R* (*trans*) by circular dichroism (CD) spectroscopy, whereas for afzelin A the 2,3-*trans* relationship was established by X-ray crystallography and NOESY correlations, but not the absolute configuration. For conrauiflavonol a specific optical rotation of +2.55 was reported in chloroform, and for afzelin A +23.5 in methanol. Although both compounds have an established 2, 3-*trans* relationship, they cannot be enantiomers since then they should have opposite specific optical rotations. The specific optical rotation for compound SA2A_10B was + 74.8. It is hypothesised that the differences in specific optical rotation between compound SA2A_10B, conrauiflavonol and afzelin A may be due to differences in enantiomeric purity, implying that compound SA2A_10B would have the highest enantiomeric purity.

The UV spectrum showed UV absorption maxima at 228, 272, 296 and 310 nm and the high resolution mass spectrum was recorded showing a pseudo molecular ion [M - H]⁻ with *m/z* 353.1038 (calculated *m/z* 353.1025) consistent with a molecular formula of C₂₀H₁₈O₆. The specific optical rotation was determined as: $[\alpha]_D^{20} + 74.8^\circ$.

Table 3.2 ¹H and ¹³C NMR assignments for compound SA2A_10B (conraui flavonol/afzelin A) recorded in CD₃CN

Position	δ_H (ppm); multiplicity; J (Hz)	δ_C (ppm)
2	5.04; d; 11.8	84.4
3	4.60; dd; 11.8, 4.1	73.2
4	-	198.7
5	-	158.9
6	-	104.0
7	-	163.2
8	5.88; s	97.0
9	-	163.6
10	-	102.2
1'	-	129.1
2'/6'	7.34; dd; 6.7, 1.9	130.6
3'/5'	6.86; dd; 6.7, 1.9	116.3
4'	-	158.9
2''	-	79.6
3''	5.62; d; 10.1	128.2
4''	6.57; d; 10.1	115.6
5''	1.40; s	28.7
6''	1.40; s	28.6
OH (3)	4.01; d; 4.1	-
OH (5)	11.86; s	-
OH (4')	7.68; s	-

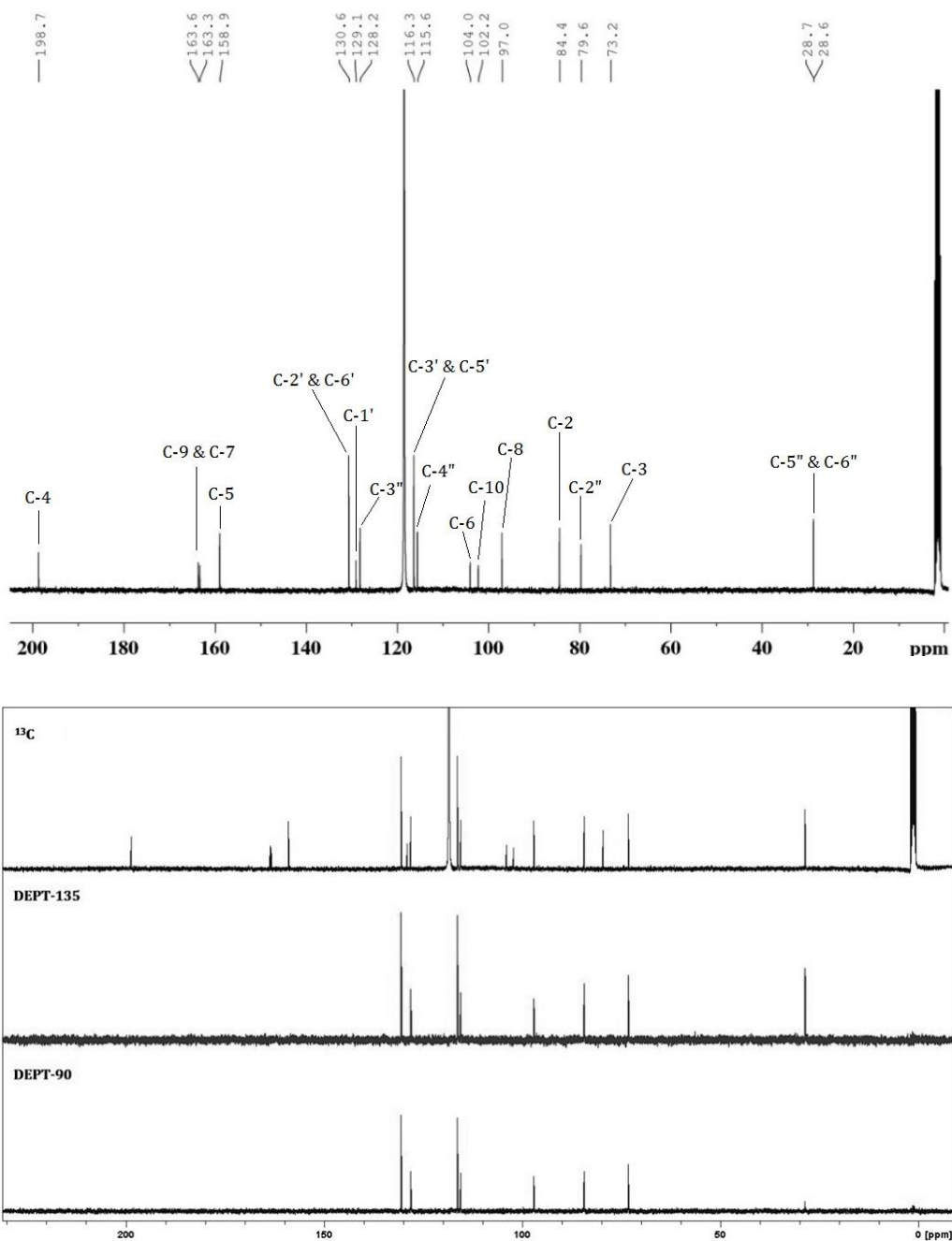


Figure 3.17 ^{13}C -NMR spectra, including DEPT-135 and DEPT-90 of compound SA2A_10B (conrauiflavinol/afzelin A)

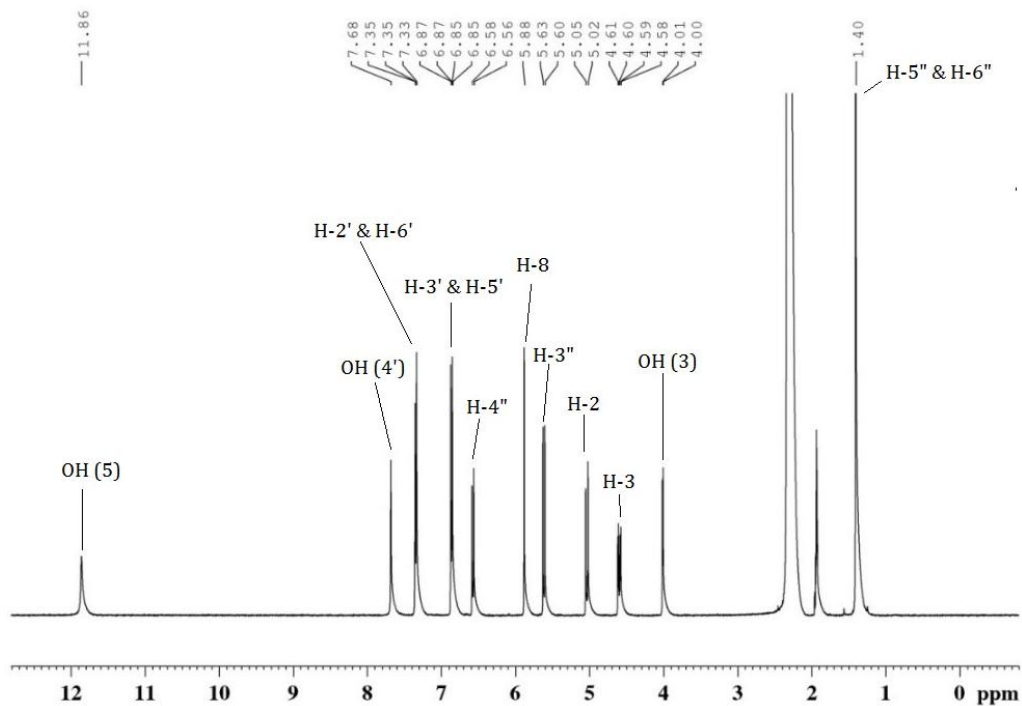


Figure 3.18 ^1H spectrum of compound SA2A_10B (conrauiflavonol/afzelin A)

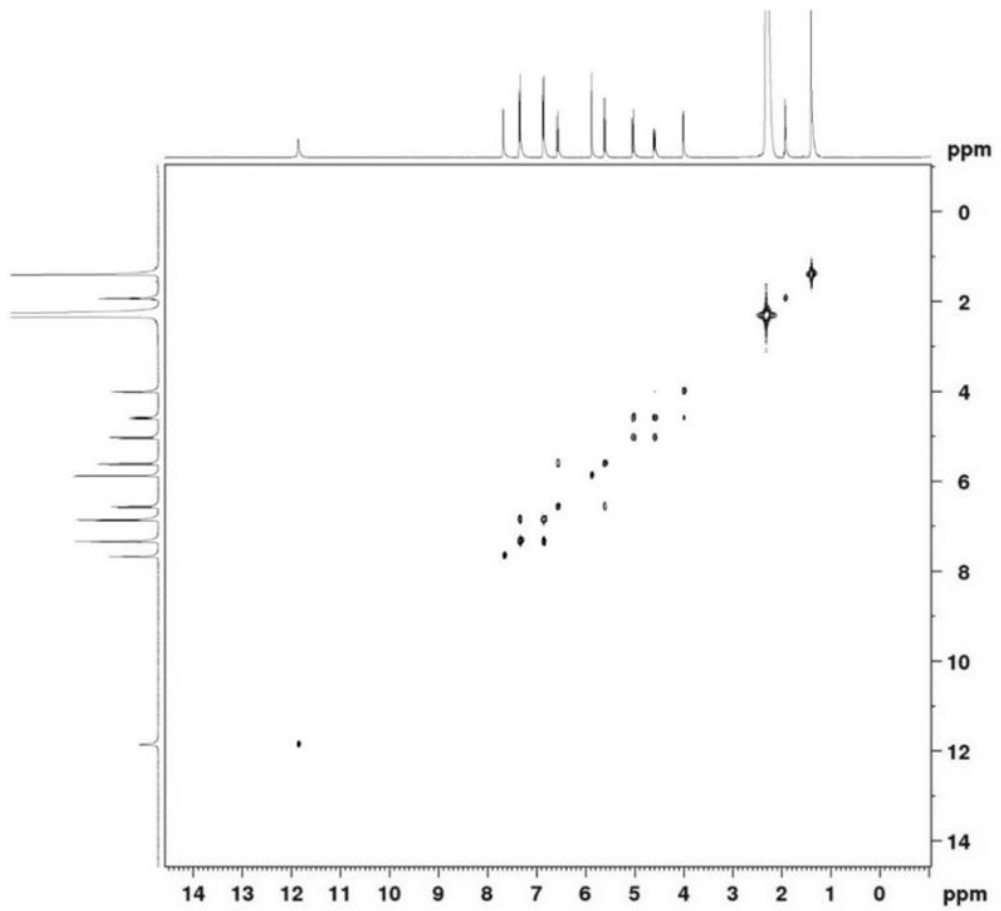


Figure 3.19 COSY spectrum of compound SA2A_10B (conrauiflavanol/afzelin A)

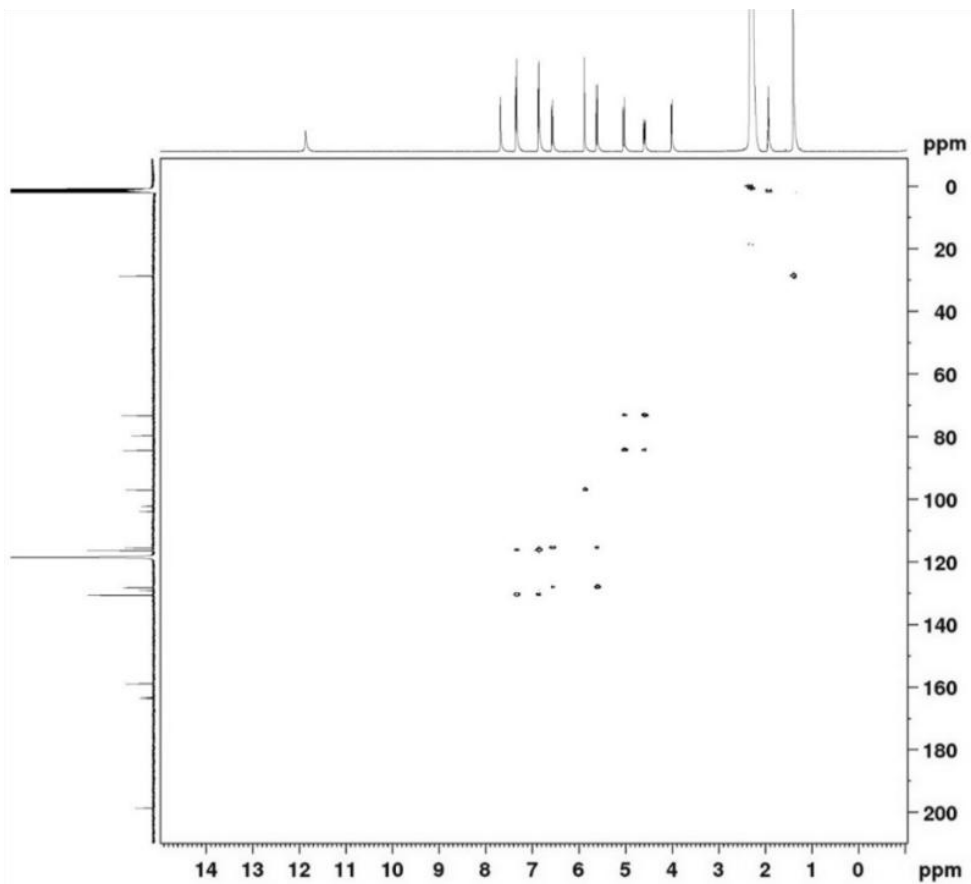


Figure 3.20 HSQC spectrum of compound SA2A_10B (conraui flavonol/afzelin A)

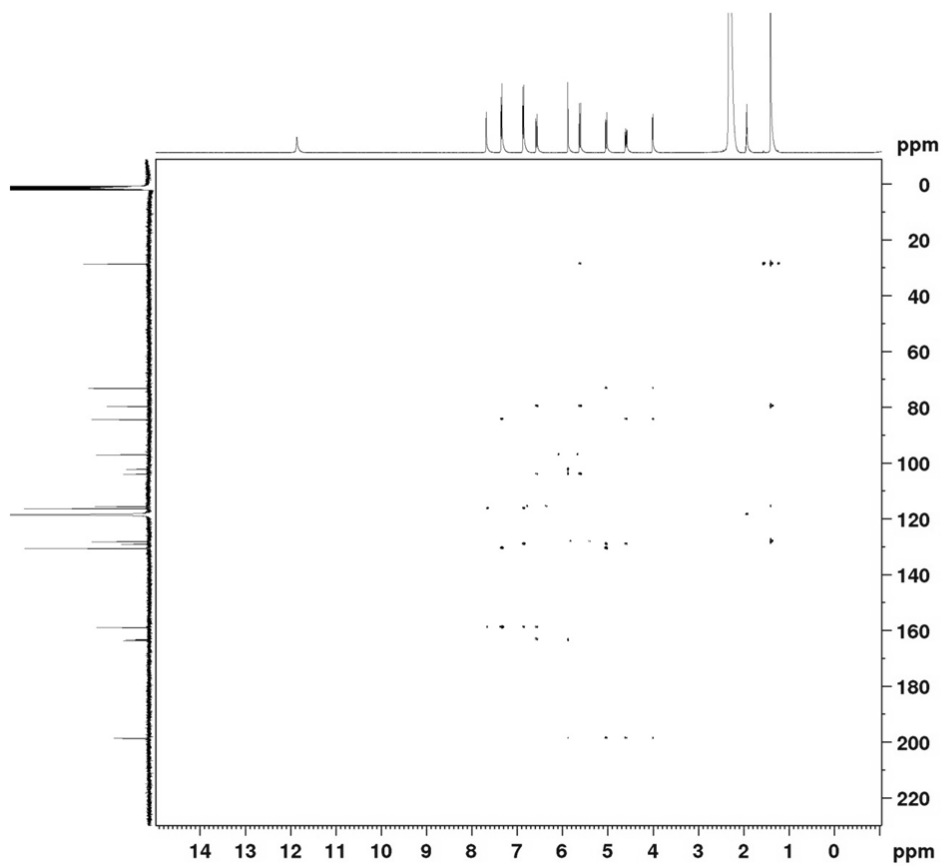


Figure 3.21 HMBC spectrum of compound SA2A_10B (conrauiflavonol/afzelin A)

3.2.7.3. Protosteganoflavanone

The structure of compound SA2A_17A was elucidated by ^1H , ^{13}C (also DEPT-135, DEPT-90) and 2D NMR (COSY, HSQC and HMBC) as 6,7-(2'',2''-dimethylpyrano)-5,1'-dihydroxy-4'-oxo-2'-enyl-flavanone for which the name **protosteganoflavanone** was adopted (Figure 3.22).

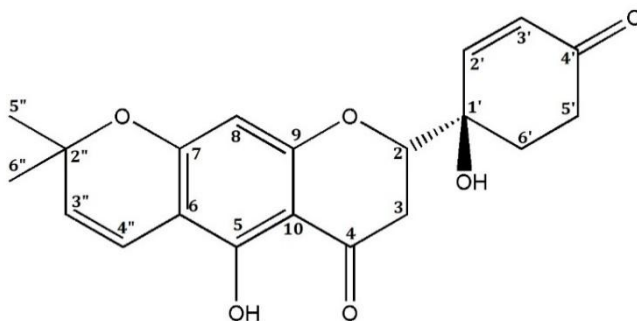


Figure 3.22 The structure of compound SA2A_17A (protosteganoflavanone)

Library search on the ^{13}C NMR data (Table 3.3 and Figure 3.23) using the NMR Predict database and the ^1H NMR data (Table 3.3 and Figure 3.24) suggested that this compound showed great similarity with SA2A_10B with a 2'',2''-dimethyl pyran ring but with a flavanone skeleton and some modifications on the B-ring. By analysis of the COSY (Figure 3.25), HSQC (Figure 3.26) and HMBC (Figure 3.27) correlations the structure was elucidated as shown. C-2 and C-3 of the flavanone skeleton showed signals at 83.0 and 36.7 ppm, respectively. The quaternary C-5, C-7 and C-9 were assigned to the signals at 159.2, 162.8 and 163.3 ppm, respectively. The quaternary carbons in position 6 and 10 showed signals at 103.9 and 103.7 ppm. The signal at 96.7 ppm was assigned to C-8 and the signal at 197.9 ppm to the carbonyl group of the flavanone. In ring B, the signals of the carbons in position 2' and 3' were assigned to the signals at 150.2 and 130.5 ppm, respectively. On the same ring C-5' and C-6' were assigned to the signals at 34.3 and 32.4 ppm and C-1' was assigned to the signal at 71.0 ppm. The signal at 199.6 indicated a carbonyl group in position 4'. The signals of the carbons of the dimethyl pyran ring were observed at 115.7 ppm (C-4''), 128.0 ppm (C-3''), 79.4 ppm (C-2'')

and the two methyl groups at 28.5 and 28.6 ppm. Here again, the HMBC correlations from H-3'' to carbons C-2'' and C-6, and from H-4'' to carbons C-2'', C-6, C-7 and C-5, indicated that the pyran ring was attached to C-7 and C-6 of the flavanone skeleton. Changes in chemical shifts of C-3 and C-1' compared to SA2A_10B, indicated that the hydroxyl group had moved from position 3 to position 1'.

The ¹H NMR spectrum showed a doublet of doublets at 4.53 ppm ($J = 13.2$ and 3.0 Hz) assigned to the proton in position 2 and a doublet of doublets at 2.66 ($J = 17.2$ and 3.0 Hz) which correlated with a doublet of doublets at 3.02 ppm ($J = 17.2$ and 13.2 Hz) corresponded to the CH₂ in position 3. The singlet observed at 5.91 ppm was assigned to H-8. The two coupled protons H-2' and H-3' ($J = 10.3$ Hz) corresponded to the signals at 7.08 and 5.97 ppm, respectively. The multiplets at 2.57, 2.43, 2.14 and 2.04 ppm were assigned to the 4 protons in position 5' and 6', respectively. H-4'' and H-3'' corresponded with the two coupled doublets ($J = 10.1$ Hz) at 6.54 and 5.59 ppm, respectively. The protons (H-5'' and H-6'') from the methyl groups at position 2'' were assigned to the singlet at 1.38 ppm. The protons of the hydroxyl groups gave signals at 12.33 ppm (5-OH) and 3.97 ppm (1'-OH).

The UV spectrum showed UV absorption maxima at 226, 270, 296 and 310 nm and the high resolution mass spectrum was recorded showing a pseudo molecular ion [M - H]⁻ with m/z 355.1197 (calculated m/z 355.1182) consistent with a molecular formula of C₂₀H₂₀O₆. The specific optical rotation was determined as: $[\alpha]_D^{20} + 228.8^\circ$.

Compound SA2A_17A has not been reported yet. It can be considered as a protoflavonoid, since it contains the typical non-aromatic B-ring and a hydroxyl group at C-1'. Therefore the trivial name protosteganoflavanone was proposed. According to a recent review, protoflavonoids are a rare class of flavonoids that until now mainly has been observed in certain genera of ferns, with the exception of *Apium graveolens*. Both *Steganotaenia araliacea* and *Apium graveolens* belong to the Apiaceae family. Protoflavonoids are considered as a promising class of anticancer compounds.^[18, 19]

Table 3.3 ¹H and ¹³C NMR assignments for compound SA2A_17A (protosteganoflavanone) recorded in CD₃CN

Position	δ_H (ppm), multiplicity, J (Hz)	δ_C (ppm)
2	4.53; dd; 13.2; 3.0	83.0
3	2.66; dd; 17.2; 3.0 3.02; dd; 17.2; 13.2	36.7
4	-	197.9
5	-	159.2
6	-	103.9
7	-	162.8
8	5.91; s	96.7
9	-	163.3
10	-	103.7
1'	-	71.0
2'	7.08; d; 10.3	150.2
3'	5.97; d; 10.3	130.5
4'	-	199.6
5'	2.57; m 2.43; m	34.3
6'	2.14; m 2.04; m	32.4
2''	-	79.4
3''	5.59; d; 10.1	128.0
4''	6.54; d; 10.1	115.7
5''	1.38; s	28.6
6''	1.38; s	28.5
OH (5)	12.33; s	-
OH (1')	3.97; s	-

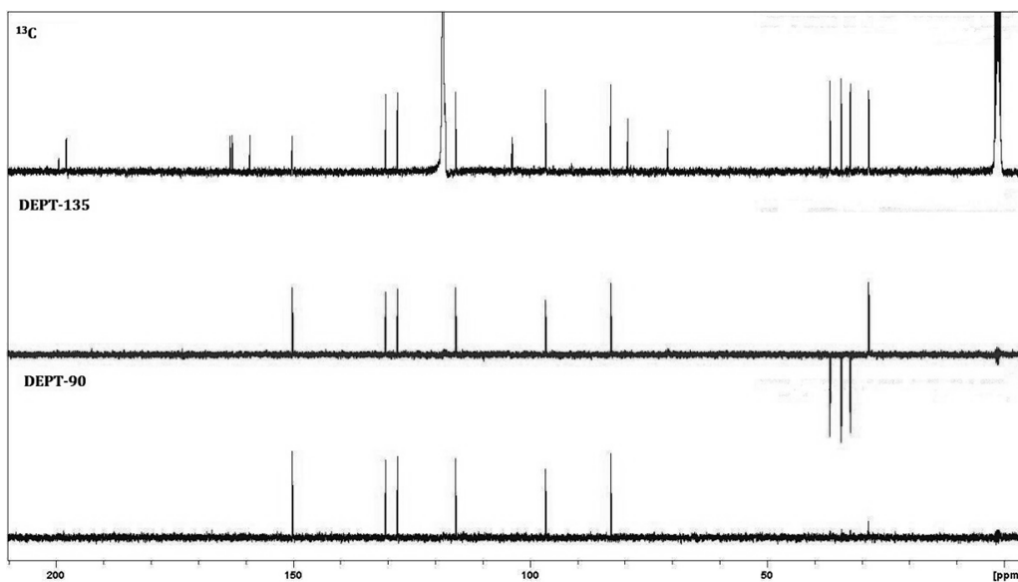
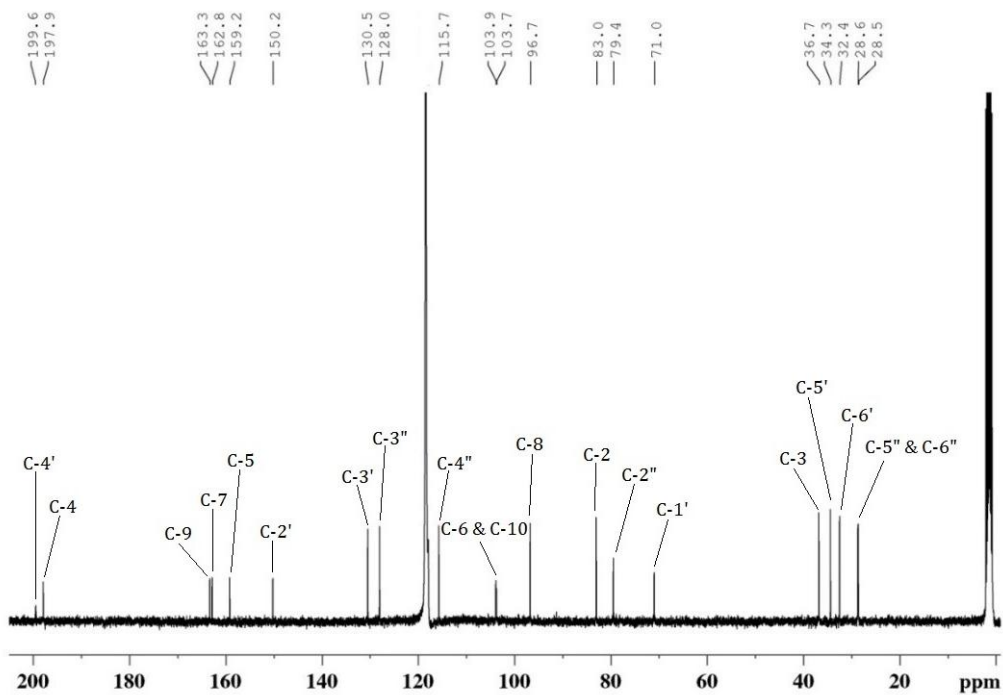


Figure 3.23 ^{13}C spectra, including DEPT-135 and DEPT-90 of compound SAZA_17A (protosteganoflavanone)

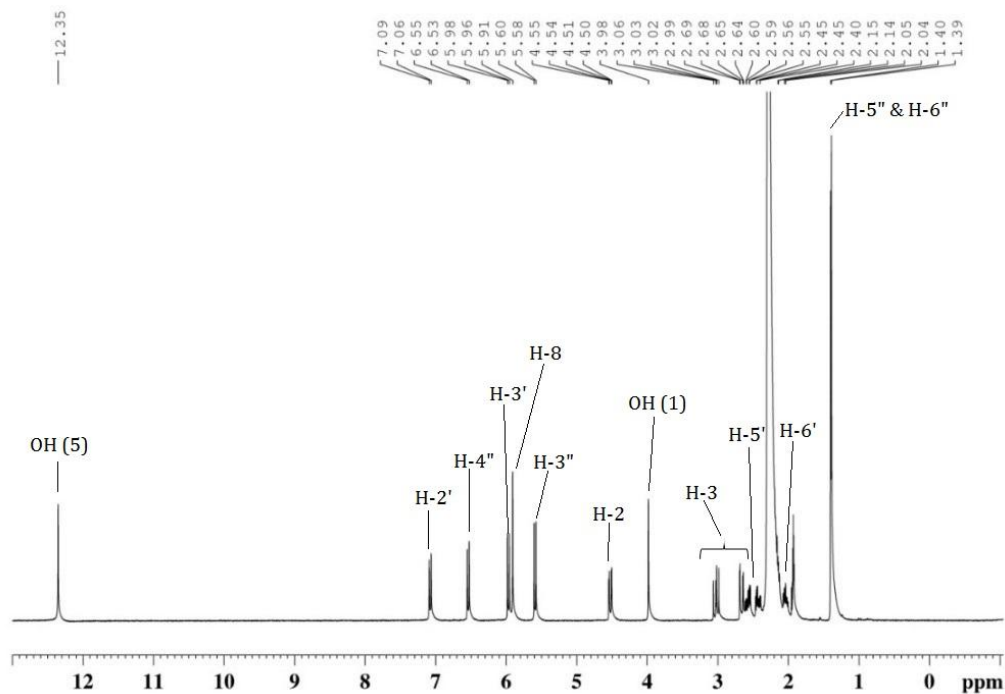


Figure 3.24 ^1H spectrum of compound SA2A_17A (protosteganoflavanone)

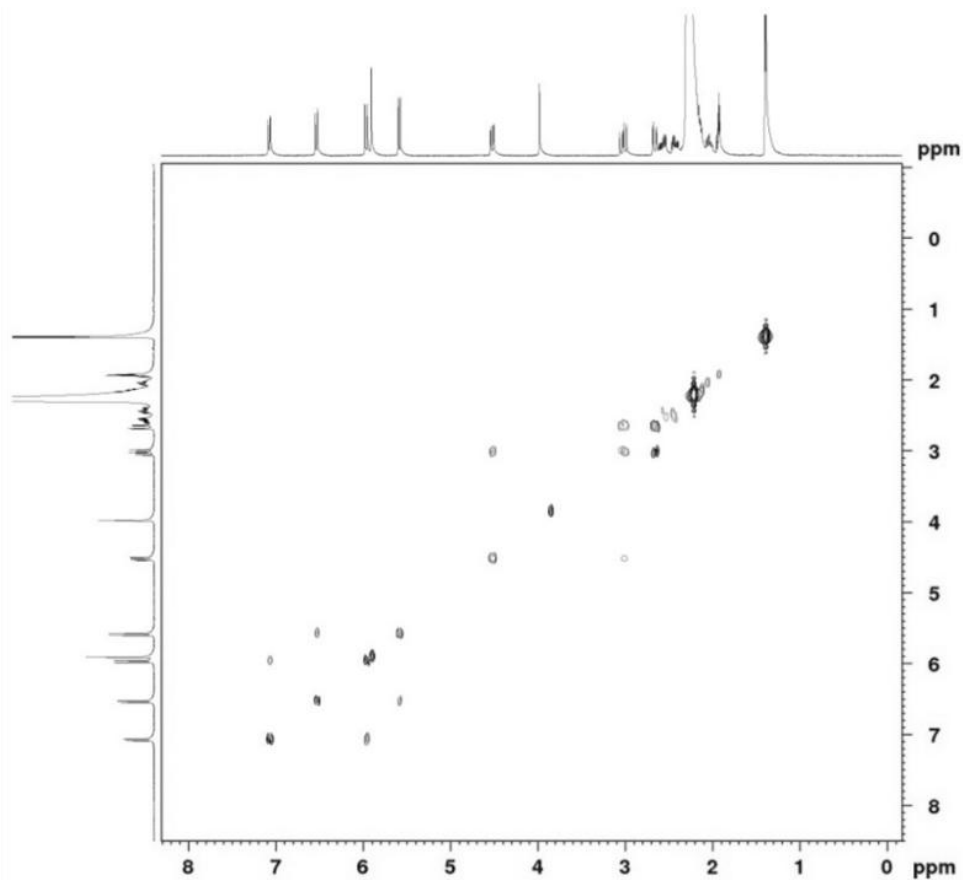


Figure 3.25 COSY spectrum of compound SA2A_17A (protosteganoflavanone)

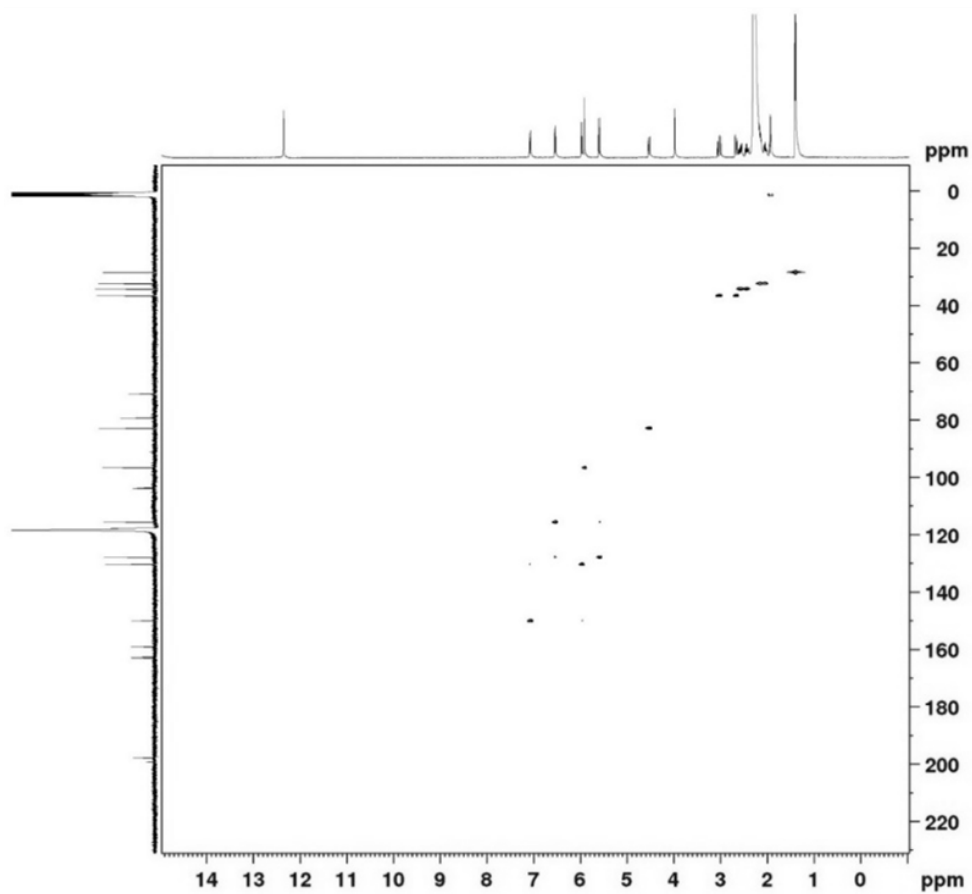


Figure 3.26 HSQC spectrum of compound SA2A_17A (protosteganoflavanone)

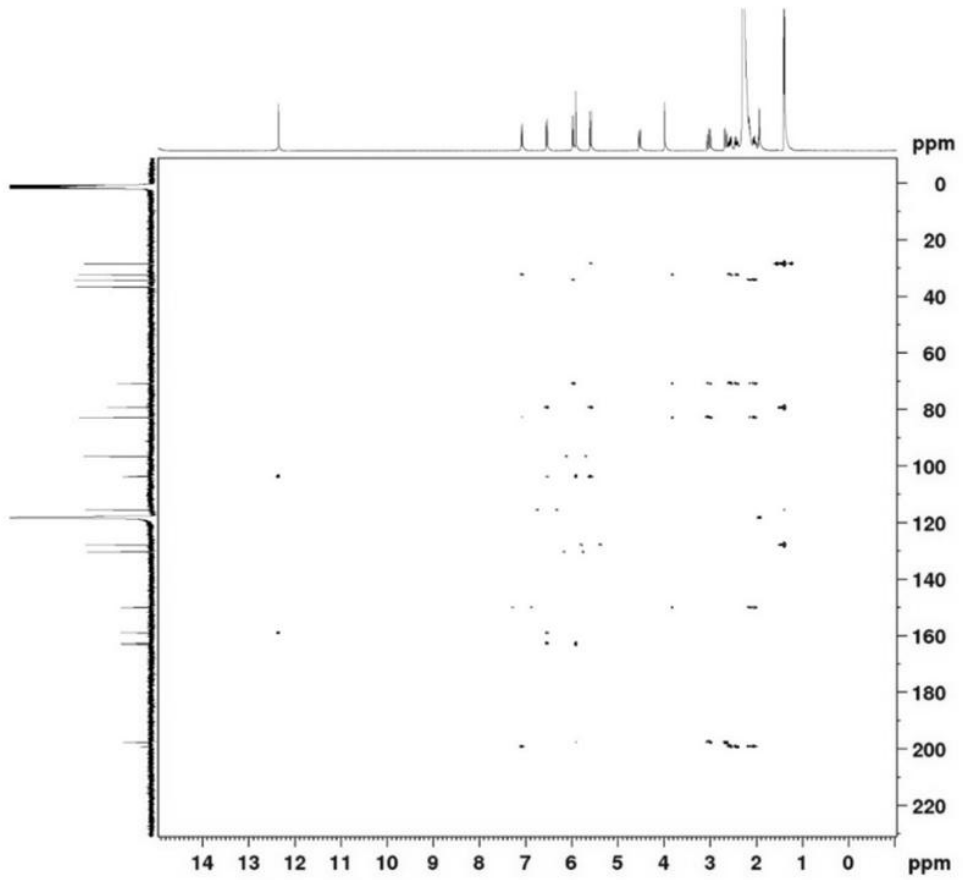


Figure 3.27 HMBC spectrum of compound SA2A_17A (protosteganoflavanone)

3.3. CYTOTOXICITY STUDY

The cytotoxicity of the *S. araliacea* crude extract (SA) (mentioned in section 3.2.2) was assessed *in vitro* on different cell lines. Not only was the effect of the extract on cancer cell lines tested, but also on normal cells. Two spectrophotometric methods were used, i.e. the SRB assay (2.3.3) and the NR assay (2.3.4).

Cytotoxicity on BEAS-2B cells, which are normal cells, was assessed by using the NR assay as shown in Figure 3.28. This graph displays the percentage of inhibition of cell viability relative to solvent control for the *S. araliacea* extract. The IC_{50} as determined from the fitted curve is included on top of the graph. To be able to test the crude extract, it needed to be dissolved. This turned out to be rather challenging. Macroscopic and microscopic evaluations were performed to see whether there were still particles in the solution. Macroscopic evaluation showed that at a concentration from 100.0 to 2.0 mg/mL dark precipitation was observed in the clear brown-yellowish solution. Precipitation led to an aspecific binding of the dye to the bottom of the well (macroscopically observed). As the dye binds to viable cells, this could result in overestimation of cell viability and underestimation of cell death. At lower concentrations (2.0 - 0.1 mg/mL), precipitates and/or particles were observed microscopically as shown in Figure 3.29. Therefore only 3 out of 7 data points were included for curve fitting and IC_{50} determination on BEAS-2B cells. Because of poor solubility and precipitation of the plant extract during the cytotoxicity assay, the estimated IC_{50} value for the BEAS-2B cells could not be considered as reliable.

Consequently, for the following experiments, the *S. araliacea* crude extract was dissolved in water. The suspension containing the precipitate was then filtered through a 0.45 μ m membrane filter and again filtered through a 0.22 μ m filter to sterilise the solution. The loss due to filtration was analysed by preparing the solution 6 times and filtering it through the membrane filters. The filtrate was then lyophilised and weighed. The average loss by filtration was then calculated and amounted to 65%. This percentage was then used to calculate the concentration of the soluble fraction of the crude extract. So the concentration used to calculate the IC_{50} is the concentration of the soluble fraction of the crude extract.

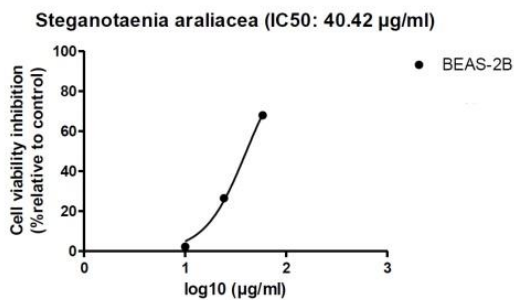


Figure 3.28 Dose-response curve and calculated IC₅₀ for effects on cell viability of BEAS-2B cells

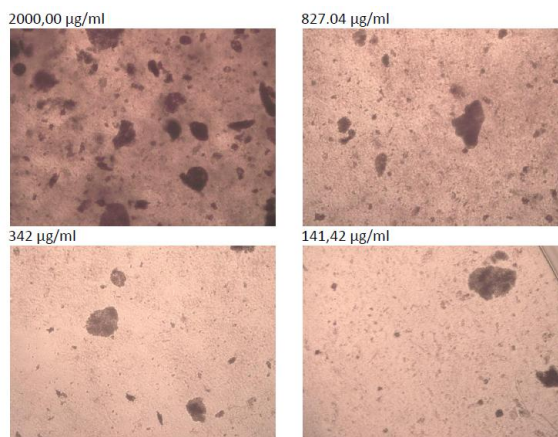


Figure 3.29 Microscopic evaluation of the solubility of the *S. araliacea* crude extract

Cytotoxicity on three cancer cell lines, i.e. MDA-MB-231, PANC-1 and HT-29 was tested by means of the SRB assay. The used concentrations of SA ranged from 3.5 – 350 µg/mL. The cytotoxicity of SA was evaluated using two different incubation times (24 h and 72 h) and all experiments were repeated three times. The survival percentages per concentration per cell line and per incubation time were calculated from the optical density measurements and are shown in the graphs (Figure 3.30). The calculated IC₅₀ values for these cell lines are summarised in Table 3.4.

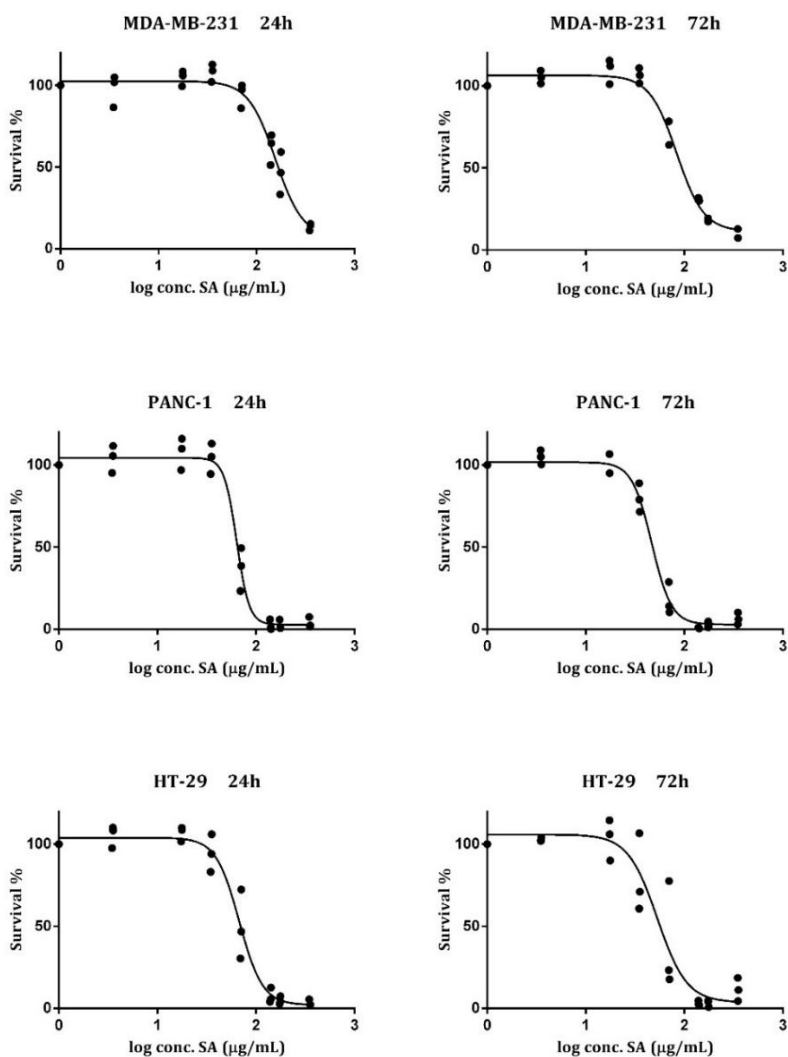


Figure 3.30 Dose-response curves of the three human cancer cell lines treated with SA

Table 3.4 IC₅₀ of *S. araliacea* crude extract on the tested cell lines

	IC ₅₀ ± SEM (µg/mL)		
	MDA-MB-231	PANC-1	HT-29
24 h	165.5 ± 8.0	64.0 ± 3.3	68.7 ± 3.9
72 h	95.7 ± 4.8	47.9 ± 1.8	55.1 ± 6.6

3.4. DISCUSSION

The MDA-MB-231 cell line is a more invasive type of breast cancer cell line that only exhibit an intermediate response to chemotherapy.^[20] This was probably the reason for the higher IC₅₀ value (165.5 and 95.7 µg/mL), compared to the other cell lines. For PANC-1 and HT-29, the crude extract exhibited only a moderate cytotoxic activity with IC₅₀ values above 20 µg/mL.

For all tested cell lines, not only a dose-response correlation could be observed, but also a time-dependent response, with the exception of BEAS-2B, which was only tested with 1 incubation time. The IC₅₀ values declined with longer incubation time. It cannot be excluded that the *S. araliacea* extract would need a longer incubation period and that the cytotoxic effect still would increase after 72 h.

Although more than 65% of the crude extract was lost during filtration, the HPLC analysis of the *in vitro* stock solution still showed the presence of the three compounds isolated during the phytochemical investigation of the crude extract.

Compounds SA2A_10B and SA2A_17A belong to the class of flavonoids, and SA2A_17A more in particular belongs to the class of the protoflavonoids. Flavonoids have been reported to possess a wide range of biological and pharmacological activities. They can influence the cascade of immunological events and modulate many biological events in cancer. Many mechanisms of action have been identified, including carcinogen inactivation, antiproliferation, cell cycle arrest, induction of apoptosis and differentiation, inhibition of angiogenesis, anti-oxidation and reversal of multidrug resistance or a combination of all these mechanisms. Therefore particular classes of flavonoids might have promising anticancer activities.^[21, 22] Recently the protoflavonoids have been proposed as a new class of potential anticancer compounds.^[18, 19]

Spiropreussomerin A is a deoxypreussomerin constituent of the endophytic fungus *Preussia* sp.^[14] Although deoxypreussomerin analogues possess a wide range of biological properties including antibacterial, antifungal, herbicidal, but also antitumour activity^[23], spiropreussomerin A did not show cytotoxicity towards human ovarian carcinoma (A2780),

human liver carcinoma (BEL-7404), colon carcinoma (HCT-8), gastric carcinoma (BGC-823) and lung adenocarcinoma (A-549).^[14]

Therefore it can be assumed that from the three compound isolated in the present work, the flavonoids and more in particular the protoflavonoid protosteganoflavanone may be responsible for the observed cytotoxicity on the cancer cell lines. It is remarkable that the lignans that have been reported before, were not among the major constituents of the batch of plant material that was analysed here. Most probably they are present in lower concentrations. They might have been isolated in a bioassay-guided fractionation scheme, but as explained above the aim of the present work was not to obtain new lead compounds, but to characterise the main constituents of a cytotoxic and potentially antitumoural plant extract to be clinically used as such. In view of the rather moderate *in vitro* activity of the *S. araliacea* crude extract, it was not prioritised for further investigations. Therefore, it was decided not to further investigate the *S. araliacea* crude extract in more detail in this project, and to give priority to the other selected plant species, i.e. *Gloriosa superba* and *Chelidonium majus*. Nevertheless, the novel constituent protosteganoflavanone might be interesting for future investigation as a possible lead compound.

3.5. SUMMARY AND CONCLUSION

S. araliacea stem bark was phytochemically investigated using chromatographic and spectroscopic techniques. Liquid-Liquid partition of the 80% ethanolic stem bark extract with petroleum ether, followed by extraction with ethyl acetate yielded the ethyl acetate fraction (SA2A). Further fractionation by flash column chromatography and LC-SPE-NMR analysis led to the identification of three constituents, i.e. spiropreussomerin A, conraui flavonol/afzelin A and a new compound 6,7-(2'',2''-dimethylpyrano)-5,1'-dihydroxy-4'oxo-2'eryl-flavanone, for which the name protosteganoflavanone was adopted.

A preliminary *in vitro* assay was performed on the *S. araliacea* crude extract to evaluate its cytotoxic effect. The results of the *in vitro* study suggested that the *S. araliacea* extract only had a moderate cytotoxic activity with IC₅₀ values far above 20 µg/mL for all tested cell lines.

One of the important pit-falls during this *in vitro* assay was the solubility of the extract and 65% of the crude extract was lost during *in vitro* evaluation. Nonetheless, analysis of the soluble crude extract still showed the presence of the three isolated compounds.

The three isolated compounds in the present work might contribute in part to the cytotoxicity of the crude extract, but more investigations are recommended.

However, because of the solubility issues and the high IC₅₀ value, further investigation of the total extract of *Steganotaenia araliacea* was considered to have less priority than the two other plants selected in this project.

REFERENCES

1. Agunu, A., E.M. Abdurahman, G.O. Andrew, and Z. Muhammed, *Diuretic activity of the stem-bark extracts of Steganotaenia araliacea hochst [Apiaceae]*. J Ethnopharmacol, 2005. 96(3): p. 471-475.
2. Orwa C, Mutua A, Kindt R, Jamnadass R, and A. S, *Agroforestry Database: a tree reference and selection guide version 4.0*. 2009.
3. Ndjonka, D., C. Agyare, K. Luersen, A. Hensel, and E. Liebau, *In vitro anti-leishmanial activity of traditional medicinal plants from Cameroon and Ghana*. International Journal of Pharmacology, 2010. 6(6): p. 863-871.
4. Lino, A. and O. Deogracious, *The in-vitro antibacterial activity of Annona senegalensis, Securidacca longipendiculata and Steganotaenia araliacea - Ugandan medicinal plants*. Afr Health Sci, 2006. 6(1): p. 31-35.
5. Musongong, G., E.N. Nukenine, M. Ngassoum, T. Gangue, and O. Messine, *In vitro Toxicity of ethanolic plant extracts from Adamawa Province, Cameroon to infective larvae of Strongyloides papillosus*. Journal of Biological Sciences, 2004. 4(6): p. 763-767.
6. Kupchan, S.M., R.W. Britton, M.F. Ziegler, C.J. Gilmore, R.J. Restivo, and R.F. Bryan, *Steganacin and steganangin, novel antileukemic lignan lactones from Steganotaenia araliacea*. J Am Chem Soc, 1973. 95(4): p. 1335-1336.
7. Wang, R.W., L.I. Rebhum, and S.M. Kupchan, *Antimitotic and antitubulin activity of the tumor inhibitor steganacin*. Cancer Res, 1977. 37(9): p. 3071-3079.
8. Sackett, D.L., *Podophyllotoxin, Steganacin and Combretastatin - Natural-Products That Bind at the Colchicine Site of Tubulin*. Pharmacology & Therapeutics, 1993. 59(2): p. 163-228.
9. Wickramaratne, D.B., T. Pengsuparp, W. Mar, H.B. Chai, T.E. Chagwedera, C.W. Beecher, N.R. Farnsworth, A.D. Kinghorn, J.M. Pezzuto, and G.A. Cordell, *Novel antimitotic dibenzocyclo-octadiene lignan constituents of the stem bark of Steganotaenia araliacea*. J Nat Prod, 1993. 56(12): p. 2083-2090.

10. Meragelman, K.M., T.C. McKee, and M.R. Boyd, *10-Demethoxystegane, a new lignan from Steganotaenia araliacea*. J Nat Prod, 2001. 64(11): p. 1480-1482.
11. Lavaud, C., G. Massiot, L. Le Men-Olivier, A. Viari, P. Vigny, and C. Delaude, *Saponins from Steganotaenia araliacea*. Phytochemistry, 1992. 31(9): p. 3177-3181.
12. Moudachirou, M., M. Abel Ayedoun, and J. Djimon Gbenou, *Composition of the essential oil of Steganotaenia araliacea Hochst from Benin and Togo*. Journal of Essential Oil Research, 1995. 7(685-686).
13. Noudjou, F., M.B. Ngassoum, P.M. Mapongmetsem, M. Marlier, M. Verscheure, and G.C. Lognagay, *Analysis by GC/FID and GC/MS of essential oil of leaflets of Steganotaenia araliacea Hochst from Cameroon*. Journal of Essential Oil Research, 2006. 18(3): p. 305-307.
14. Chen, X., Q. Shi, G. Lin, S. Guo, and J. Yang, *Spirobisnaphthalene analogues from the endophytic fungus Preussia sp.* J Nat Prod, 2009. 72(9): p. 1712-1715.
15. Kengap, R.T., G.D.W.F. Kapche, J.P. Dzoyem, I.K. Simo, P. Ambassa, L.P. Sandjo, B.M. Abegaz, and B.T. Ngadjui, *Isoprenoids and Flavonoids with Antimicrobial Activity from Ficus conraui Warburg (Moraceae)*. Helvetica Chimica Acta, 2011. 94(12): p. 2231-2238.
16. Awantu, A.F., B.N. Lenta, E.V. Donfack, J.D. Wansi, B. Neumann, H.G. Stammeler, D.T. Nounougoue, E. Tsamo, and N. Sewald, *Flavonoids and other constituents of Hymenostegia afzelii (Caesalpiniaceae)*. Phytochemistry Letters, 2011. 4(3): p. 315-319.
17. Xu, Y.J., R. Capistrano, L. Dhooche, K. Foubert, F. Lemiere, S. Maregesi, A. Balde, S. Apers, and L. Pieters, *Herbal medicines and infectious diseases: characterization by LC-SPE-NMR of some medicinal plant extracts used against malaria*. Planta Med, 2011. 77(11): p. 1139-1148.
18. Pouny, I., C. Etievant, L. Marcourt, I. Huc-Dumas, M. Batut, F. Girard, M. Wright, and G. Massiot, *Protoflavonoids from Ferns Impair Centrosomal Integrity of Tumor Cells*. Planta Medica, 2011. 77(5): p. 461-466.

19. Hunyadi, A., A. Martins, B. Danko, F.R. Chang, and Y.C. Wu, *Protoflavones: a class of unusual flavonoids as promising novel anticancer agents*. *Phytochemistry Reviews*, 2014. 13(1): p. 69-77.
20. Holliday, D.L. and V. Speirs, *Choosing the right cell line for breast cancer research*. *Breast Cancer Res*, 2011. 13(4): p. 215.
21. Batra, P. and A. Sharma, *Anti-cancer potential of flavonoids: recent trends and future perspectives*. *3 Biotech*, 2013. 3(6): p. 439-459.
22. Ren, W., Z. Qiao, H. Wang, L. Zhu, and L. Zhang, *Flavonoids: promising anticancer agents*. *Med Res Rev*, 2003. 23(4): p. 519-534.
23. Ravindranath, N., M.R. Reddy, G. Mahender, R. Ramu, K.R. Kumar, and B. Das, *Deoxypreussomerins from *Jatropha curcas*: are they also plant metabolites?* *Phytochemistry*, 2004. 65(16): p. 2387-2390.

CHAPTER 4

GLORIOSA SUPERBA

4.1. INTRODUCTION

Gloriosa superba L, commonly called glory lily, flame lily, climbing lily or creeping lily, belongs to the family of the Liliaceae.^[1] *G. superba* is native to tropical Africa, south-eastern Asia and India and is now widely cultivated throughout the world as an ornamental plant. It is a climbing herb (Figure 4.1) with tendrils to cling onto other plants that can grow up to 6 m long. The leaves are dark green and glossy and they occur in whorls of 3 to 4, alternate, sessile, lanceolate and spear shaped with curved end. Flowers are large, solitary at the ends of branches, bicoloured yellow and red, and have six erect petals. The fruits are ellipsoid capsules that split open to release several smooth red seeds. The glory lily is a tuberous plant with V- or L-shaped, finger-like tubers that are pure white when young, becoming brown with the age.^[1, 2]



Figure 4.1 *Gloriosa superba* L.

G. superba is a well-known product that has been in regular demand amongst practitioners of traditional medicine in tropical Africa and Asia. It is one of the most important exported medicinal plants of India and is still often used in Ayurveda. Five different plant parts of *G. superba* are cited as important in ethnobotanical applications, i.e. leaves, seeds, unripe fruits, tubers and the whole plant. From all plant parts the tuber is the most frequently used. It is used as a germicide, to cure ulcers, piles, haemorrhoids, inflammation, scrofula, leprosy, dyspepsia, worm infections, flatulence, intermittent fevers, debilitating arthritis and snake bites.^[1, 3, 4] The tubers are also boiled with sesame oil and applied twice a day on the joints to reduce arthritis pain.^[2] The seeds are used for relieving rheumatic pain and as a muscle relaxant.^[4]

G. superba is one of the seven semi-poisonous drugs in the Indian traditional medicine, which cure many ailments but may prove fatal on misuse. Traditional healers seem to be aware of its toxicity as the amounts they prescribe to their patients are such that the toxic symptoms are minimised. The toxins of *G. superba* have an inhibitory action on cellular division resulting in diarrhoea, depressant action on bone marrow and alopecia. Its poisonous properties are mainly due to colchicine.^[1, 2] The alkaloids of *G. superba* also showed promising cytotoxic activity against numerous cancer cells.^[2]

Recently, there has been an increased demand for the plant as a source of colchicine and colchicoside. Colchicoside is largely used for the synthesis of thiocolchicoside, which is a prominent antimuscular drug for spasmodic ailments.^[3, 5] Therefore the seeds of *G. superba* are highly priced in the world market as source of colchicine.^[1]

4.2. ALKALOIDS

4.2.1. Colchicine

The best known constituent in *G. superba* is the alkaloid colchicine. Due to the anti-inflammatory activity it is now still used for the treatment of gout and the auto-immune disease Familial Mediterranean Fever (FMF).^[1]

Colchicine, which binds to tubulin and blocks microtubules formation (see below), remains the standard of therapy for preventing attacks of urate crystal arthritis (gout) and for treating FMF, subsequently interfering with migration and degranulation of white blood cells. It also inhibits the synthesis of tumour necrosis factor α (TNF α), leukotriene B₄ and the synthesis of mononuclear phagocytes. In FMF patients, mutated pyrin fails to regulate/inhibit caspase-1-dependent C5a degradation and as a consequence, an inappropriate inflammation occurs. Colchicine interferes with this inflammation by blocking the induction of inflammasomes, which is responsible for the activation of the inflammatory processes (Figure 4.2).^[6,7]

Colchicine also blocks cyclooxygenase-2 (COX-2) activity, prostaglandin E₂ and thromboxane A₂ synthesis of mononuclear phagocytes with subsequent reduction of swelling and pain.^[8] Therefore, it is also an effective drug treatment for intense pain associated with a gout attack and FMF.^[9]

The mechanism of action at the level of the microtubules makes colchicine very interesting for the treatment of cancer. Microtubules are dynamic structures that are required for a variety of cellular processes. They play an important role during mitosis. Mitosis is an ordered series of events in which identical copies of the genome are moved to two discrete locations within the dividing cell with the help of the microtubules.^[10, 11] Microtubules consist of two different tubulin units, α - and β -tubulin, that form a heterodimer. These heterodimers assemble head-to-tail into linear protofilaments that further polymerise to the hollow microtubule cylinder. This final structure is organised in a polar manner such that the α -tubulin subunit is exposed at one end (the minus end), while the β -tubulin subunit is exposed at the other end (the plus end) (Figure 4.3).^[12-14] During the major part of the cell cycle, microtubules form an

intracellular lattice-like structure. However, when cells enter mitosis, this microtubule network is reorganised into the mitotic spindle. The process of depolymerising the interphase microtubule structure and forming the mitotic spindle, as well as finding, attaching and separating chromosomes, require highly coordinated microtubule dynamics. Most anticancer drugs that interact with these structures disturb the microtubule dynamics, causing the mitosis to stop in the metaphase and thus arresting cell division.^[13]

Colchicine is often called a spindle poison, because of its interaction with tubulin and the mitotic spindle.^[10, 14] The colchicine-binding site is located at the center of the tubulin heterodimers. Colchicine binds at the interface of the α/β -tubulin heterodimers, forming a stable tubulin-colchicine complex that effectively suppresses microtubule dynamics upon binding to microtubule ends (Figure 4.3). Colchicine does not only have an effect on the dynamics of microtubules, but also causes microtubule depolymerisation by inhibiting lateral contacts between newly formed ends of protofilaments. At low tubulin-colchicine complex concentration, the microtubules still remain intact as the loss of lateral contacts remains small, but at higher concentration ($> 0.05 \mu M$), a greater loss of lateral contacts leads to disassembly of microtubules.^[14-16]

Cancer cells are more susceptible than normal cells considering their high division rate.^[1] Drugs that interact with tubulin polymerisation are divided into two groups: the stabilising and the destabilising agents.^[12, 13] Colchicine belongs to the group of the destabilising agents, because of its mode of action in higher concentrations, which is inducing depolymerisation of microtubules.^[12, 13, 17] For pure colchicine to have an anticancer effect the dose to be given to humans was reported to be so high it was excluded for toxicity reasons.^[12, 13, 17]

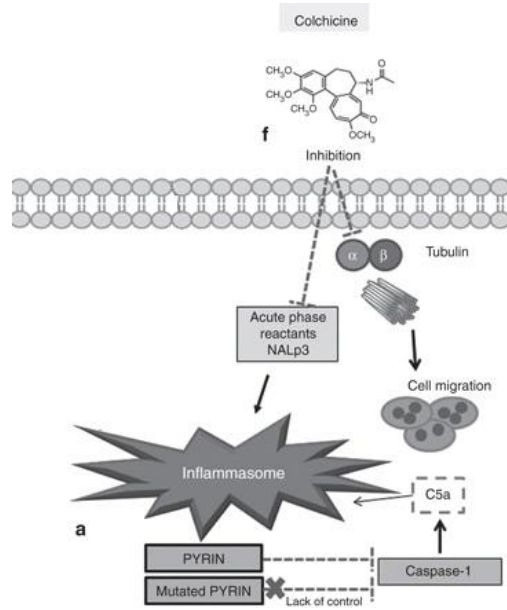


Figure 4.2 The inflammasome-pyrin interaction and mechanisms of action of colchicine in Familial Mediterranean Fever (Adapted from Grattagliano et al., 2013)

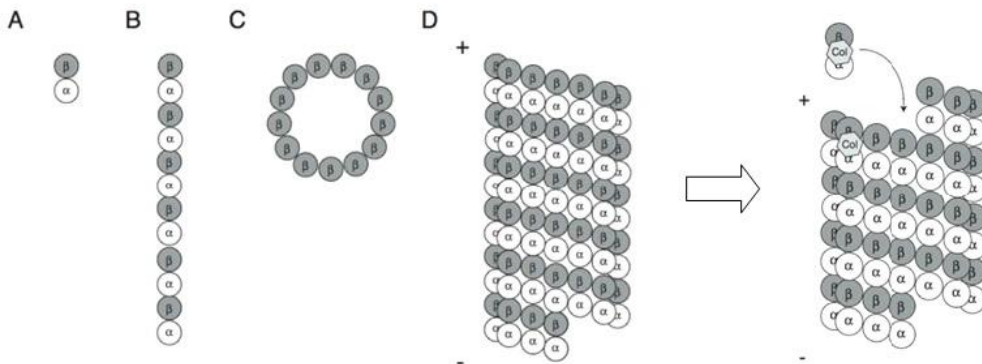


Figure 4.3 Microtubule structure. Tubulin heterodimers, composed of α- and β-subunits (A) that polymerise to form protofilaments (B) and create the hollow cylindrical structure of the microtubule (C-D) with β-tubulin at the plus end (+) and α-tubulin at the minus end (-). Colchicine (Col) binds at the α-/β-heterodimer and intercorporates into microtubules, causing a decrease of dynamicity (Adapted from Risinger et al., 2009)

4.2.2. Colchicine derivatives

Different colchicine derivatives have been isolated and identified from *G. superba*. Figure 4.4 shows the structures of the reported alkaloids.

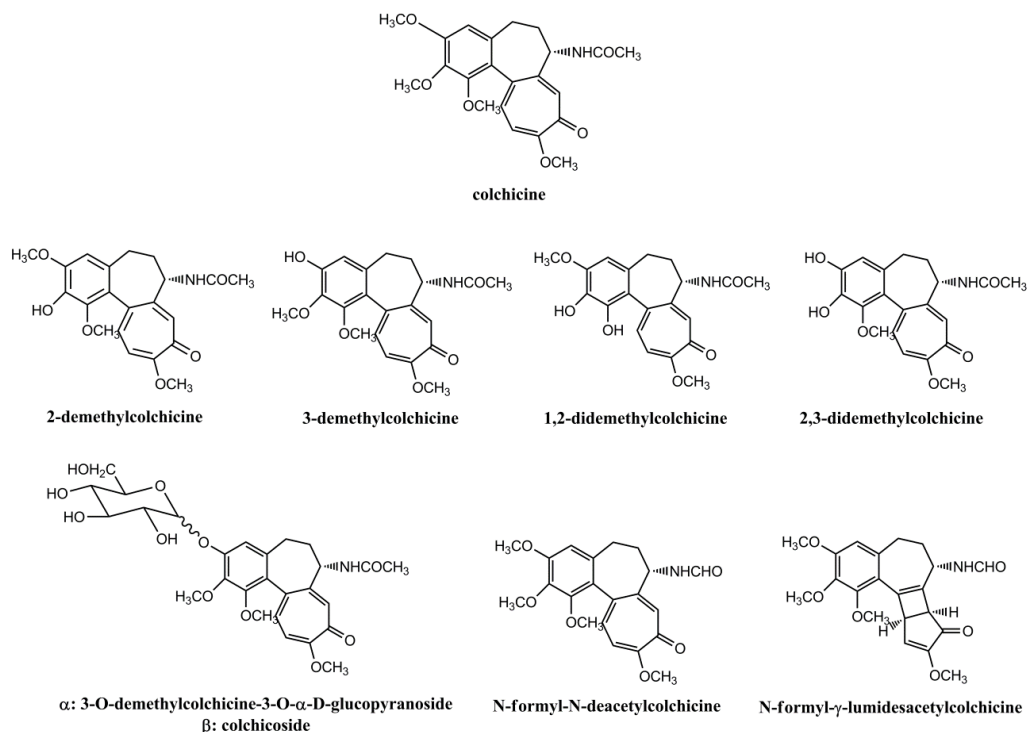


Figure 4.4 Colchicine and related alkaloids previously isolated from *Gloriosa superba* L. (Adapted from Jana et al., 2011; Chaudhuri et al., 1993; Suri et al., 2001; Nery et al., 2001)

In a study from 1975 constituents from various plant parts of *G. superba* were investigated. The seeds, tubers, leaves and flowers contained different alkaloids in different concentration. In the seeds colchicine was found together with three other alkaloids, namely N-formyl- γ -lumidesacetylcolchicine, N-formyl-N-deacetylcolchicine or gloriosine and 3-demethylcolchicine.^[18] Lumicolchicine is converted from colchicine by photolysis.^[19] In 1993, a new alkaloid was discovered from *G. superba* seeds, the 1,2-didemethylcolchicine. Other alkaloids, such as colchicine, N-formyl-N-deacetylcolchicine, 3-demethylcolchicine, 2,3-

didemethylcolchicine and 3-demethylcolchicine-3-*O*- β -D-glycoside or colchicoside were also reported in this study.^[20]

Because of the therapeutic interest in colchicoside and the lower toxicity compared to colchicine^[21, 22] colchicoside was isolated from *G. superba* seeds in 2001. In contrast to the expectation the glycoside appeared to be hydrolysed by α -glucosidase, indicating the presence of 3-*O*-demethylcolchicine-3-*O*- α -D-glucoopyranoside.^[23]

In an investigation to isolate colchicinoids from the *G. superba* seeds and to examine the anti-inflammatory activity, 2-demethylcolchicine was isolated.^[24]

Studies on the cytotoxic activity of *G. superba* extracts and pure alkaloids have also been conducted. The biological effects on cancer cells of modified colchicines were studied in 1981. Various colchicine derivatives have been synthesised, after which the activity *in vitro* and *in vivo* was compared with colchicine. This revealed a correlation between the *in vivo* potency and toxicity. The 3-demethylcolchicine (3.6 $\mu\text{mol/kg}$) structure still had a reasonable potency compared to colchicine (0.4 $\mu\text{mol/kg}$), in contrast to the 2-demethylcolchicine (13.8 $\mu\text{mol/kg}$). Colchicoside was not active *in vitro* but was not tested *in vivo*.^[25] Colchicoside, however, can act as a prodrug of the glycosidic 3-demethylcolchicine, which may explain the inactivity *in vitro*.

In 2000 an article was published on the cytotoxicity of some medicinal plants from Tanzanian traditional medicine. The methanol extracts from the plants were tested at a concentration of 10 and 100 $\mu\text{g/mL}$ in three cancer cell lines (HeLa, HT-29 and A431). The extract of *G. superba* reduced the cell proliferation in each case by at least 50% compared to the control cells, most likely due to the presence of colchicine.^[26]

4.3. PHYTOCHEMICAL CHARACTERISATION

4.3.1. **Plant material**

The *Gloriosa superba* L. seeds (Figure 4.5) were kindly provided by Indena® (batch n° C140020) and were obtained in February 2011. A certificate of analysis n° 11/0208/LSP was included as well as a proof of identification in the IDB herbarium.



Figure 4.5 *Gloriosa superba* seed

4.3.2. **Extraction**

The seeds of *G. superba* L. were dried an extra two weeks in an oven at a temperature of 45 °C. The seeds were then ground and sieved through a 2 mm sieve. The ground seeds (5.3 kg) were extracted exhaustively and consecutively by percolation and maceration with 95 L of 80% ethanol at room temperature. The ethanol was removed under reduced pressure at 40 °C and the aqueous extract was lyophilised. The yield of the crude extract was 846.7 g.

4.3.3. Isolation of the main constituents

4.3.3.1. Thin layer chromatography of the *G. superba* crude extract

Normal phase and reverse phase TLC were performed on the *G. superba* crude extract (GS). A 10 mg/mL GS solution was prepared in MeOH and 10 μ L was applied as a band of 5 mm and developed over a path of 8 cm using different mobile phases. The TLC plates were examined at a wavelength of 254 nm and 366 nm. The developed plates were also sprayed with the *p*-anisaldehyde reagent and heated at a temperature of 105 °C until maximal visualisation. The best elution was obtained by using a mixture of 75% ethyl acetate and 25% methanol. Three main zones were observed (Figure 4.6).

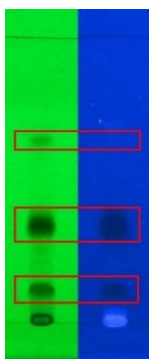


Figure 4.6 TLC profile of GS on a silica TLC plate at 254 nm and 366 nm

4.3.3.2. High performance liquid chromatography of the *G. superba* crude extract

An HPLC chromatogram was recorded of the crude extract. The sample solution was prepared with a concentration of 5.02 mg/mL in methanol. A colchicine standard solution was also prepared with a concentration of 0.31 mg/mL in methanol. The injection volume was 20 μ L for both solutions. The mobile phases were (A) water with 0.05% TFA and (B) acetonitrile. A Grace Apollo C₁₈ column was used on the Agilent 1200 HPLC system. The gradient was 0 min, 5% B; 5 min, 5% B; 55 min, 100% B; 60 min, 100% B. The flow rate was 1.0 mL/min and the column thermostat was set at 25 °C. Chromatograms were recorded at different wavelengths

(210, 230, 254, 280, 300 and 350 nm). Figure 4.7 shows the chromatograms of the *G. superba* crude extract and the colchicine standard at 350 nm. On the chromatogram of the crude extract 3 main compounds were detected of which compound C had a similar retention time as the colchicine reference compound.

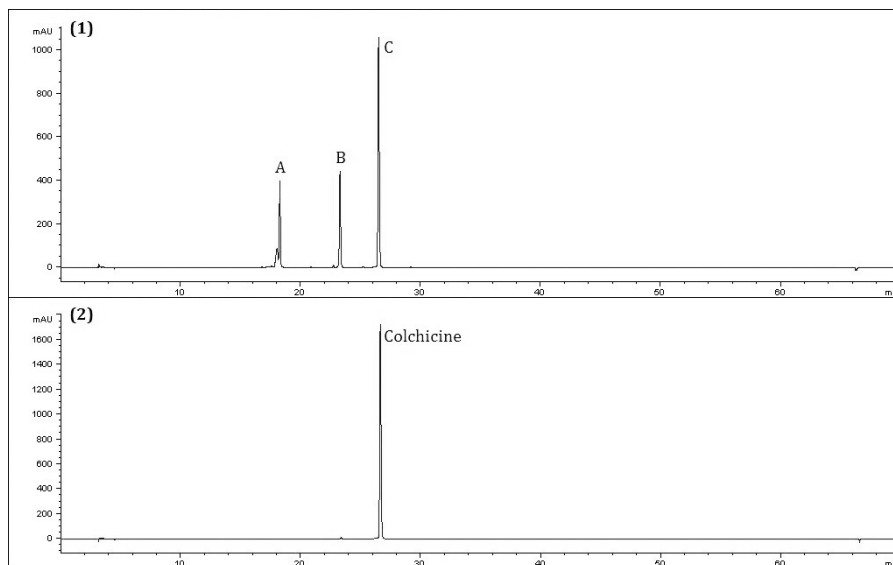


Figure 4.7 HPLC chromatograms of the crude extract of the seeds of *G. superba* (1) and colchicine standard (2)

4.3.3.3. LC-SPE-NMR of the *G. superba* crude extract

The HPLC chromatogram and TLC of the crude extract showed 3 main compounds which were isolated and identified with the help of the LC-SPE-NMR. A concentrated solution (10.3 mg/mL) of the crude extract was prepared and 30 μ L of this solution was injected. The flow rate was set at 1.0 mL/min and the detector at 350 nm. Mobile phase A was water containing TFA (0.05%) and B was acetonitrile. The gradient was optimised and the final gradient was 0 min, 5% B; 5 min, 5% B; 50 min, 32 % B; 55 min, 100% B and 60 min, 100% B. Seventeen multi-trapping were performed and repeated three times. The separated peaks were then captured on the HySphere resin GP cartridges (Figure 4.8) by setting a threshold for automatic

multi-trapping. The cartridges were dried with N₂ and the separated compounds were then eluted one by one with deuterated acetonitrile in 3 mm NMR tubes. The ¹H NMR, ¹³C NMR and 2D were recorded. The first series of multi-trappings was sufficient for compound C to record 1D (¹H and ¹³C) and 2D (COSY, HSQC and HMBC) spectra, but for compounds B and A, a second series of multi-trapping experiments was necessary. A more concentrated solution (13.2 mg/mL) was prepared and 40 µl of this solution was injected. Thirty multi-trappings were performed and repeated three times. This yielded sufficient material on the cartridges to record ¹H NMR but also 2D NMR spectra (COSY, HSQC and HMBC).

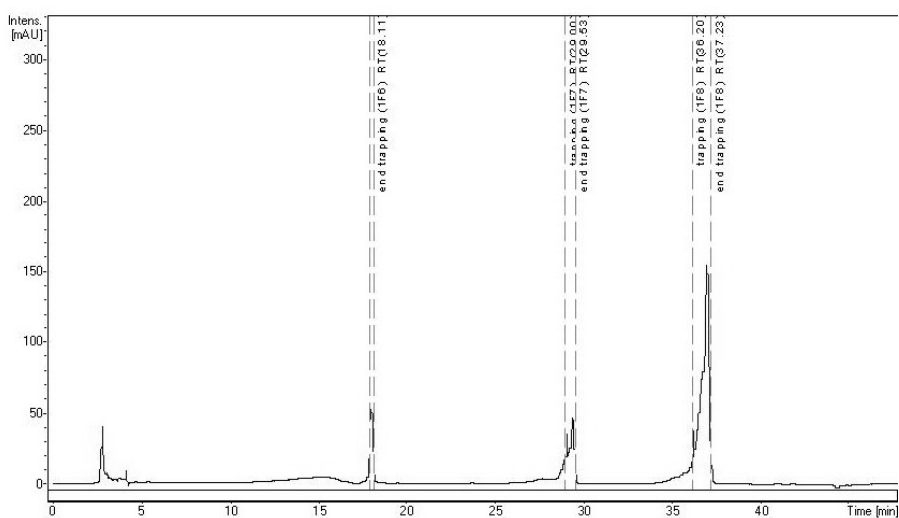


Figure 4.8 Chromatogram (UV detection at 350 nm) of the crude extract recorded on the LC-SPE-NMR instrument, showing the three compounds being trapped onto the cartridges

4.3.4. Structure elucidation of the main constituents

The structures of the isolated compounds were elucidated mainly by NMR spectroscopy, and confirmed by mass spectrometry.

4.3.4.1. Colchicine

The structure of compound C was elucidated by ^1H , ^{13}C and 2D NMR (COSY, HSQC and HMBC) as *N*-[(7*S*)-1,2,3,10-tetramethoxy-9-oxo-6,7-dihydro-5*H*-benzo[*a*]heptalen-7-yl]acetamide or **colchicine** (Figure 4.9).

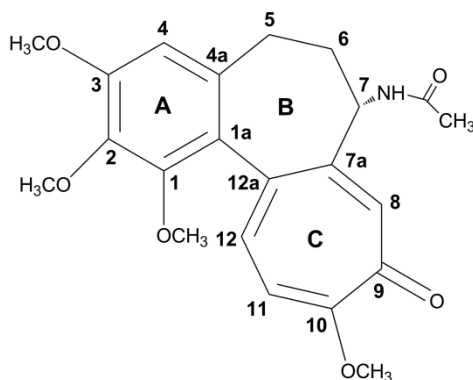


Figure 4.9 The structure of compound C (colchicine)

The structure of compound C was confirmed by comparison with spectral data found in the literature^[27-29] and by analysis of the COSY, HSQC and HMBC correlations. Table 4.1 and Figure 4.10 show the ^1H NMR spectral assignments and the ^1H NMR spectrum, respectively. The doublet observed at 6.94 ppm was assigned to the N-H proton, and the singlet at 7.17 ppm to the aromatic H-8 proton. The two other aromatic protons (H-11 and H-12) in the C ring corresponded with the two coupled doublets ($J = 10.7$ Hz) at 6.90 and 7.13 ppm. In the aromatic ring A H-4 was assigned to the singlet at 6.69 ppm. At 4.35 ppm a multiplet was assigned to H-7. The 2 protons on position 5 gave 2 multiplets at 2.34 and 2.55 ppm and in the same ring, the 2 protons on position 6 gave 2 multiplets at 1.78 and 2.07 ppm. The protons from the methoxy groups on positions 1, 2, 3 and 10 were assigned to the singlets at 3.61,

3.83, 3.86 and 3.90 ppm, respectively. The protons of the methyl group next to the amide functionality gave a singlet at 1.88 ppm. These assignments were in good agreement with the COSY (Figure 4.12). Figure 4.11 and Table 4.1 show the ^{13}C NMR spectrum and assignments, respectively. Not all carbons could be observed in the ^{13}C spectrum, due to the low concentration resulting in a low signal/noise ratio. Indeed, quaternary carbons produce small signals due to the lack of attached protons resulting in long relaxation times. The carbons that were not present in the ^{13}C NMR spectrum were determined by HSQC (Figure 4.13) and HMBC (Figure 4.14). The aromatic carbons C-11 and C-12 were assigned to the signals at 113.0 and 135.5 ppm, respectively. In the same aromatic ring C-7 and C-8 were assigned to the signals at 53.1 and 131.6 ppm, respectively. The signal at 108.8 ppm was assigned to C-4 in ring A. C-5 and C-6 were assigned to the signal at 30.5 and 37.0 ppm and the acetyl-methyl to the signal at 22.9 ppm. The acetyl-carbonyl corresponded with the signal at 170.3 ppm and the carbonyl on position 9 corresponded with the signal at 179.7 ppm. The four methoxy groups in position 1, 2, 3 and 10 gave signals at 61.8, 61.6, 56.8 and 57.0 ppm, respectively. The protons of these methoxy groups correlated in the HMBC spectrum with the carbon signals at 151.9 (C-1), 142.2 (C-2), 154.3 (C-3) and 165.1 (C-10). The remaining quaternary carbons were found at 135.6 (C-1a), 126.8 (C-4a), 151.8 (C-7a) and 136.6 (C-12a) ppm.

A mass spectrum was recorded showing a pseudo molecular ion $[\text{M} + \text{H}]^+$ with m/z 400 consistent with a molecular formula of $\text{C}_{22}\text{H}_{25}\text{NO}_6$ and the UV spectrum showed UV absorption maxima at 245 and 352 nm as reported for colchicine.^[30, 31]

Table 4.1 ¹H (400 MHz) and ¹³C (100 MHz) NMR assignments for compound **C** (colchicine) (CD₃CN)

Position	δ_{H} (ppm); multiplicity; <i>J</i> (Hz)	δ_{C} (ppm)
1	-	151.9
1a	-	135.6
2	-	142.2
3	-	154.3
4	6.69; s	108.8
4a	-	126.8
5	2.34; m 2.55; m	30.5
6	1.78; m 2.07; m	37.0
7	4.35; m	53.1
7a	-	151.8
8	7.17; s	131.6
9	-	179.7
10	-	165.1
11	6.90; d; 10.7	113.0
12	7.13; d; 10.7	135.5
12a	-	136.6
CH₃O (1)	3.61; s	61.8
CH₃O (2)	3.83; s	61.6
CH₃O (3)	3.86; s	56.8
CH₃O (10)	3.90; s	57.0
C=O (CH₃)	-	170.3
CH₃ (C=O)	1.88; s	22.9
NH	6.94; d; 7.7	

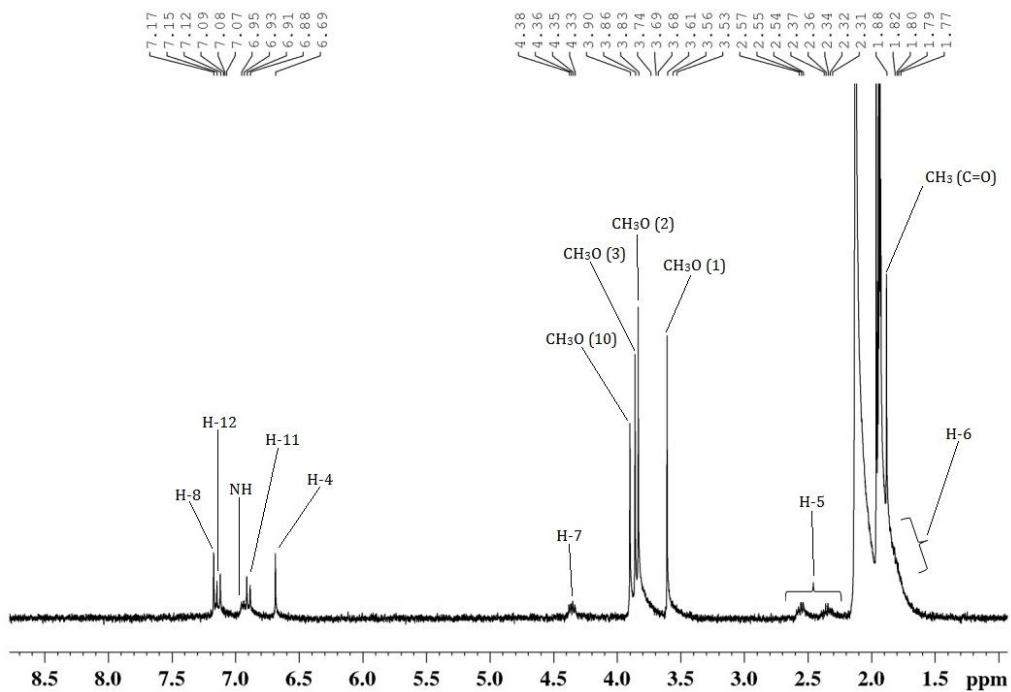


Figure 4.10 ^1H spectrum of compound C (colchicine)

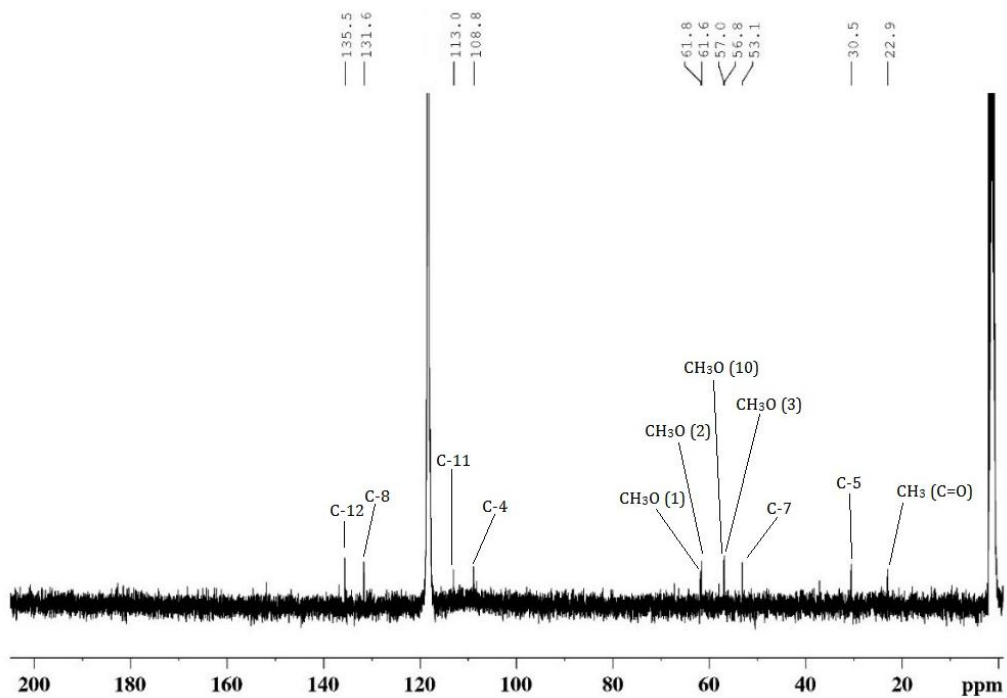


Figure 4.11 ^{13}C spectrum of compound C (colchicine)

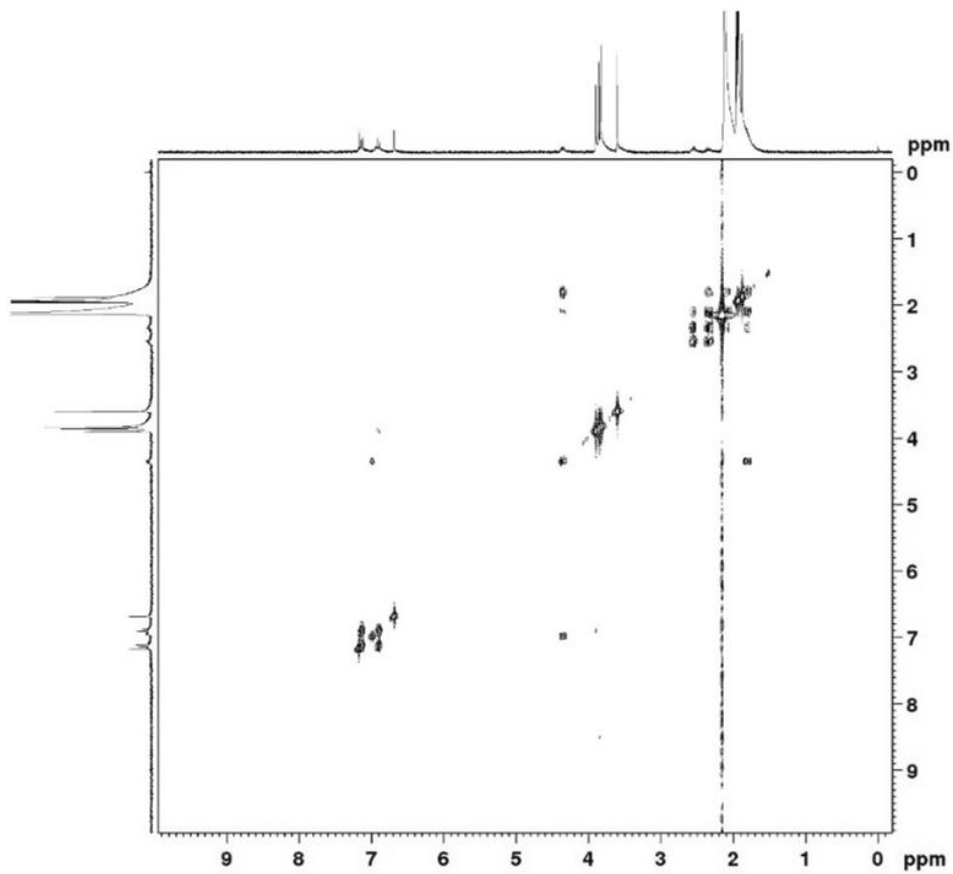


Figure 4.12 COSY spectrum of compound C (colchicine)

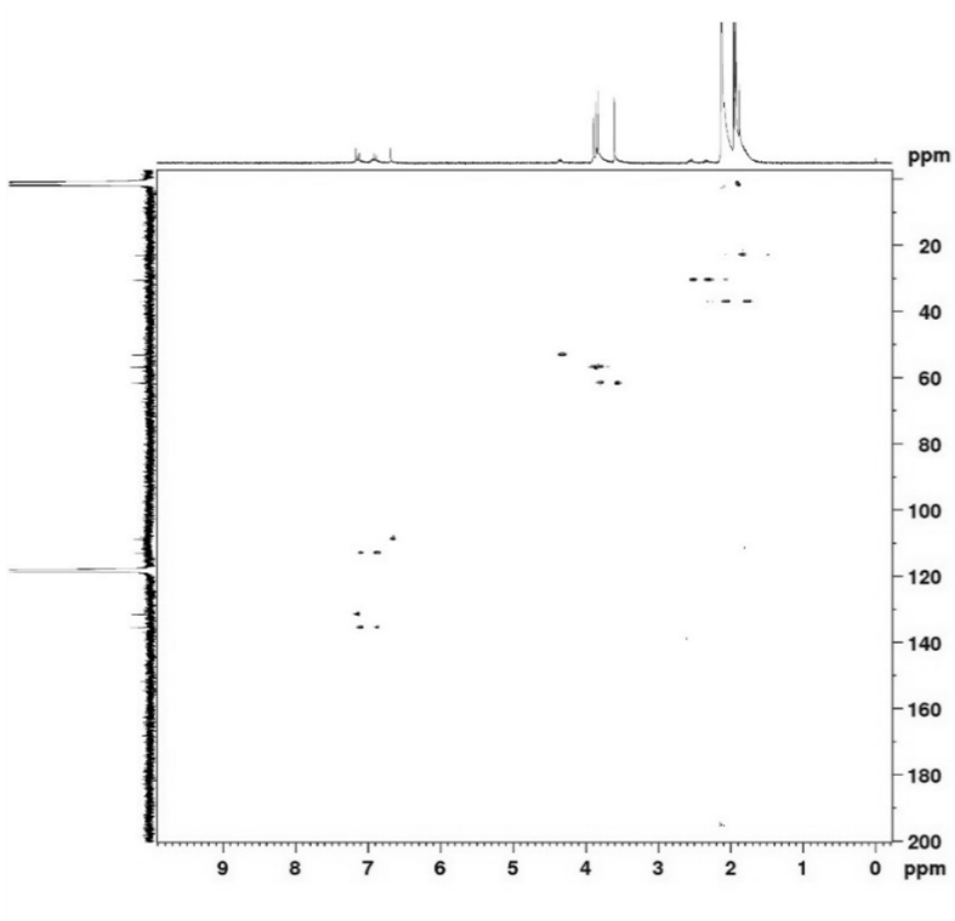


Figure 4.13 HSQC spectrum of compound C (colchicine)

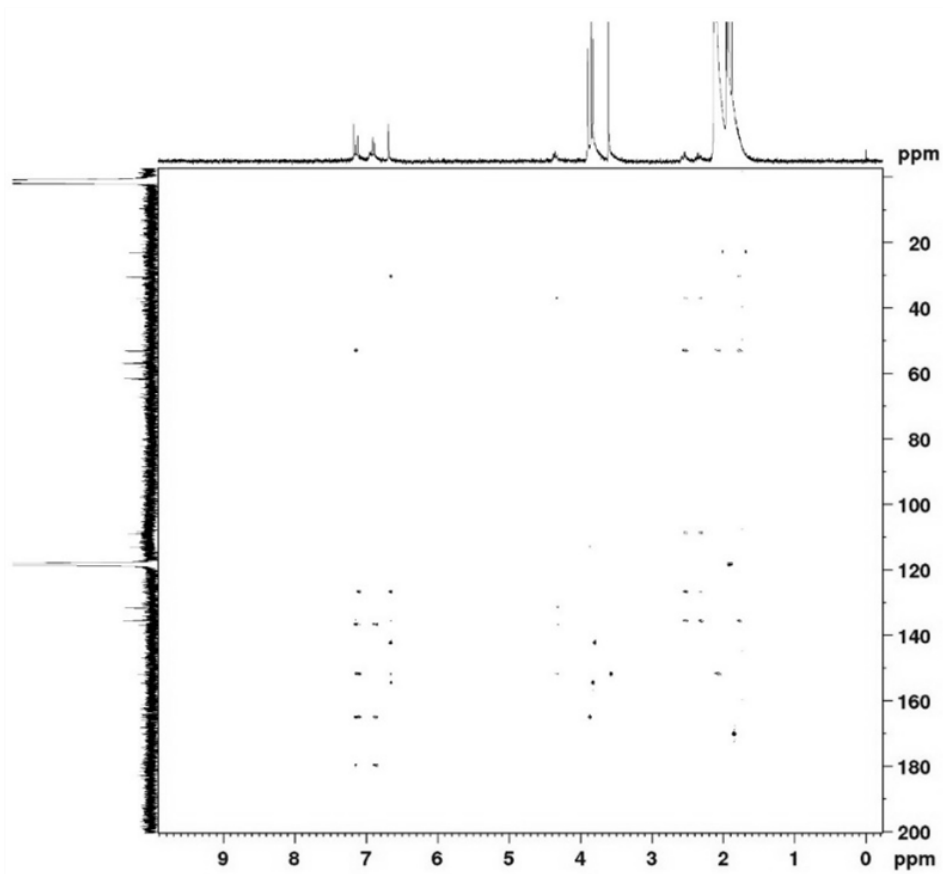


Figure 4.14 HMBC spectrum of compound C (colchicine)

4.3.4.2. 3-*O*-demethylcolchicine

The structure of compound B was elucidated by ^1H and 2D NMR (COSY, HSQC and HMBC) as *N*-[(7*S*)-3-hydroxy-1,2,10-trimethoxy-9-oxo-6,7-dihydro-5*H*-benzo[*a*]heptalen-7-yl]acetamide or **3-*O*-demethylcolchicine** (Figure 4.15).

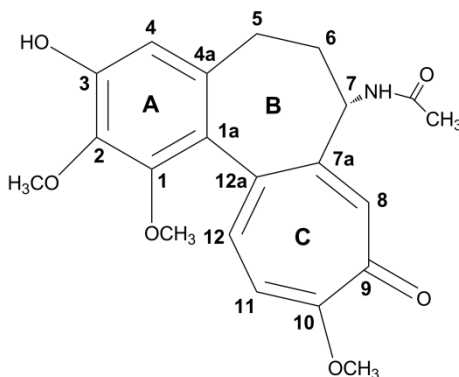


Figure 4.15 The structure of compound **B** (3-*O*-demethylcolchicine)

The structure was identified by comparing the one-dimensional spectral data with data found in the literature and by analysis of the two-dimensional spectra (COSY, HSQC and HMBC correlations).^[29] The ^1H NMR spectrum (Figure 4.16) showed similarity with that of colchicine, with 3 methoxy groups instead of 4, indicating a demethyl derivative of colchicine. The assignment of the protons is summarised in Table 4.2. The doublet observed at 6.95 ppm was assigned to the N-H proton. The singlet at 7.16 ppm was assigned to the aromatic H-8 proton. The two other aromatic protons (H-11 and H-12) in the C ring corresponded with the two coupled doublets ($J = 10.6$ Hz) at 6.89 and 7.13 ppm, respectively. In the aromatic ring A, H-4 was assigned to the singlet at 6.53 ppm. At 4.37 ppm a multiplet was assigned to H-7. The 2 protons at position 5 gave 2 multiplets at 2.29 and 2.48 ppm and in the same ring, the 2 protons at position 6 gave 2 multiplets at 1.77 and 2.08 ppm. The protons of the methyl next to the amide group gave a singlet at 1.87 ppm. The protons of the methoxy groups at position 1, 2 and 10 were assigned to the singlets at 3.59, 3.87 and 3.89 ppm, respectively. The COSY spectrum (Figure 4.17) was in good agreement with these assignments. The signals of the

carbons were derived from the analysis of the HSQC (Figure 4.18) and HMBC (Figure 4.19) spectra and are summarised in Table 4.2. The HSQC as well as the HMBC spectra showed good similarity with these of colchicine. In the HSQC spectrum the protons of the methoxy groups (3.59, 3.87 and 3.89 ppm) correlated with the carbon signals at 61.4, 61.7 and 56.8 ppm, respectively. Taking into account the ^{13}C NMR assignments of colchicine and the HMBC correlations these methoxy groups were assigned to the quaternary carbons in position 1 (151.6 ppm), 2 (140.4 ppm) and 10 (164.9 ppm), indicating that this compound is 3-*O*-demethylcolchicine.

A mass spectrum was recorded showing a pseudo molecular ion $[\text{M} + \text{H}]^+$ with m/z 386 consistent with a molecular formula of $\text{C}_{21}\text{H}_{23}\text{NO}_6$ and the UV spectrum showed UV absorption maxima at 244 and 353 nm.^[30]

Table 4.2 ¹H (400 MHz) and ¹³C (100 MHz) NMR assignments for compound **B** (3-*O*-demethylcolchicine) (CD₃CN)

Position	δ_H (ppm); multiplicity; J (Hz)	δ_C (ppm)
1	-	151.6
1a	-	136.1
2	-	140.4
3	-	151.1
4	6.53; s	111.4
4a	-	126.0
5	2.29; m 2.48; m	30.1
6	1.77; m 2.08; m	36.9
7	4.37; m	53.1
7a	-	151.8
8	7.16; s	131.5
9	-	179.6
10	-	164.9
11	6.89; d; 10.6	112.8
12	7.13; d; 10.6	135.3
12a	-	136.7
CH₃O (1)	3.59; s	61.4
CH₃O (2)	3.87; s	61.7
CH₃O (10)	3.89; s	56.8
C=O (CH₃)	-	170.0
CH₃ (C=O)	1.87; s	22.9
NH	6.95; d; 7.2	-

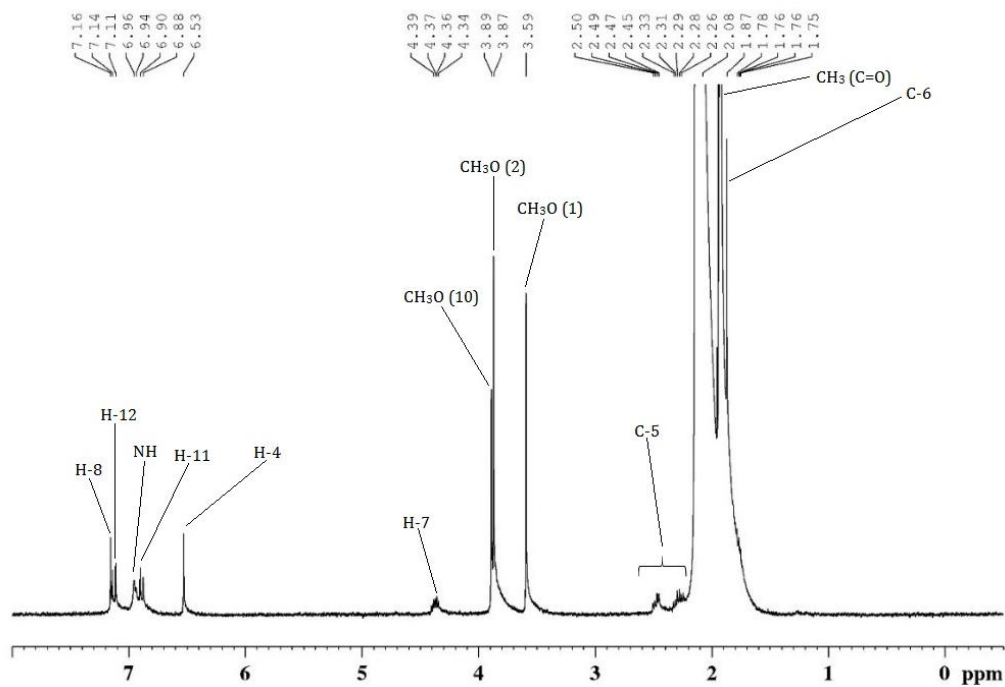


Figure 4.16 ¹H spectrum of compound **B** (3-*O*-demethylcolchicine)

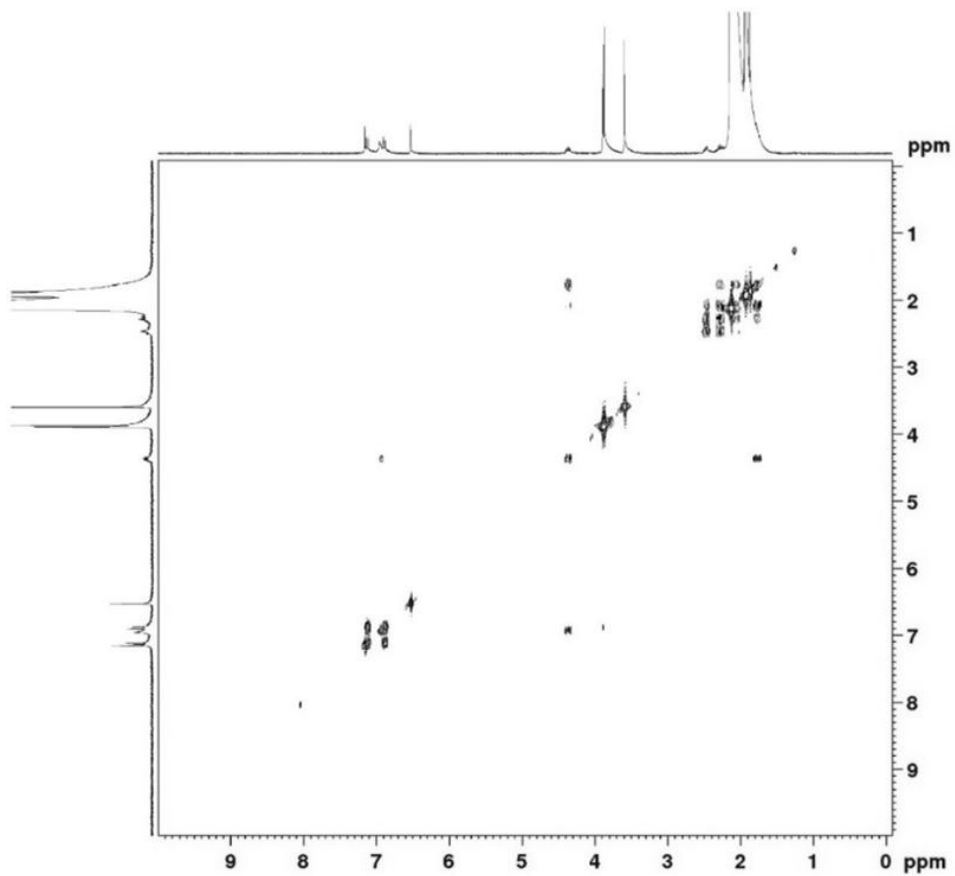


Figure 4.17 COSY spectrum of compound **B** (3-*O*-demethylcolchicine)

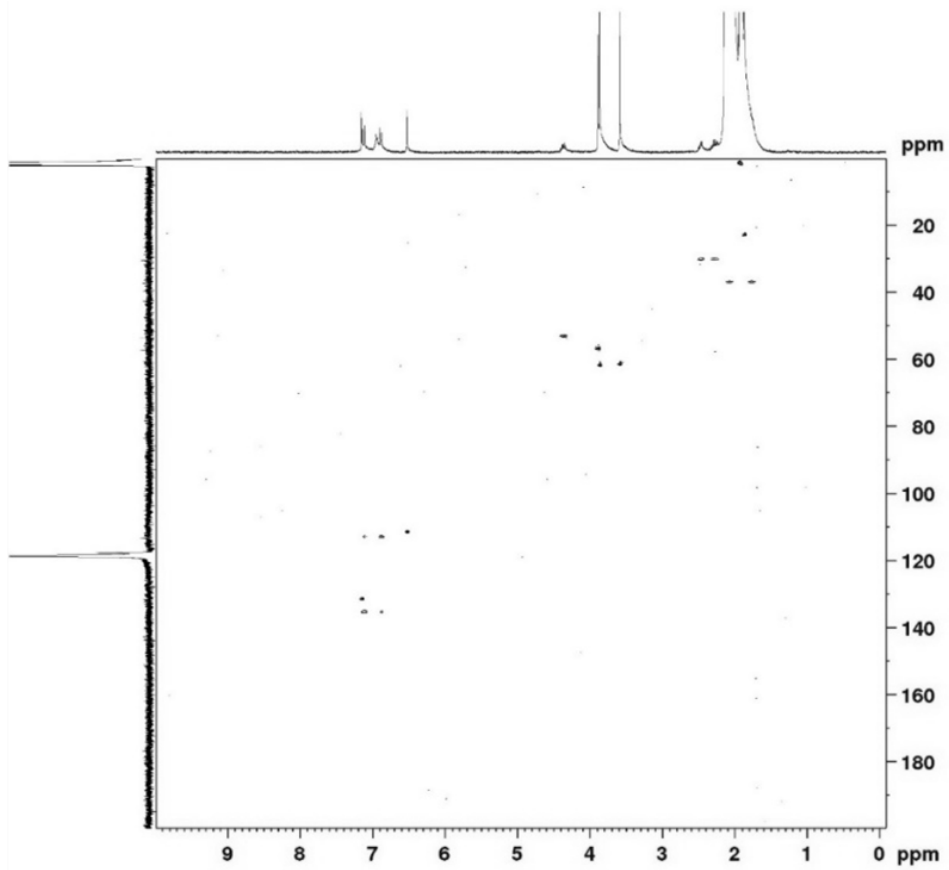


Figure 4.18 HSQC spectrum of compound **B** (3-*O*-demethylcolchicine)

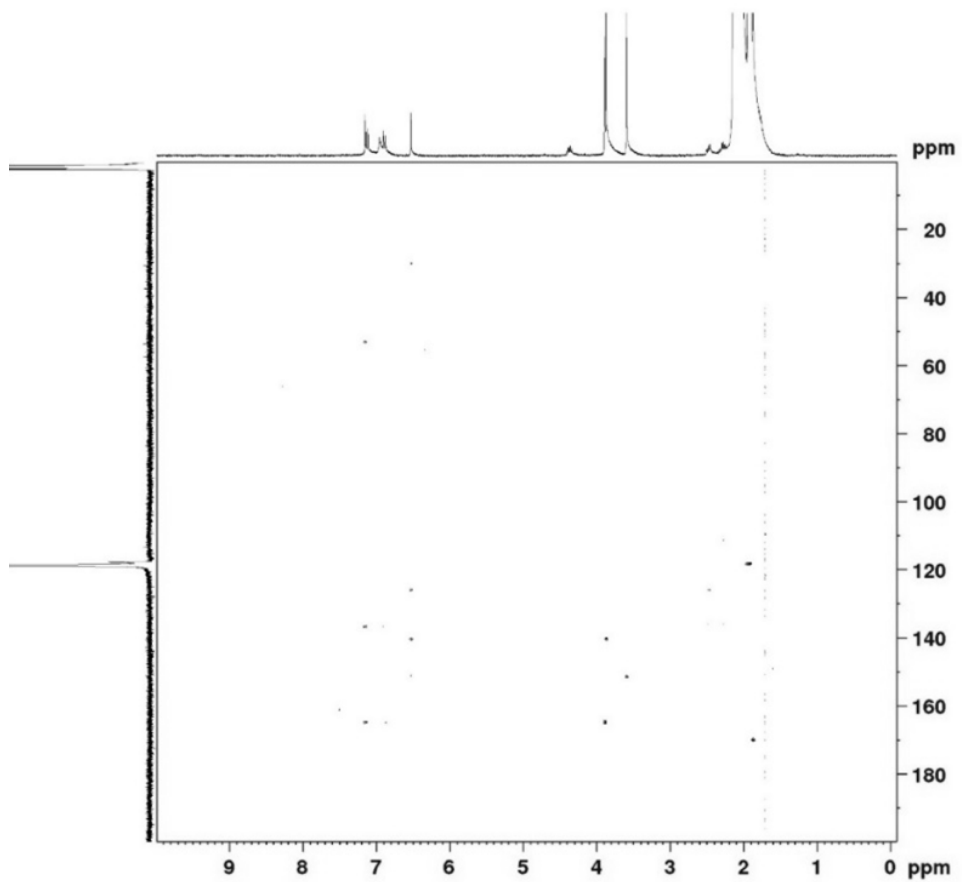


Figure 4.19 HMBC spectrum of compound B (3-O-demethylcolchicine)

4.3.4.3. Colchicoside

The structure of compound A was elucidated by ^1H and 2D NMR (COSY, HSQC and HMBC) as *N*-[(7*S*)-1,2,10-trimethoxy-9-oxo-3-[(2*S*,3*R*,4*S*,5*S*,6*R*)-3,4,5-trihydroxy-6-(hydroxymethyl)oxan-2-yl]oxy-6,7-dihydro-5*H*-benzo[*a*]heptalen-7-yl]acetamide or 3-*O*-demethyl-colchicine-3-*O*- β -*D*-glucopyranoside or **colchicoside** (Figure 4.20).

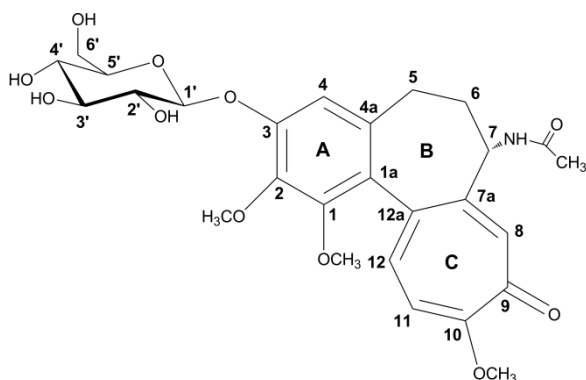


Figure 4.20 The structure of compound A (colchicoside)

The structure was identified by comparison with spectral data found in the literature and by analysis of the COSY, HSQC and HMBC correlations.^[32] The ^1H NMR spectrum (Figure 4.21) showed similarity with that of colchicine and indicated an *O*-glycoside analogue of colchicine. The ^1H NMR assignments are summarised in Table 4.3. The doublet observed at 6.95 ppm was assigned to the N-H proton. The singlet at 7.16 ppm was assigned to the aromatic H-8 proton. The two other aromatic protons (H-11 and H-12) in the C ring corresponded with the two coupled doublets ($J = 10.8$ Hz) at 6.89 and 7.13 ppm, respectively. In the aromatic ring A, H-4 was assigned to the singlet at 6.81 ppm. At 4.35 ppm a multiplet was assigned to H-7. The 2 protons at position 5 gave 2 multiplets at 2.33 and 2.52 ppm and in the same ring, the 2 protons at position 6 gave 2 multiplets at 1.77 and 2.09 ppm. The protons of the methoxy groups in position 1, 2 and 10 were assigned to the singlets at 3.62, 3.88 and 3.89 ppm, respectively. The protons of the acetyl-methyl group gave a singlet at 1.88 ppm. The anomeric proton H-1' of the glucose unit gave a doublet at 4.96 ppm with a coupling constant of $J = 7.1$

Hz, indicating a β -configuration.^[33] The multiplets at 3.42 and 3.35 ppm were assigned to the protons at position 2' and 4', respectively. The overlapping multiplets at 3.41 ppm were assigned to H-3' and H-5'. The signals of the two protons in position 6' were found at 3.62 and 3.77 ppm. The COSY spectrum (Figure 4.22) was in agreement with these assignments. ¹³C NMR was not recorded but the carbons were acquired from the HSQC (Figure 4.23) and HMBC (Figure 4.24) spectra and are summarised in Table 4.3. The carbon signals of the aglycon moiety showed great resemblance with those of 3-*O*-demethylcolchicine. Based on these signals, this compound was elucidated as a 3-*O*-demethylcolchicine-3-*O*- β -glucopyranoside. The HMBC correlations from H-1 to C-3 indicated that the glycosyl moiety was attached to C-3. This was also in agreement with the assignments for 3-*O*-demethylcolchicine.

A mass spectrum was recorded showing a pseudo molecular ion $[M + H]^+$ with m/z 548 consistent with a molecular formula of $C_{27}H_{33}NO_{11}$ and the UV spectrum showed UV absorption maxima at 245 and 349 nm.^[32]

Table 4.3 ¹H (400 MHz) and ¹³C (100 MHz) NMR assignments for compound **A** (colchicoside) (CD₃CN)

Position	δ_{H} (ppm); multiplicity; <i>J</i> (Hz)	δ_{C} (ppm)
1	-	150.9
1a	-	134.7
2	-	141.9
3	-	150.9
4	6.81; s	111.6
4a	-	127.5
5	2.33; m 2.52; m	29.3
6	1.77; m 2.09; m	35.7
7	4.35; m	51.8
7a	-	150.5
8	7.16; s	130.4
9	-	178.6
10	-	164.0
11	6.89; d; 10.8	111.7
12	7.13; d; 10.8	134.5
12a	-	135.2
CH₃O (1)	3.62; s	60.7
CH₃O (2)	3.88; s	60.9
CH₃O (10)	3.89; s	55.8
C=O (CH₃)	-	178.5
CH₃ (C=O)	1.88; s	21.7
NH	6.95; d; 6.5	-
1'	4.96; d; 7.1	101.2
2'	3.42; m	73.3
3'/5'	3.41; m	76.4
4'	3.35; m	70.0
6'	3.62; m 3.77; m	61.4

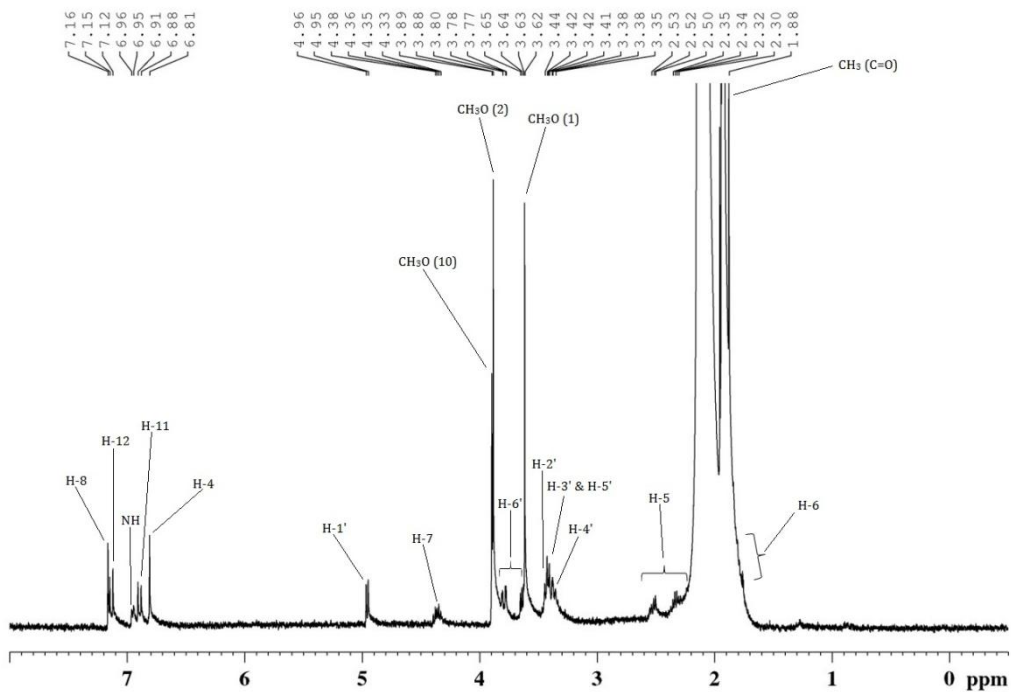


Figure 4.21 ¹H spectrum of compound A (colchicoside)

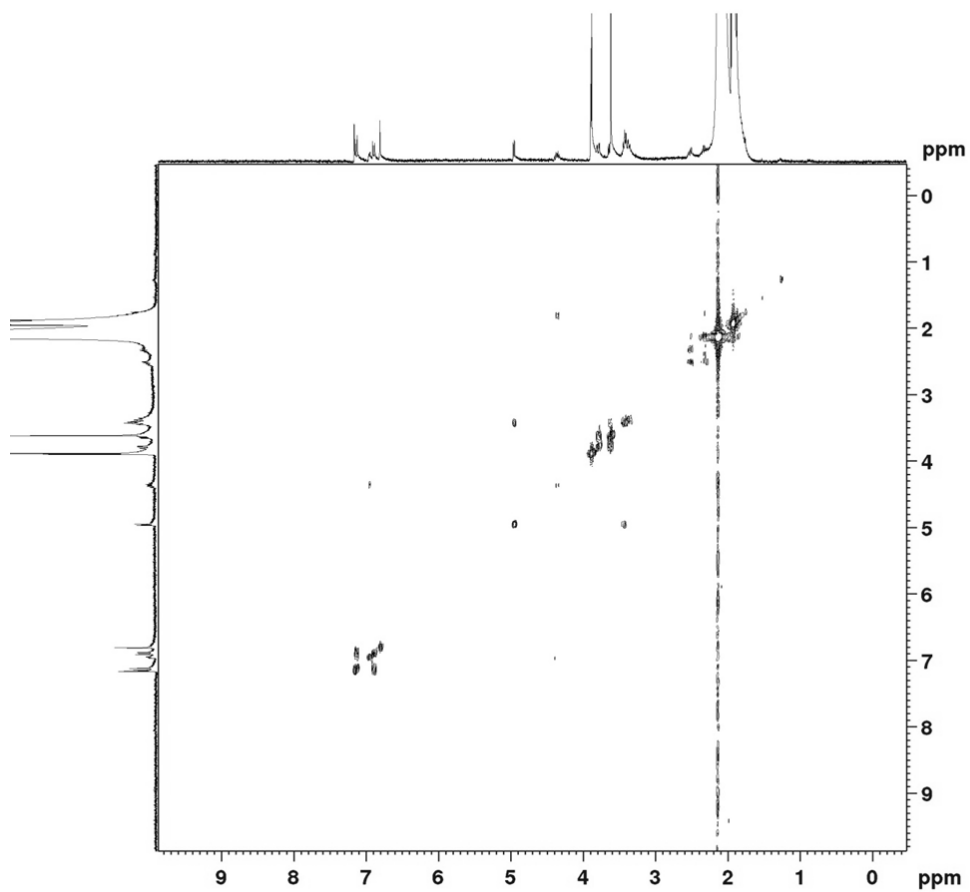


Figure 4.22 COSY spectrum of compound A (colchicoside)

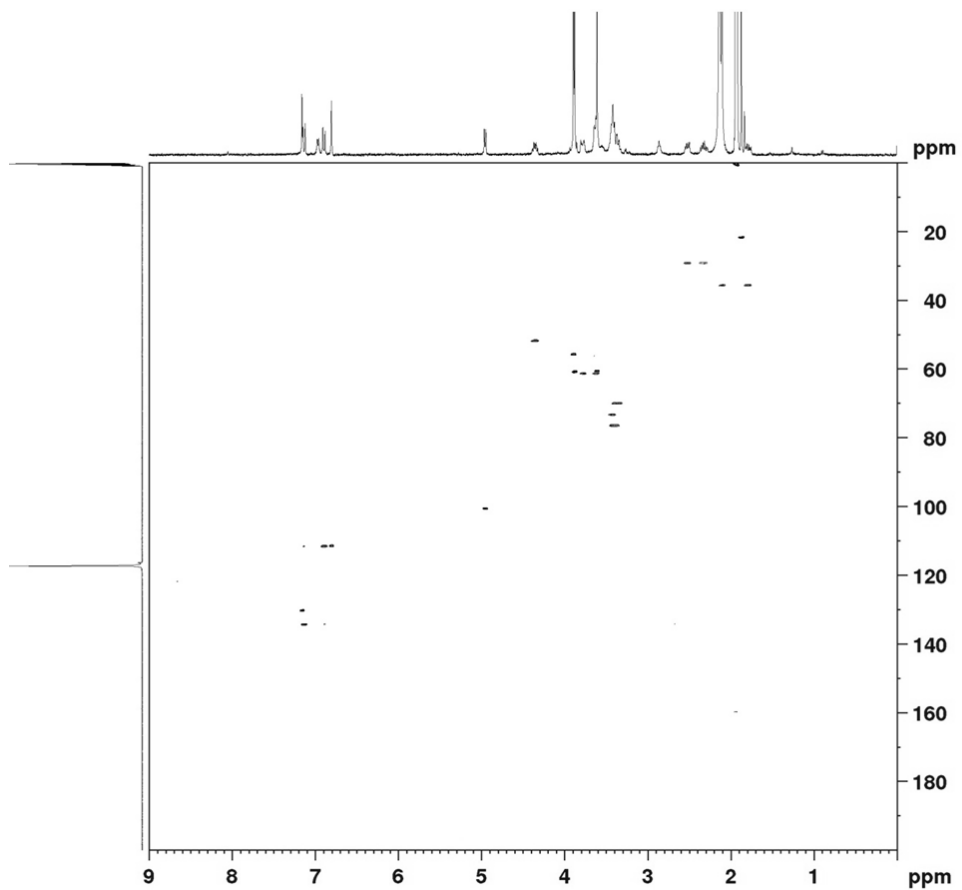


Figure 4.23 HSQC spectrum of compound A (colchicoside)

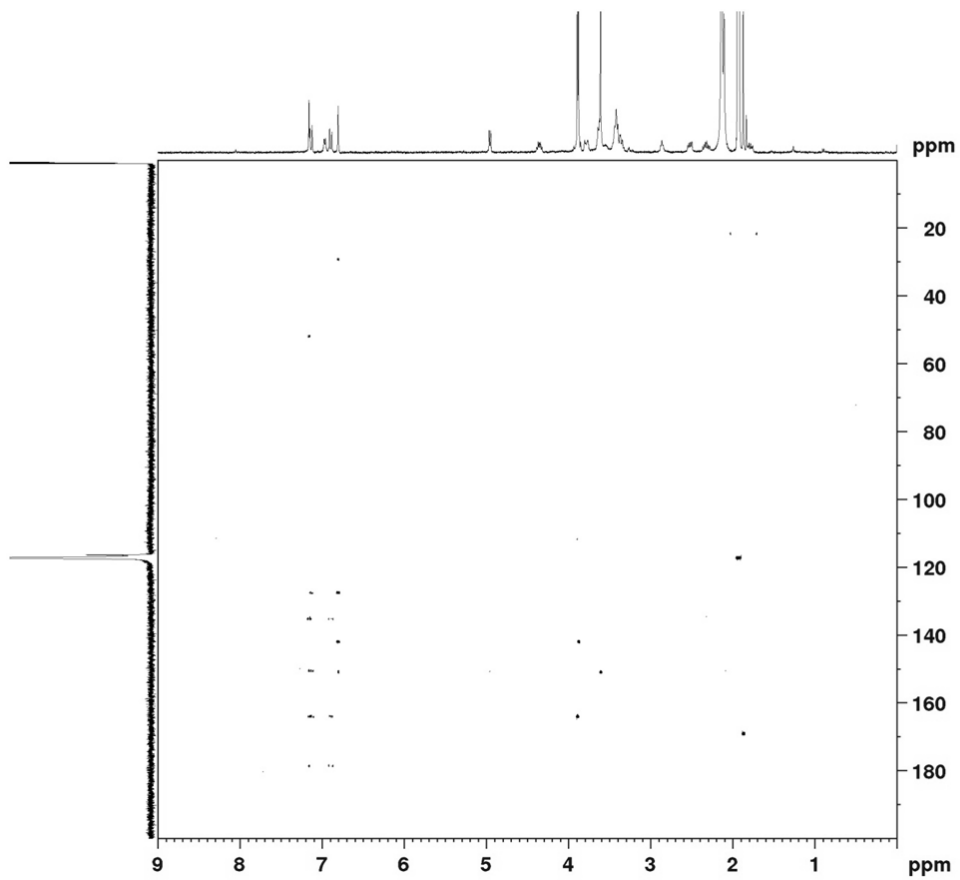


Figure 4.24 HMBC spectrum of compound A (colchicoside)

4.3.5. Colchicine-poor extract

One of the main constituents of the *G. superba* extract is colchicine. Due to known toxicity of colchicine^[13] and the presence of colchicine derivatives that may have the same activity or act as a prodrug, a second extract was prepared by means of liquid-liquid partition, starting from the crude extract, and aiming to develop an extract with a relatively low level of colchicine and a relatively high content of colchicine derivatives, especially colchicoside.

4.3.5.1. Liquid-liquid partition

Liquid-liquid partition was performed according to the scheme used by Ondra et al.^[34], Ellington et al.^[35], Al-Mahmoud et al.^[36], with some modifications. Figure 4.25 shows the scheme of the liquid-liquid partition used in this work. About 50 g of the crude dry extract (mentioned in section 4.3.2) was dissolved in 300 mL 5% acetic acid (pH 2.37). This solution was extracted three times with 300 mL diethyl ether. The organic fraction GS1A was concentrated under reduced pressure at 40 °C to 150 mL and washed once with 150 mL freshly prepared 5% acetic acid. The aqueous fractions (GS1B) were pooled and concentrated under reduced pressure at 40 °C to 300 mL. Fraction GS1B was then extracted three times with 300 mL methylene chloride. After concentrating the methylene chloride fraction to 300 mL, this organic fraction (GS2A) was washed with 300 mL freshly prepared 5% acetic acid. Again the aqueous fractions (GS2B) were pooled and evaporated to 300 mL. The aqueous fraction was made alkaline by adding ammonium hydroxide (25%) until pH 9 was reached. This fraction was then extracted three times with 300 mL methylene chloride. The organic phase was concentrated again and washed with 300 mL freshly prepared alkaline water (pH 9). The obtained fractions GS1A, GS2A and GS3A were evaporated until dryness and fraction GS3B was lyophilised. The yield of the obtained fractions was 2.58 g, 1.73 g, 0.07 g and 53.15 g, respectively. The yield of fraction GS3B was very high using this scheme, but was very hygroscopic and still contained a certain amount of water. During the partition small amounts of GS1B and GS2B were kept aside for analysis.

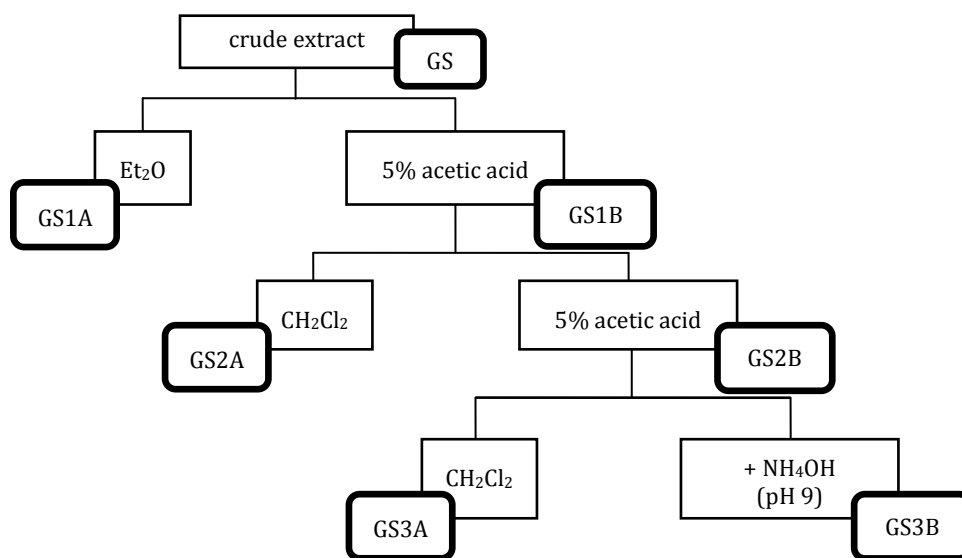


Figure 4.25 Liquid-liquid partition of the *G. superba* crude extract

4.3.5.2. Normal phase TLC analysis

NP TLC analyses were performed on the crude extract (GS), colchicine standard (COL) and the fractions obtained by liquid-liquid partition. The concentration of the crude extract amounted 5.02 mg/mL in methanol. The concentrations of the fractions were between 4.50 and 7.82 mg/mL in methanol. Ten microliter of these solutions was applied on an analytical silica gel plate. The colchicine solution had a concentration of 0.31 mg/mL in methanol and 20 μ L of the colchicine solution was applied on the same plate. The NP TLC plate was eluted over a length of 8 cm in a mixture of 40% ethyl acetate and 60% methanol. The zones on the TLC plate were visualised under UV light at 254 and 366 nm, and by spraying the plate with a *p*-anisaldehyde reagent and heating the plate to 100 – 105 $^{\circ}$ C for 5 - 10 min. Figure 4.26 shows the result of the TLC analysis of the fractions. Fraction GS1B showed all three compounds. Fraction GS2B showed mainly one compound and the two other compounds were mainly found in fraction GS2A. The same was observed for fraction GS3A and GS3B.

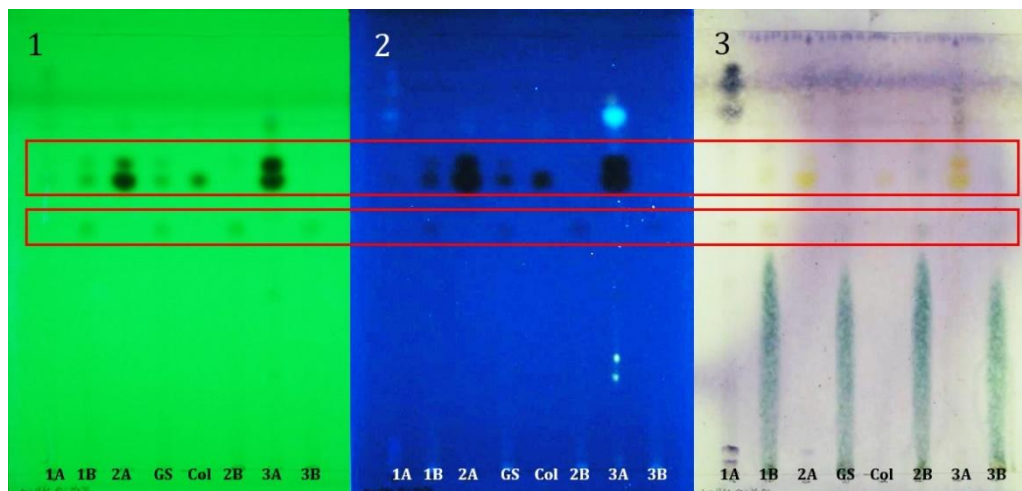


Figure 4.26 NP TLC profile of the crude extract (GS), colchicine (col) and fractions (1A, 1B, 2A, 2B, 3A and 3B) (1) 254 nm, (2) 366 nm, (3) anisaldehyde

4.3.5.3. HPLC analysis of the liquid-liquid partition fractions

The fractions were analysed by means of HPLC-DAD (Agilent 1200) and the Apollo column. Twenty microliters of the same solutions of the crude extract and the fractions (mentioned in section 4.3.5.1) were injected. Mobile phase A was water with 0.05% TFA and mobile phase B was acetonitrile. The flow rate was set at 1.0 mL/min and the DAD was set at a wavelength of 350 nm. The gradient used was 0 min, 5% B; 5 min, 5% B; 60 min, 100% B. The chromatograms are shown schematically in Figure 4.27 and the previously identified compounds A, B and C are indicated. After the first partition step colchicine (compound C) was divided into fraction GS1A and GS1B. The other compounds did not have any affinity for the organic phase. After the second partition step most of the colchicine was removed from the aqueous phase (GS2B) into the organic phase. Fraction GS2B contained mostly colchicoside (compound A) and 3-*O*-demethylcolchicine (compound B). After step three, more colchicine and 3-*O*-demethylcolchicine were removed from the aqueous phase. Due to the loss of a large amount of 3-*O*-demethylcolchicine in this last step, GS2B was selected as the colchicine-poor fraction for further preclinical investigations instead of GS3B.

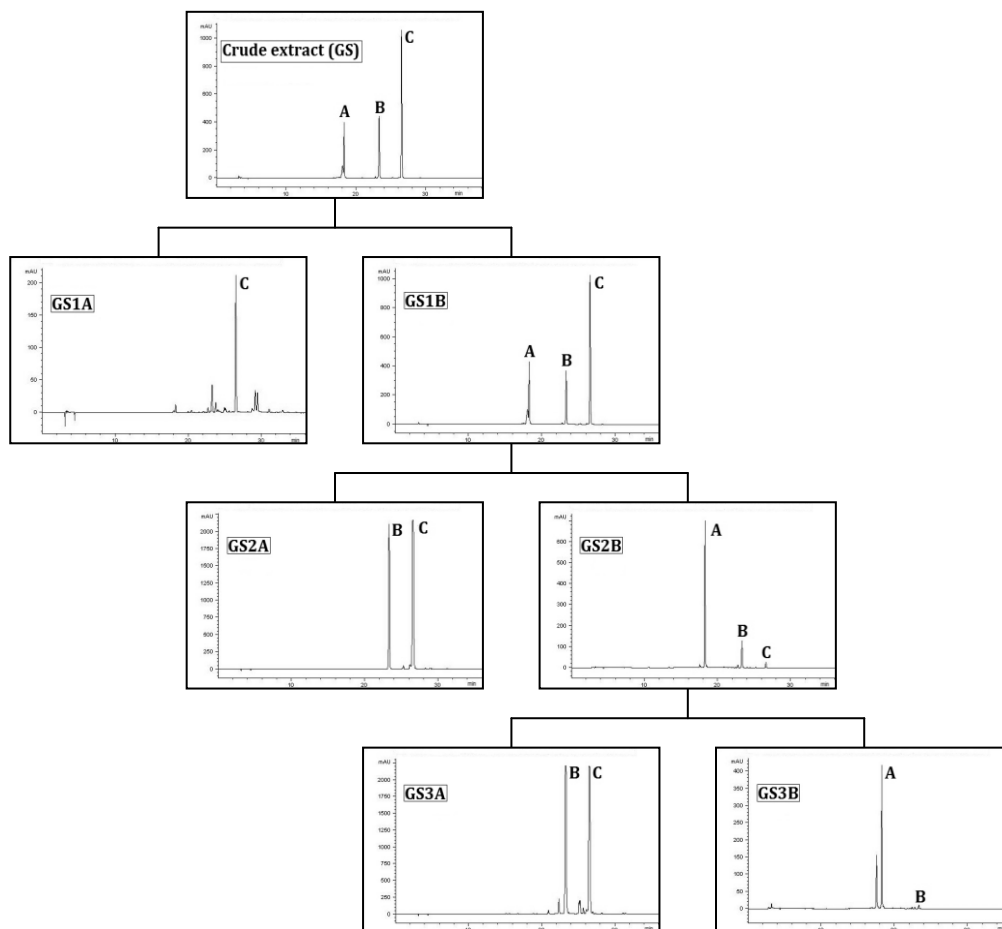


Figure 4.27 HPLC chromatograms of the fractions from the liquid-liquid partitioning (A: colchicoside, B: 3-*O*-demethylcolchicine and C: colchicine)

For the *in vivo* mouse study that was envisaged as mentioned in section 1.4 (Aims of this work), a large quantity of the colchicine-poor extract was necessary. From the ethanolic crude extract 98.7 g was used to start the liquid-liquid partition. This yielded 90.7 g of fraction GS1B. For step 2, 40.3 g of the dried GS1B fraction was used and this yielded 33.2 g of fraction GS2B, also called “colchicine-poor extract”.

4.3.5.4. Isolation of Compound D

In the HPLC chromatogram of fraction GS3B (Figure 4.28) a previously undetected peak was observed. This compound was isolated and identified by means of LC-SPE-NMR. After gradient optimisation the retention time of compound D was 35.5 min. A solution of the lyophilised fraction GS3B with a concentration 20.08 mg/mL was prepared in 50% methanol. The injection volume of each run was 60 μ L and three sequences of 30 runs were performed. The mobile phases were water with 0.05% TFA (A) and methanol (B). The flow rate was set at 1.0 mL/min and the single wavelength detector was set at 350 nm. This wavelength was selected for detection rather than UV_{max} because there was less interference. The optimised gradient was 0 min, 5% B; 5 min, 5% B; 53 min, 50% B; 55 min, 100% B and 60 min, 100% B. The Apollo column was used to separate the compounds. Compound D was then trapped on the cartridge every run and the cartridges were dried by using N_2 . Compound D was then transferred into a NMR tube with deuterated acetonitrile to record the 1H and 2D NMR spectra.

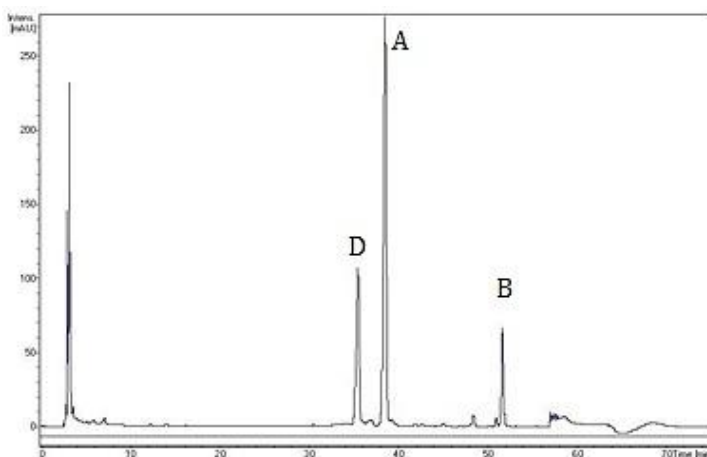


Figure 4.28 HPLC chromatogram of fraction GS3B

(A: colchicoside; B: 3-*O*-demethylcolchicine and compound D)

4.3.5.5. Identification of colchicosamide

The structure of compound D was elucidated by ^1H , and 2D NMR (COSY, HSQC and HMBC) as *N*-[(7*S*)-10-amino-1,2-dimethoxy-9-oxo-3-[(2*S*,3*R*,4*S*,5*S*,6*R*)-3,4,5-trihydroxy-6-(hydroxymethyl)oxan-2-yl]oxy-6,7-dihydro-5*H*-benzo[*a*]heptalen-7-yl]acetamide or **colchicosamide** (Figure 4.29).

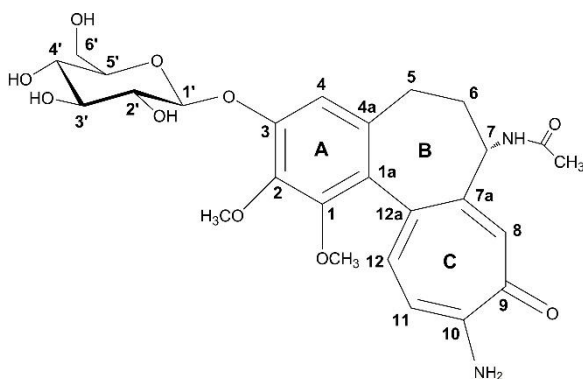


Figure 4.29 The structure of compound **D** (colchicosamide)

The UV spectrum of this compound showed UV absorption maxima at 249 and 363 nm. The ^1H NMR spectrum of compound D is displayed in Figure 4.30. It showed similarities with the ^1H NMR spectrum of colchicine and indicated again an *O*-glycoside analogue of colchicine. The proton assignments are summarised in Table 4.4 and the COSY spectrum (Figure 4.31) was in good agreement with these assignments. The ^1H NMR signals corresponded with those of colchicoside with the exception of the methoxy groups. Only 2 methoxy groups were found at 3.52 and 3.82 ppm. In the HSQC spectrum (Figure 4.32) these two methoxy protons correlated with the carbons at 60.5 and 60.8 ppm and on the HMBC spectrum (Figure 4.33) with the carbons at 151.8 and 143.1 ppm. Taking into account the relative signals found for colchicoside and the HMBC analysis, these carbons can be assigned as C-1 and C-2. The high resolution mass spectrum showed a pseudo molecular ion $[\text{M} + \text{H}]^+$ with m/z 533.2154 (calculated m/z 533.2135) consistent with a molecular formula of $\text{C}_{26}\text{H}_{32}\text{N}_2\text{O}_{10}$, indicating that a methoxy was replaced by an amine group. This was confirmed by the lowered chemical shift

of C-10 (157.0 ppm) compared to colchicoside (164.0 ppm). Once again the carbon signals were derived from the analysis of the 2D spectra and are summarised in Table 4.4. NMR and MS data suggested that this compound was colchicosamide.

Synthesis of colchicosamide has already been reported.^[37] Indeed, colchicosamide can be semi-synthesised by reaction of colchicoside with ammonia and due to the fact that this compound was isolated from the basic ammonia fraction GS3B, it could not be excluded that the found colchicosamide might be an artefact.

Table 4.4 ¹H (400 MHz) NMR assignments for compound **D** (colchicosamide) (CD₃CN)

Position	δ_{H} (ppm); multiplicity; <i>J</i> (Hz)	δ_{C} (ppm)
1	-	151.8
1a	-	129.7
2	-	143.1
3	-	151.4
4	6.75; s	111.5
4a	-	130.0
5	2.20; m 2.46; m	29.4
6	1.78; m 2.04; m	36.4
7	4.34; m	52.3
7a	-	n.d.
8	7.11; s	124.2
9	-	176.2
10	-	157.0
11	6.86; d; 10.4	110.6
12	7.10; d; 10.4	138.4
12a	-	n.d.
CH₃O (1)	3.52; s	60.5
CH₃O (2)	3.82; s	60.8
C=O (CH₃)	-	171.6
CH₃ (C=O)	1.82; s	21.7
NH	6.94; d; 6.5	-
1'	4.89; d; 7.0	100.9
2'	3.38; m	73.5
3'/5'	3.36; m	76.5
4'	3.31; m	70.1
6'	3.58; m 3.72; m	61.4

n.d. = not detected

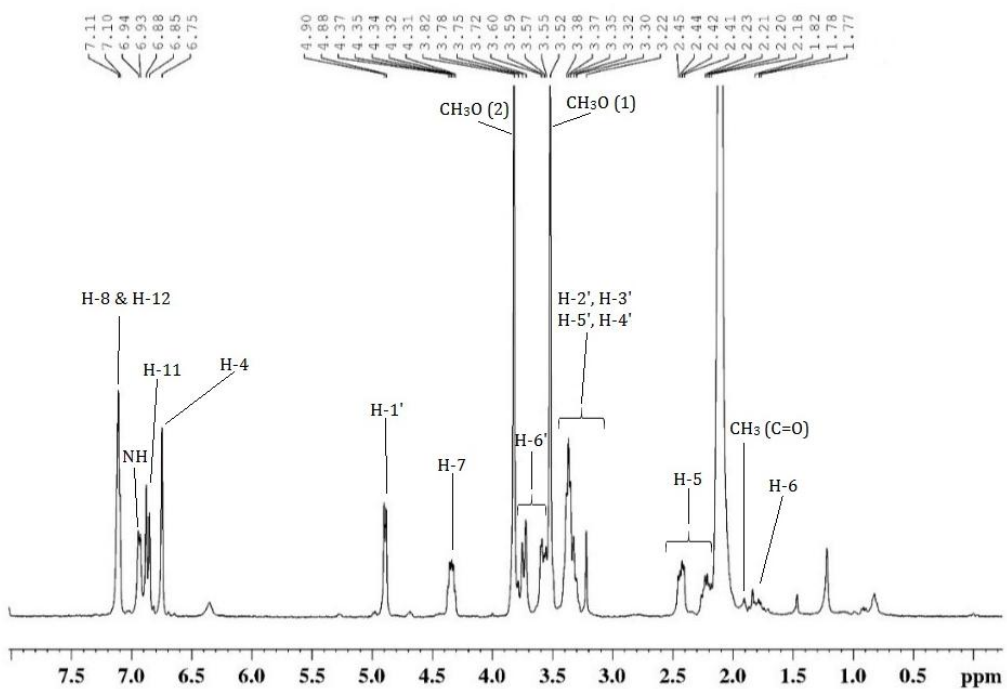


Figure 4.30 ¹H spectrum of compound D (colchicosamide)

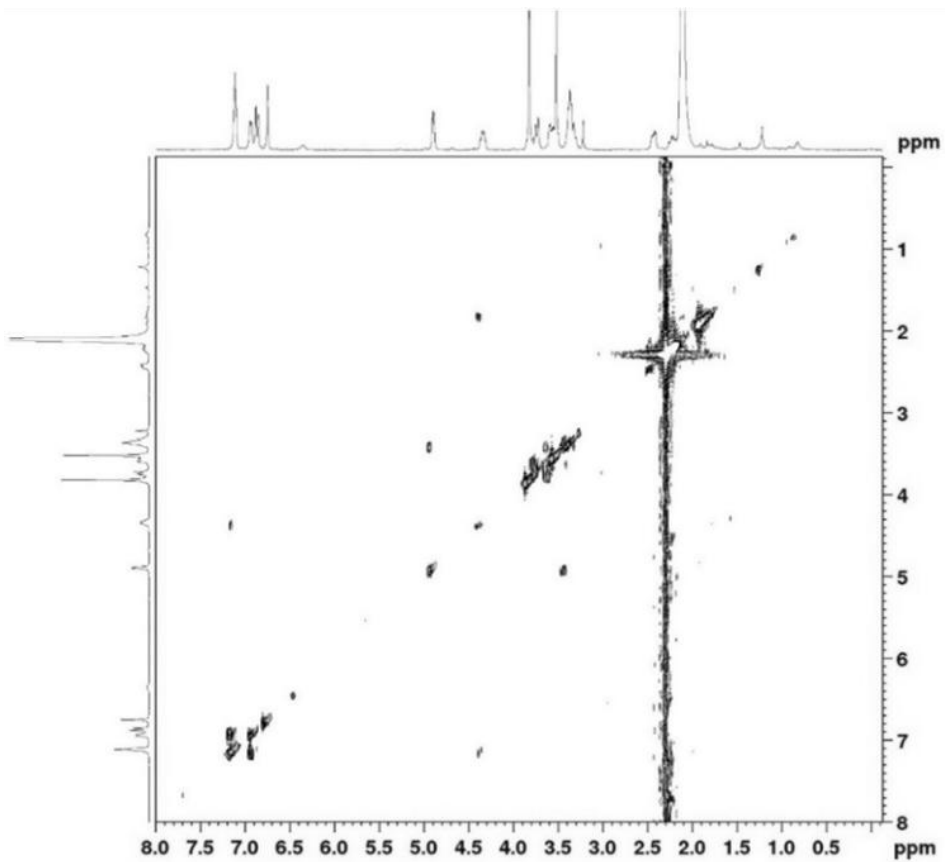


Figure 4.31 COSY spectrum of compound **D** (colchicosamide)

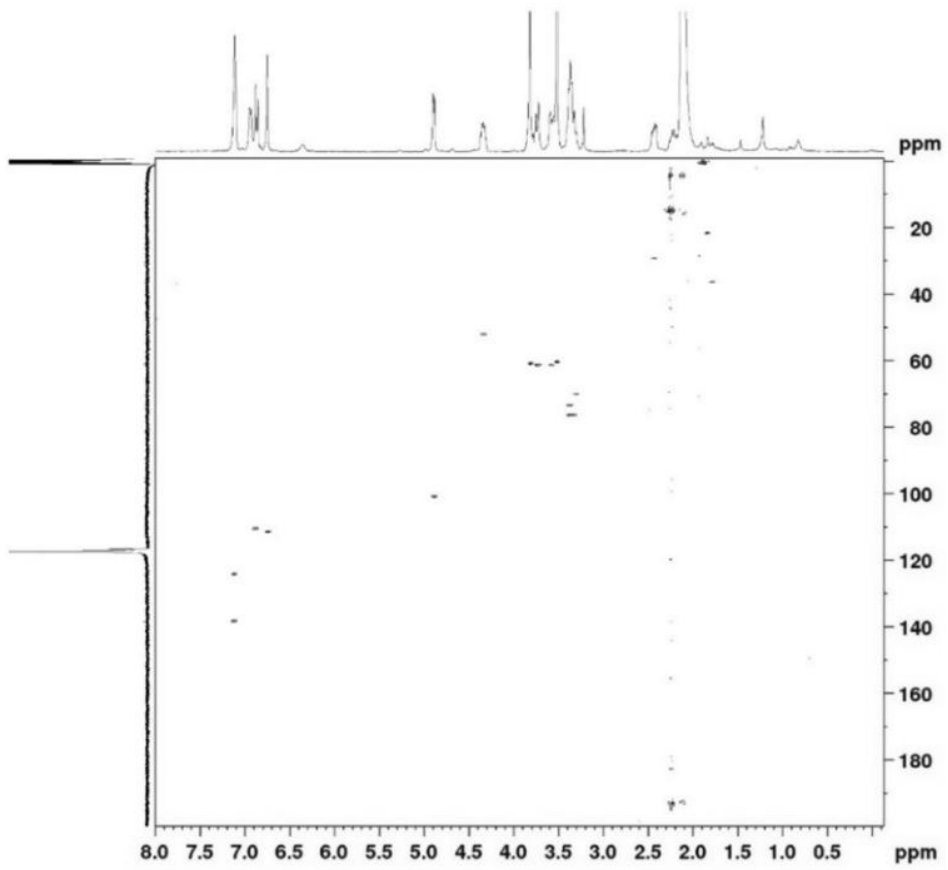


Figure 4.32 HSQC spectrum of compound **D** (colchicosamide)

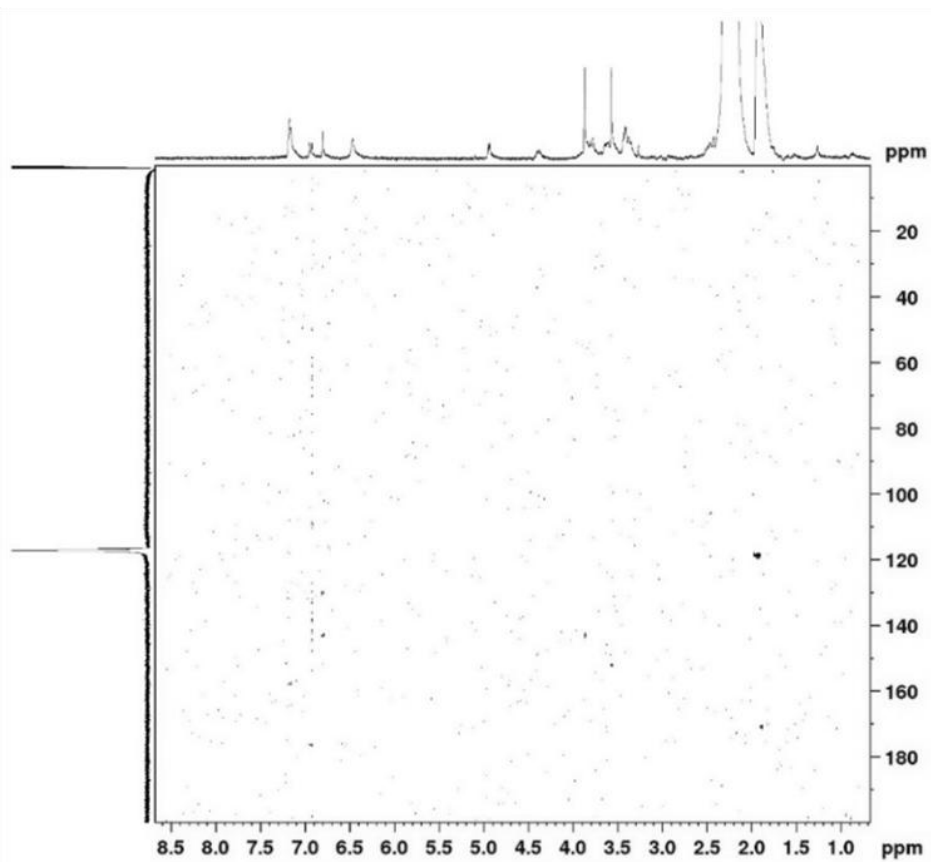


Figure 4.33 HMBC spectrum of compound **D** (colchicosamide)

4.3.6. Summary and conclusion

Gloriosa superba L. seeds were phytochemically investigated using chromatographic and spectroscopic techniques. About 5.3 kg of dried *G. superba* seeds were extracted with 80% ethanol and yielded 846.7 g crude extract. The TLC and HPLC analyses revealed three main compounds in the crude extract. These main compounds were isolated and identified by means of LC-SPE-NMR. This technique allowed to isolate and identify compounds from the crude extract with minor sample preparation and purification steps. The main compounds found in the 80% ethanolic extract of *G. superba* were colchicine, 3-*O*-demethylcolchicine and colchicoside, as reported before in the literature. After liquid-liquid partition a minor compound was also isolated and identified with the use of the LC-SPE-NMR from fraction GS3B. Compound D was identified as colchicosamide, which is an artefact derived from the reaction of colchicoside with ammonia during liquid-liquid partition.

Due to the known toxicity of colchicine, a colchicine-poor extract was prepared by means of liquid-liquid partition. By acidifying the aqueous phase and consecutive extraction steps with diethyl ether and methylene chloride, most of the colchicine was removed and fraction GS2B was created, which is an extract from *G. superba* seeds containing a higher amount of colchicine derivatives other than colchicine itself, especially colchicoside.

4.4. ANALYTICAL INVESTIGATION

The analytical part of this research project consisted in the **optimisation of an analytical procedure/method** for the quantification of the compounds identified in the extract and **validating** this analytical method/procedure. Having an analytical method offers certain advantages, such as performing batch control on every extract and to be able to quantify the (active) constituents in the extract. As previously mentioned in section 1.2, there are different types of extract, i.e. quantified, standardised and other extracts (e.g. refined). A quantified extract has one or more compounds present in a specific, guaranteed amount. The intention behind the quantification is to guarantee that the consumer is getting a product which is consistent from batch to batch. Quantification only guarantees the presence of a certain percentage of certain compounds but is not necessarily related to the therapeutic activity. Standardisation of herbal medicines involves adjusting the herbal preparation to a defined content of a constituent or a group of substances with known therapeutic activity. Standardisation is therefore based on the idea that quantified compounds are responsible for the action of a herbal preparation. Thus, it is necessary to determine the active phytochemical constituents of herbal preparations in order to ensure the reliability and repeatability of the pharmacological activities and the quality, efficacy, and safety of the preparations. Nowadays it becomes more important to create an analytical method to be able to quantify these active compounds present in the matrix/extract/plant extract.^[38-40]

Secondary metabolites of plants also have an optimum time for harvest that is not related to senescence, but often directly related to a stage of plant development. In the case of *G. superba* colchicine levels are highest during the initial growth of the plant, declining during maturation and then slightly increasing in alkaloid content when the tubers become dormant at the end of the season. Thus, colchicine content is affected by plant age and seasonality.^[41] This emphasises again the importance of quantifying the main constituents in the plant extract by using an analytical method.

4.4.1. Method development/optimisation

Different methods for the quantification of colchicine and its derivatives have already been reported in the literature. Two spectrophotometric methods were described by Narayana et al. for the determination of colchicoside. One involves the reaction of colchicoside with Fe(III) to form a complex and the other one is based on the reaction of colchicoside with $\text{NH}_2\text{OH}\cdot\text{HCl}$. The absorbance is then measured at 458 nm or 395 nm, respectively.^[21] An assay for colchicine is also described in the European Pharmacopoeia by means of potentiometric titration.^[31] The methods described are able to determine the pure individual compounds, but do not allow to individually quantify them in a mixture of similar compounds. A single method to determine all colchicine derivatives separately in the crude extract is preferable. Ondra et al. published a high-performance liquid chromatographic method for the determination of the colchicine derivatives found in different *Colchicum spp.* plants.^[34] Another HPLC-UV method was described by Chitra et al. for the quantitative analysis of active components in *G. superba* tubers.^[42] The European Pharmacopoeia also described a liquid chromatographic method to determine the related substances of colchicine.^[31] Since several analytical chromatographic methods were already reported for the determination and quantification of colchicine and its derivatives, whether or not from *G. superba*, those methods were, if possible, tested and compared. Eventually these methods were used as a starting point to optimise a new simplified method, focussing on the combined quantification of the three main compounds found in the 80% EtOH extract of the seeds of *G. superba*.

4.4.1.1. Sample preparation

Some of the sample preparation procedures from the methods listed above use one or more extraction steps. For example, the method described by Chitra et al. suggested to extract the with petroleum ether defatted plant material with methylene chloride and then adding 10% solution of ammonia followed by 10 min of vigorous shaking.^[42] Ondra et al. reported a soxhlet extraction of the plant material with methanol, after which the dried extract was dissolved in acidified water, followed by an extraction with diethyl ether, chloroform and once again an extraction with chloroform but after alkalinisation.^[34] These sample preparations were investigated and were found to generate reasonable results but they were laborious and time

consuming. The related substances test described in the monograph of colchicine only dissolves the sample in 50% MeOH^[31] and based on this one step method, a simplified sample preparation procedure was designed omitting the extensive extraction steps. Most methods started with the plant materials, while in our case the starting material was an 80% EtOH extract of *G. superba*.

Methanol, water and methanol 50% were used to dissolve the crude extract (100 mg) and the reference material colchicine. Afterwards the samples were ultrasonicated and then diluted. Every time a parameter was tested, all other parameters were kept the same. The reference material dissolved immediately in all solvents, so for the reference material the solvent was not an issue. However, the solubility of the crude extract in water and methanol 50% was not adequate compared to methanol. Methanol was therefore chosen to dissolve the extract, but because of the asymmetrical peak shape, frequently caused by injecting a 100% methanol solution, it was necessary to dilute the solution resulting in a lower percentage of methanol. The dissolved extract was diluted in methanol 50%.

The ultrasonication time was also tested. The extract was dissolved in 100% methanol and then ultrasonicated for 5, 10, 15 and 30 min. The area under the curve improved by the longer sonication time but no additional benefits were observed by sonicating longer than 15 min. Therefore, in the final method a sonication time of 15 min was used.

The final step of the development of the method was checking whether the method was also applicable in other ranges, which is usually 50% and 150% of the used amount, i.e. 100 mg in 20 mL MeOH. This was done by analysing 50 mg and 150 mg of the extract using the same conditions. Since these results were in good agreement, this sample preparation can be used.

4.4.1.2. Chromatographic conditions

Different chromatographic conditions were used in the literature.^[34, 42] In the LC-UV method of Chitra et al. an isocratic system consisting of water and acetonitrile (70:30) was used.^[42] An isocratic system consisting of phosphate buffer and methanol was also described in Ph. Eur.^[31] These systems were evaluated, but did not provide sufficient peak resolution for the crude

extract. Therefore a general gradient, which was 0 min, 5% B; 5 min, 5% B; 55 min, 100% B and 60 min, 100% B, with mobile phase A being water containing TFA (0.05%) and mobile phase B being acetonitrile, was tested. The gradient was adjusted in order to shorten the total run time, thus reducing the solvent consumption but taking into account not to decrease the quality of the separation. A good separation was reached with the gradient 0 min, 10% B; 5 min, 10% B; 25 min, 40% B; 35 min, 100% B; 40 min, 100% B. In order to see if the acid had an added value to the peak shape, different acids and water without acid were tested. It was then concluded that the acids did not improve the peak shape. The flow rate and column temperature were set at 1.0 mL/min and 25 °C. Different flow rates and column temperatures were also tested, but none of the tested parameters gave better results. Two different HPLC columns were tested, a Grace Apollo 5µm C₁₈ and a Phenomenex Luna 5 µm C₁₈. Better separation was obtained with the Luna column and therefore this column was chosen. Once an acceptable chromatogram was achieved, a suitable detection wavelength was chosen using the DAD. The wavelength was set at the UV absorption maximum of the three main compounds, which is 245 nm.

4.4.2. Final analytical method

4.4.2.1. Reference solution

About 25 mg of colchicine (97% purity) was accurately weighed into a measuring flask of 50.0 mL. This was then dissolved in 50% MeOH and ultrasonicated during 15 min. After cooling down, this solution was then diluted 12.5, 50 and 250 times resulting in concentrations of 0.002, 0.01 and 0.04 mg/mL, respectively.

4.4.2.2. Test solution

About 100 mg of *G. superba* extract was accurately weighed into a measuring flask of 20.0 mL. It was dissolved in MeOH and ultrasonicated during 15 min. After cooling down, 5.0 mL of this solution was transferred into a measuring flask of 25.0 mL. Five mL of water was added into the same flask and filled up with 50% MeOH, after cooling down.

4.4.2.3. HPLC conditions

The reference and test solution were analysed by means of HPLC by injecting 20 μ L. The following gradient was used with mobile phase A being water and B acetonitrile: 0 min, 10% B; 5 min, 10% B; 25 min, 40% B; 35 min, 100% B; 40 min, 100% B. The column used was a Phenomenex Luna 5 μ m C₁₈ 100 Å (250 x 4.6 mm) with a flow rate of 1.0 mL/min. The peaks were detected at 245 nm. The resulting chromatograms of the reference material, colchicine, and the crude extract of *G. superba* are shown in Figure 4.34.

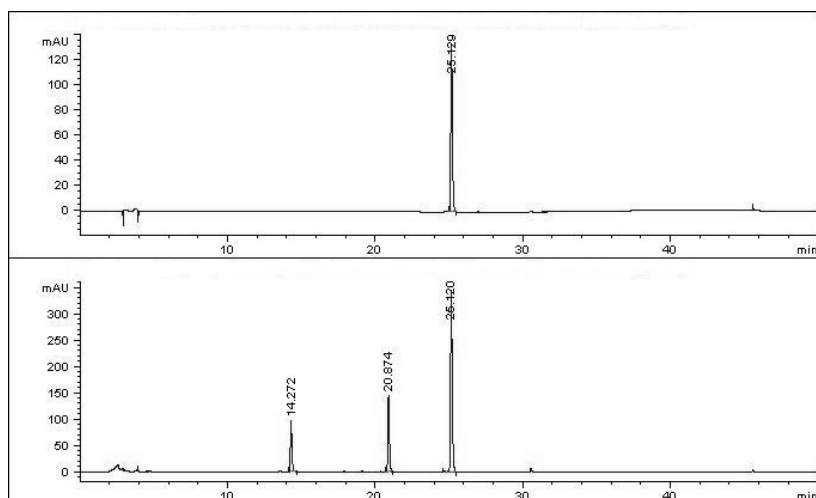


Figure 4.34 HPLC chromatogram of the reference material colchicine (upper) and the crude extract (lower), using the conditions of the optimised method

4.4.3. Validation of the analytical method

Method validation is carried out to ensure the quality of the method. There are four types of analytical procedures that can be validated, i.e. the identification tests, the quantitative tests for impurities' content, limit tests for the control of impurities, and quantitative tests of the active moiety in samples of drug substance of drug product or other selected component(s) in the drug product. This latter assay procedure represents a quantitative measurement of the major component(s) in the drug substance. Analytical procedures refer to the way of performing the analysis. This usually includes the preparation of the sample, the reference standard and the reagents, the use of apparatus, the generation of the calibration curve, and the formulae for the calculation. The fundamental parameters and experimental setup for the validation of an analytical procedure depend on the purpose of the developed/optimised method. The characteristics that needed investigation for the assay included: linearity and range (calibration model/standard curve), precision, accuracy and specificity.^[43, 44]

The **linearity** of an analytical procedure is its ability within a given range to obtain test results which are directly proportional to the concentration/amount of analyte in the sample.^[44] This is a crucial step in the establishment of an analytical method, only by establishing the correct relation between the measured response and the concentration of the analyte it can be assured that the prediction of the assumed model for an unknown concentration of the analyte will be correct.^[45] A linear relationship should be evaluated across the range of the analytical procedure. Linearity should be evaluated by visual inspection of a plot of signals as a function of concentration or content. If there is a linear relationship, test results should be evaluated by appropriate statistical methods such as by calculation of a regression line by the method of least squares. In other cases a mathematical transformation prior to the regression analysis to obtain linearity between assays and sample concentrations can be necessary. The correlation coefficient, y-intercept, slope of the regression line and residual sum of squares should be investigated. In addition, an analysis of the deviation or residuals of the actual data points from the regression line may also be necessary to evaluate the linearity. For the establishment of linearity, a minimum of 5 concentrations, within the desirable range, is recommended.^[44] The **range** of an analytical procedure is the interval between the upper and

lower concentrations/amounts of analyte in the sample for which it has been demonstrated that the analytical procedure has a suitable level of precision, accuracy and linearity. The specified range is normally derived from linearity studies and depends on the intended application of the procedure. It is established by confirming that the analytical procedure provides an acceptable degree of linearity, accuracy and precision when applied to samples containing amounts of analyte within or at the extremes of the specified range of the analytical procedure.^[44] In case of analysis of plant products, a range of at least between 40% and 200% (0.4 – 2 times) of the expected amount of the analyte of interest in the sample is recommended. A broad linear range can be expected for HPLC-UV detection. Therefore, a linear response function is expected to fit the results obtained for the absorption-concentration relationship. The regression line that best describes the linear relationship between the two variables, can be obtained and characterised by applying mathematical and statistical approaches.^[45]

The **precision** of an analytical procedure expresses the closeness of agreement or degree of scatter between a series of measurements obtained from multiple sampling of the same homogeneous sample under the prescribed conditions. Precision may be considered at three levels: repeatability, intermediate precision and reproducibility. The precision of an analytical procedure is usually expressed as the variance, standard deviation or coefficient of variation of a series of measurements. The **repeatability** expresses the precision under the same operating conditions over a short interval of time. Repeatability should be assessed using either a minimum of 9 determinations covering the specified range for the procedure or a minimum of 6 determinations at 100% of the test concentrations. **Intermediate precision** expresses within-laboratories variations: different days, different analysts, different concentration levels, different equipment, etc. The extent to which intermediate precision should be established depends on the circumstances under which the procedure is intended to be used. The effect of random events should be established on the precision of the analytical procedure. Typical variations to be studied include days, analysts, concentrations, equipment, etc. **Reproducibility** expresses the precision between laboratories.^[44]

The **accuracy** of an analytical procedure expresses the closeness of agreement between the value which is accepted either as a conventional true value or an accepted reference value and the value found.^[44] The accuracy can be investigated in three different ways: standard addition, reconstituted drug product or comparison with a standard method. The latter one can only be used if there is a standard method available. The reconstituted drug product test can only be performed on finished products when all of the constituting components are available. In the case of plant materials this is very difficult so standard addition or in other words spiking of the plant extract is the most frequently used way to investigate the accuracy. A known amount of reference material is added and after analysing the analyte using the analytical procedure it is examined if the added amount is found, so if the recovery is 100%.^[45]

The **specificity** is the ability to assess unequivocally the analyte in the presence of components which may be expected to be present. Typically this might include impurities, degradants, matrix, etc. Lack of specificity of an individual analytical procedure may be compensated by other supporting analytical procedures. In an assay, the specificity provides an exact result which allows an accurate statement on the content of the analyte in a sample. An investigation of specificity should be conducted during the validation of the assay. It is not always possible to demonstrate that an analytical procedure is specific for a particular analyte.^[44] For chromatographic procedures, representative chromatograms should be used to demonstrate specificity and individual components should be appropriately labelled. Critical separations in chromatography should be investigated at an appropriate level. For critical separations, specificity can be demonstrated by the resolution of the two components which elute closest to each other. For chromatographic procedures, peak purity tests may be used to show that the analyte chromatographic peak is not attributable to more than one component and this by investigating the UV spectra (in the case of an HPLC-DAD method) of the compounds and the standards in the beginning, the apex and the end of the peak.^[44, 45]

The **robustness** of an analytical procedure is a measure of its capacity to remain unaffected by small, deliberate variations in method parameters and provides an indication of its reliability during normal usage. The evaluation of robustness is usually considered during the development phase rather than during the validation. In the case of liquid chromatography,

examples of typical variations are: influence of variations of pH in a mobile phase, mobile phase composition, different columns, temperature or flow rate. During sample preparations typical variations are stability of analytical solutions, extraction time, extraction solvents, etc.^[44] This was investigated during method optimisation.

4.4.3.1. Response function – Calibration model

For the calibration model of colchicine ten solutions in different concentrations were prepared from a stock solution. This stock solution was prepared by dissolving 26.2 mg of colchicine standard with a purity of 97% in 50.0 mL 50% MeOH and diluting it 5 times with 50% MeOH. The concentrations of the solutions ranged from 0.0021 mg/mL to 0.0419 mg/mL and each solution was injected twice. The concentrations and the resulting peak areas for colchicine are shown in Table 4.5.

Table 4.5 The concentrations and peak areas for the calibration model of colchicine

dilution from stock	concentration (mg/ml)	peak area 1	peak area 2
1.0 mL → 50.0 mL	0.0021	187.0	187.3
2.0 mL → 50.0 mL	0.0042	378.0	376.6
4.0 mL → 50.0 mL	0.0084	752.2	756.6
5.0 mL → 50.0 mL	0.0105	945.0	936.6
8.0 mL → 50.0 mL	0.0168	1511.0	1505.1
10.0 mL → 50.0 mL	0.0210	1885.7	1891.6
5.0 mL → 20.0 mL	0.0262	2366.9	2365.8
15.0 mL → 50.0 mL	0.0314	2815.7	2817.6
7.0 mL → 20.0 mL	0.0367	3294.0	3297.6
20.0 mL → 50.0 mL	0.0419	3774.9	3787.6

The linearity for colchicine was investigated and the regression line was plotted in Figure 4.35. The least squares line was evaluated by calculating the correlation coefficient and the residuals, which were plotted in Figure 4.36. Graphical examination of the regression curve and the residual plot proved that the method was linear for colchicine. The residuals were randomly scattered and showed a condition of homoscedasticity. The highest residual corresponded to 1.5% of the signal of the 100% concentration, which is within the limit for LC-UV of 5%. The intercept, slope and their standard errors were calculated. The intercept was evaluated by calculating the confidence interval and checking whether the origin, point (0,0), was included. The slope of the calibration curve was inspected by means of the student's t-test. An analysis of variances (ANOVA) lack of fit F-test was performed and the quality coefficient was calculated. All these results are summarised in Table 4.6. The origin fell within the calibration curve since zero was included in the 95% confidence interval. The slope of the curve was significant, t_{calc} (764.56) was higher than t_{crit} (2.10). The correlation coefficient was approved since it was at least 0.999. The ANOVA showed that F_{calc} (5.20) was lower than F_{crit} (6.94). The quality coefficient was also lower than 2.50%. Thus it can be concluded that the method was found to be linear within the range 0.0021 to 0.0419 mg/mL. Although a single-point calibration is justified, since the origin fell within the calibration curve, a calibration curve with the highest, lowest and 100% concentration is constructed each time an analysis was performed, because of the very broad range of the compounds in the extract.

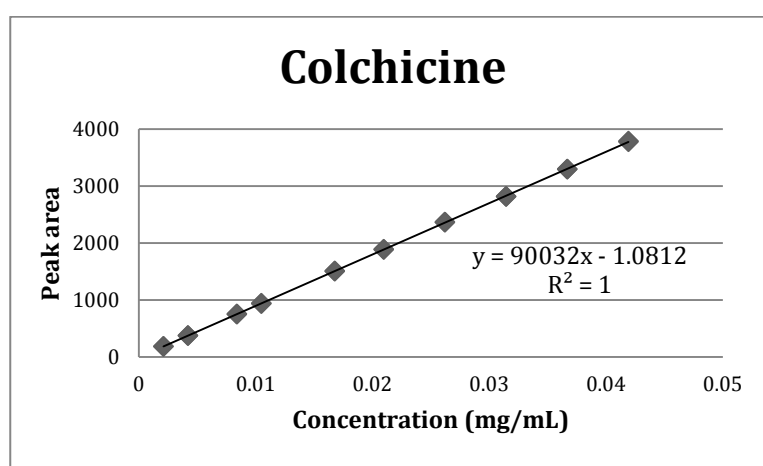


Figure 4.35 The calibration curve and corresponding equation for colchicine

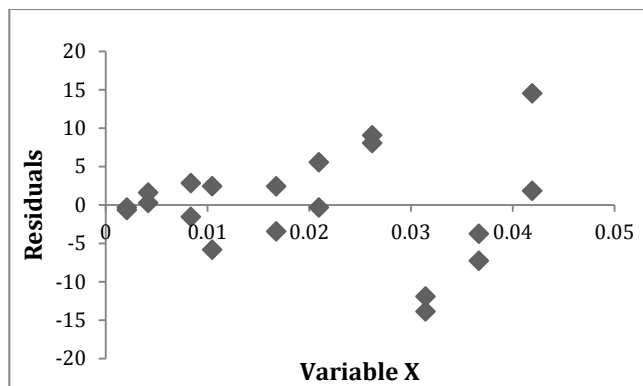


Figure 4.36 Residual plot of colchicine

Table 4.6 Overview of the linearity data of colchicine

	Colchicine
Range (mg/mL)	0.0021 – 0.0419
Number of standards	10
Intercept \pm standard error	-1.08 \pm 2.81
Confidence interval (95%)	-6.99 to 4.83
Slope \pm standard error	90032.13 \pm 117.76
t_{calc} (t_{crit})	764.56 (2.10)
Correlation coefficient	0.99997
F_{calc} (F_{crit})	5.20 (6.94)
Quality coefficient	0.32%

4.4.3.2. Precision

The **injection repeatability** was determined by injecting one of the samples six times. The concentration of each compound was then determined by injecting 3 reference solutions in duplicate (20%, 100% and 400%) and constructing a calibration curve. The determined concentrations for each compound, the standard deviation and the relative standard deviation (RSD%) are summarised in Table 4.7. Standard deviations of 0.002% (colchicoside), 0.004% (3-*O*-demethylcolchicine) and 0.006% (colchicine) were found for the three compounds. The relative standard deviations were 0.270%, 0.351% and 0.202%, respectively.

Table 4.7 Results of the injection repeatability

	Area	Conc (% m/m)		
colchicoside	693.8	0.74		
	695.1	0.74	Mean	0.741
	695.8	0.74	SD	0.002
	691.1	0.74	RSD%	0.272
	691.8	0.74		
	695.0	0.74		
3-<i>O</i>- demethylcolchicine	1007.7	1.08		
	1010.6	1.08	Mean	1.074
	1009.4	1.08	SD	0.004
	1006.6	1.07	RSD%	0.353
	1002.1	1.07		
	1002.3	1.07		
colchicine	2630.7	2.80		
	2645.9	2.82	Mean	2.810
	2641.5	2.81	SD	0.006
	2637.3	2.81	RSD%	0.202
	2638.0	2.81		
	2634.2	2.81		

For the **repeatability** six separate samples were analysed on the same day. Every sample was injected once. The calibration curve of the reference solutions was used to determine the amount of colchicine. These solutions were injected at the beginning and the end of the sequence, so each solution/concentration level was injected in duplicate.

For the **intermediate precision on different days** six separate samples (100% or 100 mg) were analysed on the same day and this was repeated on two consecutive days. Every sample was injected once. The reference solutions for the calibration curve used to determine the amount of colchicine were freshly prepared on each day and also injected at the beginning and the end of the sequence.

For the **intermediate precision on different concentration levels** six samples with half the amount (50% or 50 mg) and six samples with higher amount (150% or 150 mg) were analysed using the same method.

The amount of the individual compounds was calculated using the peak areas of the samples and the calibration curve. The mean, the standard deviation and the relative standard deviation for each compound, for each day and each concentration level were calculated and summarised in Table 4.8.

The homogeneity of the variances of the results from the different days and different concentration levels were tested, prior to conducting an ANOVA, by performing the Cochran's test. The calculated Cochran value C_{calc} was compared to the critical value at 5% level of confidence C_{crit} . The results are shown in Table 4.9. C_{calc} was smaller than C_{crit} , therefore the variances of the different days and different concentration levels were from similar magnitude and an ANOVA (one way, single factor, $\alpha = 0.05$) was performed. For the evaluation of the repeatability and intermediate precision, the within-day and within-level relative standard deviation ($RSD\%_{within}$) and the between-day and between-level relative standard deviation ($RSD\%_{between}$) were calculated. All these results are summarised in Table 4.8. These results indicated that the developed method showed acceptable precision. From the statistical point of view, the ANOVA (Table 4.9) proved that there was no significant difference between the results obtained on the different days or different concentration levels for 3-*O*-demethylcolchicine (F_{calc} was smaller than F_{crit}). For the two other compounds (colchicine and colchicoside) F_{calc} was bigger than F_{crit} , the $RSD\%_{within}$ and $RSD\%_{between}$ were also higher than the limit set by Horwitz^[43, 46], but still smaller than 5%, which was an acceptable limit. Therefore the method was considered to be precise for the three compounds with respect to time and concentration.

Table 4.8 Precision on different days and different levels

	Colchicine				
	Day 1	Day 2	Day 3	50%	150%
	100%	100%	100%		
Repeatability					
Number of replicates	6	6	6	6	6
Mean content (% m/m)	2.72	2.85	2.86	2.74	2.87
Standard deviation (% m/m)	0.05	0.03	0.05	0.04	0.03
RSD%	1.84	0.99	1.80	1.53	1.07
RSD _{within} %	1.59			1.48	
S _{within} %	0.04			0.04	
Intermediate precision					
	Time			Conc	
Number of groups	3			5	
Number of replicates	6			6	
Overall mean (% m/m)	2.81			2.81	
RSD _{between} %	3.07			2.91	
S _{between} %	0.09			0.08	
3-O-demethylcolchicine					
	Day 1	Day 2	Day 3	50%	150%
	100%	100%	100%		
	Repeatability				
Number of replicates	6	6	6	6	6
Mean content (% m/m)	1.06	1.05	1.05	1.06	1.07
Standard deviation (% m/m)	0.03	0.02	0.04	0.05	0.01
RSD%	2.97	2.07	3.84	4.52	1.34
RSD _{within} %	3.05			3.16	
S _{within} %	0.03			0.03	
Intermediate precision					
	Time			Conc	
Number of groups	3			5	
Number of replicates	6			6	
Overall mean (% m/m)	1.05			1.09	
RSD _{between} %	2.90			3.04	
S _{between} %	0.03			0.03	
Colchicoside					
	Day 1	Day 2	Day 3	50%	150%
	100%	100%	100%		
	Repeatability				
Number of replicates	6	6	6	6	6
Mean content (% m/m)	0.71	0.76	0.77	0.74	0.78
Standard deviation (% m/m)	0.02	0.01	0.02	0.01	0.01
RSD%	2.57	1.80	2.49	1.97	1.88
RSD _{within} %	2.31			2.16	
S _{within} %	0.02			0.02	
Intermediate precision					
	Time			Conc	
Number of groups	3			5	
Number of replicates	6			6	
Overall mean (% m/m)	0.75			0.75	
RSD _{between} %	4.74			4.12	
S _{between} %	0.04			0.03	

Table 4.9 Cochran and ANOVA results

	Cochran		ANOVA	
	C_{calc} (days)	C_{calc} (conc)	F_{calc} (days)	F_{calc} (conc)
Colchicine	0.447	0.307	17.49	18.13
3-O-demethylcolchicine	0.523	0.413	0.45	0.54
Colchicoside	0.418	0.282	20.31	16.81
Critical value (C_{crit} / F_{crit})	0.707	0.506	3.68	2.76

After graphical inspection of the results (Figure 4.37), the same conclusion could be made that no dependency on time or concentration of the results could be observed.

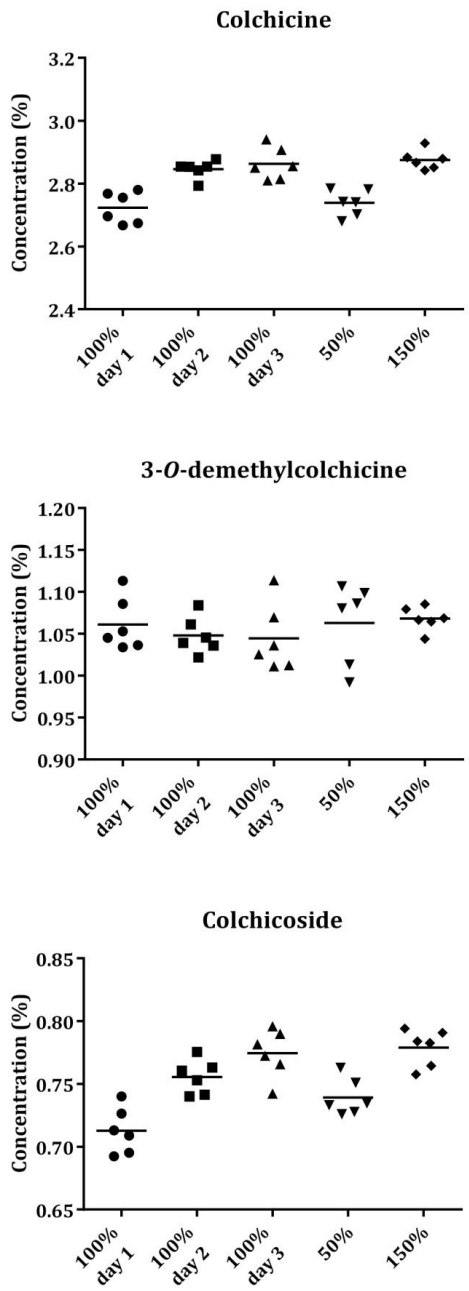


Figure 4.37 Graphical inspection of the results for repeatability and intermediate precision of the three compounds

4.4.3.3. Accuracy

The accuracy for colchicine was investigated by using the standard addition method and was tested on at least three concentration levels in triplicate. The standard addition experiment was performed by spiking different amounts of colchicine standard to 50% of the crude extract until a total concentration of 75%, 100% and 125% of colchicine was obtained. For each sample about 50 mg of the crude extract was weighed in a measuring flask of 20.0 mL. A stock solution of colchicine in MeOH with a concentration of 0.263 mg/mL was prepared and 3.0, 6.0 and 9.0 mL of this solution was added to the crude extract. This mixture was further dissolved in MeOH and ultrasonicated for 15 min. After cooling down the samples were diluted 5 times with 50% MeOH. The samples on the different concentration levels were prepared in triplicate and each sample was injected once.

The recovery percentage was calculated for each of the individually prepared samples and the content of colchicine is shown in Table 4.10.

Table 4.10 Results of the recovery experiment

Level	Colchicine content (mg)			Recovery (%)
	Total found	Added	In 50% extract	
75%	2.34	0.79	1.55	100.49
	2.36	0.79	1.61	94.93
	2.47	0.79	1.69	98.96
100%	3.10	1.58	1.51	100.88
	2.91	1.58	1.33	100.04
	2.92	1.58	1.35	99.58
125%	3.87	2.37	1.47	101.60
	3.74	2.37	1.32	102.15
	3.92	2.37	1.51	101.57

The mean recovery, the RSD% and the 95% confidence interval were calculated. A mean recovery of 100.02% with a RSD% of 2.17% was found. The confidence interval ranged from 98.36% to 101.69%. Since 100% was included in the 95% confidence interval, the recovery

percentage found was not significantly different from 100%, thus the method can be considered to be accurate for colchicine.

In order to check whether the recovery experiment was performed with the same precision as previous experiments, the values of the accuracy were compared with those of the precision in a F-test. F_{calc} (1.57) was smaller than F_{crit} (2.65) and it was then concluded that the recovery experiment was performed with the same precision. The recovery was also plotted in function of the different concentration levels and shown in Figure 4.38.

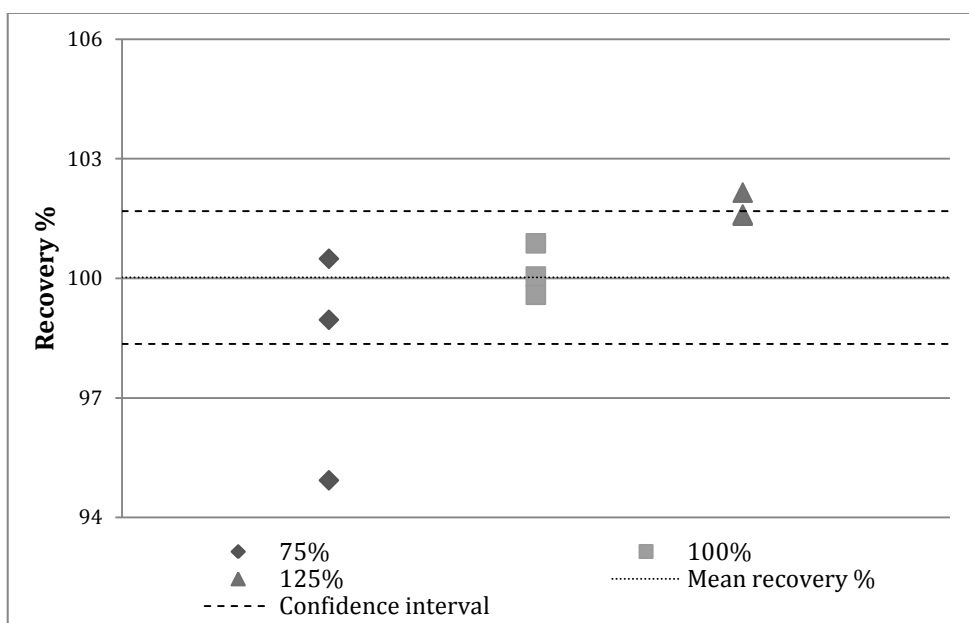


Figure 4.38 Graph of the recovery plotted in function of the different concentration levels

4.4.3.4. Specificity

In order to investigate the specificity, the peak purity of the three compounds (colchicoside, 3-*O*-demethylcolchicine and colchicine) in the crude extract was examined by using the HPLC-DAD. The UV spectra were examined throughout the peak and no deviations were observed, thus concluding that the peak purity of the three compounds was 99% and that the optimised analytical method is specific for these three compounds.

4.4.4. Correction factor

The amount of the colchicine derivatives could now be quantified by using the validated method, but was still expressed as colchicine equivalent. In order to determine the exact amount of the individual colchicine derivatives present in the crude extract, suitable reference materials were necessary. Colchicoside and 3-*O*-demethylcolchicine with a known purity would be the reference material of choice, but they were either not commercially available or very expensive. To overcome this problem a secondary standard could be used. For these two compounds, colchicine would be the ideal secondary standard considering they are derivatives of colchicine. The difference in detector response between both standards needed to be taken into account by using a correction factor. This correction factor needed to be determined and validated. For this a sufficient amount of colchicoside and 3-*O*-demethylcolchicine needed to be isolated.

4.4.4.1. Semi-preparative isolation of the two colchicine derivatives

Colchicoside and 3-*O*-demethylcolchicine were isolated from the crude extract by using the semi-preparative HPLC coupled to a mass spectrometer and a diode array detector, and an automatic fraction collector. A concentration of about 25 - 30 mg/mL in MeOH of the crude extract was prepared and 1500 - 1800 μ L of this solution was injected, after filtration. For this purpose a Phenomenex Luna 5 μ m C₁₈ 100 Å column with larger internal diameter (250 x 10 mm) was used. The mobile phase and gradient were kept the same as the analytical method. The flow rate was increased to 3.0 mL/min and the make-up pump (with an 80% MeOH/ 20% H₂O/ 0.1% formic acid solution) was set at 0.5 mL/min. The collection was triggered by mass *m/z* 386 and the two peaks were consecutively collected.

To investigate the purity, the isolated compounds were injected at a high concentration (0.1 mg/mL for colchicoside and 0.4 mg/mL for 3-*O*-demethylcolchicine) in the HPLC (Agilent 1200). The chromatogram at different wavelengths was investigated and no extra peaks were present at a wavelength different from 245 nm. All peaks that did not appear in the blank run were integrated and the area percentage of the isolated compounds was calculated. The

percentage of purity was calculated by means of the normalisation method and was 97% for colchicoside and 99% for 3-*O*-demethylcolchicine.

4.4.4.2. Validation

Linearity of the primary standard

Firstly the linearity of colchicoside and 3-*O*-demethylcolchicine was investigated. Ten solutions in different concentrations were prepared from a stock solution of 0.11 mg/mL and 0.10 mg/mL, respectively. The concentration range for colchicoside and 3-*O*-demethylcolchicine was from 0.002 to 0.04 mg/mL. Every solution was injected twice and the concentrations and peak areas are summarised in Table 4.11. Regression analysis was performed and the intercept, slope and standard errors are shown in Table 4.12 and the calibration curves were constructed (Figure 4.39). The residuals were calculated and plotted (Figure 4.40). The graphical examination of the calibration curves and the residuals proved that the method was linear, the residuals were randomly scattered and that the calibration model showed a condition of homoscedasticity. The highest residual corresponded to 1.75% of the signal of the 100% concentration for colchicoside and 1.11% for 3-*O*-demethylcolchicine, which were both within the limit for LC-UV of 5%. The confidence interval of the intercept was calculated, the slope of the calibration curve was evaluated by means of the student's t-test and the correlation factor was calculated. An ANOVA was performed and the quality coefficient was calculated. All results are shown in Table 4.12.

For colchicoside point (0,0) fell within the 95% confidence interval and the slope of the curve was significant. T_{calc} (763.2) was higher than t_{crit} (2.1). The correlation coefficient was at least 0.99. The ANOVA lack of fit showed that F_{calc} (2.6) is lower than F_{crit} (6.9) and the quality coefficient (0.43%) was lower than 2.50%. All of these data resulted that the calibration curve for colchicoside was found to be linear within the range of 0.002 to 0.041 mg/mL.

For 3-*O*-demethylcolchicine the point (0,0) fell within the 95% confidence interval and the slope of the curve was significant. T_{calc} (984.7) was higher than t_{crit} (2.1). The correlation coefficient was also at least 0.99. The ANOVA lack of fit showed that F_{calc} (13.8) is higher than F_{crit} (6.9) suggesting that there is a lack of linear fit. This is sometimes the case when the pure

error between duplicates are small compared to the lack of fit due to the use of an automatic injector, but since the quality coefficient (0.29%) was lower than 2.50%, the calibration curve for 3-*O*-demethylcolchicine was found to be linear within the range of 0.002 to 0.043 mg/mL.

Table 4.11 The concentrations and peak areas of colchicoside and 3-*O*-demethylcolchicine

Colchicoside			3- <i>O</i> -demethylcolchicine		
Conc (mg/mL)	Peak area 1	Peak area 2	Conc (mg/mL)	Peak area 1	Peak area 2
0.002	95.363	96.358	0.002	156.926	159.936
0.004	188.518	187.997	0.004	320.112	320.173
0.009	375.704	377.074	0.008	639.165	635.307
0.011	472.556	473.275	0.010	803.649	804.711
0.017	754.353	754.766	0.017	1271.265	1271.397
0.021	945.152	953.199	0.021	1596.387	1596.461
0.027	1184.854	1180.327	0.026	1988.554	1992.172
0.032	1420.960	1417.787	0.031	2399.937	2402.335
0.037	1658.195	1651.508	0.036	2789.114	2786.056
0.043	1881.905	1884.881	0.041	3193.708	3190.942

Table 4.12 Overview of the linearity data of colchicoside and 3-*O*-demethylcolchicine

	Colchicoside	3- <i>O</i> -demethylcolchicine
Range (mg/mL)	0.002 – 0.041	0.002 – 0.043
Number of standards	10	10
Intercept ± standard error	0.972 ± 1.409	0.309 ± 1.845
Confidence interval (95%)	-1.987 – 3.932	-3.568 – 4.186
Slope ± standard error	44435.5 ± 58.2	77394.1 ± 78.6
t _{calc} (t _{crit})	763.2 (2.1)	984.7 (2.1)
Correlation coefficient	1	1
F _{calc} (F _{crit})	2.6 (6.9)	13.8 (6.9)
Quality coefficient	0.43%	0.29%

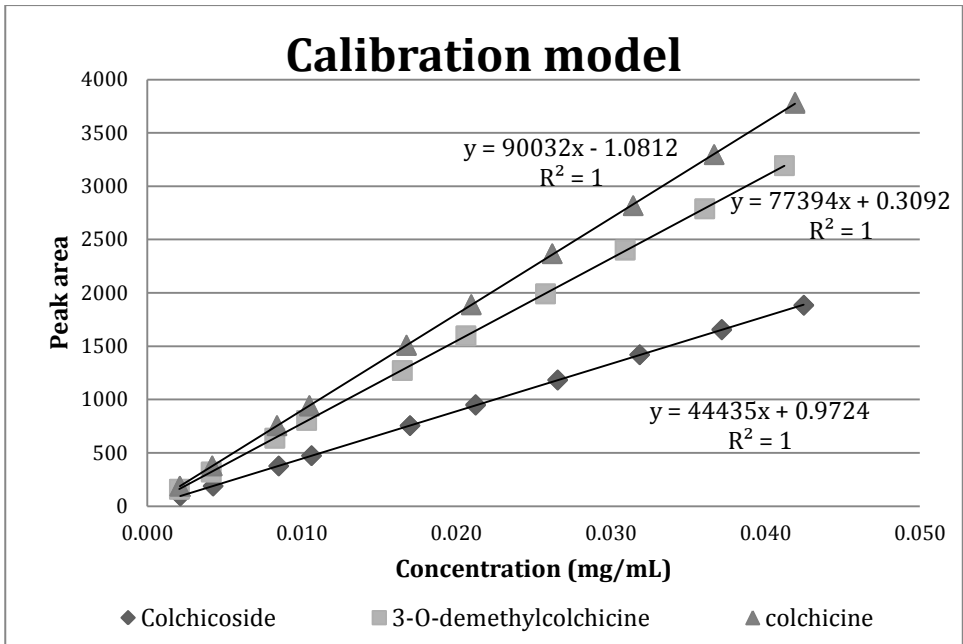


Figure 4.39 The calibration curves for colchicoside and 3-O-demethylcolchicine and the corresponding equations

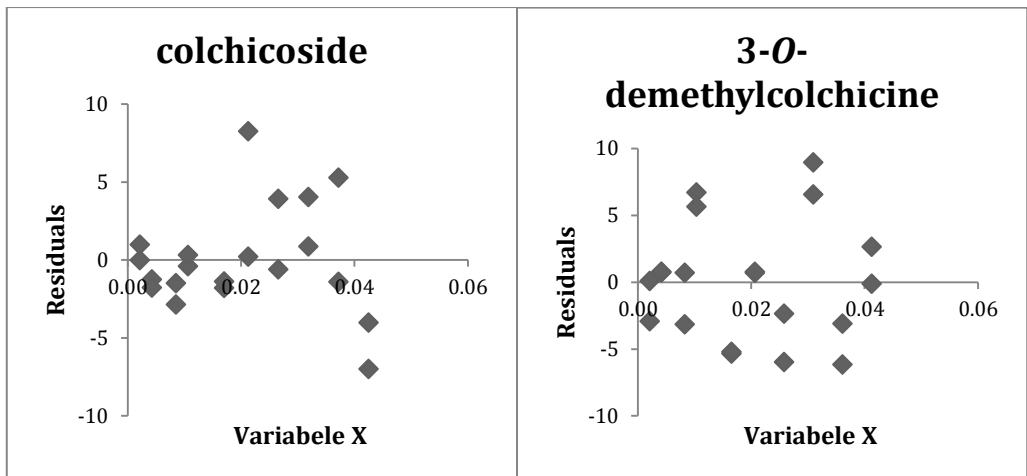


Figure 4.40 Residual plots of colchicoside and 3-O-demethylcolchicine

Precision of the correction factor for the response

For the determination and validation of the correction factor both primary standard (colchicoside and 3-*O*-demethylcolchicine) and secondary standard (colchicine) were injected on three different days. On day 1, a standard solution was prepared containing the primary and secondary standards in a concentration of 100%. On day 2, a standard solution was prepared containing the primary standard at the lowest level of the linearity range and the secondary standard in a concentration of 100%. On day 3, a standard solution was prepared containing the primary standard at the highest level of the linearity range and the secondary standard in a concentration of 100%. Fresh solutions were prepared daily and every solution was injected six times. The correction factor for the response was calculated for every injection taking into account the concentrations and peak areas of the primary and secondary standard.

For colchicoside, the concentrations, peak areas and the corresponding correction factor are shown in Table 4.13. The mean correction factors for each day were 1.93 (day 1), 1.91 (day 2), 1.97 (day 3) and the overall mean correction factor was 1.94. An ANOVA (one way, single factor, $\alpha=0.05$) was performed on all the correction factors obtained on the different days. By means of the F-test the difference between the results of the different days were investigated. The F_{calc} was 79.5, which is higher than the F_{crit} (3.68), but the $\text{RSD}\%_{\text{between days}}$, which is 1.71%, is smaller than 5%, so the mean correction factor for the response was applicable for the whole range of the method.

For 3-*O*-demethylcolchicine, the concentrations and peak areas and the corresponding correction factor are shown in Table 4.14. The mean correction factors for each day were 1.19 (day 1), 1.17 (day 2), 1.25 (day 3) and the overall mean correction factor was 1.20. An ANOVA (one way, single factor, $\alpha=0.05$) was performed on all the correction factors obtained on the different days. By means of the F-test the difference between the results of the different days was investigated. The F_{calc} was 263.12, which is higher than the F_{crit} (3.68), but the $\text{RSD}\%_{\text{between days}}$, which is 3.51%, is smaller than 5%, so the mean correction factor for the response was applicable for the whole range of the method.

Table 4.13 Correction factor colchicoside

	Concentration ($\mu\text{g/mL}$)		Peak area		Correction factor
	colchicoside	colchicine	colchicoside	colchicine	
day 1	16.80	9.68	815.8	908.3	1.93
			813.4	904.1	1.93
			815.0	910.6	1.94
			814.5	909.0	1.94
			815.1	907.8	1.93
			812.1	906.3	1.94
day 2	4.20	9.37	203.3	867.8	1.91
			205.3	871.0	1.90
			204.7	872.6	1.91
			205.6	865.4	1.89
			202.5	867.0	1.92
			205.1	869.5	1.90
day 3	27.57	10.72	1325.6	1012.4	1.96
			1330.3	1018.2	1.97
			1332.5	1013.2	1.95
			1324.2	1017.2	1.98
			1328.8	1022.2	1.98
			1331.0	1024.0	1.98

Table 4.14 Correction factor 3-O-demethylcolchicine

	Concentration ($\mu\text{g/mL}$)		Peak area		Correction factor
	3-O-demethyl colchicine	colchicine	3-O-demethyl colchicine	colchicine	
day 1	10.31	9.82	795.9	898.2	1.18
			797.6	907.7	1.19
			802.8	907.8	1.19
			802.7	908.6	1.19
			797.6	901.1	1.19
			799.0	899.5	1.18
day 2	2.02	9.93	161.0	928.0	1.17
			163.0	924.0	1.15
			160.3	921.7	1.17
			160.0	921.1	1.17
			159.8	919.5	1.17
			162.5	921.6	1.15
day 3	40.04	9.86	161.0	928.0	1.17
			3038.8	937.7	1.25
			3059.1	937.6	1.25
			3042.1	929.3	1.24
			3048.5	936.5	1.25
			3043.1	932.1	1.24
3063.6	939.5	1.25			

4.4.5. Quantification of the different batches of extract

The plant material was extracted in different batches. Not all batches contained the same amount of colchicine and colchicine derivatives. This indicates again the importance of an analytical method to quantify the constituents of a plant extract. Even though the starting plant material is the same, extraction of the constituents can differ. Therefore every batch used in this study was quantified using the validated method. The batch used to optimise and validate the method (batch 1) was already quantified in section 2.4.4. and contained 4.62% colchicine and colchicine derivatives expressed as colchicine, and the overall mean of colchicine found in this batch was 2.81%. In section 2.4.5 the individual content of the colchicine derivatives of batch 1 were calculated using the correction factor and resulted in 1.46% of colchicoside and 1.27% of 3-*O*-demethylcolchicine.

Batch 2, 3 and the colchicine-poor fraction were analysed with the method described in 2.4.3. Every sample was prepared in triplicate and a fresh stock solution of colchicine was prepared every time. Batch 2 was the batch used for the *in vitro* study and contained 5.71% of colchicine and colchicine derivatives expressed as colchicine. This batch contained 2.93% colchicine, 2.58% colchicoside and 1.74% 3-*O*-demethylcolchicine. Batch 3 was the batch used for the *in vivo* study and contained 5.79% of colchicine and colchicine derivatives expressed as colchicine. This batch contained 3.22% colchicine, 2.52% colchicoside and 1.52% 3-*O*-demethylcolchicine. The colchicine-poor extract was produced by liquid-liquid partition starting from this batch of crude extract. This colchicine-poor extract contained 1.61% of colchicine and colchicine derivatives expressed as colchicine, more in particular 0.07% colchicine, 2.26% colchicoside and 0.46% 3-*O*-demethylcolchicine. Figure 4.41 shows the chromatogram comparing the two extracts used in the *in vivo* study.

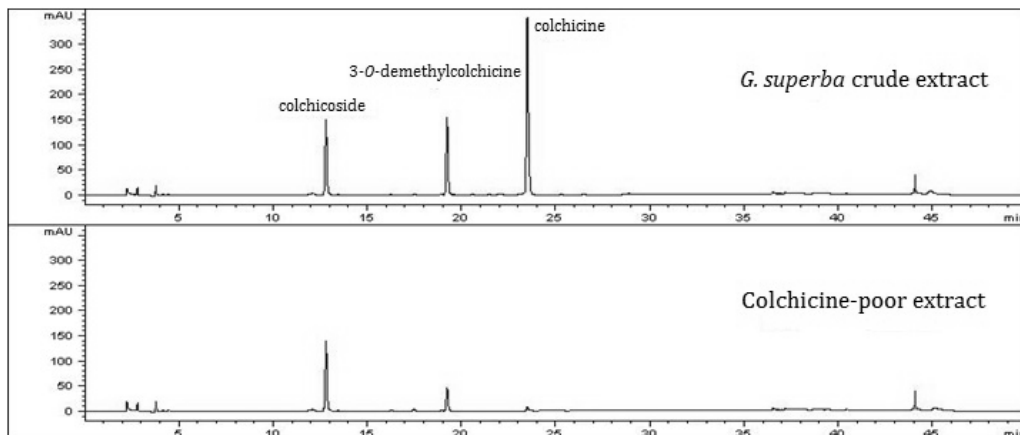


Figure 4.41 Chromatogram of the crude extract and the colchicine-poor extract

4.4.6. Summary and conclusion

An analytical method for the quantification of the 3 main constituents of the 80% ethanolic extract of *Gloriosa superba* has been optimised. This method quantifies the total amount of colchicine and colchicine derivatives expressed as colchicine. This analytical method was then validated according to the ICH guidelines. The calibration curve of colchicine indicated that the model was linear over the range of 0.0021 to 0.0419 mg/mL. The method was shown to be precise with respect to time (RSD% of 3.07% for colchicine, 2.88% for 3-*O*-demethylcolchicine and 4.74% for colchicoside, 3 days, n = 6) and with respect to the concentration (RSD% of 2.91% for colchicine, 3.04% for 3-*O*-demethylcolchicine and 4.12% for colchicoside, 3 levels, n = 6). The overall mean of colchicine and colchicine derivatives found in the crude extract of *G. superba* was 4.62% expressed as colchicine and the overall mean of colchicine found in the crude extract was 2.81%. The accuracy of the method was investigated by means of the standard addition method in which the recovery of colchicine was tested. This resulted in a mean recovery of 100.02% with a RSD% of 2.17%. Based on these results it can be concluded that the newly optimised method is suitable for its purpose, namely the quantification of the total amount of colchicine derivatives (colchicoside and 3-*O*-demethylcolchicine) and colchicine in the crude extract of *G. superba* expressed as colchicine. The correction factors for

colchicoside and 3-*O*-demethylcolchicine were also determined and validated, resulting in a correction factor of 1.94 and 1.20, respectively. By using this correction factor, the individual constituents in the crude extract could be quantified; it contained 1.46% colchicoside and 1.27% 3-*O*-demethylcolchicine.

Different batches of extract contained different amounts of colchicine and colchicine derivatives. This emphasises the importance of quality/batch control and the use of quantified/standardised extracts. Even though the starting plant material of each batch is the same, variations in extraction lead to small differences in content. The level of plant constituents is influenced by different parameters, e.g. seasonal variation, location, time of harvest. Therefore it is important to have a validated analytical method to determine the quantity of each compound in each batch of plant material/extract.

The total level of colchicine and its derivatives of the plant extract that was used in the *in vitro* experiments was 5.71% expressed as colchicine, more in particular 2.93% colchicine, 2.58% colchicoside and 1.74% 3-*O*-demethylcolchicine. The extract used in the *in vivo* experiments contained 5.79% colchicine and colchicine derivatives expressed as colchicine (3.22% colchicine, 2.52% colchicoside and 1.52% 3-*O*-demethylcolchicine), and the colchicine-poor extract 1.61% colchicine and its derivatives expressed as colchicine (0.07% colchicine, 2.26% colchicoside and 0.46% 3-*O*-demethylcolchicine).

4.5. PRECLINICAL STUDIES

4.5.1. Introduction

Because of the extreme poor prognosis of pancreatic cancer, and because conventional cancer therapy only has little impact on this disease, it was decided in an early stage of the project to focus on pancreatic cancer.^[47, 48]

In Europe, pancreatic cancer is the tenth most frequent cancer and the eighth leading cause of cancer-related death.^[49] Pancreatic cancer has an extremely poor prognosis and is one of the deadliest types of cancer. Most pancreatic cancer patients will die within the first year of diagnosis and only 6% will survive five years. The lack of progress in primary prevention, early diagnosis and treatment underscores the need for additional efforts in pancreatic cancer research.^[48]

The pancreas contains two types of glands: the exocrine glands that produce enzymes that help to digest food, and the endocrine glands that produce important hormones such as insulin. They develop completely different types of tumours with distinct risk factors, symptoms, diagnostics tests, treatment and survival rate. The exocrine tumours are by far the most common type of pancreatic cancer.^[48] The cause of pancreatic cancer is not well known, but there are several factors that increase the risk, such as obesity, tobacco use, family history, certain inherited syndromes, etc.^[47] Pancreatic cancer is typically diagnosed with the use of a CT scan. If pancreatic cancer is highly suspected but the CT scan appears normal, an endoscopic ultrasound is performed. A cancer diagnosis is typically confirmed by biopsy, but due to the deep location of the pancreas and the medical complication of a biopsy, pancreatic cancer is the least of all major cancers to be microscopically confirmed. The prognosis is largely determined by the stage of the disease at diagnosis, whether there is lymph node involvement, and the extent of spread, i.e. local as well as to distant organs. The median survival ranges from 4.5 months for the most advanced stage to 24.1 months for the earliest stage.^[48, 50] The treatment is largely determined by whether the tumour can be removed surgically. This is the only treatment that offers a chance of cure for the patients.^[51] Postoperative (adjuvant) chemotherapy either alone or in combination with radiation has

been proven to improve progression-free and overall survival in both randomised controlled trials and observational studies.^[52, 53] Gemcitabine is usually the recommended first-line chemotherapy for pancreatic cancer patients. It is given alone or in combination with other drugs or radiotherapy.^[47, 48]

In this project *in vivo* studies of the *G. superba* crude extract (GS) (section 4.3.2) as well as the colchicine-poor extract (GS2B) (section 4.3.5) were envisaged (sections 4.5.3, 4.5.4 and 4.5.5), but first some preliminary *in vitro* cytotoxicity studies were carried out using the SRB and NR assay, including the human cancer cell lines MDA-MB-231 (breast cancer), HT-29 (colon cancer) and PANC-1 (pancreatic cancer), as well as the murine pancreatic cancer cell line PANC02, in view of the planned *in vivo* experiments where this cell line would be used. In addition, The effect on two primary endometrial cancer cell lines (PC-EM005 and PC-EM002) and on the mouse fibroblast cells (3T3) was evaluated with the impedance-based *xCELLigence* Real-Time Cell Analysis or RTCA platform (2.3.5).

4.5.2. *In vitro* cytotoxicity

4.5.2.1. Results

Using the SRB assay (2.3.3) GS was tested on different human cancer cell lines (MDA-MB-231, PANC-1 and HT-29) and the murine pancreatic cancer cells PANC02.

For the MDA-MB-231 cell lines, the used concentrations of GS ranged from 0.0001 – 100 $\mu\text{g}/\text{mL}$ and at least three experiments were performed for each incubation time (24 h and 72 h). The survival percentages per concentration for these experiments are displayed in the dose-response curves (Figure 4.42). The calculated IC_{50} values, determined from the dose-response curves, are summarised in Table 4.15.

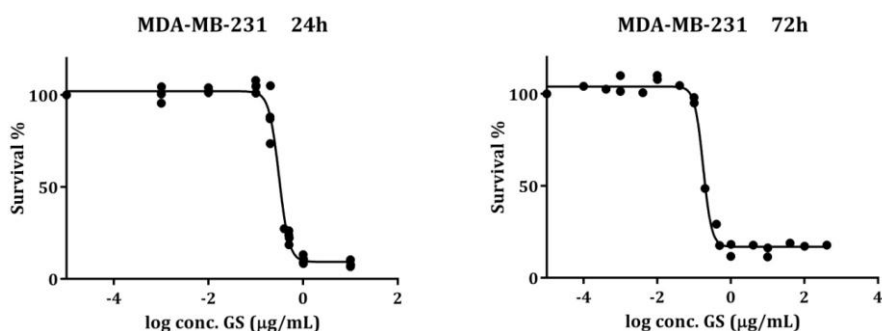


Figure 4.42 Dose-response curves of the MDA-MB-231 cell line treated with GS

The concentrations used to evaluate the effect on the PANC-1 ranged from 0.0001 – 100 $\mu\text{g}/\text{mL}$ and only two individual experiments were performed for both incubation times. However, the data were fitted in to a graph by non-linear regression (Figure 4.43) and the calculated IC_{50} values for this cell line are summarised in Table 4.15.

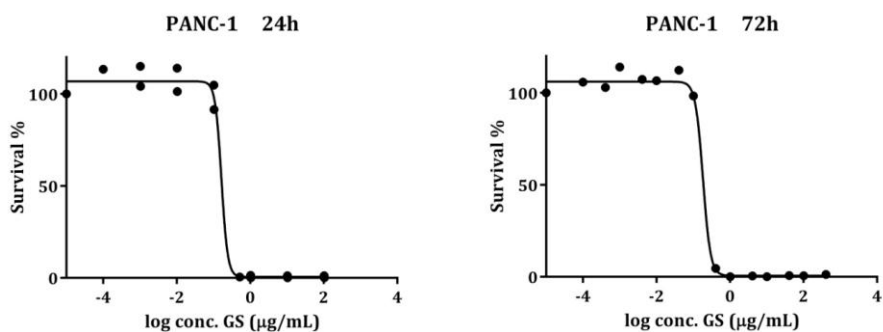


Figure 4.43 Dose-response curves of the PANC-1 cell line treated with GS

For the HT-29 cell line the concentrations ranged from 0.0001 – 100 µg/mL and three experiments were performed for the 24 h experiments, but for the 72 h only two experiments were performed. Figure 4.44 shows the graph of the results from the HT-29 experiments. The calculated IC₅₀ values for this cell line are summarised in Table 4.15.

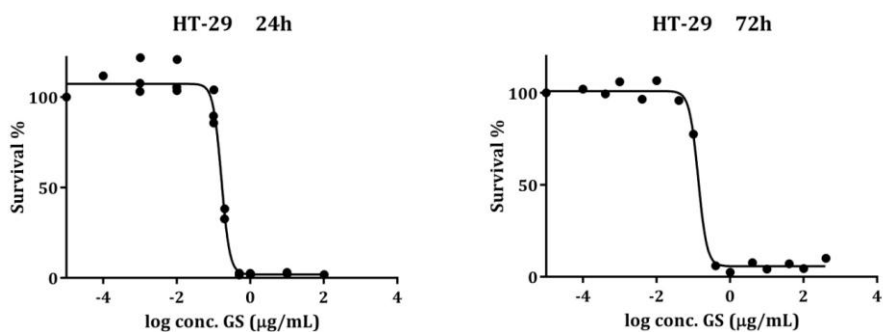


Figure 4.44 Dose-response curves of the HT-29 cell line treated with GS

For the PANC02 cell line, the used concentrations of GS ranged from 0.001 – 10 µg/mL. At least three individual experiments were performed. The colchicine-poor extract (GS2B) and colchicine (COL) were also tested *in vitro* on the PANC02 cells, but using only one incubation

time. Also at least three experiments were performed. The concentration ranged from 0.1 – 100 $\mu\text{g}/\text{mL}$ for GS2B and from 0.0001 – 10 $\mu\text{g}/\text{mL}$ for COL. The results of all these experiments are displayed in Figure 4.45. The calculated IC_{50} values for GS on this cell line are summarised in Table 4.15. IC_{50} values of 9.49 ± 0.41 and 0.098 ± 0.004 $\mu\text{g}/\text{mL}$ were determined for GS2B and COL, respectively, with an incubation time of 24 h.

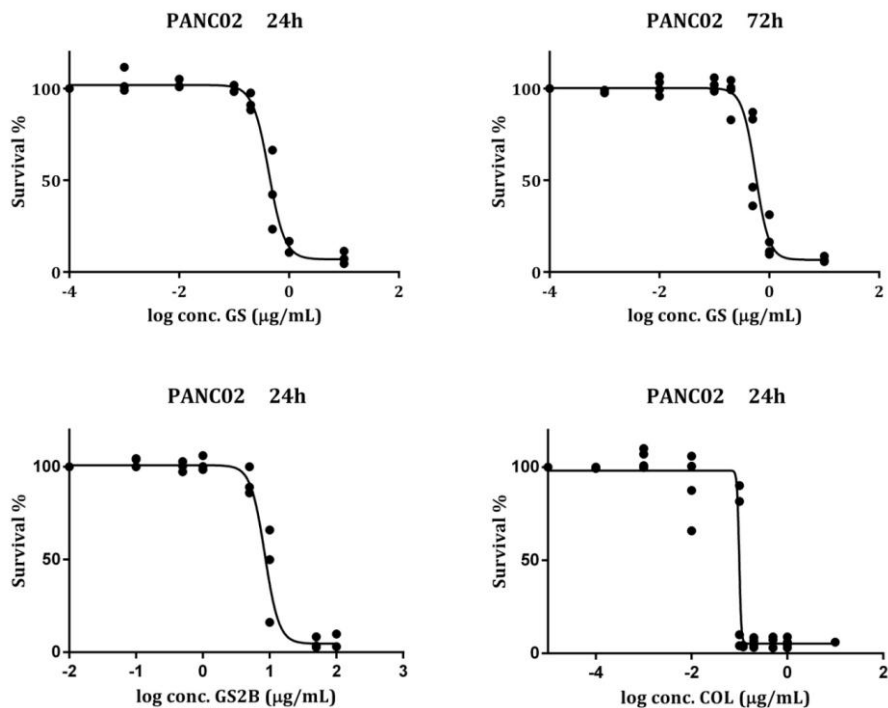


Figure 4.45 Dose-response curves of the PANC02 cell line treated with GS, GS2B and COL

Table 4.15 IC₅₀ of the *G. superba* crude extract on the tested cell lines

	IC ₅₀ ± SEM (µg/mL)			
	MDA-MB-231	PANC-1	HT-29	PANC02
24 h	0.34 ± 0.02	0.17*	0.17 ± 0.01	0.45 ± 0.03
72 h	0.24 ± 0.03	0.19 ± 0.02	0.16 ± 0.02	0.59 ± 0.04

*No standard error is shown since the best-fit value for the slope was difficult to determine, due to the low amount of data point in that area

The effect of GS on the BEAS-2B cell line was tested at 7 different concentrations (0.01 - 20 µg/mL) using the neutral red staining. A 40 mg/mL stock solution of the extract was prepared in DMSO and diluted in medium in such a way that the highest end percentage of DMSO did not exceed 0.05%. The graph (Figure 4.46) shows the percentage of cell viability inhibition relative to solvent control. The IC₅₀ as determined from the fitted curve was 0.1992 µg/mL. As reference points, the IC₅₀ values of the other human cancer cell lines, determined with the SRB assay were included in the graph. Precipitation and aspecific binding on neutral red were also examined macroscopically and microscopically, but none of these were observed for GS.

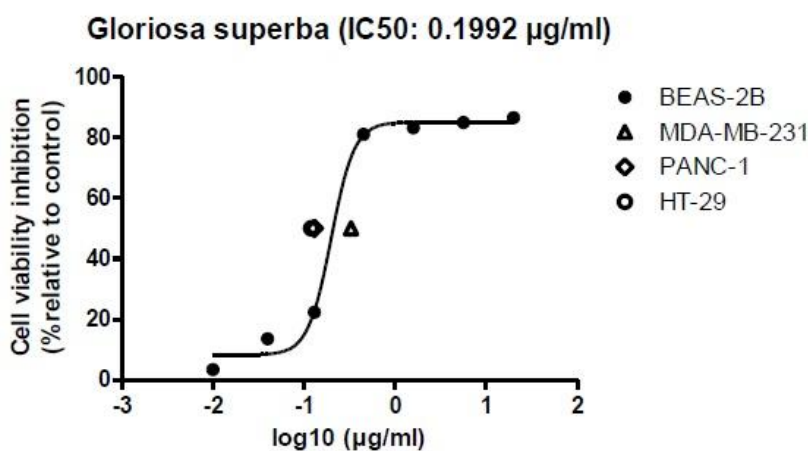


Figure 4.46 Dose-response curve and calculated IC₅₀ for effects on cell viability of BEAS-2B cells

The cytotoxicity on PC-EM005, PC-EM002 and 3T3 cells was evaluated with the impedance-based *xCELLigence* RTCA platform. Experiments were carried out using the *xCELLigence* RTCA DP instrument, where the impedance value of each well was automatically monitored by the RTCA platform and expressed as a cell index value (CI). Figure 4.47 shows the real-time plot of an *xCELLigence* cytotoxicity experiment of GS on one of the endometrial cell lines (PC-EM005). A dose-response curve (Figure 4.48) was then plotted and the IC₅₀ value was calculated and summarised in Table 4.16. The real-time plot of the two other cell lines (PC-EM002 and 3T3) are shown in Figure 4.49 and Figure 4.50 and the calculated IC₅₀ values are summarised in Table 4.16. The square R (R²) is also given in the table, which indicated the goodness of fitting of the data in a non-linear model.

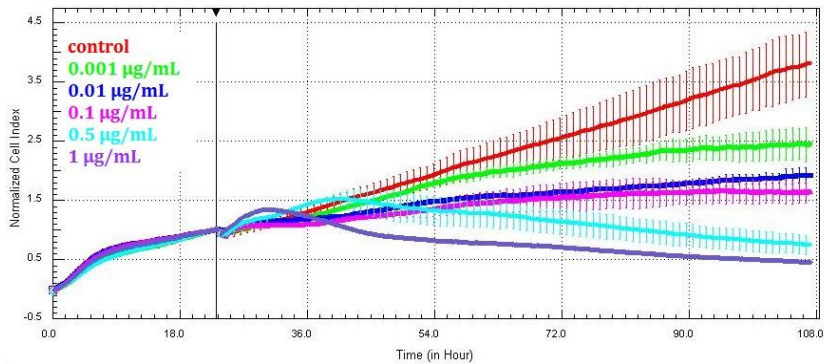


Figure 4.47 Real-time monitoring of the effect of GS on the PC-EM005 cell line

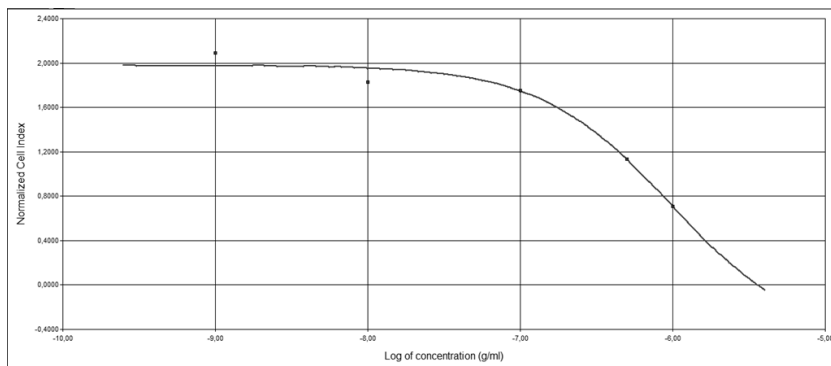


Figure 4.48 Dose-response curve of PC-EM005 treated with GS

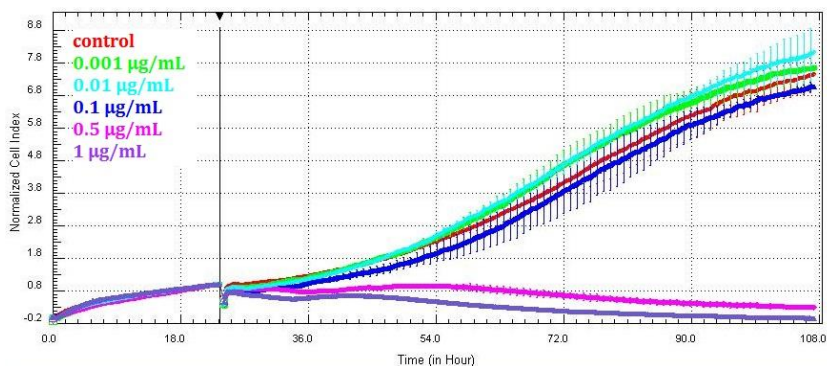


Figure 4.49 Real-time monitoring of the effect of GS on the PC-EM002 cell line

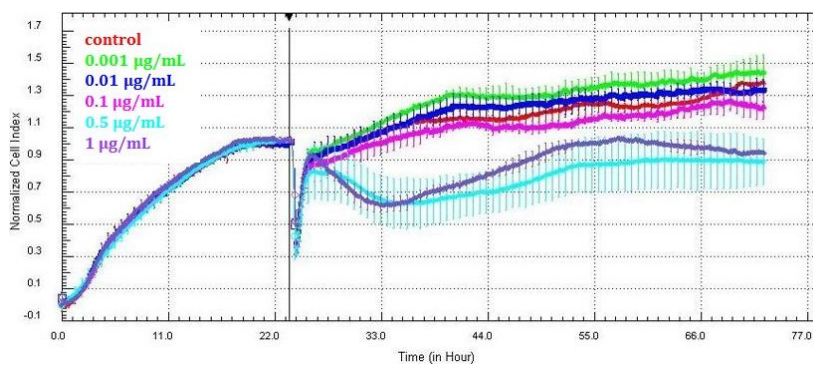


Figure 4.50 Real-time monitoring of the effect of GS on the 3T3 cell line

Table 4.16 IC₅₀ of the *G. superba* crude extract on the tested cell lines obtained with the RTCA system

	IC ₅₀ , µg/mL		
	PC-EM005	PC-EM002	3T3
48 h	0.99 (R ² : 0.99)	0.42 (R ² : 0.98)	0.19 (R ² : 0.96)

4.5.2.2. Discussion

The *G. superba* extract showed cytotoxic activity in a dose-dependent manner. Only small differences were observed between the IC₅₀ values, which were 0.34 (MDA-MB-231), 0.17 (PANC-1 and HT-29) and 0.45 µg/mL (PANC02) for the 24 h incubation time. According to the NCI plant extracts with an IC₅₀ less than 20 µg/mL are considered as highly cytotoxic.^[54] Thus, it can be concluded that GS was highly cytotoxic on all the tested cell lines, considering all determined IC₅₀ values were lower than 1 µg/mL. The cytotoxic activity did not increase greatly by prolonging the incubation time of GS and once again, the cytotoxic effect observed on the MDA-MB-231 cell line tended to be less compared to PANC-1 and HT-29. Also for PANC02, the IC₅₀ value was higher compared to the other cell lines. Nevertheless, it still showed a good dose-response and the IC₅₀ value was still lower than 1 µg/mL.

The effect on the two primary endometrial cell lines was slightly different. Although the real-time monitoring of the effect on PC-EM005 showed a dose-dependent cytotoxic effect, it seems that PC-EM005 was less susceptible to GS compared to PC-EM002, when comparing the IC₅₀ values on both cell lines. A slight proliferation inhibition on the PC-EM005 was already observed at a concentration of 0.001 µg/mL but for a decrease of the number of cells, higher concentrations were needed. For PC-EM002 no inhibition of proliferation was observed in the lower concentration range, but when treated with a concentration of 0.5 µg/mL, a cytotoxic effect was observed on the real-time plot. With regard to the 3T3 cells a cytotoxic activity was observed approximately 3 h after treatment with 0.5 µg/mL and 1 µg/mL GS.

With regard to the IC₅₀ values on the two normal cell lines (BEAS-2B and 3T3) approximately the same values were found, in the same range as observed for the cancer cells. The *in vitro* cytotoxicity of GS is mainly due to its main constituent colchicine. Nevertheless the extract also contains potential prodrugs such as colchicoside. Colchicoside can be converted by β-glucosidase activity of the microflora in the gastrointestinal tract to the cytotoxic aglycon 3-O-demethylcolchicine, one of the genuine constituents of GS. The presence of prodrugs (e.g. colchicoside), that are not active *in vitro*, can lower the concentration needed to have a certain effect *in vivo* due to the added activity of the prodrugs, and can possibly reduce *in vivo* toxicity because of a slow-release effect.

Therefore an extract (GS2B) was developed with a relatively low level of colchicine and a relatively high content of colchicine derivatives, especially colchicoside. This extract was also tested *in vitro*, but since colchicoside needs to be activated *in vivo*, not surprisingly the IC₅₀ was much higher for this extract than for GS. An IC₅₀ value of 9.49 µg/mL was observed on the PANC02 cell line, which is hundred times larger than the value observed for colchicine itself, i.e. 0.098 µg/mL. The *in vitro* cytotoxicity of GS2B is mainly due to residual colchicine and 3-*O*-demethylcolchicine.

In order to confirm the *in vitro* activity, and to verify the hypothesis that prodrugs such as colchicoside may not only add to the *in vivo* activity, but at the same time lead to reduce *in vivo* toxicity, *in vivo* experiments were scheduled as the next step.

4.5.3. Preliminary *in vivo* study

Preliminary *in vivo* studies were performed to establish the mouse model and to evaluate the growth of the subcutaneous tumour in the chosen model. Inbred wild type mice (e.g. C57BL/6, BALB/c, and C3H) have been used for > 50 years to investigate tumour growth and treatment response. These mice have fully competent immune response, which allows the study of the role of the immune system during therapy, but require mouse-strain specific murine tumour models (syngeneic tumours).^[55] An acute toxicity study was performed prior the efficacy study on a small number of non-tumour-bearing mice to evaluate whether the highest dose of *G. superba* crude extract would cause immediate clinical signs of toxicity.

4.5.3.1. Materials and methods

Cell culture

The PANC02 cells were provided (2013-04-11) by Prof. Dr. C. Gravekamp, (Albert Einstein College of Medicine, New York, USA) and were cultured in RPMI 1640 medium supplemented with 10% FBS, 1% L-glutamine, 1% sodium pyruvate and 1% penicillin/streptomycin. The cells were maintained in exponential growth in a humidified 5% CO₂ /95% air atmosphere at 37 °C.

Animals

Six-to-eight weeks old male HsdOla/MF1 (n = 3) and female C57BL/6 mice (n = 3) (16 - 20 g body weight) were purchased from Harlan laboratories (Netherlands). The mice were housed in individually ventilated cages, under a 10/14 h dark/light cycle at constant temperature and humidity and had access to tap water and food *ad libitum*. All animals were treated in accordance to the guidelines and regulations for use and care of animals. All mice experiments were approved by the local Ethical Committee of the University of Antwerp, approved study number: 2013-03.

Subcutaneous tumour model

Cultures of PANC02 cells were harvested using a 0.05% trypsin solution, washed twice in sterile PBS and resuspended in sterile PBS at a concentration of 50 x 10⁶ cells per mL. The

viable cells were counted by using the Muse® Cell Analyzer (Merck Millipore). The mice were inoculated with 100 µL of the cell suspension in the right hind limb. Tumour growth of the subcutaneous model was evaluated with calliper measurements from the moment the tumours became palpable and this three times a week. The tumour volume was calculated by means of formula $V = 0.5 \times ab^2$, with a and b being the long and short axes of the tumour, respectively.

Acute toxicity study

An acute toxicity study was carried out with the *G. superba* crude extract before performing the larger *in vivo* - efficacy study (section 4.5.4). This was carried out on healthy non-tumour-bearing C57BL/6 mice (n = 3). The mice were given a dose of 3 mg/kg body weight (BW) total amount of colchicine and its derivatives expressed as colchicine (TC) of crude extract. With the use of the validated analytical method (mentioned in section 4.4.2), the percentage of colchicine and its derivatives in GS was analysed and amounted to 5.79% (m/m) TC. Taking this percentage into account, 51.7 mg *G. superba* extract/kg BW was given during 5 consecutive days by oral gavage (p.o.). To evaluate the possible toxicological effects of the *G. superba* extract body weight was determined during therapy (5 days) and in follow-up for another 3 days. The mice were also daily inspected for clinical signs of toxicity by using an observation table employed in cancer research and toxicological studies (Table 4.17).^[56]

4.5.3.2. Results and discussion

Tumour growth

A tumour growth study was performed to test the growth of the subcutaneous tumour in the chosen mouse model and to test how long it takes to reach the desired tumour volume. The first chosen PANC02 mice model was a HsdOla/MF1 mouse strain previously reported by Casneuf et al.^[57] This model did not give the expected tumour size and 100% tumour formation. The decision was made to change the mouse strain. Because the PANC02 cell line originated from C57BL/6 mice^[58], this strain was then selected. Three C57BL/6 mice were inoculated with 5×10^6 PANC02 cells and tumour growth was evaluated ± every other day for

28 days by means of calliper measurements. Results are shown in Figure 4.51. This study showed that the C57BL/6 mouse strain developed a mean tumour volume of 300 - 400 mm³ after 19 days of inoculation and 100% tumour formation was observed.

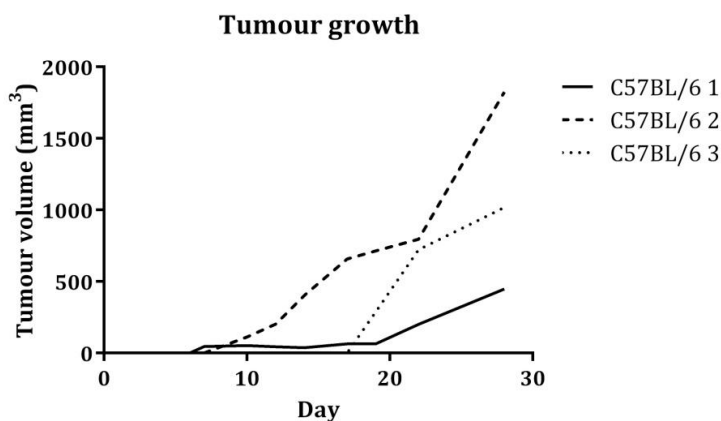


Figure 4.51 Tumour growth

Acute toxicity study

An acute toxicity study was performed by giving non-tumour-bearing C57BL/6 mice (n = 3) a high dose of GS, which was 51.7 mg/kg BW, during 5 consecutive days. This study was performed prior the *in vivo* efficacy study to exclude to possibility that a large amount of mice with induced tumours would be sacrificed at an early stage of the study due to immediate clinical signs of toxicity. The hypothesis of this toxicological study was that GS would cause immediate toxicity due to the high content of colchicine in the highest dose of extract, therefore only GS was tested in this preliminary study. However, the acute toxicity of GS and GS2B was further investigated in a longer time frame and with more animals during the efficacy study, which is described in detail in section 4.5.4. The toxicity was evaluated by weight loss and an observation table (Table 4.17). The body weight was measured daily during treatment. Figure 4.52 shows that the used dose of GS did not cause any weight loss greater than 10% of the initial body weight. Also, three days after treatment, the body weights were still stable. None of the observation criteria (Table 4.17) were met during the acute

toxicity studies. Therefore, the conclusion could be made that GS at a dose of 51.7 mg/kg did not cause any acute toxicity.

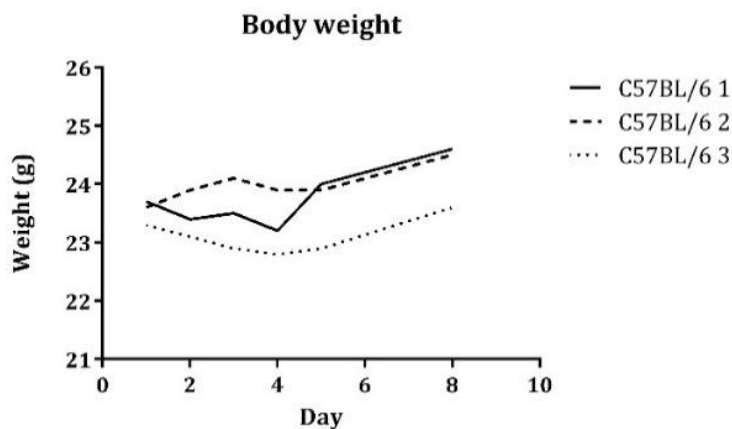


Figure 4.52 Body weight observation during 5 days of treatment and follow-up for another 3 days

Table 4.17 Selected clinical observations used in cancer research and toxicological studies (Adapted from Montgomery et al., 1990)

Parameter	What to look for	day 1	day 2	day 3	day 4	day 5
General Appearance	Dehydration, decreased body weight, missing anatomy, abnormal posture, hypothermia, fractured appendage, swelling, tissue masses, prolapse, paraphimosis	NP	NP	NP	NP	NP
Skin and fur	Discoloration, urine stain, pallor, redness, cyanosis, icterus, wound, sore, abscess, ulcer, alopecia, ruffled fur	NP	NP	NP	NP	NP
Eyes	Exophthalmos, microphthalmia, ptosis, reddened eye, lacrimation, discharge, opacity	NP	NP	NP	NP	NP
Nose, mouth, and head	Head tilted, nasal discharge, malocclusion, salivation	NP	NP	NP	NP	NP
Respiration	Sneezing, dyspnea, tachypnea, rales	NP	NP	NP	NP	NP
Urine	Discoloration, blood in urine, polyuria, anuria	NP	NP	NP	NP	NP
Feces	Discoloration, blood in the feces, softness/diarrhea	NP	NP	NP	NP	NP
Locomotor	Hyperactivity, coma, ataxia, circling, muscle tremors	NP	NP	NP	NP	NP

NP = Not present

4.5.4. ***In vivo* – efficacy study**

The *G. superba* crude extract (GS) and the colchicine-poor extract (GS2B) (mentioned in section 4.3.2 and 4.3.5) were tested *in vivo* in a murine model to evaluate their efficacy against PANC02 cells-induced tumours and to assess their toxicity.

4.5.4.1. Materials and methods

Cell culture

The same PANC02 cell culture was used as in the previous *in vivo* study, mentioned in section 4.5.3.1.

Animals

Six-to-eight weeks old female C57BL/6 mice (16 - 20 g body weight) were purchased from Harlan laboratories. The mice were housed in individually ventilated cages, under a 10/14 h dark/ light cycle at constant temperature and humidity and had access to tap water and food *ad libitum*. All animals were treated in accordance to the guidelines and regulations for use and care of animals. All mice experiments were approved by the local Ethical Committee of the University of Antwerp, approved study number: 2013-03.

Subcutaneous tumour model

Cultures of PANC02 cells were harvested using a 0.05% trypsin solution, washed twice in sterile PBS and resuspended in sterile PBS at a concentration of 30×10^6 cells per mL. The viable cells were counted by using the Muse[®] Cell Analyzer. The mice (n = 56) were inoculated with 100 μ L of the cell suspension in the right hind limb. Each mouse was randomly assigned to one of 8 groups (n = 6 - 8 mice per group) receiving a different treatment (Table 4.18). Tumour growth of the subcutaneous model was evaluated with calliper measurements from the moment the tumours became palpable and this three times a week before treatment and daily during treatment. The tumour volume was calculated with the formula mentioned in 4.5.3.1.

Table 4.18 Group treatment assignment

n°	Group	# mice	Treatment and dose
1	Negative control	7	200 µl water p.o.
2	Positive control	7	60 mg/kg BW gemcitabine IP
3	<i>Gloriosa superba</i> extract (GS)	6	0.3 mg/kg BW TC* 5.2 mg/kg BW extract p.o.
4		6	1 mg/kg BW TC* 17.2 mg/kg BW extract p.o.
5		8	3 mg/kg BW TC* 51.7 mg/kg BW extract p.o.
6	Colchicine-poor extract (GS2B)	6	0.3 mg/kg BW TC* 18.8 mg/kg BW extract p.o.
7		6	1 mg/kg BW TC* 62.5 mg/kg BW extract p.o.
8		7	3 mg/kg BW TC* 187.5 mg/kg BW extract p.o.

* Total amount of colchicine and its derivatives expressed as colchicine

Treatments

Treatment was administered during 10 days, starting 19 days after tumour inoculation when tumours had reached a volume of approximately 300 - 400 mm³. The first day of treatment was assigned "day 1" (Figure 4.53). The negative control group received 200 µL water per oral gavage (p.o.) daily. The positive control group was given 3 times/week (days 1, 3, 5, 8, 10) gemcitabine (Actavis, 38 mg/mL). It was administered at a dose of 60 mg/kg BW intraperitoneally (IP). GS and GS2B were administered by oral gavage daily at a dose of 0.3, 1 and 3 mg/kg BW total amount of colchicine and its derivatives expressed as colchicine. For both extracts the total amount of colchicine and its derivatives (calculated as colchicine) was the same, but the amount of colchicine itself in the extracts was different. The amount of colchicine in GS2B was less than 0.1% (m/m). With the use of the validated analytical method (mentioned in section 4.4.2), the percentages of colchicine and its derivatives in GS as in GS2B were analysed and amounted to 5.79% (m/m) and 1.61% (m/m) TC, respectively. Taking this percentage into account, groups 3, 4 and 5 were given 5.2, 17.2 and 51.7 mg/kg BW GS and groups 6, 7 and 8 were given 18.8, 62.5 and 187.5 mg/kg BW GS2B (Table 4.18). To evaluate

the effect of the treatment, tumour volume was measured daily during treatment and the mice were sacrificed on day 11. Toxicity caused by treatment was also evaluated by determining the body weight of the mice daily during the treatment and by daily inspection of the mice for clinical signs of toxicity by means of the observational table (Table 4.17).

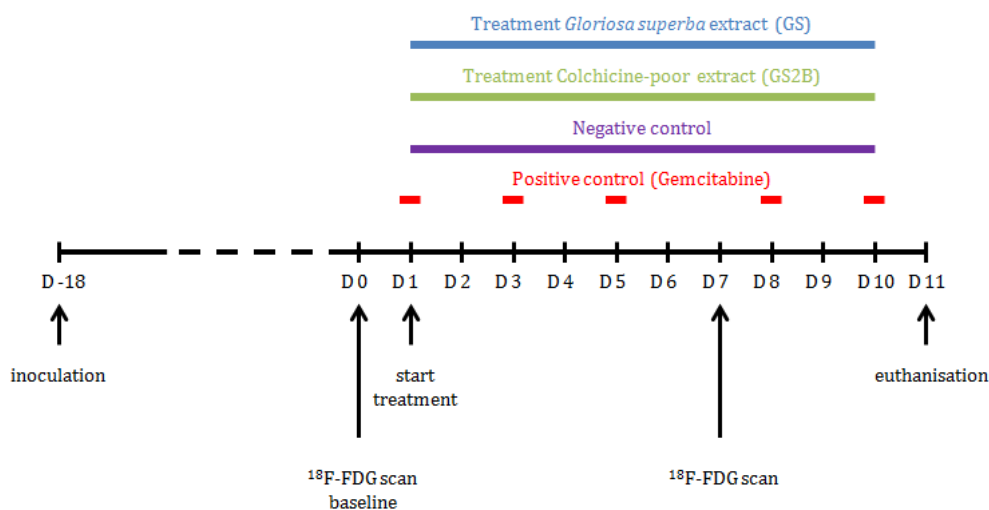


Figure 4.53 Timeline of the *in vivo* efficacy experiment

Imaging

Imaging was performed on a Siemens Inveon PET-CT scanner (Siemens Preclinical Solutions, Knoxville, TN, USA) at the Molecular Imaging Center Antwerp (MICA). Data analyses were performed using the PMOD software (PMOD Technologies, Zurich, Switzerland). Three animals per group underwent an [¹⁸F]-FDG PET/CT scan at 2 different time points: Baseline (day 0) and day 7 of treatment. Mice were anaesthetised before and during the scans with isoflurane (2-3% for induction; 0.25-2% for maintenance) (Forene®, Abbott, Louvain-La-Neuve, Belgium) in an induction chamber and body temperature was kept constant by a heating bed. Before [¹⁸F]-FDG (fludeoxyglucose) injection (0.5 mCi, intravenous), animals were fasted at least 8 h. The blood glucose levels of the mice were determined in duplicate immediately after tracer injection with an OneTouch Ultra 2 glucose meter (LifeScan, Tilburg,

The Netherlands). The mice were positioned one by one onto the micro positron emission tomography (μ PET) scan bed and scanned for 20 minutes, followed by a micro computed tomography (μ CT) scan. CT-based attenuation corrections were applied on the PET data. Delineation of the tumours were done based on CT. Averaged FDG activity concentrations (kBq/cc) for the different volume of interest (VOI) were extracted and the standard uptake values (SUVs) for these VOIs were calculated as $SUV = \text{FDG activity concentration} / \text{injected dose (kBq)} \times \text{body weight (g)}$. The SUV_{mean} were also calculated and correction for the blood glucose levels was applied. The intra-animal SUV_{mean} changes, which is the ratio of the determined SUV after treatment to the determined SUV before treatment were also calculated.

Immunohistochemistry

Tumours were harvested on day 11 and fixed in formaldehyde. At the Department of Pathology at the Antwerp University Hospital tumours were paraffin-embedded and immunohistochemical (IHC) staining was performed on 3 μm tumour slices. The tumour slices underwent haematoxylin and eosin (H&E), caspase-3 and Ki-67 staining.

Before staining, the slices were deparaffinised by incubating the slices in three washes of xylene for 5 min each, followed by incubating in two washes of 100% ethanol for 10 min each and finally by incubating in two washes of 95% ethanol for 10 min each.

For cleaved caspase-3 and Ki-67 staining, after deparaffinisation, heat induced antigen unmasking was performed for 10 or 20 min in citrate buffer (pH 6.0), respectively, after which the tissue slices were cooled down for 30 min. The endogenous peroxidase activity was blocked with 3% hydrogen peroxide for 15 min. The slices were then washed two times in deionised water and one time in washing buffer, which is a tris buffered saline with Tween[®] 20 solution (TBST) for 5 min each. After the washing steps, caspase-3 slices were blocked with blocking solution (TBST/5% normal goat serum) for 1 h at room temperature. The blocking solution was then removed, cleaved caspase-3 primary antibody or mouse specific Ki-67 primary antibody (Cell Signaling Technology, 1/400 dilution for Ki-67 and 1/300 for caspase-3 in TBST/5% normal goat serum) was added and the slices were incubated overnight at 4 °C. After washing the slices with the buffer three times for 5 min, the slices were incubated for 30 min at room temperature with a labelled polymer-HRP (horseradish peroxidase) anti-rabbit

secondary antibody (SignalStain® Boost IHC detection reagent, Cell Signaling Technology). Colour was developed using the chromogen 3,3'-diaminobenzidine (DAB) (DakoCytomation) for 10 min. After washing, the tissue slices were counterstained with Mayer's haematoxylin. TBST/5% normal goat serum instead of the primary antibody was used as negative control in order to exclude false positive response from non-specific binding of the secondary antibody. For the quantification of degree of apoptosis and proliferation, the entire tumour slice was scanned first at low power (magnification, 40x) to obtain a global view per tumour. Ten regions of interest (ROI) were then chosen at random per slice at a magnification of 200x. High necrotic regions were excluded for analysis. Per ROI the percentage of Ki-67 positive cells was determined and the mean of ten ROIs was the overall percentage of that slice. This percentage indicated the degree of proliferation. For the caspase-3 staining, the number of apoptotic bodies, which was scored between 1 to 5 with 1 being no to almost no presence of apoptotic bodies, was determined per ROI. Again the mean of ten ROIs was used to determine the degree of apoptosis. Per treatment group a mean score was calculated and this value was used for further analysis.

Statistics

Results were expressed as mean values of parameters \pm standard error (SE). The parametric ANOVA test was used to determine statistical significance, followed by a post hoc Tukey analysis to establish the statistical difference between the treatment groups. An one-way ANOVA followed by an uncorrected Fisher's LSD test was used to determine statistical differences in the intra-animal SUV_{mean} ratio between treatment groups. Non-parametric Kruskal-Wallis tests were used to determine statistical difference in degree of proliferation and apoptosis between groups, followed by a post hoc Dunn's test, for multiple comparisons. To evaluate the correlation between the relative tumour volumes and the IHC scores, a non-parametric Spearman's correlations assay was used. A p-value ≤ 0.05 was considered significant and statistical analysis was performed using GraphPad Prism 6 (Version 6.01).

4.5.4.2. Results

All mice developed subcutaneous tumours in the right hind limb (100% tumour growth). Eighteen days after inoculation, the tumours had reached a mean volume of 300 - 400 mm³ and treatment started. On day 0, which was the day before treatment, the starting mean tumour volumes per group were plotted (Figure 4.54) and tumour volumes were normalised. The mean relative tumour volumes (RTVs) were then calculated for each group for each day and plotted (Figure 4.55). The mean RTVs on day 7 and 10 were graphed and the difference between the groups was statistically determined (Figure 4.56). The two latter figures show the effect of the treatment for each group. The percentage of tumour growth inhibition (%TGI) on day 7 and 10 were calculated according to the formula: $\%TGI = 1 - (RTV_x - 1/RTV_c - 1)$, with RTV_x being the relative tumour volume from the treated group and RTV_c the relative tumour volume from the control group. The %TGI are summarised in Table 4.19. All animals were weighed daily during treatment to evaluate toxicity and the mean body weight per group was graphed (Figure 4.57). Table 4.20 summarises the mean body weight of the different treatments and the relative mean body weight at day 10. This table shows a clear gain of body weight for all groups after 10 days of treatment.

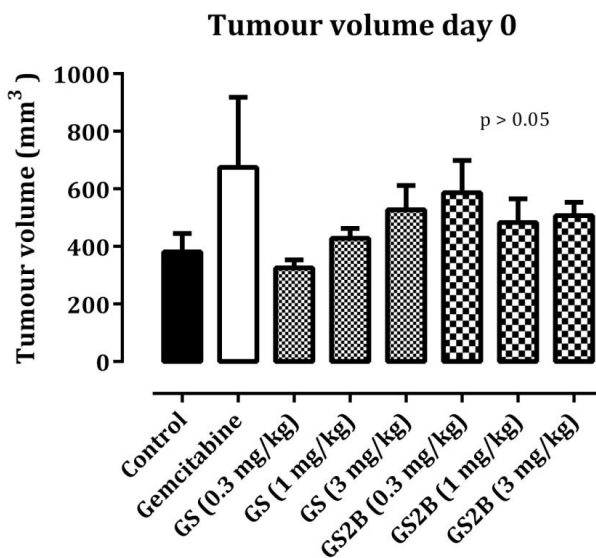


Figure 4.54 Tumour volume on day 0

Mean relative tumour volumes

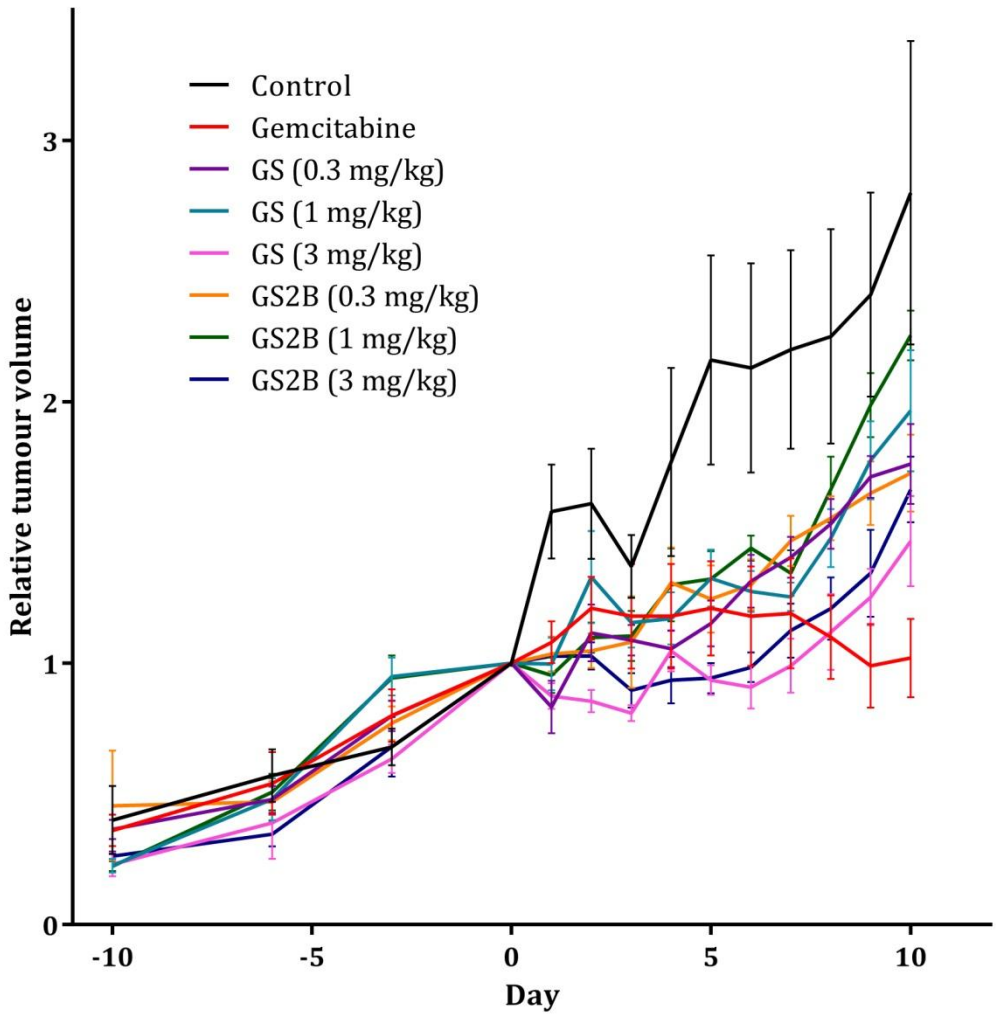


Figure 4.55 Mean relative tumour volumes

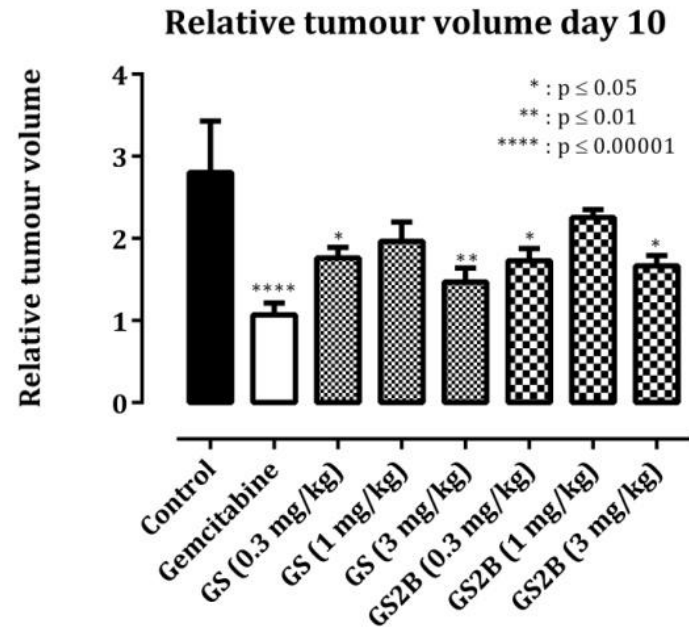
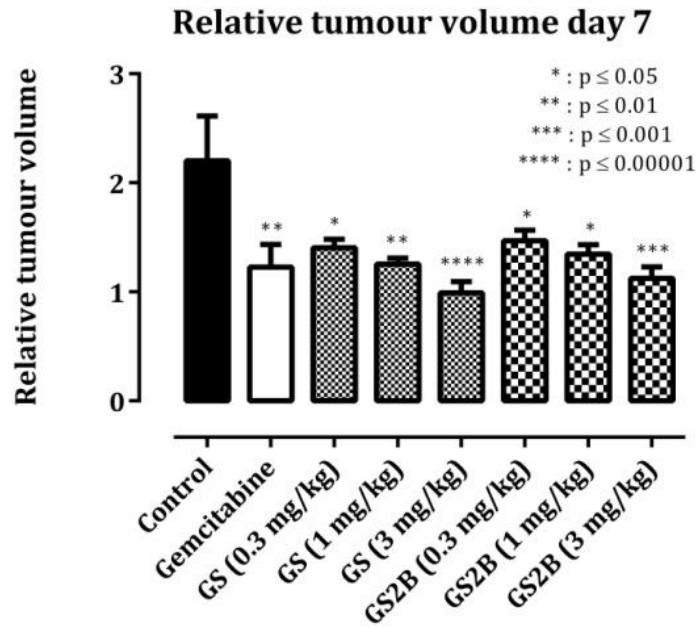


Figure 4.56 Mean relative tumour volumes on day 7 & 10

Table 4.19 Tumour growth inhibition percentage on day 7 and 10

Treatment	% TGI (day 7)	% TGI (day 10)
Gemcitabine	90%	99%
GS (0.3 mg/kg)	78%	58%
GS (1 mg/kg)	86%	46%
GS (3mg/kg)	101%	74%
GS2B (0.3 mg/kg)	74%	60%
GS2B (1 mg/kg)	81%	30%
GS2B (3mg/kg)	93%	63%

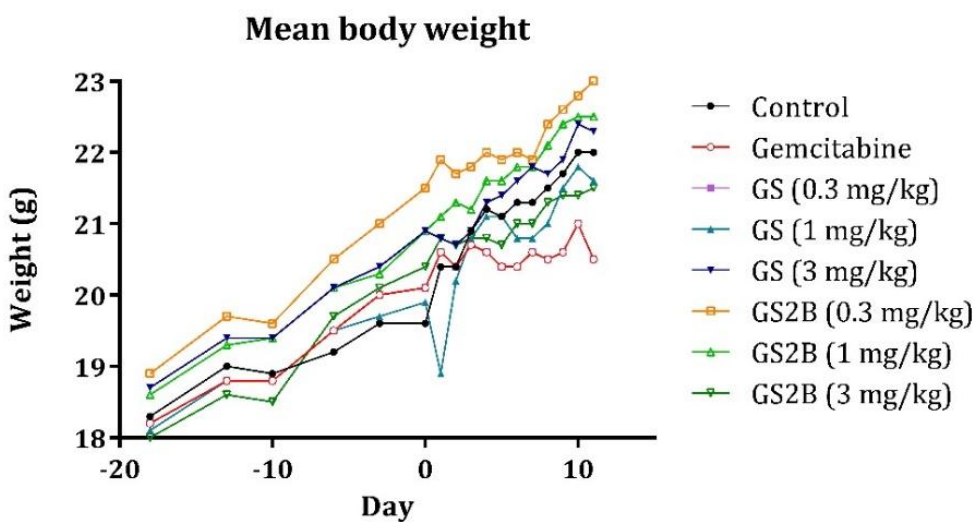


Figure 4.57 Mean body weight

Table 4.20 Mean body weight at day 0, day 10 and the relative body weight at day 10 (normalised to day 0)

Treatment group	Mean body weight \pm (SE)		
	day 0	day 10	relative body weight at day 10
Control	19.6 \pm 0.7	22.0 \pm 1.2	1.12 \pm 0.02
Gemcitabine	20.1 \pm 0.5	21.0 \pm 0.6	1.04 \pm 0.01
GS (0.3 mg/kg)	19.1 \pm 0.3	20.6 \pm 0.3	1.08 \pm 0.02
GS (1 mg/kg)	19.9 \pm 0.6	21.8 \pm 0.5	1.09 \pm 0.01
GS (3mg/kg)	20.9 \pm 0.4	22.4 \pm 0.6	1.07 \pm 0.02
GS2B (0.3 mg/kg)	21.5 \pm 0.6	22.8 \pm 0.9	1.06 \pm 0.02
GS2B (1 mg/kg)	20.9 \pm 0.5	22.5 \pm 0.4	1.08 \pm 0.03
GS2B (3mg/kg)	20.2 \pm 0.4	21.4 \pm 0.6	1.06 \pm 0.01

During the *in vivo* experiment also two kinds of imaging modalities (PET/CT scan) were performed to study the tumours (Figure 4.58). The SUV_{mean} for the different treatment groups at two different time points (baseline and day 7) corrected for blood glucose were calculated and the intra-animal SUV_{mean} changes between the two time points are shown in Figure 4.59. Correlation analysis was also performed between the measured RTV and the SUV_{mean} ratio (Figure 4.60)

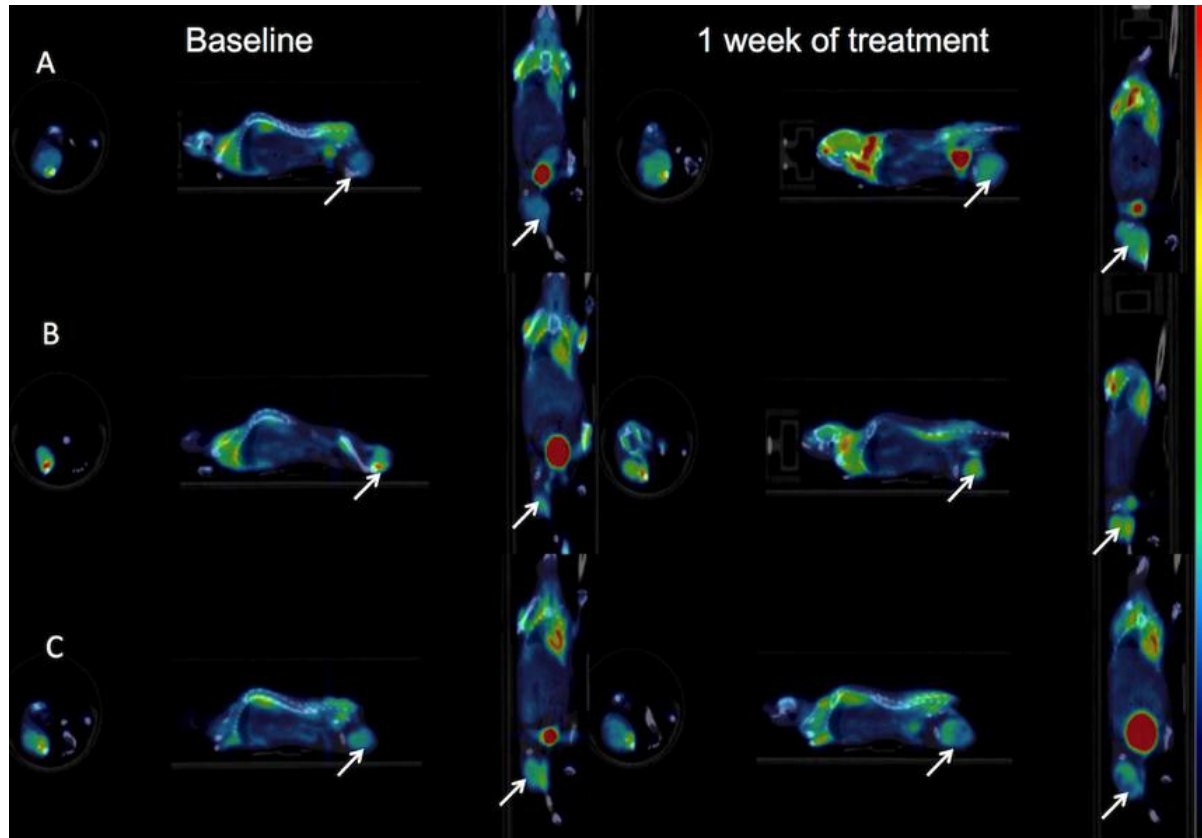


Figure 4.58 Representative PET/CT images at baseline and after 1 week of treatment. Transversal, sagittal and coronal slices are shown, with white arrows indicating the tumour. (A) control group, (B) gemcitabine group and (C) GS2B (1 mg/kg) group. SUV scale from 0 – 4.

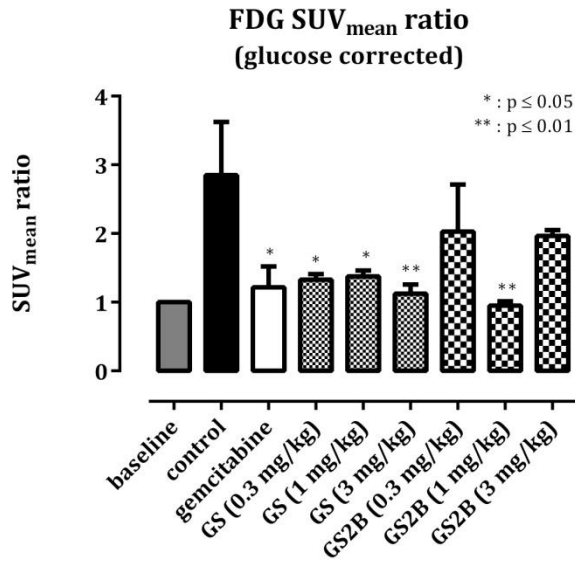


Figure 4.59 Intra-animal SUV_{mean} ratio after 7 days of treatment

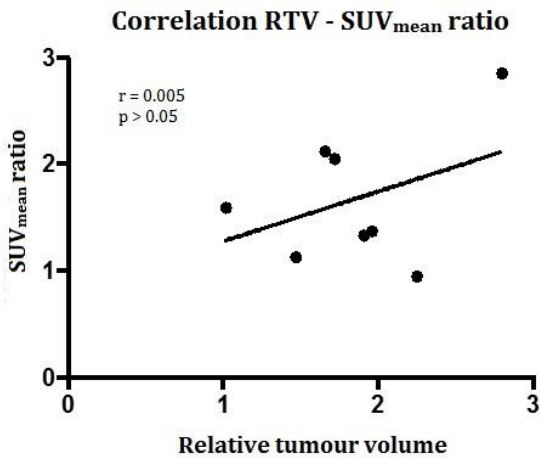


Figure 4.60 Correlation tumour volume and PET/CT

Ex vivo IHC analyses were performed on the removed tumours. Figure 4.61 shows the immunostaining of Ki-67 of tumour tissue of a mouse from the control group and treated with 3 mg/kg GS. Cells stained brown were positive for Ki-67. The result of the Ki-67 staining for the different treatment groups indicating the degree of proliferation is shown in Figure 4.62. IHC staining of cleaved caspase-3 of the tumour slices were also performed and the immunostaining of a tumour tissue derived from a mouse treated with 3 mg/kg GS is shown in Figure 4.63. Cells stained brown were positive for cleaved caspase-3 and are considered apoptotic cells. The result of the cleaved caspase-3 staining is shown in Figure 4.64. The correlations between the relative tumour volume and the IHC results were also examined and are shown in Figure 4.65.

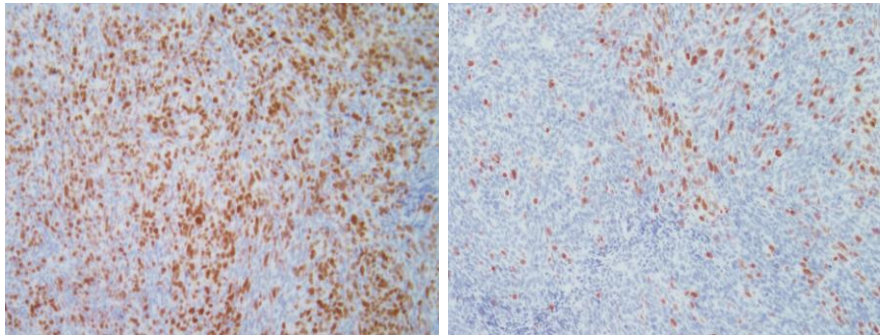


Figure 4.61 Ki-67 immunostaining of tumour tissue (200x) of the control group (left) and the 3 mg/kg GS treated group

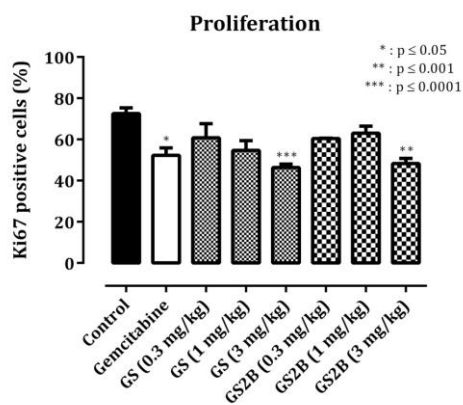


Figure 4.62 Proliferation determined by Ki-67 staining

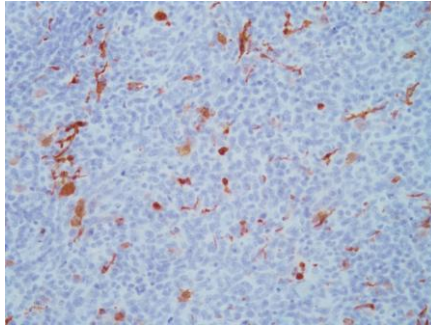


Figure 4.63 Caspase-3 immunostaining of tumour tissue (400x) of the 3 mg/kg GS treated group

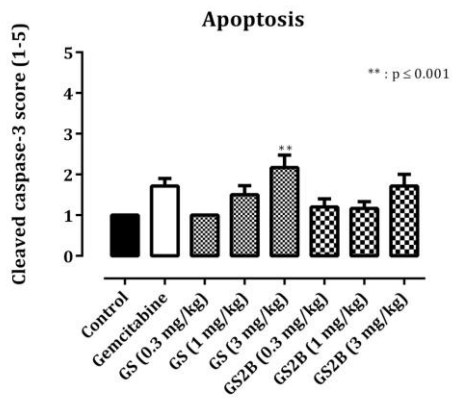


Figure 4.64 Apoptosis determined by cleaved caspase-3 staining

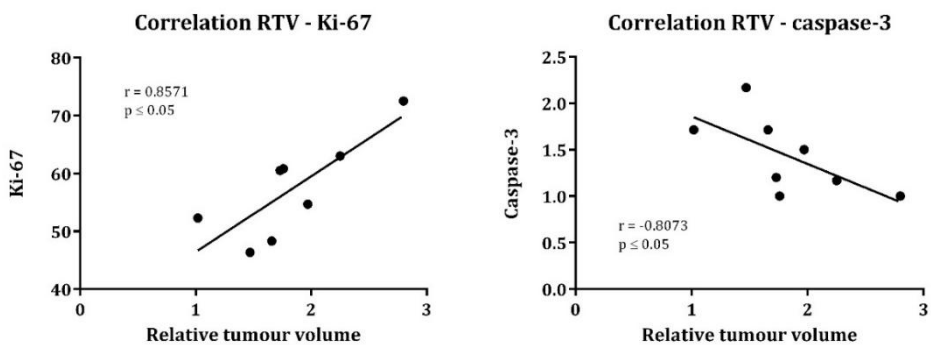


Figure 4.65 Correlation of the relative tumour volume and IHC result

4.5.4.3. Discussion

The mice were randomly divided in groups before tumour inoculation. No statistical difference ($p = 0.31$) between the groups was observed on day 0. The mean RTVs during the entire treatment period showed a difference between the treatment groups and the control group. A dose-effect relationship was observed for GS and GS2B, and although the response of the two lowest concentrations were quite the same, the biggest effect during the entire experiment was observed at the highest dose of both extracts. The RTV of the control group was higher than the treated groups and until day 7 the effect of gemcitabine was comparable to the effect of the extracts.

On day 7, the RTVs of all treatment groups were significantly smaller compared to the control group. On day 10, significantly smaller RTVs were still observed for the lowest and the highest dose of both extracts compared to the control group. The tumour growth inhibition was also calculated for the different groups. On day 7, all treatment groups showed %TGI above 50%, which is considered a relevant inhibition.^[59, 60] The greatest tumour growth inhibition was observed for the highest dose of both extracts, which is comparable with gemcitabine. On day 10, a relevant tumour growth inhibition was still observed for the lowest (0.3 mg/kg) and highest (3 mg/kg) dose of GS with a %TGI of 58 and 74%, respectively. For GS2B, also the lowest dose and highest dose showed a relevant tumour growth inhibition with a %TGI of 60% and 63%, respectively.

The treatments did not influence the body weight. No significant weight loss was observed throughout the experiment. Although the GS (1 mg/kg) group showed a downfall on day 1, the rapid gain of weight was an indication that this weight loss was due to an accidental extra fasting day rather than an effect of the treatment. Also, none of the mice showed any clinical symptoms of toxicity based on the observational table. Therefore it can also be concluded that no apparent toxicity was caused by any treatment.

For the imaging results the uptake of [^{18}F]-FDG tracer by the tumour cells is a marker for the tumour activity, the higher the uptake, the higher the tumour activity. Due to their progressive growth tumours have a high demand for energy and a high metabolic activity. FDG is a glucose

analogue extensively used in oncology for staging, restaging and recently for the evaluation of tumour response to treatment. Cancer cells demonstrate an up regulation of glucose metabolism, so an increase of uptake of glucose or glucose-analogues, such as deoxyglucose, can be observed. Labelling deoxyglucose with ^{18}F to form [^{18}F]-FDG allows to detect these cells by PET. [^{18}F]-FDG is transported into the cells by the same carrier as glucose, but at a much higher rate. It is then phosphorylated to [^{18}F]-FDG-6-phosphate, which cannot enter the normal metabolic pathways because of the presence of fluorine at C-2 position of glucose instead of the hydroxyl group, and which can only slowly leave the cell by the action of glucose-6-phosphatase. Therefore it is trapped and accumulated in the tumour cells. This 'metabolic trapping' of [^{18}F]-FDG-6-P forms the basis of the analysis of PET data.^[61] For the intra-animal SUV_{mean} ratio, there was a significant decrease of the SUV_{mean} ratio observed for the groups treated with gemcitabine, 1 mg/kg GS2B and all concentrations of GS compared to the control group, indicating a lowered metabolic activity of the tumours of these treatment groups. The other concentrations of GS2B did not showed a significant decrease of tumour activity after 7 days of treatment. Also, no correlation was observed between the RTVs and the PET/CT results. This can be due to the presence of necrotic tissue in the tumours that did not take up FDG. However for the evaluation of the RTVs, the whole tumours were measured, including the necrotic tissues. It is also possible that the extracts exhibit an additional effect on the glucose regulation, making FDG perhaps not a suitable marker for this study. Also, the use of a mouse model with an intact immune system can cause an increase of [^{18}F]-FDG uptake by macrophages at the tumour site. It is know that administration of agents that leads to apoptosis and/or necrosis of tumour cells also stimulates inflammatory response and often malignant tumours contain a variable but substantial number of macrophages.^[62, 63]

The H&E staining showed a poorly-differentiated tumour and a strong degree of proliferation of the tumour cells, which in some mice infiltrated into the muscle tissue. These characteristics and the fast growth of the tumours *in vivo*, suggested an aggressive phenotype. In some larger tumours, necrotic regions were clearly visible. The presence of small blood vessels and stroma was observed. Stroma-tissue surrounding the cancer cells plays an important role in tumour behaviour and the interaction between stromal cells and tumour cells is known to play a major role in cancer growth and progression.^[64, 65]

The expression of the human Ki-67 protein is strictly associated with cell proliferation. During interphase, the antigen can be exclusively detected within the nucleus, whereas in mitosis most of the protein is relocated to the surface of the chromosomes. The fact that the Ki-67 protein is present during all active phases of the cell cycle (G1, S, G2, and mitosis), but is absent from resting cells (G0), makes it an excellent marker for the degree of proliferation.^[66] The *ex vivo* IHC staining of Ki-67 indicated a significant decrease in proliferation observed for gemcitabine and the highest dose of both GS and GS2B. A dose-dependent decrease was observed for GS.

Ex vivo IHC staining of caspase-3, which is an apoptotic marker, indicated a significant increase of apoptotic bodies observed for the highest dose of GS. Although the highest dose of GS2B did not show significant changes, an increase of apoptotic bodies was observed comparable with gemcitabine. A dose-dependent increase of apoptotic bodies was observed for GS.

A significant positive correlation was observed between the relative tumour volumes and the Ki-67 results with $p \leq 0.05$ and a significant negative correlation was observed between the relative tumour volumes and the caspase-3 results.

All of these results led to the conclusion that GS and GS2B in a dose of 3 mg/kg TC showed promising anticancer activities in a murine pancreatic adenocarcinoma model, with relevant tumour growth inhibition, a decrease in proliferation and increase in apoptosis compared to the control group. Moreover, no toxic side effects or extreme weight loss were noticed during the daily-treatment regime of 10 days.

Most previous antitumour studies on colchicine are outdated now and were carried out in the P-388 lymphocytic leukaemia model in mice according to the protocols established by the NCI. The tumours were implanted intraperitoneally and the antitumour activity was measured in terms of T/C, which is the median survival time of the treated animals versus median survival time of the control times $\times 100$.^[25, 67, 68] A compound was considered to demonstrate good antitumour activity if duplicate tests give T/C values equal to or greater than 175%.^[67] In the study of Dumont et al. (1986) colchicine exhibited a T/C value of 245% at a dose of 0.5 mg/kg

(IP) and in the study of Rösner et al. (1980) a T/C value of 140% at a dose of 0.16 mg/kg (0.4 µmol/kg) (IM).^[25, 68] This is, however, difficult to correlate with our own study due to the fact that the extracts were given orally instead of IP or IM. After oral administration bioavailability may be a limiting factor, therefore higher doses are frequently needed. Also, the outcome in our efficacy study was the effect on the relative tumour volume and the growth inhibition of the tumour, and not in terms of survival.

From this present *in vivo* study it could be concluded that GS and GS2B have a comparable antitumoural effect in an *in vivo* model for pancreatic cancer. Our initial hypothesis is therefore confirmed that indeed, the effect was not only caused by colchicine but also by the colchicine derivatives present in larger amount in GS2B. Because of the high content of colchicoside and the very low amount (0.07%) of colchicine in GS2B, our presumption that colchicoside can act as a prodrug and adds to the antitumoural effect is hereby established.

4.5.5. ***In vivo* – survival study**

The previous *in vivo* study proved the short-term efficacy of both extracts in a murine model of pancreatic adenocarcinoma. In a follow-up experiment, a survival study and the semi-long-term toxicity of the *G. superba* crude extract and the colchicine-poor extract were determined. A combination therapy was also tested to see whether the extract had an added value to the known standard monotherapy of gemcitabine.

4.5.5.1. Materials and methods

Cell culture

The same PANC02 cell culture was used as in the previous *in vivo* study, mentioned in section 4.5.3.1.

Animals

Six-to-eight weeks old female C57BL/6 mice (16 - 20 g body weight) were purchased from Harlan laboratories. The mice were housed in individually ventilated cages, under a 10/14 h dark/light cycle at constant temperature and humidity and had access to tap water and food *ad libitum*. All animals were treated in accordance to the guidelines and regulations for use and care of animals. All mice experiments were approved by the local Ethical Committee of the University of Antwerp, approved study number: 2014-34.

Subcutaneous tumour model

Cultures of PANC02 cells were harvested using a 0.05% trypsin solution, washed twice in sterile PBS and resuspended in sterile PBS at a concentration of 30×10^6 cells per mL. The viable cells were counted by using the Muse® Cell Analyzer. Mice (n = 66) were inoculated with 100 µL of the cell suspension in the right hind limb. Tumour growth of the subcutaneous model was evaluated by means of calliper measurements from the moment the tumours became palpable and this three times a week. The tumour volume was calculated as in the previous study. Each mouse was randomly assigned to one of 6 groups (n = 11 mice per group) and assigned to a different treatment (Table 4.21).

Table 4.21 Group treatment assignment

n°	Group	# mice	Treatment and dose
1	Negative control	11	200 µl water p.o.
2	Positive control	11	60 mg/kg BW gemcitabine IP
3	Colchicine	11	4.5 mg/kg BW p.o.
4	<i>Gloriosa superba</i> extract (GS)	11	4.5 mg/kg BW TC 77.6 mg/kg BW extract p.o.
5	Colchicine-poor extract (GS2B)	11	4.5 mg/kg BW TC 281.3 mg/kg BW extract p.o.
6	Combination therapy	11	<i>G. superba</i> extract: 3.0 mg/kg BW TC p.o. (51.7 mg/kg BW extract p.o.) Gemcitabine: 60 mg/kg BW IP

Preliminary acute toxicity study

An acute toxicity study had been done before the actual survival experiment to see whether the 4.5 mg/kg dose did not cause acute toxicity. Non-tumour-bearing C57BL/6 mice (n = 3 per treatment group) were given 4.5 mg/kg colchicine, *G. superba* extract and the colchicine-poor extract during 5 consecutive days and the acute toxicity was evaluated as in the previous acute toxicity study mentioned in section 4.5.3.

Treatments

Treatment was started 12 days after tumour inoculation when tumours had reached a volume of approximately 100 mm³. The first day of treatment was assigned “day 1” (Figure 4.66). During the survival experiment the mice of the negative control group received 200 µL water p.o. (gavage) daily. The positive control group was given 3 times/week gemcitabine (Actavis, 38 mg/mL). It was administered at a dose of 60 mg/kg BW IP. GS and GS2B were administered p.o. daily at a dose of 4.5 mg/kg BW TC. Taking the percentages obtained by analysing GS and GS2B into account as in the previous *in vivo* study (4.5.4), group 4 was given 77.6 mg/kg BW

GS and group 5 was given 281.3 mg/kg BW GS2B (Table 4.21). The previous *in vivo* study with a dose of 3 mg/kg extract did not show any adverse effect and a dose-dependent response was observed. Therefore a higher dose of extract was tested in the present *in vivo* study. The dose is 1.5 times higher compared to the previous study but still below the median lethal dose (LD₅₀) of colchicine, which is 6 mg/kg p.o. for mice. Tumour growth was evaluated three times per week and the mice were sacrificed when the tumour had reached a volume of more than 1500 mm³, a tumour weight of more than 10% of the total body weight and/or a weight loss of more than 20%.

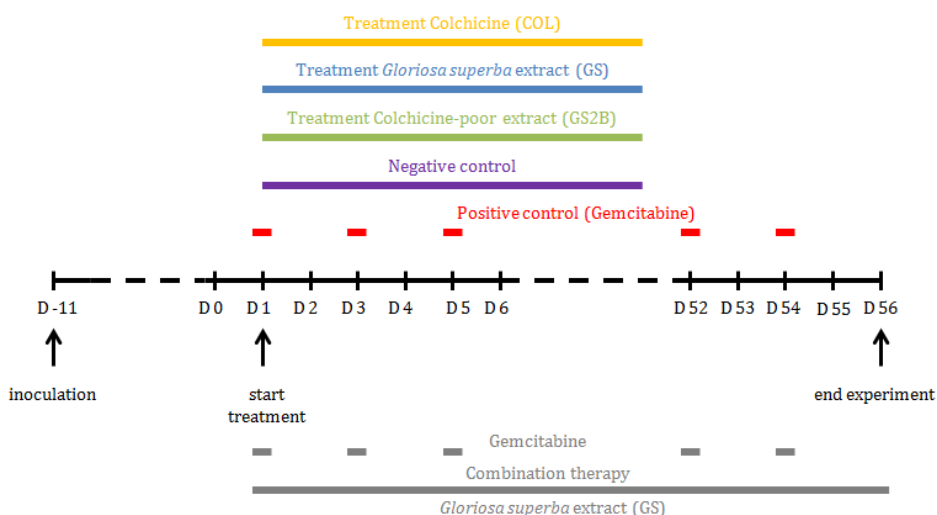


Figure 4.66 Timeline of the survival study

Statistics

Results were expressed as mean values of parameters \pm standard error (SE). The parametric ANOVA test was used to determine statistical significance, followed by a post hoc Tukey analysis to establish the statistical difference between the treatment groups. When only two groups were compared, as on day 51, a Mann-Whitney test was used to determine statistical significance. A piecewise linear regression model, in this case a so called linear mixed model

was also fitted. This is a type of regression that accounts for the dependence between observations within the same mouse. “Normal” regression assumes that all observations are independent, which is not the case in this study since multiple measurements were made per mouse. A mixed model accounts for the repeated measurements by including random effect terms into the regression equation. These terms model the effect of each individual mouse on the outcome, but were not the real interest of this study. The interesting terms, time and treatment, are referred to as the fixed effects. The construction of the fixed effects part of a linear mixed model is performed in an analogous way as model building in ordinary linear regression. So a mixed model is a statistical model containing random effects in addition to the usual fixed effects. A Kaplan–Meier survival curve was constructed and the logrank test was used to determine statistical difference between the survivals of the different treatment groups. A p-value ≤ 0.05 was considered significant and statistical analyses were performed using GraphPad Prism 6 (Version 6.01) and SPSS (version 22.0).

4.5.5.2. Results

Acute toxicity studies

This study was performed before the larger *in vivo* - survival study by giving the different treatments to non-tumour-bearing C57BL/6 mice (n = 3 per treatment group), including 4.5 mg/kg colchicine, 77.6 mg/kg GS and 281.3 mg/kg GS2B, during 5 consecutive days. The toxicity was evaluated by weight loss and the same observation table (Table 4.17) as previous acute toxicity study. Figure 4.67 shows that the given dose did not cause any weight loss greater than 10% of the initial body weight and once again none of the observation criteria were met by any animal during the acute toxicity studies. Also, five days after treatment, the body weights were still stable and still none of the mice showed any clinical symptoms of toxicity. It was concluded that the given dose of the different treatments did not cause any acute toxicity.

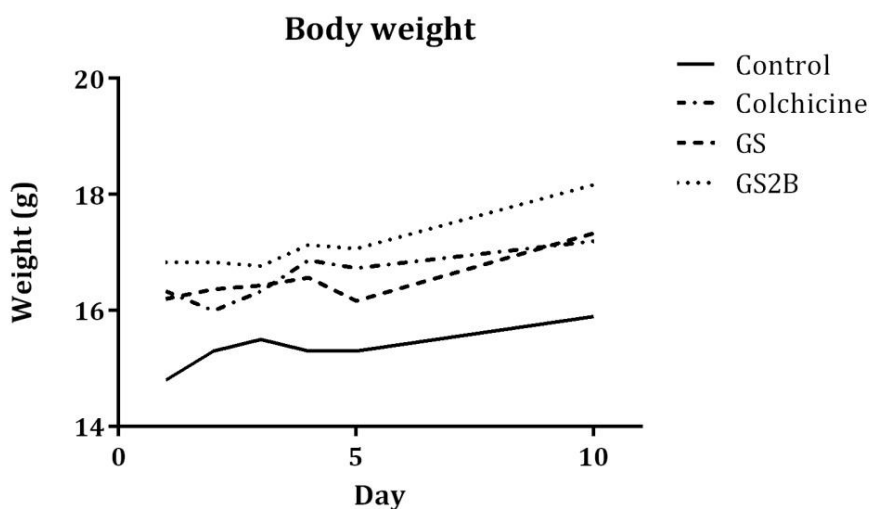


Figure 4.67 Body weight observation during 5 days of treatment and follow-up for another 5 days

Evaluation of tumour volume, tumour growth inhibition and delay, and toxicity

All mice developed subcutaneous tumours in the right hind limb (100% tumour growth). Eleven days after inoculation, the tumours had reached a mean volume of 100 mm³, the mice were randomised and treatment started. The starting mean tumour volume per group was evaluated to check whether there was no significant difference between the groups (Figure 4.68) and the tumour volumes were normalised at this time point. The mean relative tumour volumes were then calculated for each group for each day. The mean relative tumour volumes on day 11, 21 and 51 were graphed (Figure 4.69) and the difference between the groups was statistically evaluated determining the significance of the effect of each treatment. The %TGI was calculated for day 11 and 21. The tumour growth delay (TGD), which is the difference or delay in days for treated versus control groups to reach a specified volume (in this case twice the starting volume) was also determined. The %TGI and TGD are summarised in Table 4.22 All animals were weighed daily during treatment to evaluate toxicity and the mean body weight per group was graphed (Figure 4.70). Table 4.23 summarises the mean body weight of

the different treatments and the relative mean body weight at day 21. This table shows a clear gain of body weight for all groups after 21 days of treatment.

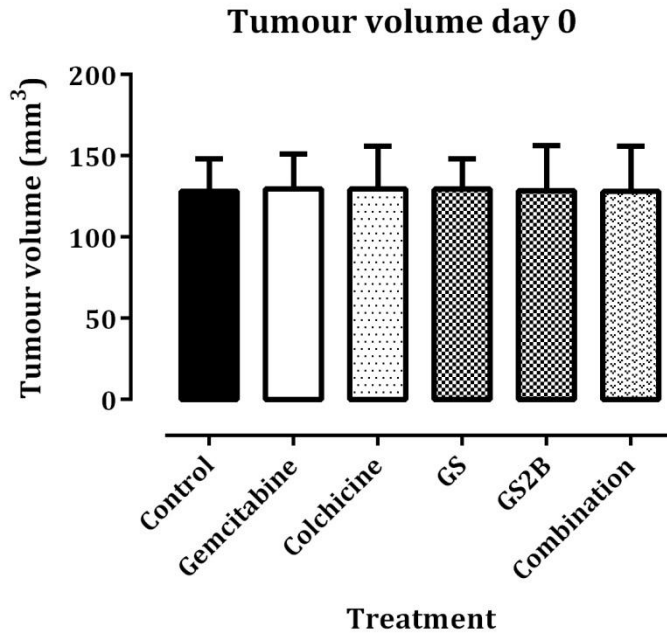


Figure 4.68 Tumour volume on day 0

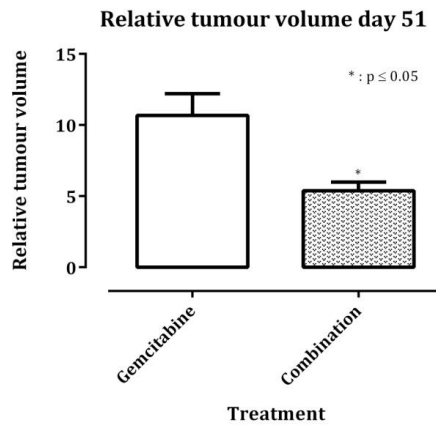
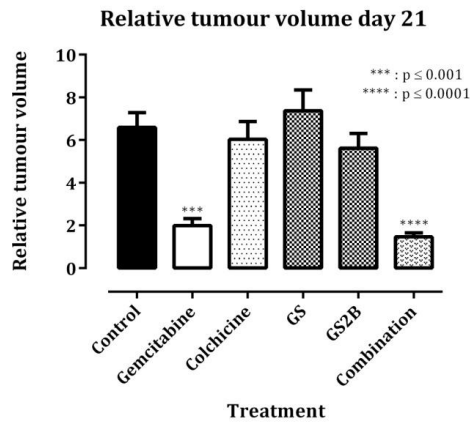
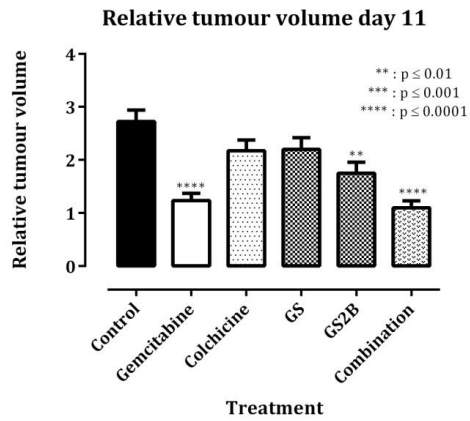


Figure 4.69 Relative tumour volume on day 11, 21 and 51

Table 4.22 Tumour growth inhibition percentage and tumour growth delay

Treatment	%TGI		TGD (in days)
	Day 11	Day 21	
Gemcitabine	86%	82%	12
Colchicine	32%	10%	1.5
GS	31%	0%	1.5
GS2B	57%	17%	5
Combination	94%	92%	21

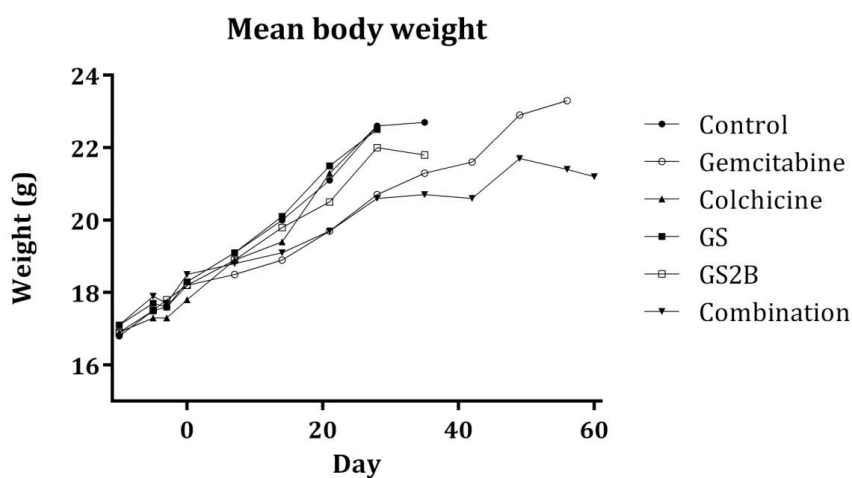


Figure 4.70 Mean body weight

Table 4.23 Mean body weight at day 0, day 21 and the relative body weight at day 21 (normalised to day 0)

Treatment group	Mean body weight \pm (SE)		
	day 0	day 21	relative body weight at day 21
Control	18.3 \pm 0.3	21.1 \pm 0.4	1.15 \pm 0.02
Gemcitabine	18.2 \pm 0.4	19.7 \pm 0.3	1.09 \pm 0.01
Colchicine	17.8 \pm 0.3	21.3 \pm 0.4	1.20 \pm 0.02
GS	18.3 \pm 0.2	21.5 \pm 0.4	1.18 \pm 0.01
GS2B	18.2 \pm 0.3	20.8 \pm 0.5	1.13 \pm 0.03
Combination	18.5 \pm 0.3	19.7 \pm 0.4	1.06 \pm 0.01

Linear mixed model

The individual scatter of each mouse was plotted (Figure 4.71 left). This graph shows the relative tumour volume of all individual mice. Each dot represents one measurement in one mouse at a given time point, with separate panels for each mouse. The strip text shows the mouse identification and the treatment. The different colours represent the different treatments. The individual scatter was also graphed per treatment group and is shown in Figure 4.71 (right). A plot of the mean relative volume (on the log scale) versus time is shown in Figure 4.72. Each dot represents the mean of the $\ln(\text{relative tumour volume})$ on one time point. The different lines represent the different treatments. These data were then fitted into a piecewise linear regression model (Figure 4.73) and in this case a linear mixed model.

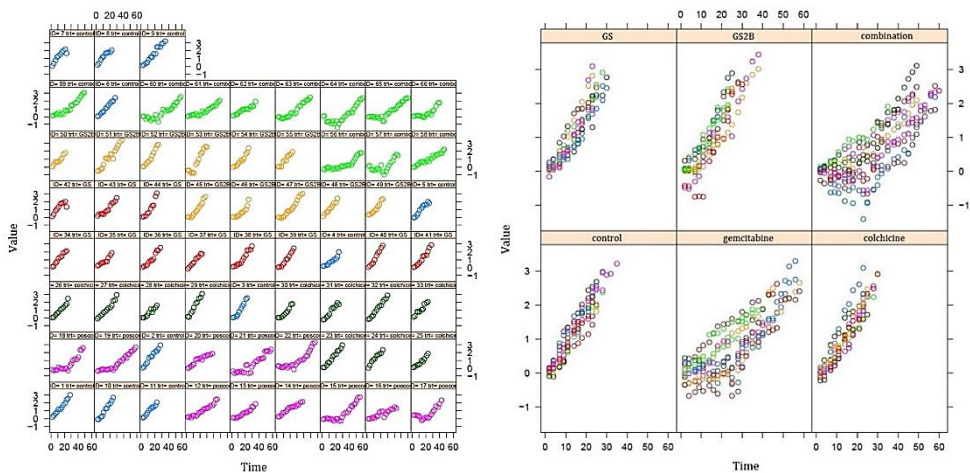


Figure 4.71 Graph of the individual scatter of the relative tumour size of all mice (left) and per treatment group (right)

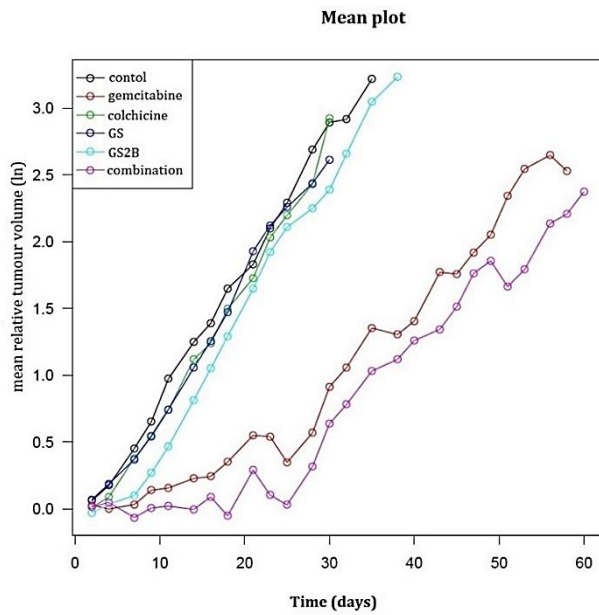


Figure 4.72 Plot of the mean relative tumour volume on the log scale

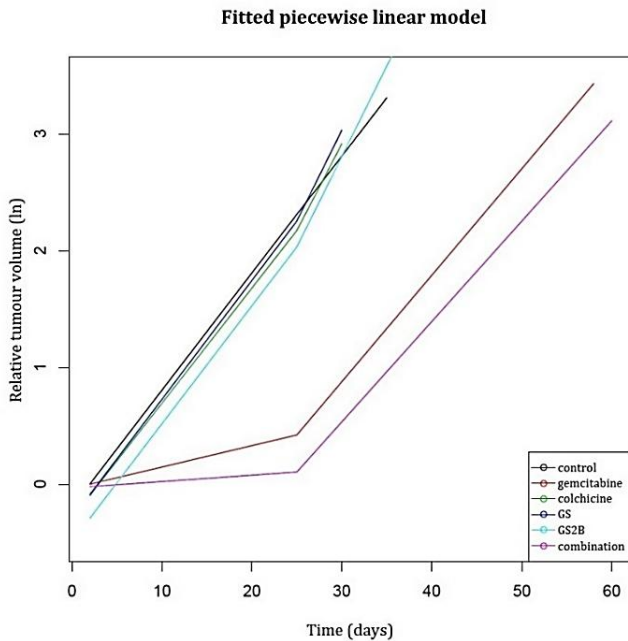


Figure 4.73 Graph of the fitted piecewise linear model

Survival study

A Kaplan-Meier survival curve was graphed and shown in Figure 4.74. The survival fraction is the fraction of mice that was still alive at a certain time point, so for each time point, the graph shows the fraction of mice still in the study per group. A drop of the line of a group indicated an event, which was in this case a removal of a mouse from the study due to one of the defined study endpoints.

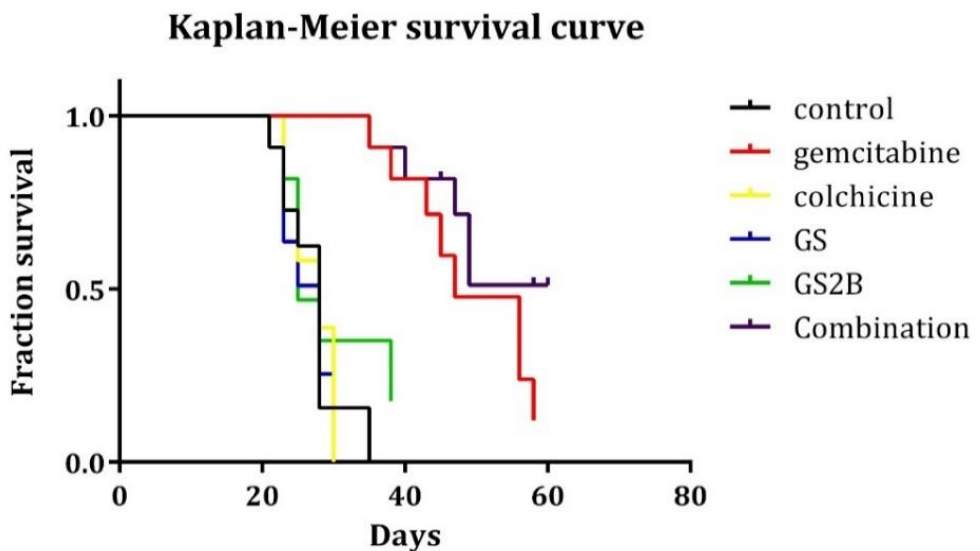


Figure 4.74 Kaplan-Meier survival curve

4.5.5.3. Discussion

The mean RTV on day 11 and 21 showed a significant difference between the control group and the gemcitabine group. A difference between the control group and the combination therapy was also observed on both days. On day 11 a significant difference was observed for GS2B, and although no significant difference was observed for colchicine and GS, a slight decrease in RTV was present. A significant lower RTV was observed for the combination

therapy at day 51 compared to the gemcitabine group. The tumour growth inhibition was also calculated for the different groups on day 11 and 21. A relevant %TGI (> 50%) was observed for gemcitabine and the combination therapy on both days with %TGI of 86% and 82% for gemcitabine and 94% and 92% for the combination therapy. A relevant %TGI (57%) was also observed for GS2B on day 11. A tumour growth delay of 12 and 21 days was observed for gemcitabine and the combination group, respectively, as well as a TGD of 5 days for GS2B.

The higher concentration of both extracts and the treatment with colchicine did not influence the body weight and no great weight loss caused by the treatments was observed throughout the experiment. No severe side effects were observed during the entire experiment. Therefore it can be concluded that no extreme toxicity, even after daily treatment of more than 23 days of higher concentrations, was caused by both extracts and colchicine.

A piecewise linear regression model, in this case the linear mixed model was also fitted. This is a type of regression that accounts for the dependence between observations within the same mouse. "Normal" regression assumes that all observations are independent, which was not the case in this study since multiple measurements were made per mouse. So a mixed model accounts for the repeated measurements by including random effect terms into the regression equation, such as missing value due to the euthanasia of mice when the tumour volume had reach 1500 mm³. The individual scatter plots and the plot of the mean relative tumour volume suggested that in the control, colchicine, GS and GS2B groups, the tumour growth was linear on the log scale from the start on. In the gemcitabine and combination group, there was a phase of slow growth until day 25, which is followed by a phase of increased growth at a pace comparable to the other 4 treatments. Due to this observation, the evolution of tumour growth with time was modelled using piecewise linear regression, accounting for the change in the slope ("knot") around day 25. This regression model included the change in slope at a given point in time. In all treatments, a knot (slope change) is modelled at day 25. However, only in the combination therapy and gemcitabine group the change in slope was substantial. The hypothesis was then tested whether the change in slope was different between the groups. So, overall comparisons between groups showed that the null hypothesis, which is that the tumour growth over time was the same in all treatment groups, was rejected with

$p < 2 \times 10^{-16}$. By rejecting the null hypothesis of an equal slope before the knot, and an equal change in slope beyond day 25, it could be concluded that there was a statistical difference in tumour growth over time between treatment groups.

For the pairwise comparisons, no significant differences were observed between the control group and the groups treated with colchicine, GS and GS2B. There was however a significant difference between the control group and the combination therapy and gemcitabine. Moreover, the combination therapy was significantly better than the gemcitabine group.

The Kaplan-Meier survival curve shows for each time point the fraction of mice still alive per group. The calculations performed in this study take censored observations into account. If the data of a certain mouse was censored, it was either because the mouse was removed from the study for reasons not related to the endpoints of the study, or because the study has ended and that mouse was still alive and no information beyond the time of censoring was available. While it seems intuitive that the curve ought to end at a survival fraction computed as the total number of subjects who died divided by the total number of mice, this is only correct if there are no censored data. A strong decline in survival fraction at a certain time point indicated that a great number of mice has reached the endpoint of 1500 mm³ and were euthanised. So, for the survival analysis, a significant longer survival time compared to the control group was observed for the group treated with gemcitabine ($p \leq 0.001$) and the combination therapy ($p \leq 0.0001$). All other treatment groups did not show a significant longer survival compared to the control group. The survival of the combination therapy compared to the gemcitabine group did not show a significant difference, however, after 58 days of treatment fewer mice treated with the combination group had died compared to the gemcitabine group due to the defined study endpoints. This result was observed on the Kaplan-Meier curve where the survival fraction at the end of the study was lower for gemcitabine compared to the combination therapy.

4.5.6. Conclusion

From the *in vitro* studies it could be concluded that the 80% ethanolic extract of *G. superba* exhibited a high cytotoxic activity on the tested cell lines with IC₅₀ values lower than 1 µg/mL. The IC₅₀ values were 0.34 (MDA-MB-231), 0.17 (PANC-1 and HT-29) and 0.45 µg/mL (PANC02) for the 24 h incubation time. The cytotoxic activity did not increase greatly by prolonging the incubation time to 72 h, with IC₅₀ values of 0.24 (MDA-MB-231), 0.19 (PANC-1), 0.16 (HT-29) and 0.59 µg/mL (PANC02). Comparing the IC₅₀ values on PC-EM005 (0.99 µg/mL) and PC-EM002 (0.42 µg/mL), it seemed that PC-EM005 was less susceptible. A slight proliferation inhibition on the PC-EM005 was observed at a concentration of 0.001 µg/mL. For PC-EM002, a cytotoxic effect was observed at concentration of 0.5 µg/mL. With regard to the 3T3 cells a cytotoxic activity was observed at a concentration of 0.5 µg/mL and 1 µg/mL. With regard to BEAS-2B and 3T3 the calculated IC₅₀ values were in the same range as observed for the cancer cells. The *in vitro* cytotoxicity of GS is mainly due to its main constituent colchicine. Nevertheless the extract also contains potential prodrugs such as colchicoside. The colchicine-poor extract GS2B, which is an extract with a relatively low level of colchicine and a relatively high content of colchicine derivatives, especially colchicoside, was evaluated on the PANC02 cell line and an IC₅₀ value of 9.49 µg/mL. The *in vitro* cytotoxicity of GS2B is mainly due to residual colchicine and 3-*O*-demethylcolchicine.

The *G. superba* crude extract and the colchicine-poor extract were tested in an *in vivo* efficacy study by using a syngeneic subcutaneous murine model of pancreatic adenocarcinoma. No toxic side effects or extreme weight loss were noticed from the treatment during the entire experiment and tumour growth inhibitions of more than 50% (74% for GS and 63% for GS2B) were observed at a dose of 3 mg/kg. Lowered FDG uptake was observed for the tumours of the gemcitabine, GS (all tested concentrations) and GS2B (1 mg/kg) treated groups, but this did not correlate with the measured relative tumour volume. Furthermore, immunohistochemical studies showed a significant decrease in proliferation and a significant increase of apoptotic bodies.

Subsequently, both extracts were submitted to an *in vivo* survival study. The mean RTV of gemcitabine and the combination therapy showed a significant difference compared to the

control group on day 11 and day 21. A significant difference between GS2B and the control group was observed only on day 11. However, a trend towards significance between the GS2B and the control group could be noted on other days, considering the smaller mean RTV observed for GS2B. A relevant %TGI of 57% for GS2B was observed only on day 11, while a %TGI of 86% and 94% was observed for gemcitabine and the combination therapy, respectively. A TGD of 5, 12 and 21 days was noticed for GS2B, gemcitabine and the combination therapy, respectively. No toxic effects or extreme weight loss due to the higher concentrations of the extracts and colchicine and/or the longer treatment period were observed during the entire study, indicating the relatively moderate toxicity of colchicine and the extracts. Furthermore, statistical analysis of the tumour growth over time between the treatment groups was assessed by using a mixed linear model and showed a significant difference for gemcitabine and the combination therapy compared to the control group. No significant difference in growth over time was observed for the groups treated with colchicine and both extracts. The combination therapy was significantly better than the monotherapy with gemcitabine. Moreover, survival analysis showed a significant prolongation of the survival of the groups treated with gemcitabine and the combination therapy. A slight difference in survival was observed between the gemcitabine and the combination therapy, the latter one being slightly better.

This study confirmed that the crude extracts and colchicine did not cause any toxicity when administered daily for more than 23 days. Indeed, it was surprising that even pure colchicine at a dose of 4.5 mg/kg still did not cause any clinical adverse effect. Our study could therefore not confirm the reported toxicity. However, extrapolation of toxicity from mouse to humans have not been studied.

No significant prolongation of survival was observed for the extracts and colchicine compared to the control group. Although a relevant tumour growth inhibition for the colchicine-poor extract and a difference of RTV compared to the control group were observed on day 11 and a slightly longer survival was noticed for the colchicine-poor extract, the most important conclusion from this study is that the *G. superba* extract might have an added value combined with gemcitabine in the treatment of pancreatic tumours.

In conclusion, our experiments have shown that the *Gloriosa superba* crude extract, as well as the colchicine-poor / colchicoside-enriched extract are active *in vivo* in a model for pancreatic cancer. The results confirm our initial hypothesis that indeed colchicoside is a prodrug that is metabolically activated after oral administration, and can provide a therapeutic alternative to colchicine, which has a connotation of high toxicity.

4.6. SUMMARY AND CONCLUSION

Gloriosa superba L. seeds were **phytochemically** investigated and three main constituents were isolated by means of LC-SPE-NMR from the crude extract. The main compounds found in the 80% ethanolic extract of *G. superba* were colchicine, 3-*O*-demethylcolchicine and colchicoside, as reported before. After liquid-liquid partition the artefact, colchicosamide, was isolated and identified. A colchicine-poor extract (GS2B) was prepared by means of liquid-liquid partition. This extract contained a high amount of colchicine derivatives and a low amount of colchicine.

An **analytical** method for the quantification of the 3 main compounds has been optimised and validated according to the ICH guidelines. This method quantifies not only the total colchicine derivatives content expressed as colchicine but by using the determined and validated correction factor the individual compounds can be quantified. The overall mean of colchicine and colchicine derivatives found in the crude extract of *G. superba* was 4.62% expressed as colchicine and contained 2.81% colchicine, 1.27% 3-*O*-demethylcolchicine and 1.46% colchicoside.

The total level of colchicine and its derivatives of the plant extract that was used in the *in vitro* experiments was 5.71% expressed as colchicine, more in particular 2.93% colchicine, 2.58% colchicoside and 1.74% 3-*O*-demethylcolchicine. The extract used in the *in vivo* experiments contained 5.79% colchicine and colchicine derivatives expressed as colchicine (3.22% colchicine, 2.52% colchicoside and 1.52% 3-*O*-demethylcolchicine), and GS2B contained 1.61% (0.07% colchicine, 2.26% colchicoside and 0.46% 3-*O*-demethylcolchicine).

During the ***in vitro*** studies the cytotoxicity of the 80% ethanolic extract of *G. superba* was assessed on different cell lines (cancerous and normal) of different origins (breast, colon, pancreas and endometrium) of different species (human and murine). From the *in vitro* experiments it could be concluded that the 80% ethanolic extract of *G. superba* exhibited high cytotoxic activity on the tested cell lines. The IC₅₀ values were all lower than 1 µg/mL. The promising IC₅₀ values observed for PANC-1 and PANC02, which were 0.17 and 0.45 µg/mL, made *G. superba* a good candidate for further investigation against pancreatic cancer.

An ***in vivo*** efficacy study was performed to determine the potential anticancer activity and toxicity of the *G. superba* crude extract and the colchicine-poor extract by using a syngeneic subcutaneous murine model of pancreatic adenocarcinoma. Six-to-eight weeks old female C57BL/6 mice were injected subcutaneously with 3 million PANC02 cells in the right hind limb. After 18 days the tumours had reached a volume of approximately 300 - 400 mm³ and therapy was started. The extracts were given daily for 10 days in a dose of 0.3, 1 and 3 mg total amount of colchicine and colchicine derivatives expressed as colchicine per kg body weight. Tumour growth was evaluated by means of calliper measurements. A tumour growth inhibition comparable with gemcitabine was noted for both extracts at a dose of 3 mg/kg 7 days after treatment. After 10 days of treatment, a tumour growth inhibition of 74% for *G. superba* crude extract and 63% for the colchicine-poor extract was still observed for the same dose. A significantly lowered FDG uptake was noticed for the crude extract in all doses and for the colchicine-poor extract at a dose of 1 mg/kg, indicating a reduced metabolic activity. No toxic or severe side effects of the treatment were seen during the entire experiment and furthermore, *ex vivo* immunohistochemical analysis of the tumour tissues showed a significant decrease in proliferation and a significant increase of apoptotic bodies, both correlated with the relative tumour volumes.

Subsequently, both extracts were submitted to an ***in vivo*** survival study with a longer treatment period and higher concentrations of extract compared to previous *in vivo* study. A significant difference in relative tumour volume of the group treated with 4.5 mg/kg colchicine-poor extract on day 11 was observed as well as relevant tumour growth inhibition of 57% and a tumour growth delay of 5 days. The combination therapy of gemcitabine with the GS extract showed a significant difference in relative tumour volume on day 11 and 21 compared to the control group, and on day 51 a significant decrease in relative tumour volume was noticed compared to the gemcitabine group. A relevant tumour growth inhibition of 94% and 92% was observed for the combination therapy, which was slightly higher than calculated for the monotherapy with gemcitabine. The tumour growth delay of 21 days for the combination therapy was also longer compared to that of the monotherapy. The mixed linear model showed a difference in growth over time for the combination therapy compared to the control group and the monotherapy. For the survival analysis a significant prolongation was

noticed for the combination therapy compared to the control but not compared to gemcitabine. All other treatments did not show a significant prolongation of survival compared to control. However, the longer treatment and higher dose of both extracts and colchicine did not cause any severe toxic effects during the entire study.

REFERENCES

1. Maroyi, A. and L.J.G. van der Maesen, *Gloriosa superba* L. (family Colchicaceae): *Remedy or poison?* Journal of Medicinal Plants Research, 2011. 5(26): p. 6112-6121.
2. Jana, S. and G.S. Shekhawat, *Critical review on medicinally potent plant species: Gloriosa superba*. Fitoterapia, 2011. 82(3): p. 293-301.
3. Nautiyal, O.P., *Isolation of 3-demethylcolchicine from Gloriosa superb sludge and coupling with α -acetobromoglucose to yield colchicoside and thiocolchicoside*. Journal of Natural Products, 2011. 4: p. 87-93.
4. Patel, R. and M. Joshi, *Isolation and Identification of Phytoconstituents in Gloriosa superba Linn*. International Journal of Pharmaceutical and research sciences, 2012. 1(3): p. 191-199.
5. Senthilkumar, M., *Phytochemical screening of Gloriosa superba L.-from different Geographical positions*. International journal of scientific and research publications, 2013. 3(1).
6. Grattagliano, I., L. Bonfrate, V. Ruggiero, G. Scaccianoce, G. Palasciano, and P. Portincasa, *Novel therapeutics for the treatment of familial Mediterranean fever: from colchicine to biologics*. Clin Pharmacol Ther, 2014. 95(1): p. 89-97.
7. Dinarello, C.A., *Anti-inflammatory Agents: Present and Future*. Cell, 2010. 140(6): p. 935-950.
8. Pouliot, M., M.J. James, S.R. McColl, P.H. Naccache, and L.G. Cleland, *Monosodium urate microcrystals induce cyclooxygenase-2 in human monocytes*. Blood, 1998. 91(5): p. 1769-1776.
9. Joshi, C.S., E.S. Priya, and C.S. Mathela, *Isolation and anti-inflammatory activity of colchicinoids from Gloriosa superba seeds*. Pharm Biol, 2010. 48(2): p. 206-209.
10. Farhat, M., A. Poissonnier, A. Hamze, C. Ouk-Martin, J.D. Brion, M. Alami, J. Feuillard, and C. Jayat-Vignoles, *Reversion of apoptotic resistance of TP53-mutated Burkitt lymphoma B-cells to spindle poisons by exogenous activation of JNK and p38 MAP kinases*. Cell Death Dis, 2014. 5: p. e1201.

11. Wood, K.W., W.D. Cornwell, and J.R. Jackson, *Past and future of the mitotic spindle as an oncology target*. *Curr Opin Pharmacol*, 2001. 1(4): p. 370-377.
12. Jordan, M.A. and L. Wilson, *Microtubules as a target for anticancer drugs*. *Nature Reviews Cancer*, 2004. 4(4): p. 253-265.
13. Yue, Q.X., X.A. Liu, and D.A. Guo, *Microtubule-Binding Natural Products for Cancer Therapy*. *Planta Medica*, 2010. 76(11): p. 1037-1043.
14. Risinger, A.L., F.J. Giles, and S.L. Mooberry, *Microtubule dynamics as a target in oncology*. *Cancer Treat Rev*, 2009. 35(3): p. 255-261.
15. Bhattacharyya, B., D. Panda, S. Gupta, and M. Banerjee, *Anti-mitotic activity of colchicine and the structural basis for its interaction with tubulin*. *Medicinal Research Reviews*, 2008. 28(1): p. 155-183.
16. Panda, D., J.E. Daijo, M.A. Jordan, and L. Wilson, *Kinetic Stabilization of Microtubule Dynamics at Steady-State in-Vitro by Substoichiometric Concentrations of Tubulin-Colchicine Complex*. *Biochemistry*, 1995. 34(31): p. 9921-9929.
17. Stanton, R.A., K.M. Gernert, J.H. Nettles, and R. Aneja, *Drugs That Target Dynamic Microtubules: A New Molecular Perspective*. *Medicinal Research Reviews*, 2011. 31(3): p. 443-481.
18. Thakur, R.S., H. Potesilova, and F. Santavy, *Substances from plants of the subfamily Wurmbaeoideae and their derivatives. Part LXXIX. Alkaloids of the plant *Gloriosa superba* L.* *Planta Med*, 1975. 28(3): p. 201-209.
19. Nery, A.L.P., F.H. Quina, P.F. Moreira, C.E.R. Medeiros, W.J. Baader, K. Shimizu, L.H. Catalani, and E.J.H. Bechara, *Does the photochemical conversion of colchicine into lumicolchicines involve triplet transients? A solvent dependence study*. *Photochemistry and Photobiology*, 2001. 73(3): p. 213-218.
20. Chaudhuri, P.K. and R.S. Thakur, *1,2-Didemethylcolchicine - a New Alkaloid from *Gloriosa-Superba**. *Journal of Natural Products*, 1993. 56(7): p. 1174-1176.
21. Narayana, B. and N.S. Divya, *Novel methods for the spectrophotometric determination of colchicoside*. *Indian Journal of Chemical Technology*, 2010. 17(4): p. 317-320.

22. Yoshida, K., T. Hayashi, and K. Sano, *Colchicoside in Colchicum-Autumnale Bulbs*. Agricultural and Biological Chemistry, 1988. 52(2): p. 593-594.
23. Suri, O.P., B.D. Gupta, K.A. Suri, A.K. Sharma, and N.K. Satti, *A new glycoside, 3-O-demethylcolchicine-3-O-alpha-D-glucopyranoside, from Gloriosa superba seeds*. Natural Product Letters, 2001. 15(4): p. 217-219.
24. Joshi, C.S., E.S. Priya, and C.S. Mathela, *Isolation and anti-inflammatory activity of colchicinoids from Gloriosa superba seeds*. Pharmaceutical Biology, 2010. 48(2): p. 206-209.
25. Rosner, M., H.G. Capraro, A.E. Jacobson, L. Atwell, A. Brossi, M.A. Iorio, T.H. Williams, R.H. Sik, and C.F. Chignell, *Biological Effects of Modified Colchicines - Improved Preparation of 2-Demethylcolchicine, 3-Demethylcolchicine, and (+)-Colchicine and Reassignment of the Position of the Double-Bond in Dehydro-7-Deacetamidocolchicines*. Journal of Medicinal Chemistry, 1981. 24(3): p. 257-261.
26. Kamuhabwa, A., C. Nshimo, and P. de Witte, *Cytotoxicity of some medicinal plant extracts used in Tanzanian traditional medicine*. Journal of Ethnopharmacology, 2000. 70(2): p. 143-149.
27. Ahmad, B., *Antioxidant activity and phenolic compounds from Colchicum luteum Baker (Liliaceae)*. African Journal of Biotechnology, 2013. 9(35).
28. Kurek, J., W. Boczon, P. Przybylski, and B. Brzezinski, *ESI MS, spectroscopic and PM5 semiempirical studies of colchicine complexes with lithium, sodium and potassium salts*. Journal of Molecular Structure, 2007. 846(1-3): p. 13-22.
29. Alali, F.Q., T. El-Elimat, C. Li, A. Qandil, A. Alkofahi, K. Tawaha, J.P. Burgess, Y. Nakanishi, D.J. Kroll, H.A. Navarro, J.O. Falkinham, 3rd, M.C. Wani, and N.H. Oberlies, *New colchicinoids from a native Jordanian meadow saffron, colchicum brachyphyllum: isolation of the first naturally occurring dextrorotatory colchicinoid*. J Nat Prod, 2005. 68(2): p. 173-178.
30. Alali, F.Q., Y.R. Tahboub, I.S. Al-Daraysih, and T. El-Elimat, *LC-MS and LC-PDA vs. phytochemical analysis of Colchicum brachyphyllum*. Pharmazie, 2008. 63(12): p. 860-865.

31. Ph. Eur., *EUROPEAN PHARMACOPOEIA 8.0 Monograph Colchicine*. 01/2008:0758.
32. Mimaki, Y., N. Ishibashi, M. Komatsu, and Y. Sashida, *Studies on the Chemical Constituents of Gloriosa rothschildiana and Colchicum autumnale*. The Japanese journal of pharmacognosy, 1991. 45(3): p. 255-260.
33. Roslund, M.U., P. Tähtinen, M. Niemitz, and R. Sjöholm, *Complete assignments of the ¹H and ¹³C chemical shifts and JH,H coupling constants in NMR spectra of d-glucopyranose and all d-glucopyranosyl-d-glucopyranosides*. Carbohydrate Research, 2008. 343(1): p. 101-112.
34. Ondra, P., I. Válka, J. Vičar, N. Sütülpinar, and V. Šimánek, *Chromatographic determination of constituents of the genus Colchicum (Liliaceae)*. Journal of Chromatography A, 1995. 704(2): p. 351-356.
35. Ellington, E., J. Bastida, F. Viladomat, V. Simanek, and C. Codina, *Occurrence of colchicine derivatives in plants of the genus Androcymbium*. Biochemical Systematics and Ecology, 2003. 31(7): p. 715-722.
36. Al-Mahmoud, M.S., F.Q. Alali, K. Tawaha, and R.M. Qasaymeh, *Phytochemical study and cytotoxicity evaluation of Colchicum stevenii Kunth (Colchicaceae): A Jordanian meadow saffron*. Natural Product Research, 2006. 20(2): p. 153-160.
37. Bellet, P., *Colchicosamides, method of making, and compositions containing same*. 1957, Google Patents.
38. Kunle, O.F., H.O. Egharevba, and P.O. Ahmadu, *Standardization of herbal medicines - A review*. International Journal of Biodiversity and Conservation, 2012. 4(3): p. 101-112.
39. Liang, Y.Z., P.S. Xie, and K. Chan, *Quality control of herbal medicines*. Journal of Chromatography B-Analytical Technologies in the Biomedical and Life Sciences, 2004. 812(1-2): p. 53-70.
40. Vlietinck, A., L. Pieters, and S. Apers, *Legal Requirements for the Quality of Herbal Substances and Herbal Preparations for the Manufacturing of Herbal Medicinal Products in the European Union*. Planta Medica, 2009. 75(7): p. 683-688.

41. Finnie, J.F. and J. Vanstaden, *Isolation of Colchicine from Sandersonia-Aurantiaca and Gloriosa-Superba - Variation in the Alkaloid Levels of Plants Grown Invivo*. Journal of Plant Physiology, 1991. 138(6): p. 691-695.
42. Chitra, R. and K. Rajamani, *A rapid high-performance liquid chromatographic method for quantitative analysis of anti-cancerous active components in gloriosa superba tubers*. Pharmacognosy Journal, 2009. 1(2): p. 138-142.
43. ICH, *Text on validation of analytical procedures*. ICH Harmonised Tripartite Guidelines, 1994.
44. ICH, *Validation of analytical procedures: methodology*. ICH Harmonised Tripartite Guideline, 1996.
45. Dhooghe, L., *Antimalarial agents from plants: investigations of Ormocarpum Kirkii, Phyllanthus amarus, Nauclea pobeguini, and neocryptolepine derivatives*. PhD Thesis, 2009, University of Antwerp.
46. Horwitz, W. and R. Albert, *The concept of uncertainty as applied to chemical measurements*. Analyst, 1997. 122(6): p. 615-617.
47. Li, D., K. Xie, R. Wolff, and J.L. Abbruzzese, *Pancreatic cancer*. Lancet, 2004. 363(9414): p. 1049-1057.
48. American Cancer Society, *Cancer Facts & Figures 2013*. American Cancer Society, 2013.
49. Cascinu, S., S. Jelic, and E.G.W. Group, *Pancreatic cancer: ESMO clinical recommendations for diagnosis, treatment and follow-up*. Ann Oncol, 2009. 20 Suppl 4: p. 37-40.
50. Bilimoria, K.Y., D.J. Bentrem, C.Y. Ko, J. Ritchey, A.K. Stewart, D.P. Winchester, and M.S. Talamonti, *Validation of the 6th Edition AJCC Pancreatic Cancer Staging System - Report from the National Cancer Database*. Cancer, 2007. 110(4): p. 738-744.
51. Shaib, Y., J. Davila, C. Naumann, and H. El-Serag, *The impact of curative intent surgery on the survival of pancreatic cancer patients: a U.S. Population-based study*. Am J Gastroenterol, 2007. 102(7): p. 1377-1382.

52. O'Reilly, E.M., *Refinement of adjuvant therapy for pancreatic cancer*. JAMA, 2010. 304(10): p. 1124-1125.
53. Neoptolemos, J.P., *Adjuvant treatment of pancreatic cancer*. Eur J Cancer, 2011. 47 Suppl 3: p. S378-380.
54. Boik, J., *Natural compounds in cancer therapy*. 2001, Minnesota USA: Oregon Medical Press.
55. Campbell, E.J. and G.U. Dachs, *Current limitations of murine models in oncology for ascorbate research*. Front Oncol, 2014. 4: p. 282.
56. Montgomery, C.A.J., Cancer Bulletin, 1990. 42: p. 230-237.
57. Casneuf, V., P. Demetter, T. Boterberg, L. Delrue, N. Van Damme, and M. Peeters, *Antiangiogenic Versus Cytotoxic Therapeutic Approaches in a Mouse Model of Pancreatic Cancer: An Experimental Study with Sunitinib, Gemcitabine and Radiotherapy*. Annals of Oncology, 2009. 20: p. 56-56.
58. Corbett, T.H., B.J. Roberts, W.R. Leopold, J.C. Peckham, L.J. Wilkoff, D.P. Griswold, and F.M. Schabel, *Induction and Chemotherapeutic Response of 2 Transplantable Ductal Adenocarcinomas of the Pancreas in C57bl-6 Mice*. Cancer Research, 1984. 44(2): p. 717-726.
59. Yamazaki, S., *Translational Pharmacokinetic-Pharmacodynamic Modeling from Nonclinical to Clinical Development: A Case Study of Anticancer Drug, Crizotinib*. Aaps Journal, 2013. 15(2): p. 354-366.
60. Buck, E., A. Eyzaguirre, M. Rosenfeld-Franklin, S. Thomson, M. Mulvihill, S. Barr, E. Brown, M. O'Connor, Y. Yao, J. Pachter, M. Miglarese, D. Epstein, K.K. Iwata, J.D. Haley, N.W. Gibson, and Q.S. Ji, *Feedback Mechanisms Promote Cooperativity for Small Molecule Inhibitors of Epidermal and Insulin-Like Growth Factor Receptors*. Cancer Research, 2008. 68(20): p. 8322-8332.
61. Miele, E., G.P. Spinelli, F. Tomao, A. Zullo, F. De Marinis, G. Pasciuti, L. Rossi, F. Zoratto, and S. Tomao, *Positron Emission Tomography (PET) radiotracers in oncology--utility of 18F-Fluoro-deoxy-glucose (FDG)-PET in the management of patients with non-small-cell lung cancer (NSCLC)*. J Exp Clin Cancer Res, 2008. 27: p. 52.

62. Kubota, R., S. Yamada, K. Kubota, K. Ishiwata, N. Tamahashi, and T. Ido, *Intratumoral distribution of fluorine-18-fluorodeoxyglucose in vivo: high accumulation in macrophages and granulation tissues studied by microautoradiography*. J Nucl Med, 1992. 33(11): p. 1972-1980.
63. Brepoels, L., S. Stroobants, P. Vandenberghe, K. Spaepen, P. Dupont, J. Nuyts, G. Bormans, L. Mortelmans, G. Verhoef, and C. De Wolf-Peeters, *Effect of corticosteroids on 18F-FDG uptake in tumor lesions after chemotherapy*. J Nucl Med, 2007. 48(3): p. 390-397.
64. Mesker, W.E., G.J. Liefers, J.M. Junggeburst, G.W. van Pelt, P. Alberici, P.J. Kuppen, N.F. Miranda, K.A. van Leeuwen, H. Morreau, K. Szuhai, R.A. Tollenaar, and H.J. Tanke, *Presence of a high amount of stroma and downregulation of SMAD4 predict for worse survival for stage I-II colon cancer patients*. Cell Oncol, 2009. 31(3): p. 169-178.
65. Wiseman, B.S. and Z. Werb, *Stromal effects on mammary gland development and breast cancer*. Science, 2002. 296(5570): p. 1046-1049.
66. Scholzen, T. and J. Gerdes, *The Ki-67 protein: From the known and the unknown*. Journal of Cellular Physiology, 2000. 182(3): p. 311-322.
67. Brossi, A., H.J.C. Yeh, M. Chrzanowska, J. Wolff, E. Hamel, C.M. Lin, F. Quin, M. Suffness, and J. Silverton, *Colchicine and its analogues: Recent findings*. Medicinal Research Reviews, 1988. 8(1): p. 77-94.
68. Dumont, R., A. Brossi, C.F. Chignell, F.R. Quinn, and M. Suffness, *A novel synthesis of colchicine and analogs from thiocolchicine and congeners: reevaluation of colchicine as a potential antitumor agent*. Journal of Medicinal Chemistry, 1987. 30(4): p. 732-735.

CHAPTER 5

CHELIDONIUM MAJUS

5.1. INTRODUCTION

Chelidonium majus L., commonly known as greater celandine (Figure 5.1), is a perennial plant native to Europe and Asia. It is one of the most investigated plants of the Papaveraceae family. The name '*Chelidonium*' came from 'chelidon', a Greek word which means swallow bird, as the plant begins to flower when the swallows return. It is widely distributed across the world. It can be found in Europe, Asia, Northwest Africa and North America. *C. majus* has been used since the Middle Ages for bile and liver disorders. The fresh latex was used for the treatment of warts but also for other skin diseases. The *C. majus* tincture in combination with *Thuya occidentalis* tincture and salicylic acid (Aporil®) is still used against warts. It is a typical rural plant that grows on nitrogenous soil. It is a rich source of biologically active substances used for the treatment of various diseases.^[1]



Figure 5.1 *Chelidonium majus* L.

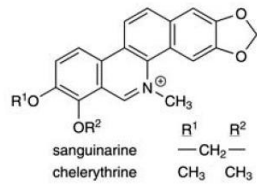
5.1.1. Constituents

The plant contains as major constituents benzyloisoquinoline alkaloids. Alkaloids are a group of biological substances, which exhibit a wide spectrum of biological activities such as anti-inflammatory, antimicrobial, antitumour, analgesic and spasmolytic properties.^[2, 3] More than 20 benzyloisoquinoline alkaloids have been identified from this plant including benzophenanthridines (e.g. chelerythrine, chelidonine, sanguinarine, isochelidonine), protoberberines (e.g. berberine, coptisine, stylopine) and protopines (e.g. protopine) (Figure 5.2). Sanguinarine and chelerythrine are the most prominent alkaloids obtained from roots while coptisine, chelidonine and berberine are usually obtained from the aerial parts.^[4] Sanguinarine is an alkaloid first isolated from the root of *Sanguinaria canadensis* and is a structural homologue of chelerythrine.^[5] Chelidonine is a tertiary benzophenanthridine alkaloid and was isolated from *C. majus* in 1839.^[6] Berberine is the most widely distributed quaternary protoberberines alkaloid and is found in many members of the Berberidaceae (e.g. *Berberis*, *Mahonia*), the Ranunculaceae (e.g. *Hydrastis*), and other families.^[7] *Chelidonium* alkaloids have been thoroughly studied and their potential application as anticancer agents has already been reported.^[8, 9]

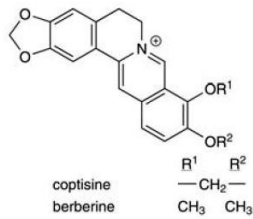
The plant also contains flavonoids, phenolic acids (e.g. chelidonic acid) and caffeic acid esters (e.g. (-)-2-(*E*)-caffeoyl-D-glyceric acid, (-)-4-(*E*)-caffeoyl-L-threonic acid, (-)-2-(*E*)-caffeoyl threonic acid lactone, (+)-(*E*)-caffeoyl-L-malic acid) (Figure 5.3).^[9-12]

Benzylisoquinoline alkaloids

Benzophenanthridines



Protoberberines



Protopines

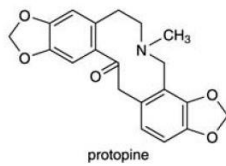
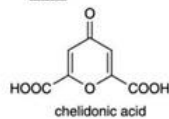


Figure 5.2 Alkaloids of *C. majus* (From Barnes et al., 2007)

Acids



Caffeic acid esters

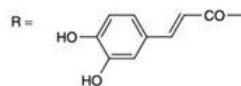
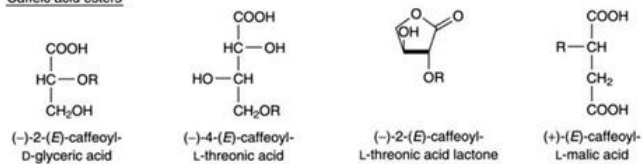


Figure 5.3 Constituents of *C. majus* (From Barnes et al., 2007)

5.1.2. **Biological activities**

Both the crude extract and the purified compounds exhibit a wide variety of biological activities, e.g. anti-inflammatory, antimicrobial, immunomodulatory, cholerectic activities, hepatoprotective, analgesic, and antitumoural, which are mostly in accordance with the traditional uses of *C. majus*.^[10, 11, 13-15]

The antiproliferative effects of *C. majus* were evaluated *in vitro* on rapidly multiplying human keratinocyte (HaCaT) cell lines resulting in an IC₅₀ value of 1.9 µg/mL for the dry extract containing 0.68% alkaloids expressed as chelidonine. Sanguinarine, chelerythrine and chelidonine gave IC₅₀ values of 0.2, 3.2 and 3.3 µmol/L, respectively, whereas berberine showed only low potency with an IC₅₀ of 30 µmol/L. The lactate dehydrogenase assay showed a cytostatic activity rather than cytotoxic activity.^[16, 17] The polysaccharide fraction from a water extract of *C. majus* also showed an inhibition of the proliferation of several tumour cell lines *in vitro*. A 100 µg/mL fraction showed over 50% cytotoxicity for the mastocytoma (P815) and melanoma (B16F10) cell lines.^[18]

The antileukaemic activity of the protoberberine alkaloids was reported in 1982 to be related to the structural conformation of the molecule and its DNA-binding properties.^[19] Two years later, Smekal et al. reported that the biological effects of sanguinarine are caused by the intercalation into the DNA helix forming a sanguinarine-DNA-complex.^[20] Sanguinarine is known to have a wide range of biological properties including antimicrobial, antifungal, anti-inflammatory and antineoplastic activity. It has been shown to inhibit a variety of human tumour cell types.^[5]

Most *in vitro* studies suggested that sanguinarine, chelidonine, chelerythrine and berberine are responsible for the antitumoural effect of the *C. majus* extract. The strongest antitumour agent was found to be sanguinarine, which intercalates strongly with DNA. Chelidonine, chelerythrine and berberine are also active but are less potent.^[1]

Chelidonine has shown promising anticancer potential with the ability to overcome multidrug resistance of different cancer cell lines. It was also reported that chelidonine and an alkaloid

extract of *C. majus* inhibited growth and induced apoptosis in resistant cancer cells. Their cytotoxic effect was more prominent in the sensitive leukaemia cells (CCRF-CEM) than in the other cancer cells overexpressing ABC transporters. The overexpression of ABC transporters is associated with treatment failure in many cancers and has been correlated with drug resistance. Chelidonine causes DNA damage by mutation and additionally, it is a DNA intercalator. Its action leads to frame shift mutations, which can lead to changes in amino acid sequences of important proteins. In addition, intercalation may influence promoters and other regulatory DNA sequences. DNA damage can lead to cell death via apoptosis. The intercalation can disturb replication and transcription processes, because the DNA double helix is stabilised. Furthermore, some *C. majus* alkaloids target tubulin and microtubules arresting cell cycle progression, which eventually leads to apoptotic cell death. Chelidonine is reported to inhibit tubulin polymerisation with an IC_{50} value of $24 \mu M$.^[6, 21-23] It also showed a significant antiproliferative effect on planarian stem cells in a dose-dependent manner. Mitotic abnormalities were also observed and the number of cells able to proceed to anaphase appeared significantly reduced.^[24]

Chelerythrine was shown to mediate a broad variety of biological activities, such as antimicrobial and anti-inflammatory effects.^[25-28] It was also reported to exert cell growth inhibitory effect via the induction of apoptosis in numerous cancer cells, suggesting their potential application as proapoptotic drugs in cancer therapy. Furthermore, it was effective against certain tumours that are otherwise resistant to standard therapies.^[29-31]

The use of berberine has been mentioned in the Indian Ayurvedic, Unani, and Chinese traditional medicine.^[32] Several pharmacological properties have been attributed to berberine including antidiarrheal, vasorelaxant, antimicrobial, antioxidative and anti-inflammatory properties.^[7, 33-37] The antiproliferative properties of berberine indicate promising antitumour activity. Berberine has shown to promote cell death in several cell lines and is capable of inducing apoptosis in a caspase- and apoptosis inducing factor (AIF)-dependent manner. The involvement of caspase, an increase of Bax expression, DNA fragmentation, and cytochrome c release, suggested a role of the mitochondria in the process.^[32, 33, 38-41]

Protopine is mainly found in plants of the Papaveraceae family. It has been investigated in a large number of biological studies in which it exhibited antiparasitic activity, anti-arrhythmic, antithrombotic, anti-inflammatory and hepatoprotective effects. In comparison with other types of isoquinoline alkaloids, protopine exhibited weak cytotoxic activity on the human promyelocytic leukaemia (HL-60) cell line, but it was found to be cytoprotective against oxidative stress-induced cell death *in vitro*.^[42-46] The biological activity of protopine may be associated with its ability to inhibit calcium and potassium channels.^[47-50]

5.1.3. **Ukrain™**

Ukrain™, an anticancer drug, has been described as a semi-synthetic *Chelidonium majus* alkaloid derivative, consisting of three chelidonine molecules combined to thiophosphoric acid (thiotepa) (Figure 5.4). It is claimed to be effective against a range of cancers and has drug licenses in several states of the former Soviet Union. Numerous preclinical investigations and randomised clinical trials (RCT) suggest that Ukrain™ is pharmacologically active and clinically effective as an anticancer drug. However, these studies show several limitations. While common anticancer drugs are cytotoxic both against cancer and normal cells, Ukrain™ is allegedly only cytotoxic against cancer cells. Some studies suggest that there was no evidence to suggest selective cytotoxicity previously reported for Ukrain™. The methodological quality of most studies was poor. The Jadad score of most RCT was low. Their sample size was usually small, and a sample size calculation to define the number of patients required was lacking in most cases. The majority of RCT were conducted in Ukrainian research institutes and published in only two different journals. In several trials, there are clear signs of involvement of the manufacturer of Ukrain™. Moreover, Panzer et al. found the actions of Ukrain™ to be similar to the *C. majus* alkaloids it is prepared from and chemical analyses of Ukrain™ were inconsistent with the proposed trimeric structure and demonstrated that at least some commercial preparations of Ukrain™ consist of a mixture of *C. majus* alkaloids (including chelidonine). Research carried out at the NCI where Ukrain™ was tested on the screening panel with 60 cell lines from eight human cancer types revealed Ukrain™ to be cytotoxic against all the solid cancer cell lines tested. At least 35 *in vitro* and 45 animal experiments have been published that all assess the biological mechanism of Ukrain™

which suggest that Ukrain™, a drug based on the extract of the plant *C. majus*, has anticancer activity in a wide range of cell lines.^[51-54]

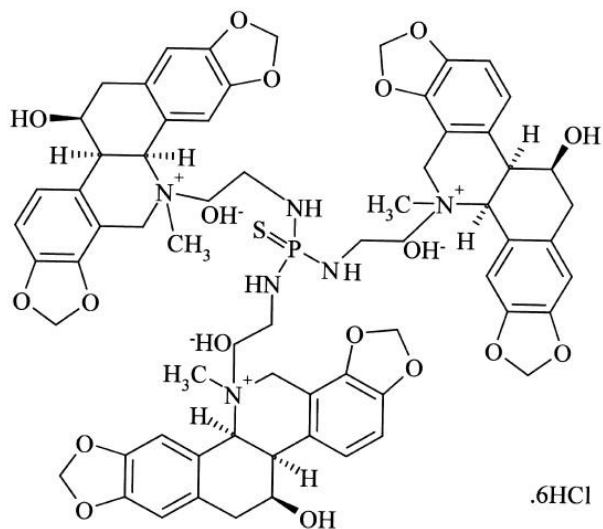


Figure 5.4 The proposed chemical structure of Ukrain™ (From Panzer et al., 2000)

5.2. PHYTOCHEMICAL INVESTIGATION

5.2.1. Plant material

The first batch of plant material that was used was the pulverised dried *Chelidonium majus* herb (Figure 5.5) purchased from Pharmaflores NV (batch number 10K25). The second batch plant material was uncut dried *Chelidonium majus* herb identified and provided by Dr. Olaf Kelber from Steigerwald Arzneimittelwerk GmbH and a voucher specimen was kept in the laboratory. Both batches of herbs were ground and passed through a sieve of 1 mm.



Figure 5.5 *Chelidonium majus* herb

5.2.2. Extraction

The first batch *Chelidonium majus* herb (6.5 kg) was extracted exhaustively and consecutively with 136.5 L of 80% ethanol by percolation and maceration at room temperature. The ethanol was removed under reduced pressure at 40 °C and the aqueous extract was lyophilised. The crude extract of the first batch *C. majus* (CM1) yielded 1.6 kg. The second batch *C. majus* herb (930 g) was extracted with 33.9 L of 80% ethanol and yielded 192 g crude extract (CM2).

An assay on both batches of plant material was performed according to the European Pharmacopoeia.^[55] The requirement was that the dried plant material should contain minimum 0.6% of total alkaloids expressed as chelidonine. In batch 1 0.77% total alkaloids

were found with a RSD% of 2.60%. Batch 2 contained 1.26% total alkaloids with a RSD% of 4.76%. Because of the higher content of alkaloids in batch 2, the crude extract derived from the second batch of plant material was used in further experiments.

5.2.3. Defatting

The lipophilic components of the crude extract were removed by means of liquid-liquid extraction with *n*-hexane. Approximately 30 g of crude extract was dissolved in 400 mL of water and extracted three times with 400 mL of *n*-hexane. The very lipophilic components, such as waxes and lipids, had more affinity for the *n*-hexane phase compared to the more hydrophilic components that had more affinity for the aqueous phase. This aqueous phase (CM2B) was then lyophilised and yielded 21.8 g. This defatted extract contained 2.87% total alkaloids.

The *C. majus* crude extract (CM2) and the defatted extract (CM2B) were used to test the efficacy of the extract *in vitro*.

5.2.4. High performance liquid chromatography

HPLC chromatograms were recorded for CM2B, as well as reference standards, i.e. chelidonine, sanguinarine, chelerythrine, protopine and berberine. The analytical method, according to Sarközi et al. with minor modification, was used.^[11] Solid phase extraction was performed on CM2B before injection. CM2B (98.0 mg) was dissolved in 3 mL 0.5% HCL in methanol. About 1.25 mL from this solution was diluted with 3.75 mL of 0.05 M *n*-heptanesulfonic acid aqueous solution (HS) and was homogenised by sonication. The supernatant was loaded onto an octadecyl SPE column, previously activated with 5 mL of 5% HS (0.05 M) in methanol and 5 mL of 100% HS (0.05 M). The SPE column was then washed with 5 mL of a 70% HS (0.05 M) solution in methanol to remove the matrix. The compounds were then eluted with 2.5 mL of 5% HS (0.05 M) in methanol. The reference standards were dissolved in a concentration ranging from 0.08 – 0.23 mg/mL in methanol. Twenty microliter was injected and separation was performed on the Phenomenex Luna C₁₈ coupled with a precolumn. Column temperature was set at 30 °C and the flow rate was 1 mL/min. The mobile

phases were (A) 30 mM ammonium formate (pH 2.80) and (B) methanol. The gradient was 0 min, 5% B; 5 min, 5% B; 55 min, 100% B; 60 min, 100% B. The chromatograms were recorded at 280 nm and retention time and UV spectrum of the reference standards were compared with the compounds found in CM2B. Figure 5.6 shows the chromatogram of the defatted *C. majus* extract and the determined alkaloids.

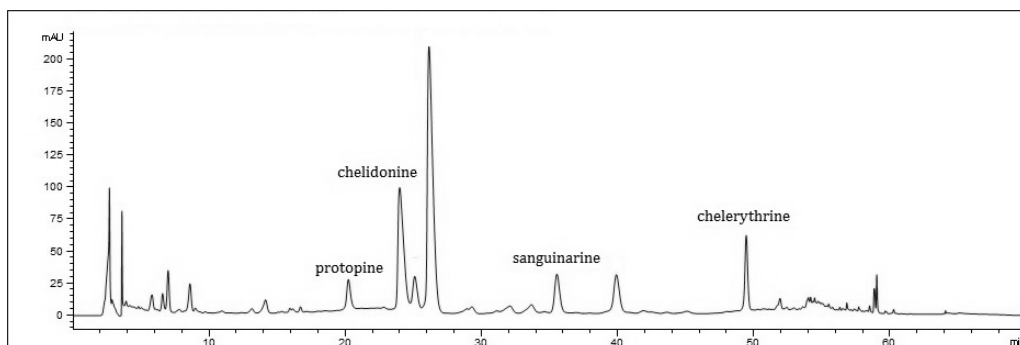


Figure 5.6 Chromatogram of CM2B and the determined alkaloids

5.3. PRECLINICAL STUDIES

5.3.1. *In vitro* cytotoxicity

The cytotoxicity of the *C. majus* crude extract (CM2) and the defatted extract (CM2B) (mentioned in section 5.2.2 and 5.2.3) were assessed *in vitro* in different cell lines, i.e. human and murine (cancer) cells. Different techniques were used such as spectrophotometric methods (the SRB assay and the NR assay) and the RTCA system.

5.3.1.1. Results

CM2 was evaluated on different human cancer cell lines, i.e. MDA-MB-231, PANC-1 and HT-29 by the SRB assay (2.3.3).

The used concentrations ranged from 10 – 1000 µg/mL and at least three individual experiments were performed for both incubation times. The survival percentages per concentration for these experiments were plotted in dose-response curves and are displayed in Figure 5.7. The calculated IC₅₀ values for these cell lines are summarised in Table 5.1.

The cytotoxic effect of CM2 was also evaluated on the PANC02 cell line, using concentrations ranging from 1 – 1000 µg/mL. Two experiments were performed with an incubation time of 24 h and four with 72 h incubation time. The calculated IC₅₀ values for this cell line are summarised in Table 5.1.

Table 5.1 IC₅₀ of the *C. majus* crude extract on the tested cell lines

		IC ₅₀ ± SEM (µg/mL)			
		MDA-MB-231	PANC-1	HT-29	PANC02
<i>C. majus</i>	24 h	73.9*	20.7 ± 1.0	20.6 ± 2.5	34.4 ± 2.8
	72 h	57.8 ± 5.1	19.8 ± 2.7	19.4 ± 1.6	33.4 ± 1.4

*No standard error is shown since the best-fit value for the slope was difficult to determine, due to the low amount of data point in that area

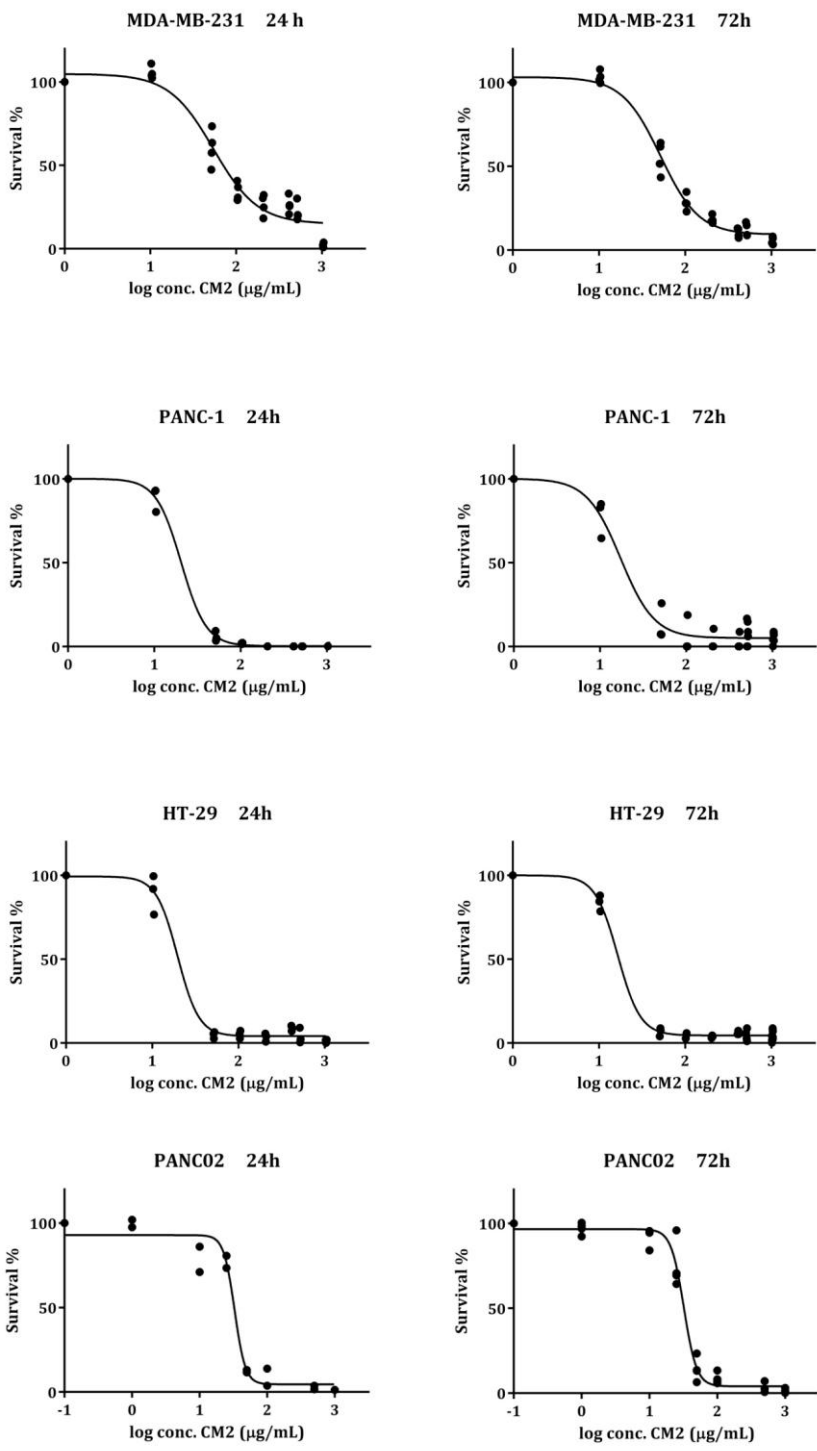


Figure 5.7 Dose-response curves of the different cancer cell lines treated with CM2

CM2B was also evaluated *in vitro* on different cell lines using different methods. The cytotoxic experiment on the BEAS-2B cell line was performed using the NR assay. CM2B was tested on the BEAS-2B cells at 7 different concentrations (1 - 1000 $\mu\text{g}/\text{mL}$). A 100 mg/mL stock solution of the extract was prepared in 5% DMSO and diluted in media in such a way that the highest end percentage of DMSO did not exceed 0.05%. The graph (Figure 5.8) shows the percentage of cell viability inhibition relative to the solvent control. The IC_{50} as determined from the fitted curve was 64.38 $\mu\text{g}/\text{mL}$. As reference point, the IC_{50} values of the other cellular models that were previously determined are indicated in the graph. Precipitation and aspecific binding of neutral red were also examined and were not observed.

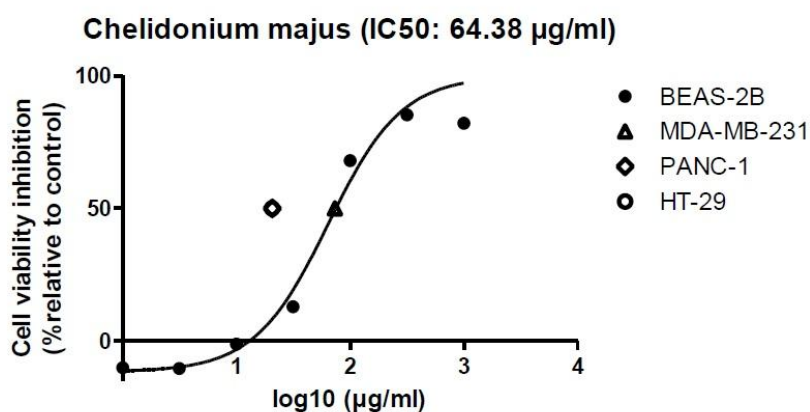


Figure 5.8 Dose-response curve and calculated IC_{50} for effects on cell viability of BEAS-2B cells

CM2B was also tested against the PANC02 cells, again by using the SRB assay. The concentrations of CM2B ranged from 0.1 - 1000 $\mu\text{g}/\text{mL}$ and the dose-response curves are shown in Figure 5.9. Three experiments were performed with an incubation time of 24 h and four with an incubation time of 72 h. The calculated IC_{50} values for this cell line treated with CM2B were 36.0 ± 2.6 for 24 h and 30.1 ± 0.7 for 72 h.

The effect on two primary endometrial cancer cell lines (PC-EM005 and PC-EM002) and on the mouse fibroblast cells (3T3) was evaluated with the use of the RTCA system (2.3.5). Figure 5.10 shows the real-time plot of the cytotoxicity experiment of CM2B on the PC-EM005 cell line. The real-time plot of the two other cell lines (PC-EM002 and 3T3) are shown in Figure 5.11 and Figure 5.12. Again, a dose-response curve was plotted and the IC₅₀ value was calculated and all calculated IC₅₀ values are summarised in Table 5.2.

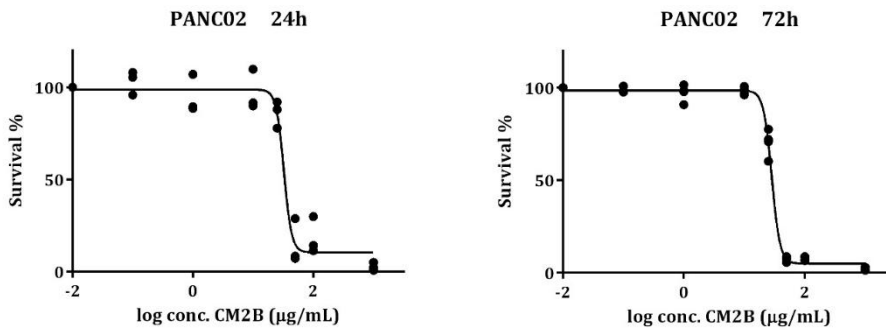


Figure 5.9 Dose-response curves of the PANC02 cell lines treated with CM2B

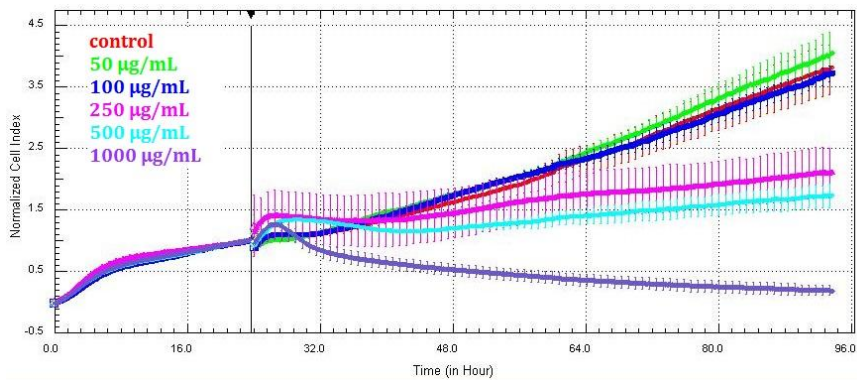


Figure 5.10 Real-time monitoring of the effect of CM2B on the PC-EM005 cell line

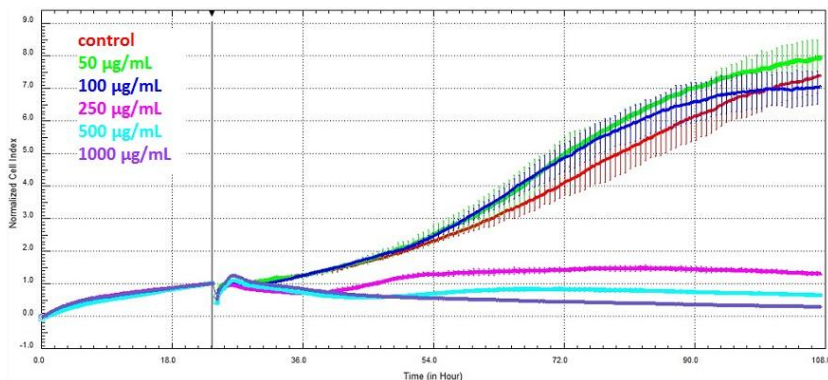


Figure 5.11 Real-time monitoring of the effect of CM2B on the PC-EM002 cell line

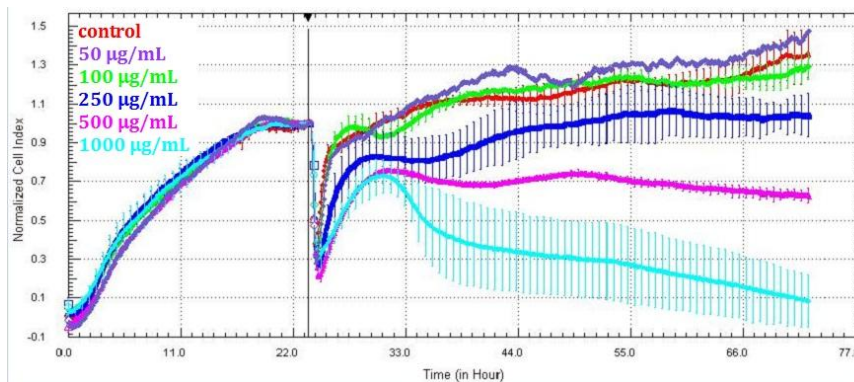


Figure 5.12 Real-time monitoring of the effect of CM2B on the 3T3 cell line

Table 5.2 IC₅₀ of the defatted *C. majus* extract on the tested cell lines

		IC ₅₀ ± SEM (µg/mL)				
		PANC02	PC-EM005	PC-EM002	3T3	
<i>defatted C. majus</i>	24 h	36.0 ± 2.6	48h	1400	100	1600
	72 h	30.1 ± 0.7		(R ² : 0.98)	(R ² : 0.98)	(R ² : 0.99)

5.3.1.2. Discussion

The *C. majus* crude extract only exerted a moderate effect on the MDA-MB-231 cells with an IC_{50} above 20 $\mu\text{g}/\text{mL}$ for both incubation times. This was probably due to the invasive type of this cell line, making it more resistant to therapy. A lower IC_{50} value was observed for an incubation time of 72 h compared to 24 h. This can indicate that the crude extract from this plant perhaps needed a longer incubation period for this specific cell line. For all other cell line this effect was not observed.

A relevant cytotoxic effect was revealed against PANC-1 and HT-29 for CM2 with IC_{50} value around 20 $\mu\text{g}/\text{mL}$ for both incubation times.

The results observed for the defatted *C. majus* extract on the PANC02 cell line did not differ from the results observed for the crude extract. The IC_{50} values for both extracts all ranged around 35 $\mu\text{g}/\text{mL}$ and both extracts were considered having a moderate to high cytotoxic effect on the PANC02 cell line.

Although for the *xCELLigence* experiment no effect was observed on the PC-EM005 cells at a concentration of 100 $\mu\text{g}/\text{mL}$, an inhibition of proliferation was noticed when treated at a concentration of 250 $\mu\text{g}/\text{mL}$ and 500 $\mu\text{g}/\text{mL}$ CM2B. Approximately 3 h after adding treatment, a decline in cell numbers (decline of cell index) was observed at a concentration of 1 mg/mL. It was then concluded that CM2B only exhibited a low activity due to the high concentration needed for the cytotoxic effect. The high IC_{50} value led to the same conclusion.

For the PC-EM002 cells again no effect was observed at a concentration of 100 $\mu\text{g}/\text{mL}$, but a decline in number of cells was observed starting from a concentration of 250 $\mu\text{g}/\text{mL}$. Approximately 15 h after adding treatment, the cells treated with 250 $\mu\text{g}/\text{mL}$ showed a slight increase in number of cells, but after a couple of hours a proliferation inhibition was observed. For the cells treated with 500 $\mu\text{g}/\text{mL}$ again a decline in cell number was observed 3 h after treatment was added and a proliferation inhibition was observed 24 h after treatment was added. For the cells treated with 1 mg/mL a slow decrease in cell number was observed during the entire incubation period

For the 3T3 cell line, a great decrease of cell number for all concentrations was observed after adding CM2B, followed by a recuperation period and a slow growth. However, for the cells treated with 500 µg/mL a slow decrease of cell number was observed and for 1 mg/mL a large decrease in cell numbers was observed.

In conclusion, for the defatted *C. majus* extract, high IC₅₀ values were observed for PC-EM005 and 3T3 cells, thus having no relevant cytotoxic effect on these cell lines. For the PC-EM002 cell line a low cytotoxic effect was observed with an IC₅₀ of 0.1 mg/mL.

5.3.2. ***In vivo* – effect on metastases**

An *in vivo* study was performed to evaluate the effect of the *C. majus* defatted extract (CM2B) (mentioned in section 5.2.2 and 5.2.3) on a highly metastatic pancreatic murine model. This study was executed at the department of Microbiology and Immunology, Albert Einstein College of Medicine (NY, USA) in the laboratory of Prof. Claudia Gravekamp.

5.3.2.1. Materials and methods

Cell Culture

The PANC02 was provided by Chandan Guha, Albert Einstein College of Medicine. The cells were cultured in McCoy's medium supplemented with 10% FBS, glutamine (2 mM), nonessential amino acids, sodium pyruvate (1 mM), HEPES (10 mM), and penicillin/streptomycin (100 U/mL) and were maintained in exponential growth in a humidified 5% CO₂/95% air atmosphere at 37 °C.

Animals

Six-to-eight weeks old female C57BL/6 mice were obtained from Charles River and maintained in the animal husbandry facility of the Albert Einstein College of Medicine according to the Association for Assessment and Accreditation of Laboratory Animal Care guidelines, and according the guidelines of the Albert Einstein Institute for Animal Studies. The mice were housed under a 10/14 h dark/light cycle at constant temperature and humidity and had access to tap water and food *ad libitum*.

Acute toxicity study

A short acute toxicity study has been done with the different treatments before the actual metastasis experiment. Non-tumour-bearing C57BL/6 mice (n = 3 per dose) were given different doses of *C. majus* extract (0.4, 1.2 and 2.4 mg/kg BW). These doses were given IP daily for 3 days and the acute toxicity was then evaluated.

Metastatic tumour model and evaluation

Cultures of PANC02 cells were harvested using a 0.05% trypsin solution, washed twice in sterile PBS and resuspended in sterile PBS at a concentration of 20 x 10⁶ cells per mL. The

viable cells were counted by using a haemocytometer and trypan blue. Mice (n = 21) were inoculated with 100 µL of the cell suspension in the mammary fat pad on day 0. In this PANC02 metastatic model, the primary tumour extends to the chest cavity lining, which is palpable 5 à 7 days after tumour cell injection, but primary tumours stay relatively small, whereas metastases (visible by eye) predominantly developed in the portal liver, resulting in the production of ascites in the peritoneal cavity within approximately 20 days. In addition, the pancreas is heavily infiltrated with PANC02 tumour cells, but less frequently in the mesenteric lymph nodes, diaphragm, spleen, and kidneys.^[56] After 3 days of tumour cell injection, treatment started. Each mouse was randomly divided in 3 experimental groups (n = 5 per treatment group and n = 3 per control group) and assigned to a different treatment (Table 5.3). All mice were euthanised at day 20 and analysed for tumour weight, location and frequency of metastases.

Treatments

Treatment was administered during 19 days, starting 3 days after tumour inoculation. The first day of treatment was assigned “day 1” (Figure 5.13). The control mice received 300 µL saline IP daily, while the positive control group were given 3 times/week gemcitabine (Sigma Aldrich) dissolved in saline. It was administered IP at a dose of 60 mg/kg BW. CM2B was administered IP daily at a dose of 1.2 mg/kg BW and Ukrain™ was given 3 times/week at a dose of 3.6 mg/kg IP (Table 5.3).

Statistics

Statistical analysis of the results was performed using a non-parametric Mann-Whitney test. Values of $p \leq 0.05$ were considered significant and statistical analysis was performed using GraphPad Prism 6 (Version 6.01).

Table 5.3 Group treatment assignment

n°	Group	# mice	Treatment and dose
0	Negative control	9	300 µl saline IP
1	Positive control	5	60 mg/kg BW gemcitabine IP
2	<i>Chelidonium majus</i> extract	5	1.2 mg/kg BW IP
3	Ukrain™	5	3.6 mg/kg BW IP

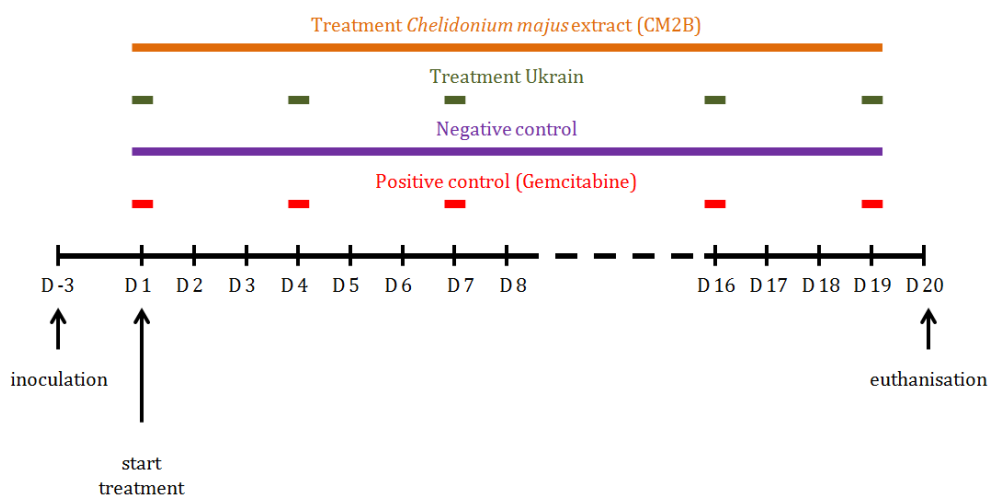


Figure 5.13 Time line of the *in vivo* metastasis study

5.3.2.2. Results and discussion

An acute toxicity study was performed prior to the metastasis experiment. The mice that were given the two lowest doses (0.4 and 1.2 mg/kg BW) did not show any adverse effects. Two mice died within 3 h after receiving an injection of the highest dose (2.4 mg/kg BW) and the last mouse died immediately after the second injection. Therefore it was preferred to perform the metastasis experiment with a dose of 1.2 mg CM2B/kg BW.

During the metastasis experiment, three different experimental groups were set up. Every treatment had its own experiment and its own control (n = 3). At day 20 all mice were checked for ascites by palpation of the abdomen. All control mice had developed ascites and all mice were then sacrificed. The primary tumours were removed and weighed. The metastases in the abdominal cavity and organs were counted manually. The amount of metastases per group is shown in Figure 5.14.

The first parameter that was evaluated was the degree of ascites for each group. Each mouse was scored based on the degree of ascites (bloody, translucent or no ascites). The gemcitabine treated mice did not show any ascites. All mice of the control groups had developed bloody ascites. One mouse of the *C. majus* treated group did not show any ascites, while the four others showed translucent ascites. For the Ukrain™ treated group, 3 mice had bloody ascites and 2 mice had no ascites.

The second and third parameters were the weight of the primary tumour and the number of metastases. For the *C. majus* extract significantly less metastases were counted compared to the control group. The extract, however, did not affect the weight of the primary tumours. For Ukrain™ no significant difference in amount of metastases was observed compared to the control group and also no decrease in tumour weight. For the positive control group treated with gemcitabine, significantly less metastases was counted in comparison with the control group, but again no significant decrease in tumour weight was observed

Although the positive control confirmed that the used model was suitable to evaluate the effect on the number of metastases, this was merely a pilot study with promising preliminary results. Therefore further investigation with for example a bigger sample size is needed. It might also be useful to have an idea about the number of metastases just before treatment to exclude the possibility of badly performed inoculation.

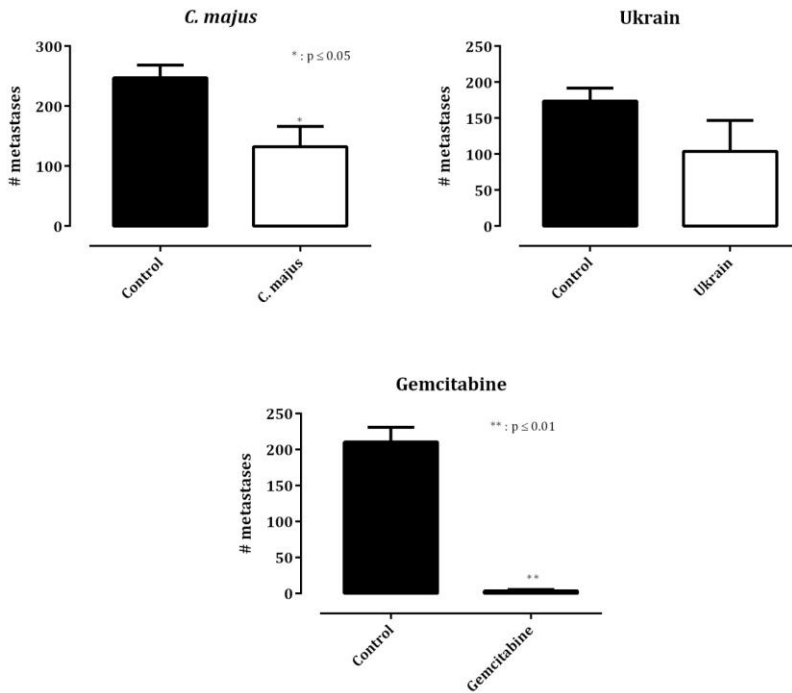


Figure 5.14 Bar charts of the counted metastases

5.4. SUMMARY AND CONCLUSION

The *Chelidonium majus* L. herb was phytochemically investigated. The dried plant material contained 1.26% of total alkaloids expressed as chelidonine. About 930 g dried herb was extracted with 33.9 L of 80% ethanol and yielded 192 g crude extract (CM2). This crude extract was then defatted with *n*-hexane, resulting in a defatted *C. majus* extract (CM2B). Four main benzylisoquinoline alkaloids, i.e. chelidonine, sanguinarine, chelerythrine and protopine, were identified from CM2B by means of HPLC-UV. Both extracts were evaluated *in vitro* in different cell lines, i.e. human and murine (cancer) cells for their cytotoxic activity. CM2 showed a high cytotoxic activity against PANC-1 and HT-29, and a moderate cytotoxic activity against MDA-MB-231. CM2 as well as CM2B showed a moderate to high cytotoxic activity against the PANC02 cell lines. Low to almost no cytotoxic activity was observed for PC-EM005, PC-EM002 and 3T3 cell lines, when treated with CM2B.

A preliminary *in vivo* study was performed to evaluate the antitumoural effect of CM2B on a highly metastatic murine pancreatic model. Significantly less metastases were counted for the mice treated with 1.2 mg/kg BW CM2B compared to the control group. The extract, however, did not affect the weight of the primary tumours.

REFERENCES

1. Committee on Herbal Medicinal Products (HMPC), *Assessment report on Chelidonium majus L., herba*. European Medicines Agency, 2011. EMA/HMPC/369801/2009.
2. Jursky, F. and M. Baliova, *Differential effect of the benzophenanthridine alkaloids sanguinarine and chelerythrine on glycine transporters*. *Neurochemistry International*, 2011. 58(6): p. 641-647.
3. Wink, M., T. Schmeller, and B. Latz-Bruning, *Modes of action of allelochemical alkaloids: Interaction with neuroreceptors, DNA, and other molecular targets*. *Journal of Chemical Ecology*, 1998. 24(11): p. 1881-1937.
4. Colombo, M.L. and E. Bosisio, *Pharmacological activities of Chelidonium majus L (Papaveraceae)*. *Pharmacological Research*, 1996. 33(2): p. 127-134.
5. Serafim, T.L., J.A.C. Matos, V.A. Sardao, G.C. Pereira, A.F. Branco, S.L. Pereira, D. Parke, E.L. Perkins, A.J.M. Moreno, J. Holy, and P.J. Oliveira, *Sanguinarine cytotoxicity on mouse melanoma K1735-M2 cells-Nuclear vs. mitochondrial effects*. *Biochemical Pharmacology*, 2008. 76(11): p. 1459-1475.
6. Panzer, A., A.M. Joubert, P.C. Bianchi, E. Hamel, and J.C. Seegers, *The effects of chelidonine on tubulin polymerisation, cell cycle progression and selected signal transmission pathways*. *European Journal of Cell Biology*, 2001. 80(1): p. 111-118.
7. Dewick, P., *Medicinal Natural Products*. 2006. p. 339-340.
8. Kemeny-Beke, A., J. Aradi, J. Damjanovich, Z. Beck, A. Facsko, A. Berta, and A. Bodnar, *Apoptotic response of uveal melanoma cells upon treatment with chelidonine, sanguinarine and chelerythrine*. *Cancer Letters*, 2006. 237(1): p. 67-75.
9. Barnes, J., L. Anderson, and D. Philipson, *Herbal Medicines: A Guide for Healthcare*. 2007: Pharmaceutical Press, London. p. 136-145.
10. Gilca, M., L. Gaman, E. Panait, I. Stoian, and V. Atanasiu, *Chelidonium majus--an integrative review: traditional knowledge versus modern findings*. *Forsch Komplementmed*, 2010. 17(5): p. 241-248.

11. Sarkozi, A., G. Janicsak, L. Kursinszki, and A. Kery, *Alkaloid composition of *Chelidonium majus* L. studied by different chromatographic techniques*. *Chromatographia*, 2006. 63: p. S81-S86.
12. Hahn, R. and A. Nahrstedt, *Hydroxycinnamic Acid-Derivatives, Caffeoylmalic and New Caffeoylaldonic Acid-Esters, from *Chelidonium-Majus**. *Planta Medica*, 1993. 59(1): p. 71-75.
13. Kulp, M., O. Bragina, P. Kogerman, and M. Kaljurand, *Capillary electrophoresis with led-induced native fluorescence detection for determination of isoquinoline alkaloids and their cytotoxicity in extracts of *Chelidonium majus* L.* *Journal of Chromatography A*, 2011. 1218(31): p. 5298-5304.
14. Vahlensieck, U., R. Hahn, H. Winterhoff, H.G. Gumbinger, A. Nahrstedt, and F.H. Kemper, *The Effect of *Chelidonium-Majus* Herb Extract on Choleresis in the Isolated-Perfused Rat-Liver*. *Planta Medica*, 1995. 61(3): p. 267-271.
15. Mazzanti, G., A. Di Sotto, A. Franchitto, C.L. Mammola, P. Mariani, S. Mastrangelo, F. Menniti-Ippolito, and A. Vitalone, **Chelidonium majus* is not hepatotoxic in Wistar rats, in a 4 weeks feeding experiment*. *Journal of Ethnopharmacology*, 2009. 126(3): p. 518-524.
16. Vavreckova, C., I. Gawlik, and K. Muller, *Benzophenanthridine alkaloids of *Chelidonium majus* .1. Inhibition of 5- and 12-lipoxygenase by a non-redox mechanism*. *Planta Medica*, 1996. 62(5): p. 397-401.
17. Vavreckova, C., I. Gawlik, and K. Muller, *Benzophenanthridine alkaloids of *Chelidonium majus* .2. Potent inhibitory action against the growth of human keratinocytes*. *Planta Medica*, 1996. 62(6): p. 491-494.
18. Song, J.Y., H.O. Yang, S.N. Pyo, I.S. Jung, S.Y. Yi, and Y.S. Yun, *Immunomodulatory activity of protein-bound polysaccharide extracted from *Chelidonium majus**. *Archives of Pharmacal Research*, 2002. 25(2): p. 158-164.
19. Maiti, M., R. Nandi, and K. Chaudhuri, *Sanguinarine: a monofunctional intercalating alkaloid*. *FEBS Lett*, 1982. 142(2): p. 280-284.

20. Smekal, E., N. Kubova, and V. Kleinwachter, *Interaction of Benzophenanthridine Alkaloid Sanguinarine with DNA*. *Studia Biophysica*, 1984. 101: p. 125-132.
21. El-Readi, M.Z., S. Eid, M.L. Ashour, A. Tahrani, and M. Wink, *Modulation of multidrug resistance in cancer cells by chelidonine and Chelidonium majus alkaloids*. *Phytomedicine*, 2013. 20(3-4): p. 282-294.
22. Wink, M., *Molecular modes of action of cytotoxic alkaloids: from DNA intercalation, spindle poisoning, topoisomerase inhibition to apoptosis and multiple drug resistance*. *Alkaloids Chem Biol*, 2007. 64: p. 1-47.
23. Fletcher, J.I., M. Haber, M.J. Henderson, and M.D. Norris, *ABC transporters in cancer: more than just drug efflux pumps*. *Nat Rev Cancer*, 2010. 10(2): p. 147-156.
24. Isolani, M.E., D. Pietra, L. Balestrini, A. Borghini, P. Deri, M. Imbriani, A.M. Bianucci, and R. Batistoni, *The in vivo effect of chelidonine on the stem cell system of planarians*. *Eur J Pharmacol*, 2012. 686(1-3): p. 1-7.
25. Vavreckova, C., I. Gawlik, and K. Muller, *Benzophenanthridine alkaloids of Chelidonium majus; II. Potent inhibitory action against the growth of human keratinocytes*. *Planta Med*, 1996. 62(6): p. 491-494.
26. Vavreckova, C., I. Gawlik, and K. Muller, *Benzophenanthridine alkaloids of Chelidonium majus; I. Inhibition of 5- and 12-lipoxygenase by a non-redox mechanism*. *Planta Med*, 1996. 62(5): p. 397-401.
27. Lenfeld, J., M. Kroutil, E. Marsalek, J. Slavik, V. Preininger, and V. Simanek, *Antiinflammatory activity of quaternary benzophenanthridine alkaloids from Chelidonium majus*. *Planta Med*, 1981. 43(2): p. 161-165.
28. Colombo, M.L. and E. Bosisio, *Pharmacological activities of Chelidonium majus L. (Papaveraceae)*. *Pharmacol Res*, 1996. 33(2): p. 127-134.
29. Chmura, S.J., M.E. Dolan, A. Cha, H.J. Mauceri, D.W. Kufe, and R.R. Weichselbaum, *In vitro and in vivo activity of protein kinase C inhibitor chelerythrine chloride induces tumor cell toxicity and growth delay in vivo*. *Clin Cancer Res*, 2000. 6(2): p. 737-742.

30. Ma, L., N. Krishnamachary, and M.S. Center, *Phosphorylation of the multidrug resistance associated protein gene encoded protein P190*. *Biochemistry*, 1995. 34(10): p. 3338-3343.
31. Kemeny-Beke, A., J. Aradi, J. Damjanovich, Z. Beck, A. Facsko, A. Berta, and A. Bodnar, *Apoptotic response of uveal melanoma cells upon treatment with chelidonine, sanguinarine and chelerythrine*. *Cancer Lett*, 2006. 237(1): p. 67-75.
32. Mantena, S.K., S.D. Sharma, and S.K. Katiyar, *Berberine, a natural product, induces G1-phase cell cycle arrest and caspase-3-dependent apoptosis in human prostate carcinoma cells*. *Mol Cancer Ther*, 2006. 5(2): p. 296-308.
33. Kuo, C.L., C.W. Chi, and T.Y. Liu, *The anti-inflammatory potential of berberine in vitro and in vivo*. *Cancer Lett*, 2004. 203(2): p. 127-137.
34. Stermitz, F.R., P. Lorenz, J.N. Tawara, L.A. Zenewicz, and K. Lewis, *Synergy in a medicinal plant: antimicrobial action of berberine potentiated by 5'-methoxyhydnocarpin, a multidrug pump inhibitor*. *Proc Natl Acad Sci U S A*, 2000. 97(4): p. 1433-1437.
35. Ko, W.H., X.Q. Yao, C.W. Lau, W.I. Law, Z.Y. Chen, W. Kwok, K. Ho, and Y. Huang, *Vasorelaxant and antiproliferative effects of berberine*. *Eur J Pharmacol*, 2000. 399(2-3): p. 187-196.
36. Maiti, M. and G.S. Kumar, *Molecular aspects on the interaction of protoberberine, benzophenanthridine, and aristolochia group of alkaloids with nucleic acid structures and biological perspectives*. *Med Res Rev*, 2007. 27(5): p. 649-695.
37. Shirwaikar, A., A. Shirwaikar, K. Rajendran, and I.S. Punitha, *In vitro antioxidant studies on the benzyl tetra isoquinoline alkaloid berberine*. *Biol Pharm Bull*, 2006. 29(9): p. 1906-1910.
38. Pereira, G.C., A.F. Branco, J.A.C. Matos, S.L. Pereira, D. Parke, E.L. Perkins, T.L. Serafim, V.A. Sardao, M.S. Santos, A.J.M. Moreno, J. Holy, and P.J. Oliveira, *Mitochondrially targeted effects of berberine [natural yellow 18, 5,6-dihydro-9,10-dimethoxybenzo(g)-1,3-benzodioxolo(5,6-a) quinolizinium] on K1735-M2 mouse melanoma cells: Comparison with direct effects on isolated mitochondrial fractions*. *Journal of Pharmacology and Experimental Therapeutics*, 2007. 323(2): p. 636-649.

39. Hwang, J.M., H.C. Kuo, T.H. Tseng, J.Y. Liu, and C.Y. Chu, *Berberine induces apoptosis through a mitochondria/caspases pathway in human hepatoma cells*. Arch Toxicol, 2006. 80(2): p. 62-73.
40. Serafim, T.L., P.J. Oliveira, V.A. Sardao, E. Perkins, D. Parke, and J. Holy, *Different concentrations of berberine result in distinct cellular localization patterns and cell cycle effects in a melanoma cell line*. Cancer Chemother Pharmacol, 2008. 61(6): p. 1007-1018.
41. Pinto-Garcia, L., T. Efferth, A. Torres, J.D. Hoheisel, and M. Youns, *Berberine inhibits cell growth and mediates caspase-independent cell death in human pancreatic cancer cells*. Planta Med, 2010. 76(11): p. 1155-1161.
42. Vrba, J., E. Vrublova, M. Modriansky, and J. Ulrichova, *Protopine and allocryptopine increase mRNA levels of cytochromes P450 1A in human hepatocytes and HepG2 cells independently of AhR*. Toxicology Letters, 2011. 203(2): p. 135-141.
43. Satou, T., M. Koga, R. Matsushashi, K. Koike, I. Tada, and T. Nikaido, *Assay of nematocidal activity of isoquinoline alkaloids using third-stage larvae of Strongyloides ratti and S-venezuelensis*. Veterinary Parasitology, 2002. 104(2): p. 131-138.
44. Wang, G.X., Z.A. Zhou, D.X. Jiang, J. Han, J.F. Wang, L.W. Zhao, and J. Li, *In vivo anthelmintic activity of five alkaloids from Macleaya microcarpa (Maxim) Fedde against Dactylogyrus intermedius in Carassius auratus*. Veterinary Parasitology, 2010. 171(3-4): p. 305-313.
45. Rathi, A., A.K. Srivastava, A. Shirwalkar, A.K.S. Rawat, and S. Mehrotra, *Hepatoprotective potential of Fumaria indica Pugsley whole plant extracts, fractions and an isolated alkaloid protopine*. Phytomedicine, 2008. 15(6-7): p. 470-477.
46. Saeed, S.A., A.H. Gilani, R.U. Majoo, and B.H. Shah, *Anti-thrombotic and anti-inflammatory activities of protopine*. Pharmacological Research, 1997. 36(1): p. 1-7.
47. Xiao, X.H., J.T. Liu, J.W. Hu, X.P. Zhu, H. Yang, C.Y. Wang, and Y.H. Zhang, *Protective effects of protopine on hydrogen peroxide-induced oxidative injury of PC12 cells via Ca²⁺ antagonism and antioxidant mechanisms*. European Journal of Pharmacology, 2008. 591(1-3): p. 21-27.

48. Ko, F.N., T.S. Wu, S.T. Lu, Y.C. Wu, T.F. Huang, and C.M. Teng, *Ca²⁺-Channel Blockade in Rat Thoracic Aorta by Protopine Isolated from Corydalis Tubers*. Japanese Journal of Pharmacology, 1992. 58(1): p. 1-9.
49. Song, L.S., G.J. Ren, Z.L. Chen, Z.H. Chen, Z.N. Zhou, and H.P. Cheng, *Electrophysiological effects of protopine in cardiac myocytes: inhibition of multiple cation channel currents*. British Journal of Pharmacology, 2000. 129(5): p. 893-900.
50. Jiang, B., K. Cao, and R. Wang, *Inhibitory effect of protopine on K-ATP channel subunits expressed in HEK-293 cells*. European Journal of Pharmacology, 2004. 506(2): p. 93-100.
51. Boehm, K., E. Ernst, and CAM-Cancer Consortium. *Ukrain*. [cited 2014/08/31]; Available from: <http://www.cam-cancer.org/CAM-Summaries/Herbal-products/Ukrain>.
52. Panzer, A., E. Hamel, A.M. Joubert, P.C. Bianchi, and J.C. Seegers, *Ukrain(TM), a semisynthetic Chelidonium majus alkaloid derivative, acts by inhibition of tubulin polymerization in normal and malignant cell lines*. Cancer Lett, 2000. 160(2): p. 149-157.
53. Panzer, A., A.M. Joubert, J.N. Eloff, C.F. Albrecht, E. Erasmus, and J.C. Seegers, *Chemical analyses of Ukrain, a semi-synthetic Chelidonium majus alkaloid derivative, fail to confirm its trimeric structure*. Cancer Lett, 2000. 160(2): p. 237-241.
54. Ernst, E. and K. Schmidt, *Ukrain - a new cancer cure? A systematic review of randomised clinical trials*. BMC Cancer, 2005. 5: p. 69.
55. Ph. Eur., *EUROPEAN PHARMACOPOEIA 8.0 Monograph Greater Celandine*. 07/2012:1861.
56. Quispe-Tintaya, W., D. Chandra, A. Jahangir, M. Harris, A. Casadevall, E. Dadachova, and C. Gravekamp, *Nontoxic radioactive Listeria(at) is a highly effective therapy against metastatic pancreatic cancer*. Proc Natl Acad Sci U S A, 2013. 110(21): p. 8668-8673.

CHAPTER 6
GENERAL CONCLUSION & PERSPECTIVES

The aim of this thesis was to evaluate some promising plant extracts for their potential in the treatment of cancer. One of the possibilities to improve therapy is by using a combination of compounds/drugs acting on different targets. In this case, the dose of each individual product can be lowered, resulting in fewer side effects. Plants are a source of chemically diverse constituents that can act on different targets and furthermore, the generally low concentration of these constituents creates often low toxicity. Synergistic effects in plant extracts have been a long time established fact and together with the presence of inactive prodrugs that gradually become active by metabolism, these two aspects help to reduce toxicity and improve the pharmacological profile. So this work focused on the scientific approach concerning herbal medicinal products to evaluate and demonstrate their added value to cancer treatment taking efficacy, safety and quality into account.

For *Steganotaenia araliacea*, the already reported cytostatic lignans have not been found during our investigation. However, a new protoflavonoid, named protosteganoflavanone, was isolated. The class of protoflavonoid has been promoted to exhibit antitumoural activity. Although the crude extract only exerted moderate activity *in vitro*, the new protoflavonoid can still be an interesting compound with perhaps potential cytotoxic properties and therefore a suited candidate for further *in vitro* investigation. Further phytochemical investigation on the plant extracts to check whether more protoflavonoid are present in *S. araliacea* can provide more affirmation to test a more purified fraction of *S. araliacea*. In the case *in vitro* studies are performed more different types of cell lines can be tested to see whether the moderate activity was only characteristic for the tested cell line and perhaps better activity can be seen on other types of cell lines.

Chelidonium majus showed higher *in vitro* activity compared to *S. araliacea*. The *C. majus* crude extract as well as the defatted extract showed relevant cytotoxic properties. Our pilot study with *C. majus* against a highly metastatic mouse model also showed promising efficacy. Therefore it is worthwhile to investigate this plant extract more in detail. Before performing more *in vivo* tests, it would be preferable to do more chromatographic profiling. Although the major known constituents of *C. majus* were identified, quantification of the compounds together with the identification of the remaining unknown compounds would be advisable. So

further investigation with perhaps LC-SPE-NMR could possibly identify the other compounds. The probability that the unidentified compounds are new, is very low due to the fact that *C. majus* has been thoroughly phytochemically studied. It would be desirable to quantify the active constituents so that future *in vivo* investigations can be performed with quantified extract as it was performed for *Gloriosa superba*.

This thesis consisted mainly of the investigation of *Gloriosa superba*. At an early stage *G. superba* exhibited high cytotoxic activity, which was much higher compared to the two other plant extracts. The simple chromatographic profile of the crude extract made it possible to isolate the main active compounds without further purification steps and to quantify them using the optimised and validated HPLC-UV method. Therefore the ability existed to perform *in vivo* studies with quantified extracts.

The *in vivo* study of the *Gloriosa superba* extract, as well as the colchicine-poor extract have shown efficacy in a mouse model for pancreatic cancer. These results confirmed the initial hypothesis that indeed colchicoside, a prodrug that is metabolically activated after oral administration, can provide a therapeutic alternative to colchicine, which has a connotation of high toxicity. However, combination therapy of a standard drug with a herbal medicine may be therapeutically more acceptable for cancer than a monotherapy with a herbal medicine. The *in vivo* experiment combining gemcitabine with the *Gloriosa superba* extract showed a higher efficacy of the combination therapy than monotherapy with gemcitabine. The same results can be expected for the colchicine-poor extract. Therefore further investigations of the combination of the colchicine-poor extract with gemcitabine might be beneficial, as well as using higher concentration of extract. A higher dose can be use since even at the highest concentration in our experiment no signs of toxicity were observed. In a next step, PANC-1 cells can be used in a xenograft model to test the *in vivo* antitumoural effect on human pancreatic cancer cell induced models.

Although the mechanism of action of colchicine is well known, the possibility that other mechanisms may contribute to the activity of the extract cannot be excluded. Therefore further investigations into the mechanisms of action is also a step to be consider.

In conclusion, for the three plant species initially selected for this project, i.e. *Steganotaenia araliacea* Hoechst, *Gloriosa superba* L. and *Chelidonium majus* L., phytochemical investigations have been carried out resulting in the identification of cytotoxic constituents. For *Chelidonium majus* a preliminary *in vivo* experiment was executed. For *Gloriosa superba* analytical methods were developed to quantify their extracts, and *in vivo* experiments were carried out. The *in vivo* antitumoural activity of the *Gloriosa superba* extract was demonstrated in a pancreatic tumour model. Our hypothesis that naturally occurring prodrugs such as colchicoside may contribute to the activity was confirmed by demonstrating the *in vivo* efficacy of a colchicine-poor / colchicoside-enriched extract, especially in combination with the standard drug gemcitabine. The latter observation, together with the absence of obvious toxicity, may open promising therapeutic options for the treatment of human pancreatic cancer.

SUMMARY

Cancer is the second leading cause of death worldwide and has become the most challenging disease to cure. The burden of cancer is still increasing despite diagnostic and therapeutic advancements. The death rate due to cancer increases every year. Cancer can be defined as a disease in which a group of abnormal cells grows uncontrollably by disregarding the normal rules of cell division.

Many of the current cancer drugs are from natural origin or derived from natural products. Plants are an interesting source because of their chemically diverse constituents. A plant extract is a complex mixture of different, often closely related compounds that can act on different targets. Because of the generally low concentration of these constituents, there is a low toxicity, whereas with regard to the activity often synergism is observed. Usually the plant preparations in their crude or refined form show a more interesting combination of activities than the isolated constituents. In addition, the presence of prodrugs can add to the activity. So there is a huge potential in the use of medicinal plant extracts. Natural products represent valuable sources for drug development given the fact that a considerably large amount of drugs is of natural origin.

In this thesis several medicinal plants with previously reported cytotoxic activity and/or traditional use were investigated for their potential use against cancer.

The phytochemical investigation of the *Steganotaenia araliacea* **Hoechst.** stem bark led to the identification of three constituents that to the best of our knowledge had never been reported before in this plant species. These constituents were spiropreussomerin A, which is a secondary metabolite of the endophyte *Preussia sp.*, conrauiflavonol/afzelin A and a new compound 6,7-(2",2"-dimethylpyrano)-5,1'-dihydroxy-4'oxo-2'eryl-flavanone, for which the name protosteganoflavanone was adopted. The *in vitro* studies of the *S. araliacea* extract only resulted in a moderate cytotoxic activity for the tested cell lines, i.e. breast (MDA-MB-231), pancreas (PANC-1) and colon (HT-29) cancer cell lines and bronchial epithelial (BEAS-2B) cells with IC₅₀ values above 20 µg/mL. However, the identified protosteganoflavanone belongs to a rare class of flavonoids, i.e. the protoflavonoids. It is considered as a promising class of anticancer compounds. Therefore future investigations on protosteganoflavanone may be

promising together with the *in vitro* evaluation of the ethyl acetate fraction, in which this protoflavonoid was present as major compound. This ethyl acetate fraction could then be used as a refined extract. However in this project, further investigation of the total extract of *S. araliacea* was considered having less priority than the two other plants selected due to its seemingly moderate *in vitro* activity.

The study on *Gloriosa superba* L. seeds comprised not only a phytochemical investigation, during which four compounds were isolated and identified from the 80% EtOH crude extract, i.e. colchicine, 3-*O*-demethylcolchicine, colchicoside and the artefact, colchicosamide, but also in an analytical investigation, in which the three main compounds in the crude extract were quantified.

For the quantitative analysis of the main compounds in the crude extract, an HPLC-UV method was optimised with respect to the sample preparation and chromatographic separation in order to obtain a correct and quantitative result. This method was validated and has proven to be efficient for the quantification of the total amount of colchicine and colchicine derivatives expressed as colchicine and for the simultaneous quantification of the three individual compounds (colchicoside, 3-*O*-demethylcolchicine and colchicine). Different batches of extract contained different amounts of colchicine and colchicine derivatives. This emphasises the importance of quality/batch control and the use of quantified extracts.

The cytotoxicity of the *G. superba* crude extract was assessed *in vitro* on different cell lines (cancerous and normal) of different origins (breast, colon, pancreas and endometrium (PC-EM005 and 002)) of different species (human and murine (PANC02 and 3T3)). Different assays were used with their own advantages and disadvantages. The results of the *in vitro* studies led to the conclusion that the *G. superba* crude extract exhibited a high cytotoxic activity on the tested cell lines with IC₅₀ values lower than 1 µg/mL.

An *in vivo* efficacy study was performed to determine the potential anticancer activity and toxicity of the *G. superba* crude extract. In addition, a colchicine-poor but colchicoside-enriched extract was prepared, in which colchicoside served as a prodrug of 3-*O*-demethylcolchicine, the active metabolite. Both extracts were evaluated in a syngeneic

immunocompetent murine model of pancreatic cancer. A relevant tumour growth inhibition was observed at a dose of 3 mg/kg total amount of colchicine and colchicine derivatives expressed as colchicine with a tumour growth inhibition of 74% for the crude extract and 63% for the colchicine-poor extract. No severe side effects or toxicity due to the treatment were observed during the entire study. Significant lowered tumour metabolic activity was observed for the crude extract at all given dose and for the colchicine-poor extract at a dose of 1 mg/kg. Furthermore, *ex vivo* immunohistochemical analysis of the tumour tissues showed a significant decrease in proliferation and a significant increase of apoptotic bodies.

An *in vivo* survival study was also performed. No prolongation of survival was observed for the treatment groups with the exception of the combination therapy, which is gemcitabine together with the *G. superba* crude extract, and the gemcitabine monotherapy. Statistical analysis of the data showed a significant difference in relative tumour volume and growth over time for the combination therapy compared to the control group and the gemcitabine monotherapy. A significant difference of relative tumour volume between the colchicine-poor extract and the control group was only observed on day 11 together with a tumour growth inhibition of 56.6%. A trend towards significance between the colchicine-poor extract and the control group was observed on other days, considering a smaller mean relative tumour volume observed for the colchicine-poor extract group. Although the crude extract did not showed a significant effect, the combination therapy with the crude extract and gemcitabine showed a significant effect on the tumour compared to the control group and the gemcitabine monotherapy. No toxicity caused by any treatment was observed during the entire study.

During the phytochemical investigation of the *Chelidonium majus* L. herb four main benzyloisoquinoline alkaloids, i.e. chelidonine, sanguinarine, chelerythrine and protopine, were identified from the defatted *C. majus* extract by means of HPLC-UV. The *C. majus* crude extract as well as the defatted extract were evaluated *in vitro* on the same cell lines as the *G. superba* extract for their cytotoxic activity. The *C. majus* crude extract showed a moderate cytotoxic activity against a human breast cancer cell line, however a high cytotoxic activity was observed against human pancreatic and colon cancer cell lines. The crude extract and defatted extract also exhibited a moderate to high cytotoxic activity against the murine pancreatic

cancer cell lines. Low to almost no cytotoxic activity was observed on the two endometrium cancer cell lines as well as for the murine fibroblast cells, when treated with the defatted extract.

A preliminary *in vivo* study was performed to evaluate the antitumoural effect of the defatted *C. majus* extract on a highly metastatic pancreatic murine model. Significantly less metastases were counted for the mice treated with 1.2 mg/kg defatted *C. majus* extract compared to the control group. The extract, however, did not affect the weight of the primary tumours.

SAMENVATTING

Kanker is de tweede belangrijkste doodsoorzaak wereldwijd en is dan ook uitgegroeid tot de meest uitdagende ziekte om te genezen. Het sterftecijfer als gevolg van kanker neemt elk jaar toe en dit ondanks diagnostische en therapeutische vooruitgang. Kanker kan worden gedefinieerd als een ziekte waarbij abnormale cellen ongecontroleerd groeien door de normale regels van celdeling te schenden.

Veel van de huidige antikankermedicijnen zijn van natuurlijke oorsprong of afkomstig van natuurlijke producten. Planten zijn een interessante bron vanwege hun diverse chemische samenstelling. Een plantenextract is een complex mengsel van verschillende, vaak nauw verwante componenten die op verschillende doelwitten kunnen werken. Door de doorgaans lage concentratie van deze componenten is er weinig toxiciteit, terwijl wat betreft de activiteit vaak synergisme wordt waargenomen. Meestal zijn de (ruwe) plantenextracten in vergelijking met de geïsoleerde componenten interessanter omwille van de combinatie van de activiteiten. Bovendien kan de aanwezigheid van prodrugs aan de activiteit bijdragen. Het gebruik van medicinale plantenextracten heeft dus veel potentieel. Natuurlijke producten zijn waardevolle bronnen voor de ontwikkeling van geneesmiddelen gezien het feit dat een aanzienlijk aantal geneesmiddelen van natuurlijke oorsprong zijn.

In dit doctoraatsproefschrift werden verschillende geneeskrachtige planten met eerder gerapporteerde cytotoxische activiteit en/of traditioneel gebruik onderzocht voor hun potentieel gebruik tegen kanker.

Het fytochemisch onderzoek van de *Steganotaenia araliacea* **Hoechst.** schors leidde tot de identificatie van drie componenten die zover onze kennis reikt, nog nooit werden gerapporteerd voor deze plant. Deze componenten waren spiropreussomerin A, een secundaire metaboliet afkomstig van het endofyt of de symbiotische schimmel *Preussia sp.*, conrauiflavonol/afzelin A en een nieuwe component 6,7-(2",2"-dimethylpyrano)-5,1'-dihydroxy-4'oxo-2'eryl-flavanon, aan welke de triviale naam protosteganoflavanone werd gegeven. De *in vitro* studies van het *S. araliacea* extract resulteerden slechts in een matige cytotoxische activiteit voor alle geteste cellijnen, i.e. borst- (MDA-MB-231), pancreas- (PANC-1) en colon- (HT-29) kankercellijnen en bronchiale epitheliale cellen (BEAS-2B) met een IC₅₀ waarde hoger dan 20 µg/mL. Het geïdentificeerde protoflavonoïd, protosteganoflavanone,

behoort tot een zeldzame klasse van flavonoiden die beschouwd wordt als een veelbelovende klasse van antikankerverbindingen. Daarom zou een toekomstig onderzoek naar de activiteit van protosteganoflavanone interessant zijn, daar nog niets gekend is over deze component. Een *in vitro* evaluatie van de ethylacetaatfractie van *S. araliacea*, waarvan dit protoflavonoïd één van de hoofdcomponenten is, kan ook veelbelovend zijn om te onderzoeken en om eventueel als opgezuiverd extract te dienen. In dit doctoraatsproject werd echter prioriteit gegeven aan de twee andere planten omwille van de op het eerste zicht matige *in vitro* resultaten van het ruw extract van *S. araliacea*.

De studie op de *Gloriosa superba* L. zaden resulteerde niet alleen in een fytochemisch onderzoek, waarbij vier componenten, namelijk colchicine, 3-*O*-demethylcolchicine, colchicoside en de artefact colchicosamide werden geïsoleerd en geïdentificeerd uit het ruw extract, maar ook in een analytisch onderzoek, waarbij de drie hoofdcomponenten van het ruw extract werden gekwantificeerd.

Voor deze kwantitatieve analyse werd een HPLC-UV methode geoptimaliseerd met betrekking tot de staalvoorbereiding en chromatografische scheiding om een juist en kwantitatief resultaat te bekomen. Deze methode werd gevalideerd en heeft bewezen efficiënt te zijn voor de kwantificatie van de totale hoeveelheid colchicine en colchicine derivaten uitgedrukt als colchicine en voor de simultane kwantificatie van de drie afzonderlijke componenten (colchicoside, 3-*O*-demethylcolchicine en colchicine). Verschillende loten van het plantenextract bevatten verschillende hoeveelheden colchicine en colchicine derivaten. Dit benadrukt nogmaals het belang van een kwaliteit/batchcontrole en het gebruik van gekwantificeerde extracten.

De cytotoxiciteit van het *G. superba* ruw extract werd *in vitro* geëvalueerd op verschillende cellijnen (kanker en normaal) van verschillende oorsprong (borst, colon, pancreas en endometrium (PC-EM005 en 002)) en van verschillende species (mens en muis (PANC02 en 3T3)). Verscheidene biologische methoden werden gebruikt met elk hun eigen voordelen en nadelen. Uit de resultaten van de *in vitro* studies kon geconcludeerd worden dat het *G. superba* ruw extract een hoge cytotoxische activiteit op de geteste cellijnen vertoonde met IC₅₀ waarden lager dan 1 µg/mL.

Een *in vivo* efficaciteitsonderzoek werd uitgevoerd om de potentiële antikankeractiviteit en de toxiciteit van het *G. superba* ruw extract. Daarnaast werd een colchicine-arm doch colchicoside-rijk extract bereid, waarbij colchicoside de prodrug is van de actieve metabooliet, 3-*O*-demethylcolchicine. Beide extracten werden in een syngeneïsch immunocompetent muismodel van pancreaskanker geëvalueerd. Een relevante tumorgroei inhibitie werd waargenomen bij een dosis van 3 mg/kg totaal colchicine en colchicine derivaten uitgedrukt als colchicine voor beide extracten met een tumorgroei inhibitie van 74% voor het ruw extract en 63% voor het opgezuiverd colchicine-arm extract. Gedurende de hele studie werden bij geen van de ingestelde therapieën toxiciteit of ernstige bijwerkingen waargenomen. Een significante daling van de metabole activiteit van de tumor werd geconstateerd voor alle dosissen van het ruw extract en voor een dosis van 1 mg/kg colchicine-arm extract. Bovendien vertoonde de *ex vivo* immunohistochemische analyse van de tumorweefsels een significante afname van proliferatie en een aanzienlijke toename van apoptotische lichamen en dus van apoptose.

Een *in vivo* overlevingsonderzoek werd vervolgens uitgevoerd. Voor de verschillende behandelingen werd er geen verlenging van de overleving waargenomen, met de uitzondering van de combinatietherapie, namelijk een behandeling met gemcitabine en het *G. superba* ruw extract samen, en de gemcitabine monotherapie. Uit de statistische analyse van de gegevens werd een significant verschil in relatief tumorvolume en tumorgroei over tijd voor de combinatietherapie waargenomen vergeleken met de controle groep en de monotherapie. Bovendien werd een significant verschil in relatief tumorvolume tussen het colchicine-arm extract en de controle groep waargenomen op dag 11 samen met een tumorgroei inhibitie van 57%. Op andere dagen kan er echter een trend naar significantie tussen de groep behandeld met het colchicine-arm extract en de controle groep worden waargenomen, aangezien een kleiner gemiddeld relatief tumorvolume geobserveerd werd voor de groep behandeld met het colchicine-arm extract. Hoewel geen significant effect werd geconstateerd voor het ruw extract, vertoonde de combinatietherapie met het ruw extract en gemcitabine wel een significant effect op de tumor in vergelijking met de controle groep en de gemcitabine monotherapie. Gedurende de hele studie werd bij geen van de ingestelde therapieën toxiciteit waargenomen.

Tijdens het fytochemisch onderzoek van het *Chelidonium majus* L. kruid werden vier hoofdcomponenten van de klasse van de benzyloquinoline alkaloiden geïdentificeerd uit het ontvet *C. majus* extract door middel van HPLC-UV. Deze vier hoofdcomponenten waren chelidonine, sanguinarine, chelerythrine en protopine. De cytotoxische activiteit van het ruw en het ontvet *C. majus* extract werd ook *in vitro* geëvalueerd in dezelfde cellijnen als het *G. superba* extract. Voor het ruw extract werd een matige cytotoxische activiteit tegen de humane borstkankercellijn en een hoge cytotoxische activiteit tegen de humane pancreas- en colonkankercellijn waargenomen. Beide extracten vertoonden een matige tot hoge cytotoxische activiteit tegen de muis pancreaskankercellijn. Bij een behandeling met het ontvet extract werd weinig tot bijna geen cytotoxische activiteit waargenomen op de endometriumcellijnen.

Een preliminair *in vivo* onderzoek werd uitgevoerd om het antitumoraal effect van het ontvet extract te bepalen op een zeer metastatisch pancreas muismodel. Er werden statistisch minder metastasen geteld bij de muizen behandeld met 1.2 mg ontvet *C. majus* extract/kg lichaamsgewicht in vergelijking met de controle groep. Het extract had echter geen invloed op het gewicht van de primaire tumoren.

ACKNOWLEDGEMENT

-

DANKWOORD

Na enkele duizenden woorden, neem ik nu even tijd om enkele woorden van dank te typen. Want het is slechts met de hulp van anderen dat zo'n eindresultaat tot stand kan komen.

In de eerste plaats wil ik mijn promotoren, Prof. Luc Pieters en Prof. Sandra Apers, bedanken voor de kans die ze me gaven om dit doctoraatswerk uit te voeren. In het begin heb ik getwijfeld of ik dit wel zou kunnen, maar jullie bleven in me geloven. Bedankt voor alles wat ik van jullie heb kunnen en mogen leren.

Ik wil ook Prof. Arnold Vlietinck bedanken. Desondanks ik geen doctoraatstudente van hem was, heeft hij mij altijd bijgestaan tijdens mijn doctoraat. Zijn encyclopedische kennis en de "drive" om het met ons te delen zijn legendarisch.

Zonder financiële steun is het moeilijk om een doctoraat uit te voeren. Daarom wens ik het Agentschap voor Innovatie door Wetenschap en Technologie te bedanken voor het verlenen van een doctoraatsbeurs.

Ik zou ook het Antikankerfonds of destijds Reliable Cancer Therapies willen bedanken. Niet enkel voor de financiële steun van dit project, maar ook om hun kennis te delen. Vooral een enorme dank u wel aan Klara, die mijn project al van het begin in goede banen heeft geleid.

Mijn dank gaat ook uit naar alle (ex)-collega's van de onderzoeksgroep NatuRA: Rudy, Nina, Francis, Ariane, Adnan, Roger, Tess en de vele buitenlandse passanten en studenten. Maar in het bijzonder enkele mensen die extra in de bloemetjes moeten gezet worden zoals o.a.

Liene, jij verdient zeker een plaatsje in dit dankwoord. Ook dankzij jou is er sprake van een doctoraat. Bedankt! Niet alleen voor mij zo goed te begeleiden tijdens mijn masterproef, maar ook tijdens de eerste jaren van mijn doctoraat. Een IWT indienen en verdedigen werd een eitje met jou aan mijn zijde.

Kenne, mijn bureaugenoot, A.112 zou niet hetzelfde zijn zonder jou. Het liedje "Sweet Caroline" blijf ik eeuwig aan jou linken. Ook jij verdient een bloemetje. Ik kon altijd bij jou terecht met mijn vragen over MS. Maar jij was ook degene waar ik terecht kon i.v.m. activiteitstudies, dierproeven en allerlei andere dingen. Dus voor jou een bloemetje of misschien liever een paar schoenen? ☺

Vasiliki, our NMR-specialist, at the end we finally found something to collaborate. Thanks for sharing all your knowledge about NMR. And also thanks for all the wise advice you gave me and all the nice talks we had. I really hope we can stay in touch.

Hans, mijn labomaatje, de voorbije 4 jaren waren "vlot" verlopen doordat ik altijd tegen jou mocht zagen, zuchten en blazen als het weeral niet ging. Ik zou je willen bedanken voor de vriendschap van de voorbije jaren en voor alle hulp. En nog veel succes met het afronden van je doctoraat.

Emmy, bedankt voor alle leuke tijden! Ik vond het super dat ik met jou naar congressen kon gaan en samen frustraties konden delen. Nog veel succes met je eigen doctoraat!

Ines, ook jij bedankt voor de leuke momenten en nog veel succes met je doctoraat.

Tania, mega Tania, bij jou kon ik altijd terecht voor ALLES! Als de toestellen weeral niet deden wat ik wou. Voor analytische en praktische vragen die ik had. Of als ik het gewoon even niet zag zitten. Bij jou kon ik met alles terecht.

Mart, voor jou ook een dikke merci, voor alle professionele hulp tijdens die 4 jaren. Ook bij jou kon ik met ontelbare vragen terecht.

Hanne, dikke merci voor mij te helpen met de dieren. Zonder jou zou het niet elke dag vlotter en vlotter gegaan zijn.

En dan nog de Anneliesjes, bedankt om de laatste maanden naar mijn ontzettend vele problemen en ergernissen te willen luisteren en sorry dat ik misschien te veel in jullie bureau heb staan zagen de voorbije maanden.

Vervolgens zou ik het Centrum voor Oncologisch Onderzoek (CORE) willen bedanken en in het bijzonder Prof. Filip Lardon om mij de kans te geven om het *in vitro* luik van mijn thesis te kunnen uitvoeren in hun labo. Ook een dank u wel aan An om mij bij te staan bij al het *in vitro* onderzoek. Dikke merci aan Hilde en Greet voor al het hulp bij de celkweek en ook aan Christophe voor het snijden van de coupes. Ik zou ook Prof. Marc Peeters willen bedanken voor zijn betrokkenheid in mijn project en Prof. Patrick Pauwels voor alle hulp bij de immunohistochemische studies.

Mijn dank gaat ook uit naar Prof. Steven Staelens en het hele team van het Molecular Imaging Center Antwerp (MICA) en vooral in het bijzonder Christel en Philippe voor al de hulp tijdens de *in vivo* proeven.

Graag zou ik ook nog Prof. Claudia Gravekamp willen bedanken. Niet alleen voor het doneren van de PANC02 cellen, maar ook voor het onderzoek dat ik mocht uitvoeren in haar labo en al de technieken die ze mij heeft aangeleerd.

Mijn dank gaat ook uit naar Dr. Lieve Coenegrachts van het Gynaecologische Oncologie Laboratorium van de KU Leuven om de *xCELLigence* te mogen gebruiken.

Cédéric, Bieke en Arthur, bedankt dat jullie een weekje hebben willen helpen met de gavage van de muizen.

Onder het motto: we work hard, we play hard, zou ik ook graag mijn vrienden willen bedanken die mij al die jaren hebben gesteund en de nodige ontspanningen hebben gebracht. Vooral een dikke merci aan Ina en Janne. We hebben samen Farmacie overleefd en hebben zoveel leuke tijden beleefd en hopelijk komen er nog meer van die leuke tijden in de toekomst. If a friendship lasts longer than 7 years, psychologists say it will last a lifetime...

Ik zou het thuisfront ook willen bedanken. De hoeveelheid aanmoediging die uit deze hoek is gekomen valt moeilijk in woorden uit te drukken. In het bijzonder mijn ouders die mij altijd hebben gesteund tijdens mijn studies. Bedankt om mij alle kansen te geven om te kunnen slagen. Dit is niet enkel mijn succes, maar ook die van jullie. Mijn schoonmoeder zou ik ook extra willen bedanken. Niet enkel om mij in huis te nemen, maar ook voor de enorme steun de voorbije jaren.

And last but not least,...

Sander, wij hebben een lange weg afgelegd. Samen begonnen aan de opleiding Farmacie, samen gedoopt bij UFKA, labo-partners tijdens fysica, feest/studie-partners tijdens onze jaren Farmacie en nu mijn wettelijk samenwonende partner ☺! Jij hebt mij altijd proberen te steunen waar je kon. De voorbije maanden waren voor mij mentaal super zwaar. Maar ik ben blij dat dit doctoraat eindelijk afgerond is en dat wij aan het volgend hoofdstuk kunnen beginnen.

Daar het onmogelijk is om alle personen te vermelden die een bijdrage hebben geleverd aan dit doctoraat een algemene bedankt aan iedereen die ik eventueel ben vergeten.

Rica

... I have not failed. I've just found 10000 ways that won't work. – Thomas Edison

SCIENTIFIC CURRICULUM VITAE

SCIENTIFIC CURRICULUM VITAE

PERSONALIA

Name	Rica Capistrano I.
Date of birth	November 30th, 1985
Place of birth	Manilla, Philippines
E-mail	rica.capistrano@uantwerpen.be

EDUCATION

1998 – 2004	Secondary, option Science-Mathematics Instituut Dames van het Christelijk Onderwijs Antwerp, Belgium
2004 – 2008	Academic Bachelor in Pharmaceutical Sciences, distinction University of Antwerp, Belgium
2008 – 2010	Master of Drug development: Pharmacist, distinction University of Antwerp, Belgium
2010 – 2015	PhD student in Pharmaceutical Sciences PhD fellowship from the <i>Agency for Innovation by Science and Technology in Flanders (IWT)</i> Natural Products & Food – Research & Analysis University of Antwerp, Belgium

SCIENTIFIC EXPERIENCE

- Oct 2010 – Present Natural Products & Food – Research & Analysis
PhD thesis: Phytochemical, Analytical and Preclinical
Investigations on Plant Extracts as Potential Antitumoural
Therapy
- Feb 2010 – June 2010 Laboratory of Pharmacognosy and Pharmaceutical Analysis
Master thesis: Phytochemical investigation on *Bafodeya benna*

SCIENTIFIC PUBLICATIONS

Papers in peer-reviewed journals

- 2011 Xu Yong-Jiang, Capistrano I. Rica, Dhooghe Liene, Foubert Kenn, Lemièrè Filip, Maregesi Sheila, Baldé Aliou, Apers Sandra, Pieters Luc - Herbal medicines and infectious diseases : characterization by LC-SPE-NMR of some medicinal plant extracts used against malaria - *Planta Medica* yr:2011 vol:77 iss:11 pg:1139 - 1148. <http://dx.doi.org/doi:10.1055/s-0030-1270719>
- 2015 Capistrano Rica, Wouters An, Foubert Kenn, Baldé Aliou, Apers Sandra, Lardon Filip, Pieters Luc, Exarchou Vassiliki - Phytochemical Characterisation of a Cytotoxic Stem Bark Extract of *Steganotaenia araliacea* and Identification of a Protoflavanone by LC-SPE-NMR – *Phytochemistry Letters*. Submitted.

Oral presentations

- 2014 Potential use of a standardized *Gloriosa superba* extract for the treatment of cancer – 62nd International Congress and Annual Meeting of the Society for Medicinal Plant and Natural Product Research (GA) – Guimaraes, Portugal
- 2012 The use of standardized plant extracts for the treatment of cancer – 16th forum of Pharmaceutical Sciences – Belgian Society of Pharmaceutical Sciences - Blankenberge, Belgium

Poster presentations

- 2014 Capistrano I. Rica, Wouters An, Vlietinck Arnold, Lardon Filip, Apers Sandra, Pieters Luc - In vitro cytotoxic activity of alkaloid-containing plant extracts – 62nd International Congress and Annual Meeting of the Society for Medicinal Plant and Natural Product Research (GA) – Guimaraes, Portugal
- 2013 Capistrano I. Rica, Foubert Kenn, Wouters An, Lardon Filip, Apers Sandra, Pieters Luc - Investigation of the potential use of a *G. superba* extract for the treatment of cancer - 61st International Congress and Annual Meeting of the Society for Medicinal Plant and Natural Product Research (GA) - Münster, Germany
- 2012 Capistrano I. Rica, Foubert Kenn, Dhooghe Liene, Wouters An, Lardon Filip, Vlietinck Arnold, Apers Sandra, Pieters Luc - Standardized plant extracts in the treatment of cancer - Natural anticancer drugs congress - Olomouc, Czech Republic
- 2010 Capistrano I. Rica, Dhooghe Liene, Foubert Kenn, Baldé Aliou, Apers Sandra, Pieters Luc - Phytochemical investigations on the leaves of *Bafodeya benna* using LC-SPE-NMR - Drug Analysis – Antwerp, Belgium